

For Reference

NOT TO BE TAKEN FROM THIS ROOM

Ex LIBRIS
UNIVERSITATIS
ALBERTAEANAE



THE UNIVERSITY OF ALBERTA

THE REACTIVITY OF ELECTRONS SOLVATED IN METHANOL AND
ETHANOL

BY



GERALD LLOYD BOLTON

A THESIS

SUBMITTED TO THE FACULTY OF GRADUATE STUDIES AND RESEARCH
IN PARTIAL FULFILMENT OF THE REQUIREMENTS FOR THE DEGREE

OF

DOCTOR OF PHILOSOPHY

DEPARTMENT OF CHEMISTRY

EDMONTON, ALBERTA

FALL, 1974

A B S T R A C T

At 295K, the e_s^- absorption peak (E_{\max}) and the width of the band at half height ($W_{\frac{1}{2}}$) were, respectively, 1.80 and 1.4 eV in ethanol. At temperatures between 170 and 350K, $\Delta E_{\max}/\Delta T = 3.2 \times 10^{-3}$ eV deg⁻¹ in ethanol. Increasing T increased $W_{\frac{1}{2}}$ slightly. The product of the e_s^- free ion yield per 100 eV of energy absorbed (G_{fi}) and the molar absorptivity at the band maximum ($\epsilon_{\lambda_{\max}}$) was independent of T in neutral ethanol, but increased slightly with T in $\sim M$ basic solution. The spectrum shape and position was not affected by the addition of base, but the maximum absorbance (A_{\max}) was increased due to scavenging of H_s^+ in the spurs.

Increasing the pressure between 1 bar and 2 kb caused E_{\max} to increase by 0.10 eV per kb in methanol and 0.075 eV per kb in ethanol. The $W_{\frac{1}{2}}$ increased by about 0.1 eV per kb in both alcohols. A_{\max} decreased by 25% per kb in methanol, due mostly to a decrease in $\epsilon_{\lambda_{\max}}$.

In many solvents $W_{\frac{1}{2}} \cdot \epsilon_{\lambda_{\max}}$, which is related to the oscillator strength (f), is $139 \times 10^6 \text{ M}^{-1} \text{ cm}^{-2}$.

Using this value, and measured values of $G_{fi} \cdot \epsilon_{\lambda_{\max}}$ and $W_{\frac{1}{2}}$, values of 1.5 and 1.4 were predicted for G_{fi} in methanol and ethanol, respectively. The value of f decreases with decreasing T and increasing P in both alcohols. The Arrhenius activation energy (E_a) for the decomposition

of e_s^- was 4.8 ± 0.2 kcal mol $^{-1}$. Values of E_a for a number of reactions of efficient electron scavengers with e_s^- were 3.0 ± 0.3 kcal mol $^{-1}$, which suggests a common rate determining step, such as diffusion of e_s^- . Benzene and phenol are poor e_s^- scavengers, and E_a 's for the reaction are 6.4 and 4.5, and 6.0 and 4.4 kcal mol $^{-1}$ in methanol and ethanol, respectively. The higher E_a 's were attributed to the increased binding energy of e_s^- in the solvent with decreasing T.

The ratio of rate constants for e_s^- scavenging (k_5) in ethanol and methanol ($k_{5,EtOH}/k_{5,MeOH}$) was 0.6 for diffusion controlled reactions, which is nearly equal to the ratio of diffusion coefficients of e_s^- in the two solvents. For slower reactions, the ratio increased, reaching 7.5 for phenol. This was attributed to the higher binding energy of e_s^- in methanol ($E_{max} = 1.97$ eV) than in ethanol ($E_{max} = 1.80$ eV).

The volume of activation (ΔV^\ddagger) for the decomposition reaction of e_s^- was -23.4 cm 3 mol $^{-1}$ in ethanol and -16.7 cm 3 mol $^{-1}$ in methanol. Values of ΔV^\ddagger for e_s^- scavenging reactions were determined for a number of scavengers. For reaction rates near the diffusion controlled value, $\Delta V^\ddagger > 0$. For slower reactions $\Delta V^\ddagger < 0$.

Values of k_5 at 295K and 1 bar were determined for seven gaseous solutes in the solvents water, methanol and ethanol. A comparison with values calculated from steady state radiolysis results was made.

ACKNOWLEDGEMENTS

The author expresses appreciation to the many persons associated with him during the time this thesis was researched and written.

Thanks are due to the staff of the Radiation Research Centre, the non-academic staff of the Chemistry Department, Mrs. M. Waters who typed this thesis, and Mr. G. Johanson who drew a number of the figures.

Special thanks go to my wife Lynne, my children Barbara and Grant, and my parents, whose patience and encouragement made the conclusion of this work inevitable.

My rewarding association with Dr. G. R. Freeman, who directed the research reported here, is gratefully acknowledged.

Finally, thanks are extended to the National Research Council of Canada and the Government of the Province of Alberta for financial assistance.

T A B L E O F C O N T E N T S

	<u>Page</u>
GLOSSARY OF SYMBOLS AND TERMS USED	1
INTRODUCTION	4
A GENERAL	4
1. RADIATION CHEMISTRY	4
a. Steady State Radiolysis	6
b. Pulse Radiolysis	7
2. ABSORPTION OF HIGH ENERGY RADIATION .	10
a. Interaction of photons (γ or X Rays) With Matter.	10
b. Interaction of Fast Electrons With Matter.	11
c. Linear Energy Transfer (LET)	11
d. Spur Formation	12
3. THE TIME SCALE OF EVENTS IN RADIOLYSIS	14
4. RADIOLYSIS OF ALCOHOLS	17
C THE SOLVATED ELECTRON.	19
1. HYPOTHESES CONERNING THE FATE OF NEARLY THERMAL ELECTRONS	19
2. THE OPTICAL AND KINETIC PROPERTIES OF SOLVATED ELECTRONS	21
3. THEORETICAL MODELS FOR THE SOLVATED ELECTRON IN POLAR LIQUIDS	23
D THE VARIATION OF PRESSURE.	25
E THE VARIATION OF TEMPERATURE	28
F THE OBJECT OF THE PRESENT WORK	31

	<u>Page</u>
EXPERIMENTAL	33
A MATERIALS	33
1. SOLVENTS	33
a. Water	33
b. Methanol	33
c. Ethanol	34
2. SOLUTES	35
a. Solid Compounds Used as Solutes	35
b. Liquid Compounds Used as Solutes	36
c. Gaseous Compounds Used as Solutes	37
d. Miscellaneous Compounds	38
B APPARATUS	39
1. THE SAMPLE CELLS	39
2. THE OPTICAL DETECTION SYSTEM . . .	44
3. THE TEMPERATURE CONTROL SYSTEM . .	49
4. THE HIGH PRESSURE SYSTEM.	52
5. THE BUBBLING SYSTEM	57
a. Samples in Quartz Cells	57
b. Samples for High Pressure Cell	60
c. The Gaseous Solute Bubbler . .	62
6. GAS CHROMATOGRAPHY	65
a. Analysis of Water in Alcohols	65
b. Analysis of Gaseous Solutes. .	65

	<u>Page</u>
7. THE VAN DE GRAAFF ACCELERATOR	65
8. THE SECONDARY EMISSION MONITOR (SEM)	67
C TECHNIQUES.	70
1. SAMPLE PREPARATION	70
a. Samples in Type (a) Cells.	70
b. Samples in Type (b) Cells	71
c. Samples in Type (c) Cells	73
d. Samples in the High Pressure Cell	73
e. Samples Containing Sodium Alkoxide	74
2. CHROMATOGRAPHY	74
a. Analysis of Water in Alcohols.	74
b. Analysis of Gaseous Solutes.	75
3. SODIUM-POTASSIUM ALLOY PREPARATION	77
4. ANALYSIS OF POLAROID PHOTOGRAPHS.	80
a. Analysis of the Kinetics from Photograph i	81
b. Analysis of Optical Absorption from Photograph i	86
c. Analysis of Optical Absorption from Photograph ii	89
D TIMING OF A FAST ABSORPTION EXPERIMENT	90
E IRRADIATION AND DOSIMETRY	95
1. IRRADIATION	95
2. DOSIMETRY	95
F DIELECTRIC CONSTANT (ϵ) AND DENSITY (ρ)	97
1. THE EFFECT OF TEMPERATURE	97

	<u>Page</u>
2. THE EFFECT OF PRESSURE	97
RESULTS	103
A SOLVATED ELECTRON OPTICAL ABSORPTION SPECTRA	103
1. THE EFFECT OF TEMPERATURE CHANGE .	103
a. Neutral Ethanol	103
b. $\sim \text{mM}$ KOH in Ethanol	109
c. The effect of Temperature on E_{\max} and $G_{fi} \mathcal{E}_{\lambda_{\max}}$	112
2. THE EFFECT OF KOH CONCENTRATION .	116
3. THE EFFECT OF IMPURITIES THAT SCAVENGE e_s^-	120
4. THE EFFECT OF PRESSURE	122
5. THE EFFECT OF PULSE DOSE ON ABSORBANCE	131
6. THE EFFECT OF ADDED WATER.	131
B TEMPERATURE EFFECTS ON e_s^- REACTION KINETICS	135
1. NEUTRAL AND $\sim \text{lmM}$ KOH SOLUTIONS OF ETHANOL.	135
2. E_a FOR THE REACTION OF e_s^- WITH SCAVENGERS IN METHANOL AND ETHANOL	137
a. Acetone $((\text{CH}_3)_2\text{CO})$ as e_s^- Scavenger.	140
b. Nitrobenzene $(\text{C}_6\text{H}_5\text{NO}_2)$ as the e_s^- Scavenger.	146
c. Naphthalene $(\text{C}_{10}\text{H}_8)$ as the e_s^- Scavenger.	146

	<u>Page</u>
d. Perchloric Acid (HClO_4) as the e_s^- Scavenger	153
e. Benzene (C_6H_6) as the e_s^- Scavenger	157
f. Phenol ($\text{C}_6\text{H}_5\text{OH}$) as the e_s^- Scavenger	163
C PRESSURE EFFECTS ON e_s^- REACTION KINETICS.	168
1. THE EFFECT OF PRESSURE ON THE e_s^- DECOMPOSITION REACTION	169
a. Pure Neutral Methanol and Ethanol	169
b. The Effect of Base on ΔV^\ddagger of e_s^- Decomposition	172
c. The effect of Water on ΔV^\ddagger of e_s^- Decomposition in Ethanol . .	176
2. THE EFFECT OF PRESSURE ON THE SCAVENGING OF e_s^-	176
a. Naphthalene (C_{10}H_8) as e_s^- Scavenger	179
b. Acetonitrile (CH_3CN) as e_s^- Scavenger	179
c. Perchloric Acid (HClO_4) as e_s^- Scavenger	190
d. Nitrobenzene ($\text{C}_6\text{H}_5\text{NO}_2$) as e_s^- Scavenger	193
e. Acetone ($(\text{CH}_3)_2\text{CO}$) as e_s^- Scavenger	197
f. Ethyl Acetate ($\text{CH}_3\text{CO}_2\text{C}_2\text{H}_5$) as e_s^- Scavenger	197
g. Cadmium Chloride (CdCl_2) as e_s^- Scavenger	211

	<u>Page</u>
5. THE EFFECTS OF PRESSURE ON A _{max}	284
6. THE OSCILLATOR STRENGTH f OF THE e _s ⁻ OPTICAL ABSORPTION	286
a. The Relative f for e _s ⁻ in Various Solvents	286
b. The Effects of Temperature and Pressure on W _{1/2} · E _λ ^{max} in Methanol and Ethanol	289
7. THE EFFECT OF ADDED WATER ON THE e _s ⁻ OPTICAL ABSORPTION SPECTRUM IN ETHANOL	291
 B TEMPERATURE EFFECTS ON e _s ⁻ REACTION KINETICS	295
1. GENERAL	295
2. NEUTRAL AND ~mM KOH SOLUTIONS OF ETHANOL	297
3. THE REACTION OF e _s ⁻ WITH SCAVENGERS	299
4. OTHER EFFECTS OF BENZENE-SOLVATED ELECTRON REACTIONS.	302
 C PRESSURE EFFECTS ON e _s ⁻ REACTION KINETICS	307
1. GENERAL	307
2. THE EFFECT OF PRESSURE ON THE e _s ⁻ DECOMPOSITION REACTION	309
a. Pure Neutral Methanol and Ethanol	309
b. The Effect of Base on ΔV [‡] of e _s ⁻ Decomposition.	311
c. The Effect of Water on ΔV [‡] of e _s ⁻ Decomposition in Ethanol	312
3. THE EFFECT OF PRESSURE ON THE SCAVENGING OF e _s ⁻	313

	<u>Page</u>
D REACTION RATE CONSTANTS (k_5) FOR e_s^- WITH GASEOUS SOLUTES IN WATER, METHANOL AND ETHANOL	316
E THE EFFECT OF PULSE DOSE ON THE e_s^- HALF-LIFE	323
F COMPARISON OF REACTION RATES OF e_s^- IN METHANOL AND ETHANOL	325
 BIBLIOGRAPHY	 333

L I S T O F T A B L E S

<u>Table</u>		<u>Page</u>
I-1	Time Scale for Events in an Irradiated Polar Liquid at Room Temperature	15
II-1	Column Conditions for Gaseous Solutes Analysis	76
III-1	Solvated Electron Optical Absorption Properties. Neutral Ethanol and Methanol	106
III-2	Solvated Electron Optical Absorption Properties. 1 <u>mM</u> KOH in Ethanol	111
III-3	$G_{fi} \cdot \epsilon_{\lambda_{max}}$ in Neutral and $\sim \text{mM}$ KOH in Ethanol	115
III-4	Solvated Electron Optical Absorption Properties in Basic Ethanol, $294 \pm 1\text{K}$	119
III-5	Pressure Effects on the Solvated Electron Optical Absorption Spectrum	125
III-6	The Effect of Temperature on the e_s^- Decomposition Reaction. Neutral Ethanol	138
III-7	The Effect of Temperature on the e_s^- Decomposition Reaction. $\sim \text{mM}$ KOH in Ethanol	139
III-8	The k 's and E_a 's for the Reaction of e_s^- with Acetone	145
III-9	The k 's and E_a 's for the Reaction of e_s^- with Nitrobenzene	149
III-10	The k 's and E_a 's for the Reaction of e_s^- with Naphthalene	152
III-11	The k 's and E_a 's for the Reaction of e_s^- with Perchloric Acid	156
III-12	The k 's and E_a 's for the Reaction of e_s^- with Benzene	161
III-13	The k 's and E_a 's for the Reaction of e_s^- with Phenol	167

<u>Table</u>		<u>Page</u>
III-14	The Effect of Pressure on e_s^- Decomposition in Methanol and Ethanol	171
III-15	The Effect of Base on ΔV^\ddagger in Methanol	175
III-16	The Effect of Base on ΔV^\ddagger in Ethanol	175
III-17	The Effect of H_2O on ΔV^\ddagger of e_s^- Decomposition in Ethanol	178
III-18	The k 's and ΔV^\ddagger 's for $e_s^- +$ Naphthalene	184
III-19	The k 's and ΔV^\ddagger 's for $e_s^- +$ Acetonitrile	189
III-20	The k 's and ΔV^\ddagger 's for $e_s^- + H_s^+$	194
III-21	The k 's and ΔV^\ddagger 's for $e_s^- +$ Nitrobenzene	200
III-22	The k 's and ΔV^\ddagger 's for $e_s^- +$ Acetone	205
III-23	The k 's and ΔV^\ddagger 's for $e_s^- +$ Ethyl Acetate	210
III-24	The k 's and ΔV^\ddagger 's for $e_s^- +$ Cadmium Chloride	216
III-25	The k 's and ΔV^\ddagger 's for $e_s^- +$ Toluene	224
III-26	The k 's and ΔV^\ddagger 's for $e_s^- +$ Benzene	229
III-27	Data Summary for Effect of Pressure on $e_s^- +$ Scavenger Reaction, $295 \pm 1K$	230
III-28	k for $e_s^- + N_2O$ in Water	235
III-29	k for $e_s^- + N_2O$ in Methanol	236
III-30	k for $e_s^- + N_2O$ in Ethanol	237
III-31	k for $e_s^- + SF_6$ in Water	239
III-32	k for $e_s^- + SF_6$ in Methanol	241
III-33	k for $e_s^- + SF_6$ in Ethanol	242
III-34	k for $e_s^- +$ Oxygen in Methanol	245
III-35	k for $e_s^- +$ Oxygen in Ethanol	246

<u>Table</u>		<u>Page</u>
III-36	k for e_s^- + Carbon Dioxide in Water	248
III-37	k for e_s^- + Carbon Dioxide in Methanol	249
III-38	k for e_s^- + Carbon Dioxide in Ethanol	250
III-39	k for e_s^- + 1,3-Butadiene in Water	252
III-40	k for e_s^- + 1,3-Butadiene in Methanol	253
III-41	k for e_s^- + 1,3-Butadiene in Ethanol	254
III-42	k for e_s^- + Acetylene in Water	255
III-43	k for e_s^- + Acetylene in Methanol	256
III-44	k for e_s^- + Acetylene in Ethanol	257
III-45	k for e_s^- + Ethene	259
III-46	$G(OH) \cdot \epsilon_{\lambda_{max}} (SCN)_2^-$ Relative to the Fe^{+2}/Fe^{+3} Dosimeter	266
IV-1	Comparison of e^- Spectral Data from Different Solvents	272
IV-2	The Estimation of $\epsilon_{\lambda_{max}}$ in Ethanol and Methanol	283
IV-3	Comparison of $W_{\frac{1}{2}} \cdot \epsilon_{\lambda_{max}}$ for the e_s^- Spectrum in a Variety of Solvents	288
IV-4	The Effect of T on $W_{\frac{1}{2}} \cdot \epsilon_{\lambda_{max}}$ in Alcohols and Water	290
IV-5	The Effect of P on $W_{\frac{1}{2}} \cdot \epsilon_{\lambda_{max}}$ in Alcohols and Water	292
IV-6	Summary of Arrhenius Activation Energy Data for the Reaction of e_s^- with Scavenger. Methanol as Solvent	300
IV-7	Summary of Arrhenius Activation Energy Data for the Reaction of e_s^- with Scavenger. Ethanol as Solvent	301
IV-8	The Effect of Benzene Concentration on the Absorbance in Methanol and Ethanol	304

<u>Table</u>		<u>Page</u>
IV-9	Comparison of ΔV^\ddagger Data from Pulse Radiolysis and Steady State Radiolysis Studies	315
IV-10	Gaseous Solute Rate Constant Data Summary Water, 295 \pm 3K	318
IV-11	Gaseous Solute Rate Constant Data Summary Methanol, 295 \pm 3K	319
IV-12	Gaseous Solute Rate Constant Data Summary Ethanol, 295 \pm 3K	321
IV-13	Comparison of k_5 in Methanol and Ethanol for a Variety of Electron Scavengers	327

L I S T O F F I G U R E S

<u>Figure</u>		<u>Page</u>
II-1	Suprasil Quartz Optical Cells	40
II-2	The High Pressure Optical Cell	42
II-3	The Optical Detection System	45
II-4	The Amplifier Linearity and Rise Time	48
II-5	The High Pressure System	53
II-6	The High Pressure Bomb and Bellows Position Indicator	56
II-7	The Bellows Position Indicator Circuit	58
II-8	The Sample Bubbler Manifold for Use with Quartz Cells	59
II-9	The High Pressure Sample Preparation System	61
II-10	The Gaseous Solute Stock Solution Preparation Apparatus	63
II-11	The Secondary Emission Monitor (SEM)	68
II-12	The Sealing Technique for Type (b) Cells	72
II-13	Gas Chromatograph Calibration Plots	78
II-14	The Na-K Alloy Preparation Apparatus	79
II-15	Typical Oscilloscope Trace Photographs	82
II-16	The First Order Decay of Solvated Electrons in Ethanol	84
II-17	The Geometric Method of Determining λ_{\max}	88
II-18	The Timing Sequence of an Absorption Experiment	91
II-19	The Effect of Temperature on the Density of Methanol and Ethanol	98
II-20	The Effect of Temperature on the Static Dielectric Constant of Methanol and Ethanol	99

<u>Figure</u>		<u>Page</u>
II-21	The Effect of Pressure on the Density of Methanol and Ethanol	100
II-22	The Effect of Pressure on the Dielectric Constant of Methanol and Ethanol	102
III-1	e_s^- Absorption Spectra in Ethanol	105
III-2	Time Dependent Shape of Solvated Electron Spectrum in Ethanol at 166K	108
III-3	e_s^- Absorption Spectra in $\sim 1 \text{ mM}$ KOH in Ethanol	110
III-4	Temperature Dependence of E_{\max} for e_s^- Absorption in Ethanol	113
III-5	Temperature Dependence of $G_{fi} \cdot \epsilon_{\lambda_{\max}}$ in Ethanol	114
III-6	e_s^- Absorption Spectra in Ethanol	117
III-7	e_s^- Absorption Spectra in Ethanol	118
III-8	The Effect of Scavenger on the Solvated Electron Spectrum in Ethanol	121
III-9	e_s^- Absorption Spectra in Methanol	123
III-10	e_s^- Absorption Spectra in Ethanol	124
III-11	Relative A in Methanol as a Function of Electron Beam Energy	127
III-12	Diagram Showing Area of Solution Sampled by Analyzing Light Beam	129
III-13	The Decrease in A in Methanol with Increasing Pressure	132
III-14	The Effect of Pulse Dose on the A of e_s^- in Ethanol	133
III-15	The Effect of Water on the A_{\max} of e_s^- in Ethanol	134
III-16	E Plots for e_s^- Decomposition Reaction in EtOH	136

<u>Figure</u>		<u>Page</u>
III-17 A-F	The Effect of T on e_s^- + Acetone	141-143
III-17 G	E_a for e_s^- + Acetone	144
III-18 A-C	The Effect of T on e_s^- + Nitrobenzene	147-148
III-18 D	E_a for e_s^- + Nitrobenzene	148
III-19 A-C	The Effect of T on e_s^- + Naphthalene	150-151
III-19 D	E_a for e_s^- + Naphthalene	151
III-20 A,B	The Effect of T on e_s^- + H_s^+	154
III-20 C	E_a for e_s^- + H_s^+	155
III-21 A-D	The Effects of T on e_s^- + Benzene	158-159
III-21 E	E_a for e_s^- + Benzene	160
III-22 A-E	The Effect of T on e_s^- + Phenol	164-166
III-22 F	E_a for e_s^- + Phenol	166
III-23	ΔV^\ddagger for the e_s^- Decomposition Reaction in MeOH or EtOH	170
III-24	The Effect of [KOH] on ΔV^\ddagger of e_s^- Decomposition in Methanol	173
III-25	The Effect of [KOH] on ΔV^\ddagger of e_s^- Decomposition in Ethanol	174
III-26	The Effect of $[H_2O]$ on ΔV^\ddagger of e_s^- Decomposition in Ethanol	177
III-27 A-C	The Effect of P on e_s^- + Naphthalene in MeOH	180-181
III-27 D	ΔV^\ddagger for e_s^- + Naphthalene in MeOH	181
III-28 A-C	The Effect of P on e_s^- + Naphthalene in EtOH	182-183
III-28 D	ΔV^\ddagger for e_s^- + Naphthalene in EtOH	183
III-29 A-C	The Effect of P on e_s^- + Acetonitrile in MeOH	185-186

FIGURE

		<u>Page</u>
III-29 D	ΔV^\ddagger for $e_s^- +$ Acetonitrile in MeOH	186
III-30 A-C	The Effect of P on $e_s^- +$ Acetonitrile in EtOH	187-188
III-30 D	ΔV^\ddagger for $e_s^- +$ Acetonitrile in EtOH	188
III-31 A-C	The Effect of P on $e_s^- + H_s^+$ in EtOH	191-192
III-31 D	ΔV^\ddagger for $e_s^- + H_s^+$ in EtOH	192
III-32 A-C	The Effect of P on $e_s^- +$ Nitrobenzene in MeOH	195-196
III-32 D	ΔV^\ddagger for $e_s^- +$ Nitrobenzene in MeOH	196
III-33 A-C	The effect of P on $e_s^- +$ Nitrobenzene in EtOH	198-199
III-33 D	ΔV^\ddagger for $e_s^- +$ Nitrobenzene in EtOH	199
III-34 A-C	The Effect of P on $e_s^- +$ Acetone in MeOH	201-202
III-34 D	ΔV^\ddagger for $e_s^- +$ Acetone in MeOH	202
III-35 A-C	The Effect of P on $e_s^- +$ Acetone in EtOH	203-204
III-35 D	ΔV^\ddagger for $e_s^- +$ Acetone in EtOH	204
III-36 A-C	The Effect of P on $e_s^- +$ Ethyl Acetate in MeOH	206-207
III-36 D	ΔV^\ddagger for $e_s^- +$ Ethyl Acetate in MeOH	207
III-37 A-C	The Effect of P on $e_s^- +$ Ethyl Acetate in EtOH	208-209
III-37 D	ΔV^\ddagger for $e_s^- +$ Ethyl Acetate in EtOH	209
III-38 A-C	The Effect of P on $e_s^- + CdCl_2$ in MeOH	212-213
III-38 D	ΔV^\ddagger for $e_s^- + CdCl_2$ in MeOH	213
III-39 A-C	The Effect of P on $e_s^- + CdCl_2$ in EtOH	214-215
III-39 D	ΔV^\ddagger for $e_s^- + CdCl_2$ in EtOH	215

<u>Figure</u>	<u>Page</u>
III-40 A-C The Effect of P on e_s^- + Toluene in MeOH	217-218
III-40 D ΔV^\ddagger for e_s^- + Toluene in MeOH	218
III-41 A-C The Effect of P on e_s^- + Toluene in EtOH	219-220
III-41 D ΔV^\ddagger for e_s^- + Toluene in EtOH	220
III-42 A-C The Effect of P on e_s^- + Untreated Toluene in EtOH	221-222
III-42 D ΔV^\ddagger for e_s^- + Toluene (untreated) in EtOH	222
III-43 A-C The Effect of P on e_s^- + Benzene in MeOH	225-226
III-43 D ΔV^\ddagger for e_s^- + Benzene in MeOH	226
III-44 A-C The Effect of P on e_s^- + Benzene in EtOH	227-228
III-44 D ΔV^\ddagger for e_s^- + Benzene in EtOH	228
III-45 The Effect of Dose on $t_{\frac{1}{2}}$ of e_s^- in MeOH	261
III-46 The Effect of Dose on $t_{\frac{1}{2}}$ of e_s^- in EtOH	262
III-47 The $(SCN)_2^-$ Absorption Spectrum in Water	269
III-48 The Effect of $[SCN^-]$ on A of $(SCN)_2^-$ in Aqueous Solution	270
IV-1 Plot of E_{max} vs $\epsilon.p$ for Ethanol, Methanol and Water	276
IV-2 The Effect of Benzene Concentration on the e_s^- Absorbance	303
IV-3 Comparison of e_s^- Scavenging Reaction Rates (k_5) in Methanol and Ethanol	328

GLOSSARY OF SYMBOLS AND TERMS USED

A, ^{1a}
Absorbance.

$$A = \log_{10} \left(\frac{I_0}{I} \right) = \epsilon bc$$

I_0 is incident light intensity

I is transmitted light intensity

ϵ is the molar absorptivity in $M^{-1} \text{ cm}^{-1}$

b is the path length

c is the molar concentration of absorber

Bar, A unit for pressure. 1 bar = 0.9869 atmospheres
= 14.50 psi. 1 kb = 10^3 bars.

E, The energy of an optical absorption, in units
of ev. E_{\max} is the energy of maximum absorption.

E_a , The Arrhenius activation energy in kcal/mol.

f, ^{1b}
Oscillator strength.

$$f = 4.32 \times 10^{-9} [9\eta_0 / (\eta_0^2 + 2)^2] \int \epsilon_{\bar{v}} d\bar{v}$$

η_0 is the refractive index of the solvent

$\epsilon_{\bar{v}}$ is the molar absorptivity at wave number \bar{v}

The term in brackets is an internal field cor-
rection.

G, The yield of a radiolysis reaction in units of
species per 100 ev of absorbed dose. G_{fi} re-
presents the yield of free ions/100 ev, G_{gem}

represents the yield of geminate ions/100 eV.

L, Ostwald coefficient

$$L = V_G/V_L$$

V_G is the volume of dissolved gas

V_L is the volume of liquid

Both are at the same temperature and pressure.

In the literature, λ and γ are also used to represent the Ostwald coefficient. It should not be confused with the Bunsen coefficient, α , for which V_G is the gas volume corrected to 760 torr and 273K.

LET, Linear energy transfer. The average energy loss per unit distance travelled by an ionizing particle, in units of eV/nm.

M, Used to express the units of molarity, which are moles of solute per litre of solution.

mol, Mole.

S, Scavenger, a purposely added or already present solute which preferentially reacts with a particular intermediate formed in radiolysis.

ΔV^\ddagger , Volume of activation 1c in $\text{cm}^3 \text{mol}^{-1}$.

$$\Delta V^\ddagger = \frac{-RT \left(\ln \frac{k_b}{k_a} \right)_T}{P_b - P_a}$$

R is the gas constant

T is the Kelvin temperature

k_b and k_a are the reaction rate constants at P_b and P_a , respectively

P_b and P_a are pressures, in units consistent with the units of R.

$W_{1/2}$, Half-width, the width of an optical absorption spectrum at half its height, in units of ev.

ϵ , Dielectric constant (static).

λ , Wavelength in nm.

ϵ , Molar absorptivity in $M^{-1} \text{ cm}^{-1}$.

ρ , Density in g/cm^3 .

→ Signifies a reaction induced by the absorption of radiation by the species to the left of the arrow.

INTRODUCTION

A. GENERAL

1. RADIATION CHEMISTRY

Radiation chemistry is the study of the chemical effects resulting from the absorption of high energy radiation by material.^{2,3} Absorption of ionizing energy by a liquid results in the production of a variety of reactive intermediates. These may be a combination of excited species, positive and negative ions, and free radicals.



The products of (I-1) are usually reactive, and they may react with each other, with the solvent, or with solutes. Analysis to determine the identities and yields of intermediate and final products provides much of the data available to radiation chemists. The determination of reaction rate constants furnishes additional information.

When it is possible to exert some control over the reactions of intermediates, much more instructive data may be obtained. Addition of a solute which preferentially reacts with a particular intermediate is one way of gaining this control. Such a solute is called a scavenger (S).

The effect of a scavenger on the yield of a final product infers the identity of the product's precursor. Furthermore, if the scavenging reaction gives a measurable product, the yield of the scavenged intermediate may be determined. Illustrative examples of electron scavengers are N_2O ⁴ and SF_6 .⁵



The ions formed by (I-2) and (I-3) react further to yield one molecule of N_2 ⁶, or six F^- ions⁷, respectively, for each electron scavenged. The scavengable yield of electrons can be found by increasing the scavenger concentration until there is no further change in the amount of final product. At that point, the yield of electrons is equal to the yield of N_2 if N_2O was the scavenger, or one sixth the yield of F^- if SF_6 was the scavenger.

Scavenging studies have led to the identification of the electron as a precursor of molecular hydrogen. Removal of electrons from solution by reaction with a solute inhibits (I-4). This is reflected by a reduced H_2 yield due to (I-5).





The subscripts s in (I-4) denote that the electron and ion are solvated. The maximum possible suppression of the yield by addition of an electron scavenger indicates how much H_2 results from electron reactions. The remainder must be attributed to other sources. Data of this type are utilized when postulating mechanisms.

There are two common methods of irradiating materials. These are the steady state and the pulse radiolysis methods. The two provide complimentary data.

a. Steady State Radiolysis

The most common source of radiation for steady state radiolysis is ^{60}Co . The decay of this man made radioisotope results in the emission of γ photons of 1.25 MeV average energy.

In these studies, data are obtained by identification of the final products and measurement of their yields. Since analysis is done after completion of the reactions involving the products of (I-1), it is impossible to establish absolutely the rate of reaction for any of them. However, rate constant ratios may be obtained when known concentrations of two different scavengers are competing for a particular intermediate. Using (I-2) and (I-3) as the example, the rate constant

ratio k_{I-2}/k_{I-3} can be determined from (I-6) if the final product yields are measured.

$$k_{I-2}/k_{I-3} = \frac{[SF_6]}{[N_2O]} \frac{(N_2 \text{ yield})}{1/6(F^- \text{ yield})} \quad (I-6)$$

In summary, analysis of results obtained by steady state methods can give the identities and yields of final products, as well as relative kinetic data. The identities of the reactive intermediates and the overall reaction mechanism can only be inferred from these data. Incorrect conclusions might sometimes be drawn when different intermediates can give rise to the same final products. The most apparent error of this type in the pre ~1960⁸ literature was the assignment of H atoms as the primary reducing species in irradiated liquids. It is now recognized that the solvated electron (e_s^-) is a more abundant primary reducing species.

b. Pulse Radiolysis

The pulse radiolysis technique is a relatively new addition to radiation chemistry. The radiation source is an electrical machine, most often a linear accelerator (lineac) or van de Graaff accelerator. It became electronically feasible in the late 1950's for these machines to deliver radiation in an intense single pulse. The first accounts of work done using the pulse radiolysis

method appeared in 1960.⁹⁻¹¹

Typical pulse duration is from 0.01 to 1 μ s, although both longer and shorter pulses are used. The system with the shortest time resolution (~20 ps) in use was developed by Hunt and co-workers¹²⁻¹⁶, and utilizes the 35 ps fine structure pulses from a 40 MeV lineac. Beam energies used vary by several orders of magnitude, but the most common is a few MeV. Peak pulse currents vary from milliamps to amps, depending upon the type of machine and the pulse length.

Two criteria should be considered when choosing a machine for a pulse radiation source. First, the pulse should be short compared with the time scale of the reactions being investigated. Second, there must be enough energy per pulse to create an adequate concentration of reactive species for detection. With the variety of machines available, it is usually possible to meet these criteria. Many of the machines available and their characteristics are briefly described in a number of books^{3,17-21} and articles.^{22,23}

Spectrophotometry^{17-21,24} and electrical conductivity²⁵⁻²⁹ are the most used methods for the detection of short-lived intermediates. The latter method measures the radiation induced transient conductivity in a solution, and has advantages where the charged intermediates cannot be conveniently detected optically. Information

on primary yields and reaction rates of charged species may be found.

It is the combination of kinetic spectrophotometry and pulse radiolysis though, that has been most productive. The method is versatile, and reactions of both charged and radical intermediates may be followed. The only criterion is that the species must absorb light strongly in a region of the spectrum where fast detection is possible. Fortunately this criterion is met by the solvated electron, and some radicals, in many solvents. Optical detection makes identification less ambiguous, and absolute rate constants can be readily determined by observing the effect of solute concentration on the rate of decay of the optical absorption. The primary yield may also be found if the molar absorptivity is known. Unfortunately, it seldom is. More work is necessary to establish the value of ϵ in most systems.

The events which precede the chemical reaction of intermediates are of considerable interest. One of these events is the localization of extra electrons in a medium. It has recently become possible to detect the final stages of the localization process in low temperature alcohols.³⁰⁻³² This is done by observing the time dependent changes in the shape and position of the absorption spectrum. Knowledge of the physical processes will enable a more complete empirical understanding of

irradiated systems.

2. ABSORPTION OF HIGH ENERGY RADIATION

a. Interaction of photons (γ or X Rays) With Matter

At energies normally used for studies in radiation chemistry, there are three processes which contribute to the absorption of a photon's energy by matter. These are, with the photon energy at which they are most important in brackets, the photoelectric effect (<0.1 MeV), the Compton effect (~0.01 - 20 MeV), and pair production (>5 MeV).

When energy is absorbed via the photoelectric effect, a photon is completely absorbed by an atom or molecule, and an extranuclear electron is ejected. The ejected electron has kinetic energy equal to the photon energy, less the binding energy of the electron in the atom.

In the Compton effect, a photon on "collision" with bound or free electrons gives up part of its energy. The result is production of electrons in the system which have various amounts of excess kinetic energy. The Compton effect is by far the most important energy loss process for photon energies of about 1 MeV. Cobalt 60 γ rays are near this energy.

Pair production results when interaction of a photon with the field of a nucleus produces an electron-

positron pair. This requires a theoretical minimum energy of 1.02 MeV.³³ In practise, somewhat more energy is required, and the excess is found in the kinetic energy of the electron-positron pair.

In each case, after a photon interacts with matter, energetic electrons are produced. These primary electrons in turn produce many secondary electrons. It is these energetic electrons which are responsible for most of the chemical change which is observed. Therefore, the chemical changes will be the same if fast electrons, rather than photons, are used initially. This is an important consideration, as will be evident in the discussion of linear energy transfer (LET) which follows.

b. Interaction of Fast Electrons With Matter

Fast electrons primarily produce ionization and excitation by coulombic interaction with the orbital electrons of atoms or molecules in the medium. Elastic collisions with nuclei, radiative collisions, and Cerenkov radiation generally contribute much less to the energy loss of fast electrons.^{17,33,34}

c. Linear Energy Transfer (LET)

The rate at which fast electrons lose their energy to a medium is given by the Bethe equation.³⁵ The value of the energy loss per unit distance ($-dE/dx$) is

called the linear energy transfer (LET). For primary electrons produced by γ photons, and ~ 1 MeV electrons, the initial LET in water is of the order of 10^{-2} eV/ \AA .

The LET is an average quantity, and increases as the particle slows down. It also increases as the square of the charge on the particle. Slower moving doubly charged α particles deposit their energy in a much shorter distance than do fast electrons. This leads to a much different distribution of reactive intermediates in the liquid, and consequently a different yield of final products.^{17,34,37} Therefore, when comparing data from different studies, it is important to know the LET of the radiation used.

d. Spur Formation

The deposition of energy in a liquid by a fast electron is not a uniformly continuous process. Energy is lost at random intervals in amounts of $10^2 \pm 1$ eV. The resulting volumes of excitation or ionization are called spurs. There is a wide distribution of spur sizes and shapes created by primary and secondary electrons of different LET. A spur exists as long as there is a significant probability that the intermediates in it will react with each other.³⁸

After their formation in spurs, the reactive intermediates may suffer one of several fates. Some

may react to form stable products while still in the spur. Some may recombine, as is often the case with electrons and their parent positive ions. This is called geminate recombination, and the ions are called geminate ions. Some ions and radicals will evade reaction or recombination in the spurs. These diffuse into the bulk solution and become free species.

The proportion of ions which become free ions increases with the dielectric constant of the medium. The number of ions which become free for each 100 ev of energy absorbed by the system is called G_{fi} . Water, methanol and ethanol have G_{fi} of about two for solvated electrons. In hydrocarbons of low dielectric constant, solvated electrons usually have a G_{fi} of only about 0.1, even though the total ionization is similar in the different types of liquids.

Reactions which occur in spurs do not obey homogeneous kinetics. This is because there is not a random distribution of reactants. A nonhomogeneous kinetics model must be used.^{39,40} Application of nonhomogeneous kinetics to pulse irradiated systems has been made by Vermeer and Freeman⁴¹ to the geminate recombination reaction in low temperature n-propyl ether. Baxendale and Wardman³¹ have pointed out that an initial portion of the solvated electron decay in low temperature alco-

holes also follows nonhomogeneous kinetics.

For those ions which diffuse into the bulk medium, homogeneous kinetics are used. Most pulse radiolysis studies have examined the reactions of only free ions, and therefore involve homogeneous kinetics.

3. THE TIME SCALE OF EVENTS IN RADIOLYSIS

The time scale of events occurring in an irradiated polar liquid at room temperature may be approximately as represented in Table I-1. The first entry is based on the time required for an electron of 2 MeV energy to traverse an average molecular diameter of 0.5 nm. The speed of such an electron is ninety eight percent of the speed of light, so it would pass by the molecule in 2×10^{-18} s. The formation of the excited state of the molecule following passage of the fast electron occurs in a time comparable to an electronic oscillation ($10^{-16} - 10^{-15}$ s). This, as recognized by the Franck-Condon principle, is a short time compared to a molecular vibration period ($10^{-14} - 10^{-13}$ s), during which excited molecules will dissociate. Very little is known about the autoionization of excited or superexcited states, but it is thought to be a major source of the ions formed as a result of the radiation of molecules.^{17,36}

At present, the best estimate for the time re-

TABLE I-1

Time Scale for Events in an Irradiated Polar Liquid at
Room Temperature

<u>Time, s</u>	<u>Event</u>
10^{-18}	Fast electron traverses molecule
	Secondary electron traverses molecule
10^{-16}	Excitation or ionization occurs
10^{-15}	Time between successive ionizations along a track
10^{-14}	Autoionization of superexcited states
10^{-13}	Molecular vibration, dissociation of excited states
	Electrons slowed to near thermal energy
10^{-12}	Time between molecular collisions, reactive intermediates makes one diffusive jump
	Electron solvation
10^{-10}	Geminate neutralization occurring
10^{-8}	Spur reactions complete
10^{-7}	Lifetime of solvated electrons in presence of $\sim mM$ reactive solute
10^{-5}	Lifetime of solvated electrons in pure methanol and ethanol

quired for electron solvation is 10^{-12} s. Earlier estimates were about 10^{-11} s, based on the dielectric relaxation time at constant field. However, as solvation proceeds, the electrostatic force rapidly weakens, and there is less relaxation than would occur in a constant field. The shorter relaxation time at constant charge is probably a better approximation, as pointed out by Freeman and Fayadh^{42a}, Schiller^{42b}, and others.^{42c} Hunt and coworkers¹² have reported experimental data indicating that electron solvation is complete in less than 10 ps in water, methanol and ethanol at room temperature. A more recent report by Rentzepis et al^{42d} indicates that electron solvation in water may be complete as early as 4 ps after localization.

Most pulse radiolysis studies using spectrophotometry have observed only the events occurring on a μ s time scale, which includes only the last two entries in Table I-1. Lowering the temperature increases the time for most of the events listed. In low temperature alcohols, the increase may be more than two orders of magnitude in time. The time resolution of optical detection systems is also improving. Faster resolution and low temperatures have enabled optical detection of the occurrence of solvation and of spur reactions.

There is considerable overlap in the times indicated for many of the events. Some may be occurring

over several orders of magnitude in time. The times indicated are those thought to be the most important to a particular event.

4. RADIOLYSIS OF ALCOHOLS

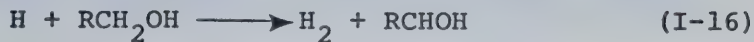
A general, but oversimplified, ionic mechanism for the radiolysis of alcohols ³⁷ is represented by the following reactions. Square brackets indicate that the enclosed species are within a spur.



It is assumed that the positive ions also become solvated.

In the pulse radiolysis of ethanol, reactions (I-7) and (I-10) result in the formation of acetaldehyde, which is an efficient scavenger of electrons, having a reaction rate constant of $4.0 \times 10^9 \text{ M}^{-1} \text{ s}^{-1}$.⁴³⁻⁴⁵ Acetaldehyde is also formed by free radical reactions

(I-16) and (I-17), the total yield being $G \approx 3.7$ ^{43,46}



At a dose of $4 \times 10^{20} \text{ eV} \ell^{-1}$ (about 10 pulses in this work), the acetaldehyde concentration would be $2.5 \times 10^{-5} \text{ M}$ in ethanol. There would then be competition between (I-19) and (I-14) for solvated electrons.



Therefore, frequent sample changes are necessary when irradiating ethanol to avoid as much as possible the occurrence of (I-19).

In the irradiation of methanol, formaldehyde is formed ($G = 2.0$). ⁴⁷ However, formaldehyde is a poor electron scavenger ($k_{I-19} < 10^7 \text{ M}^{-1} \text{ s}^{-1}$ in water) ^{48,49}, so samples may be subjected to many pulses with no observable effect on the solvated electron half-life.

The other major products of the radiolysis of methanol and ethanol are H_2 and the appropriate diol (I-18). Neither of these are electron scavengers.

The e_s^- from (I-13) is what is normally detected optically, although those from (I-9) have also been observed at low temperature in the alcohols. ³⁰⁻³²

C. THE SOLVATED ELECTRON1. HYPOTHESES CONCERNING THE FATE OF NEARLY THERMAL ELECTRONS

Prior to the advent of the pulse radiolysis method, there were two hypotheses as to the fate of secondary (tertiary, etc.) electrons in an irradiated liquid. The Samuel-Magee hypothesis ³⁹ predicted that an electron would lose energy through inelastic collisions with the medium, but fail to escape from the coulombic attraction of the parent positive ion. Geminant recombination would follow, resulting in an excited molecule, which could then split into radicals. Any chemical change in the irradiated system was attributed to the reactions of the radicals. The hypothesis satisfactorily accounted for many of the known facts when applied to the radiolysis of water. The hydrogen atom was considered to be the primary reducing species.

It was suggested by Stein ⁵⁰ and theoretically predicted by Lea ⁵¹, Gray ⁵² and Platzman ^{53,54} that electrons experience quite the opposite fate. The hypothesis assumed that by the time an electron approached thermal energy, it was at least 50 Å from the parent positive ion, and was no longer subject to strong coulombic attractive forces. It therefore polarized the surrounding medium and became a solvated free

ion. Platzman predicted that these electrons would absorb light in the visible region when solvated in water.

The observation in 1962 of a strong absorption of visible light in pulse irradiated water was the first major success of the pulse radiolysis method.⁵⁵ The absorption was ascribed to the solvated electron. There are at least nine pieces of evidence indicating that this was the correct assignment.⁵⁶ Examples of the evidence are: (i) the kinetic salt effect had shown that a reducing species in irradiated water had unit negative charge⁵⁷, (ii) the value for $G(e_s^-)$ agrees well with the best estimates made from steady state radiolysis⁵⁸, (iii) addition of known electron scavengers suppressed the absorption signal, and (iv) the spectrum was similar in shape (but not position) to that obtained in metal-ammonia solutions.⁵⁹ The discovery of the solvated electron confirmed Platzman's prediction, but not the hypothesis. The actual situation in an irradiated liquid must be explained by a combination of the two hypotheses. The Samuel-Magee treatment is more correct in non-polar liquids where free ions comprise five percent or less of the total ionization. However, the more polar the liquid, the higher the free ion yield becomes, exceeding fifty percent of the total ionization in water.

2. THE OPTICAL AND KINETIC PROPERTIES OF SOLVATED ELECTRONS

Since its discovery and identification, the solvated electron has been subjected to intensive scrutiny. Its optical properties ⁶⁰ in water ^{55, 60-63}, methanol ^{30-32, 64-69}, ethanol ^{30-32, 64-71} and a number of other solvents ^{41, 72-75} and solvent mixtures ^{70, 75-77} have been studied. In all solvents in which the solvated electron has been observed, its optical absorption spectrum is a broad ($W_{1/2} = 0.88$ eV in water ⁶³, 1.3 eV in methanol ^{64, 65} and 1.4 eV in ethanol ^{64, 65} at room temperature) structureless ^{63, 71} band. The band is bell shaped on a wavelength scale, but is skewed towards high energies when plotted on an energy scale.

^{63, 65} The molar absorptivity is quite large ($\epsilon_{(\bar{v}_{\max})} = 9.4 \times 10^3 \text{ M}^{-1} \text{ cm}^{-1}$ in ethanol, $10.2 \times 10^3 \text{ M}^{-1} \text{ cm}^{-1}$ in methanol and $18.9 \times 10^3 \text{ M}^{-1} \text{ cm}^{-1}$ in water) making detection of very low concentrations possible. For example, in this work, the concentration of solvated electrons in ethanol at the end of a typical pulse was $1 \mu\text{M}$ (calculated assuming $G(e_s^-)_{\text{fi}} = 1.7$ and absorbed dose = 4×10^{16} eV/ml). In water, and the alcohols, the maximum absorbance occurs in the visible region.

Despite the fact that the solvated electron was the last of the reactive intermediates to be identified, more is now known about it than any other.¹⁷ Several

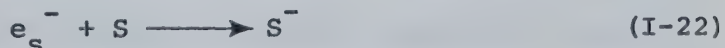
hundred rate constants have been determined for the reaction of the electron solvated in water. A wide variety of solutes have been used, and reported rates vary by nine orders of magnitude. The lowest rate constant which has been determined is for reaction with the solvent itself.



The reported value for k_{I-20} is $16 \text{ M}^{-1} \text{ s}^{-1}$.⁷⁸ However, (I-20) may be more properly written as the unimolecular decomposition (I-21), in which case k_{I-21} is $8.9 \times 10^2 \text{ s}^{-1}$.



The majority of the reported rate constants for the reaction of e_s^- with a solute (I-22) are near the diffusion controlled limit. That is, they are of the order of $10^{10} \text{ M}^{-1} \text{ s}^{-1}$.



The S denotes an electron scavenger.

A comprehensive bibliography of pulse radiolysis of water, covering the years 1960 to 1969⁷⁹, lists nearly 200 papers and 40 review articles^{56, 80-84} and

books.¹⁸ The alcohols have received much less attention as solvents for electrons. Of the alcohols, methanol³⁰⁻
32, 85-88 and ethanol^{30-32,43,44,67,68,88-96} have been used most often. Recent reviews list the data obtained in both the steady state and pulse radiolysis of methanol⁴⁷ and ethanol.⁴⁶ Similar results are often obtained in the alcohols and in water, as is shown in this thesis.

3. THEORETICAL MODELS FOR THE SOLVATED ELECTRON IN POLAR LIQUIDS

Theories for extra electrons in materials were initiated in the treatment of F-centers in alkali-halide crystals, and dilute solutions of alkali metal in liquid ammonia. The former gave rise to the polaron model^{97,98} among others. The latter gave rise to the cavity model.⁹⁹ The ideas advanced in these treatments are incorporated in present theories.

The polaron model suggested a "self-trapping" mechanism for electron localization. The electron, by its presence, was thought to create a potential field due to the polarization of molecules in its locality. No physical cavity was postulated. Such a locality containing an extra negative charge was called a polaron.

A self-trapping mechanism was also postulated for

the cavity model. Here however, a physical cavity containing the electron, surrounded by the positive ends of solvent dipoles, was used to describe the site of electron localization.

It might be thought that these theories are not mutually exclusive. Such was shown to be the case by Jortner ¹⁰⁶, who accomplished a merger of the two viewpoints. The treatment, when applied to the ammoniated electron, was successful in predicting the optical excitation energy and the blue shift in the spectrum with increasing pressure or decreasing temperature. The solvent was viewed as a dielectric continuum.

A further modification used the self-consistent field (SCF) scheme ¹⁰¹ to calculate the transition energy in water. In the SCF treatment, the electronic polarization contributes to the binding energy of the electron.

Semicontinuum models ¹⁰²⁻¹⁰⁵ recognize the molecular nature of the solvent surrounding the localized electron. These models have had some success in correlating spectral properties. Beyond a solvation shell, often taken to be four molecules, the liquid is regarded as an isotropic continuous dielectric.

Several treatments have made use of a molecular approach, where electron localization is considered only on the basis of electron interaction with a limited

number of solvent molecules. Dimers ¹⁰⁶ and tetramers ¹⁰⁷ have been considered. An extension of these treatments is the stabilized cluster model. ¹⁰⁸

The various ideas have been discussed and reviewed. ¹⁰⁹⁻¹¹⁴ It is agreed that no single model yet proposed is able to satisfactorily correlate all of the experimental data, even in a single solvent. Finding a quantitative explanation for the width of the solvated electron optical absorption spectrum has proven to be particularly difficult.

More experimental data against which model calculations could be tested are required. In particular, data which are obtained under the variation of temperature and pressure would assist in further theoretical development.

D. THE VARIATION OF PRESSURE

There have been very few reports of pulse radiolysis of liquids at high hydrostatic pressures. Of the studies presented until now, all but one ¹¹⁵ used water as the solvent. ¹¹⁵⁻¹¹⁹ More use of pressure has been made in steady state radiolysis, both with water ¹²⁰⁻¹²³ and alcohols ¹²⁴⁻¹²⁶ as solvents. However, even these reports are not numerous, and come from only two laboratories.

As noted by Laidler ¹²⁷, pressure studies provide at least as much insight into mechanisms as do temperature studies. This should be particularly true of solvated electrons, in view of the cavity model.

According to present theories, increase in pressure should result in a blue shift (to higher energy) of the solvated electron optical absorption spectrum. This would arise as a result of, among other things, compression of the cavities in which the electrons are localized. This effect has been observed for pulse irradiated water ¹¹⁵⁻¹¹⁹ and ethanol ¹¹⁵, dilute alkali metal ammonia solutions ¹²⁸ and F centres in alkali halide crystals. ¹²⁹ Also, the effect of pressure on the yield of solvated electrons might provide data which indicate whether cavities suitable for electron solvation pre-exist, or are created by the electron itself. Pressure would be expected to affect yields more in the former case through destruction of the necessary cavities. It seems apparent that pressure variation could be used to provide data which would test models presently available.

The effects of pressure on the solvated electron reaction kinetics would also provide valuable data for use in postulating mechanisms. Changes in reaction rates due to pressure change are generally expressed in terms of the volume of activation (ΔV^\ddagger), which is the

change in volume in passing from the initial state to the activated state.

$$\Delta V^\ddagger = -RT \left(\frac{\partial \ln k}{\partial P} \right)_T \quad (I-23)$$

In (I-23), k is the rate constant determined at the pressure P . The equation shows that ΔV^\ddagger is negative when increasing the pressure increases the rate constant. That is, when the activated state occupies less volume than the initial state, then pressure favours the lower volume state. The opposite is true when ΔV^\ddagger is positive, which means that the initial state has a smaller volume than the activated state. Increasing the pressure then inhibits the volume increase necessary to reach the activated state. Application of Le Chatelier's principle results in the same conclusions.

Interpretation of volume of activation data must include two effects. First is the change due to structural factors of the reactants themselves as they enter the activated state, which should be of minor importance in solvated electron reactions. The second is the volume change resulting from reorganization of the solvent molecules. This should be larger and mainly due to electrostriction.

It would also be interesting to see how pressure effects differ from temperature effects for similar

changes in solvent properties such as density and dielectric constant⁶⁵, since these properties have been used in attempts to correlate different sets of data obtained in studies of the solvated electron.

E. THE VARIATION OF TEMPERATURE

A great many chemical reactions adhere to the Arrhenius law expressed in (I-24).

$$k = Ae^{-E_a/RT} \quad (I-24)$$

A is the frequency factor and has the same units as the rate constant, k.

E_a is the activation energy

To test the law for a particular reaction, data must be obtained at different temperatures. Conformity to the law is indicated if a plot of $\ln k$ versus $1/T(K)$ is linear. The value of E_a is determined from the slope of the plot.

From the standpoint of this law, it is necessary to understand the activation energy and frequency factor in order to be able to understand the factors which determine the rate constant. Information about the activation energies for solvated electron reactions would assist in achieving a better understanding of the reaction mechanisms.

Most of the reported values of E_a for solvated electron reactions were obtained with water as the solvent. Under normal conditions, this restricts the range of possible temperature variation to less than 100°C. A number of the first activation energies determined were near 3.5 kcal mol⁻¹. This led to speculation that the lowest activation energy possible for solvated electron reactions in water was the same as that for diffusion in water¹³⁰, which is 3.5 kcal mol⁻¹. This was disproved when values for E_a as low as 1.7 kcal mol⁻¹ were measured.¹³¹ New theories about the diffusion mechanism of solvated electrons in water were necessary. It was suggested that hydrated electrons may diffuse by migrating between existing potential traps instead of through creation of new holes, as in conventional diffusion.¹³²

The effects of changing temperature on the optical absorption spectrum of solvated electrons can also yield valuable data.^{41,65,133,134} Low temperature pulse radiolysis of alcohols has given a greater insight into the electron solvation process. Baxendale and Wardman³⁰⁻³² found that the solvated electron spectrum is very time dependent. Initially there was a structureless absorption rising steadily from 350 nm to 1,350 nm. It resembled the spectrum found for trapped electrons in hydrocarbon glasses. It was postulated that the

spectrum resembled that found in a medium of low dielectric constant because the solvent had not yet reacted to the presence of the charge. This spectrum decayed rapidly ($t_{1/2} = 3$ ns in ethanol at 166K) in the infrared with a simultaneous growth in the known "long time" visible absorption spectrum. Within several hundred ns, no further change in the spectrum shape could be observed. The subsequent slower change was only in intensity, and was due to reaction of the solvated electrons.

Solvation times for electrons were estimated from the decay of the near infrared absorption. With these data, and those of Hunt and coworkers ¹² obtained at room temperature, an activation energy of 4-5 kcal mol⁻¹ was estimated for the solvation of the electron. Knowledge about the energy of activation is helpful in understanding how solvation begins. For example, it is estimated that the breaking of hydrogen bonds in the alcohols requires an activation energy of 4-5 kcal mol⁻¹, and this may therefore be rate determining in the solvation process.

The variations of both temperature and pressure are valuable aids in obtaining data for testing theories and postulating mechanisms. The role of physical properties of the solvent can be elucidated by comparing the results from pressure and temperature variations which had a similar effect on the particular solvent property.

F. THE OBJECT OF THE PRESENT WORK

When this work began, very few data were available concerning the pulse radiolysis of alcohols at other than ambient temperature and pressure. The effect of temperature on the e_s^- optical absorption spectrum had not been fully investigated.⁶⁷ Information was especially lacking about temperature effects on the scavenging or decomposition reactions of solvated electrons in alcohols. The wide liquid range of methanol and ethanol made these solvents especially good media for obtaining activation energies.

No kinetic data had been obtained in the pulse radiolysis of alcohols at high pressure. The optical data were limited to a single publication.¹¹⁵ Results from γ and pulse radiolysis of water at high pressures, even though incomplete and sometimes contradictory, were proving useful in postulating mechanisms and testing models. Data from the alcohols would be equally valuable. It was therefore undertaken to determine temperature and pressure effects on the solvated electron optical and kinetic properties in methanol and ethanol.

Reaction rate constants for (I-22) were determined for a number of gaseous solutes in the solvents water, methanol and ethanol. This work was first deemed necessary because the rate constants for the reaction of solvated electrons with N_2O or SF_6 were not known in

the alcohols. These gases are frequently used as electron scavengers in competition kinetics, and knowing their rate constants would allow rate constant ratios to be solved. When a technique for rapid sample preparation was developed, the study was expanded to include seven other gases.

It is hoped the work reported in the following chapters will contribute eventually to a more complete understanding of the solvated electron and its reactions.

E X P E R I M E N T A L

A. MATERIALS

1. SOLVENTS

a. Water

Water was always freshly triply distilled from a Pyrex system and collected in a quartz receiver. The second distillation was from alkaline potassium permanganate solution.

b. Methanol

Sources of methanol were:

- (1) Baker Chemical Company, Reagent Spectrophotometric Grade,
- (2) Fisher Scientific Company, Certified A.C.S. Spectroanalyzed,
- (3) Monsanto Company, Commercial Grade.

Typical impurity levels reported by Monsanto were 5 ppm carbonyl, 20 ppm acid and 70 ppm water. The best Fisher methanol was of similar purity and that from Baker was less pure, as indicated by the solvated electron lifetime in each.

Routine purification was therefore carried out in an apparatus constructed of Pyrex with grease free ground glass joints. A slight positive pressure was maintained in the system by a continuous flow of Ultra High Purity (U. H. P.) argon which could only escape

through U-tubes containing mercury. Sulphuric acid (1.0 ml/litre of alcohol) and 2,4-dinitrophenylhydrazine (1.5 gms/litre of alcohol) were added to the methanol. The solution was gently refluxed for at least eight hours, then slowly distilled through a one meter column packed with glass helices. Receivers were rinsed several times with fresh distillate before being used to collect the middle fraction.

An alternative purification used the same apparatus and methods, but the methanol was treated from a solution containing sodium (1 gm/litre) and sodium borohydride (1 gm/litre).

Both methods yielded a nearly odorless product in which the solvated electron lifetime had been similarly increased. Distillation from acid media in the first method precludes the increased electron lifetime being due to contamination by base. Gas chromatographic analysis showed that neither method increased the water content within the detection limit of 500 ppm.

Treated methanol was stored under U.H.P. argon in Pyrex flasks with stoppers wrapped in Parafilm "M". No deterioration in purity occurred over several months at room temperature.

c. Ethanol

Absolute-Reagent Grade ethanol was obtained from

the U. S. Industrial Chemical Company. Experience had shown this to be the best available,⁴⁴ having reported maximum impurity levels of 50 ppm water, 5 ppm methanol, and less than 1 ppm benzene, halogen compounds or carbonyl compounds. Treatment by either of the purification methods used with methanol resulted in no improvement or even a decrease in purity.

Contact with oxygen or moisture had to be avoided. This was accomplished by fitting the ethanol bottle with a Pyrex syphon and applying several pounds of U.H.P. argon pressure. Alcohol could be obtained by opening a Teflon stopcock on the syphon tubing.

2. SOLUTES

a. Solid Compounds Used as Solutes

	<u>Solute</u>	<u>Supplier</u>
(1)	biphenyl	Matheson, Coleman and Bell
(2)	cadmium chloride	Baker Chemical Company
(3)	naphthalene	Eastman Organic Company
(4)	phenol	B.D.H. Chemicals Limited
(5)	potassium hydroxide	Fisher Scientific Company
(6)	sodium	B.D.H. Chemicals Limited
(7)	sodium hydroxide	Fisher Scientific Company

All solid additives were of reagent quality. Some received the following treatment before use.

- (1), (3) Sublimed under vacuum
- (4) Melted under vacuum in a modified sublimation apparatus. Sodium-potassium alloy was then added with vigorous stirring. After reaction was complete, phenol was sublimed, then transferred to the stock solution under an atmosphere of U.H.P. argon.
- (5), (7) Only translucent pellets free of carbonate spots were used
- (6) Fresh metal surfaces were obtained by cutting under n-hexane. The metal was then dried in a stream of U.H.P. argon and rapidly transferred to the solvent.

b. Liquid Compounds Used as Solutes

	<u>Solute</u>	<u>Supplier</u>
(1)	acetone (spectro A.C.S.)	Eastman Organic Company
(2)	acetonitrile (spectroquality)	Matheson, Coleman and Bell
(3)	acrylonitrile	B.D.H. Chemicals Ltd.
(4)	benzene (research grade)	Phillips Petroleum Company
(5)	1,3-cyclohexadiene (99%)	Chemical Samples Company
(6)	ethyl acetate (spectroquality)	Matheson, Coleman and Bell
(7)	nitrobenzene	Fisher Scientific Company
(8)	perchloric acid (70 wt. %)	Baker and Adamson
(9)	toluene	Fisher Scientific Company

(10) trimethyl borate	Stauffer Chemical Company
(11) o-xylene (99.9%)	Chemical Samples Company

Liquid additives were of reagent quality except where otherwise indicated. They were used as received with the following exceptions:

- (4) (9) (11) Vacuum degassed in a grease free system, then distilled onto sodium-potassium alloy and stirred at room temperature overnight. The final distillate was collected in 10 ml Pyrex bulbs and sealed under vacuum.
- (5) (7) (10) Distilled in an atmosphere of U.H.P. argon, only the middle fraction being retained.

c. Gaseous Compounds Used as Solutes

	<u>Solute</u>	<u>Supplier</u>
(1) argon (U.H.P.)		Matheson Company
(2) 1,3-butadiene		Phillips Petroleum Company
(3) carbon dioxide (99.5%)		Matheson Company
(4) ethylene		Phillips Petroleum Company
(5) ethyne (99.8%)		Matheson Company
(6) nitrous oxide (98.5%)		Matheson Company
(7) oxygen (99.95%)		Alberta Oxygen Ltd.
(8) sulphur hexafluoride (99.8%)		Matheson Company

Gases obtained from Phillips Petroleum Company were research grade, and were used as received. Others were treated in the following ways:

- (1) Argon was run through a column of Labor-Absorber Oxisorb "G" obtained from Messer Griesheim GMBH Industriegase. This was to remove the 2-3 ppm of oxygen the argon was reported to contain.
- (3) (7) (8) The gas was bubbled through two "scrubbers" containing triply distilled water, then through a trap held at 266K by an ice-salt bath, before use.
- (5) The same as for (3) with the addition prior to the scrubbers of a trap held at 210K by a chloroform slush bath.

d. Miscellaneous Compounds

	<u>Compound</u>	<u>Supplier</u>
(1)	acetaldehyde (Research grade)	Eastman Organic Chemicals
(2)	chloroform	Mallinckrodt Chemical Works
(3)	2,4-dinitrophenylhydrazine	Eastman Organic Chemicals
(4)	ferrous ammonium sulphate	Mallinckrodt Chemical Works
(5)	helium	Canadian Liquid Air
(6)	n-hexane (99 mole %)	Fisher Scientific Company

(7) nitric acid	Baker Chemical Company
(8) potassium	B.D.H. Chemicals Ltd.
(9) potassium permanganate	B.D.H. Chemicals Ltd.
(10) potassium thiocyanate	Fisher Scientific Company
(11) sodium borohydride (98%)	American Drug and Chemicals Co.
(12) sodium chloride	B.D.H. Chemicals Ltd.
(13) sulphuric acid	Canadian Industries Ltd.

All were used as received and where purity is not indicated, they were of reagent quality.

B. APPARATUS

1. THE SAMPLE CELLS

Cells of Suprasil quartz from Pyrocell Manufacturing Company were used at atmospheric pressure. They were of 1.0 x 1.0 x 4.5 cm inside dimensions giving a cell volume of 4.5 cm³. Two opposite faces were frosted, and the cell was topped by a graded seal so that it could easily be attached to Pyrex glass tubing. Different cell designs are illustrated in Figure II-1.

Cells of type (a) were used for samples containing solid or liquid solutes for irradiation at room temperature or above. The Pyrex No. 7782 Teflon stop-cocks (Canadian Laboratory Supplies Ltd.) provided a good seal and could be closed rapidly. These cells

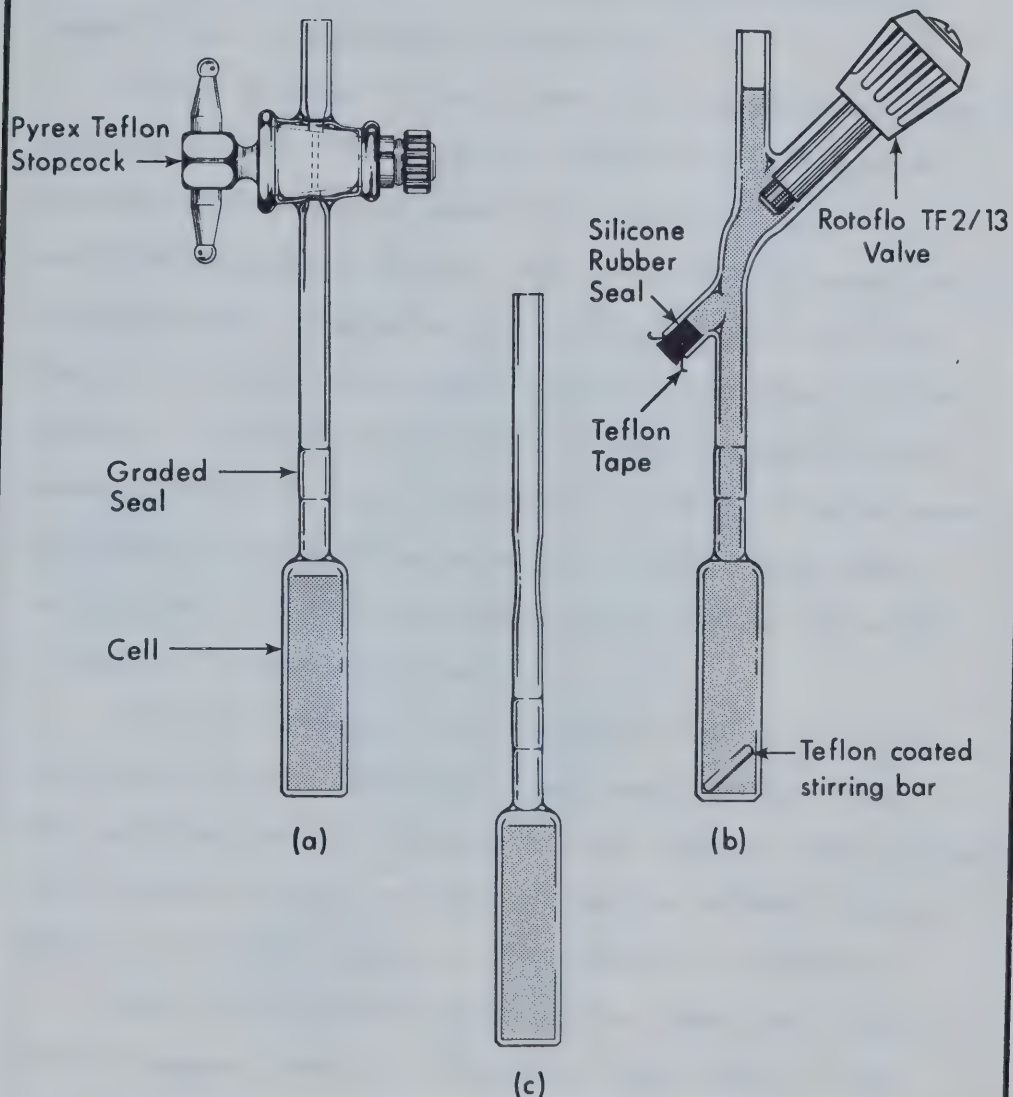


FIGURE II-1. Suprasil Quartz Optical Cells.

could not be used at low temperature due to air leaks at the stopcock. Cells of type (b) were used for irradiation at low temperatures. The technique for sealing these cells is described on page 71.

Cells of type (c) were used for samples containing a gaseous solute. The silicone rubber seal was soaked in ethanol before use to leach out soluble compounds. It was then wrapped in Teflon tape to further prevent sample contamination. Agitation of a Teflon coated stirring bar (1/8" x 1/2") included in the cell assured uniform mixing. A Rotoflo TF2/13 Teflon valve (Canadian Laboratory Supplies Ltd.) was used to provide a large opening during sample de-oxygenation. Cell volumes were calibrated from the weight difference before and after filling with absolute ethanol.

The high pressure cell shown in Figure II-2 was fabricated in the chemistry department machine shop. The cell body of 410 stainless steel was not heat treated. The electron window cap and the optical window caps of 416 s.s. were heat treated to 36 Rockwell C hardness.

The optical windows of sapphire (American Instruments Company, part No. A4-62065) were fixed to the caps with a very thin layer of Elmer's epoxy (The Borden Chemical Company). These windows could withstand working pressures in excess of seven kilobars.

The electron window was fabricated of Vascomax

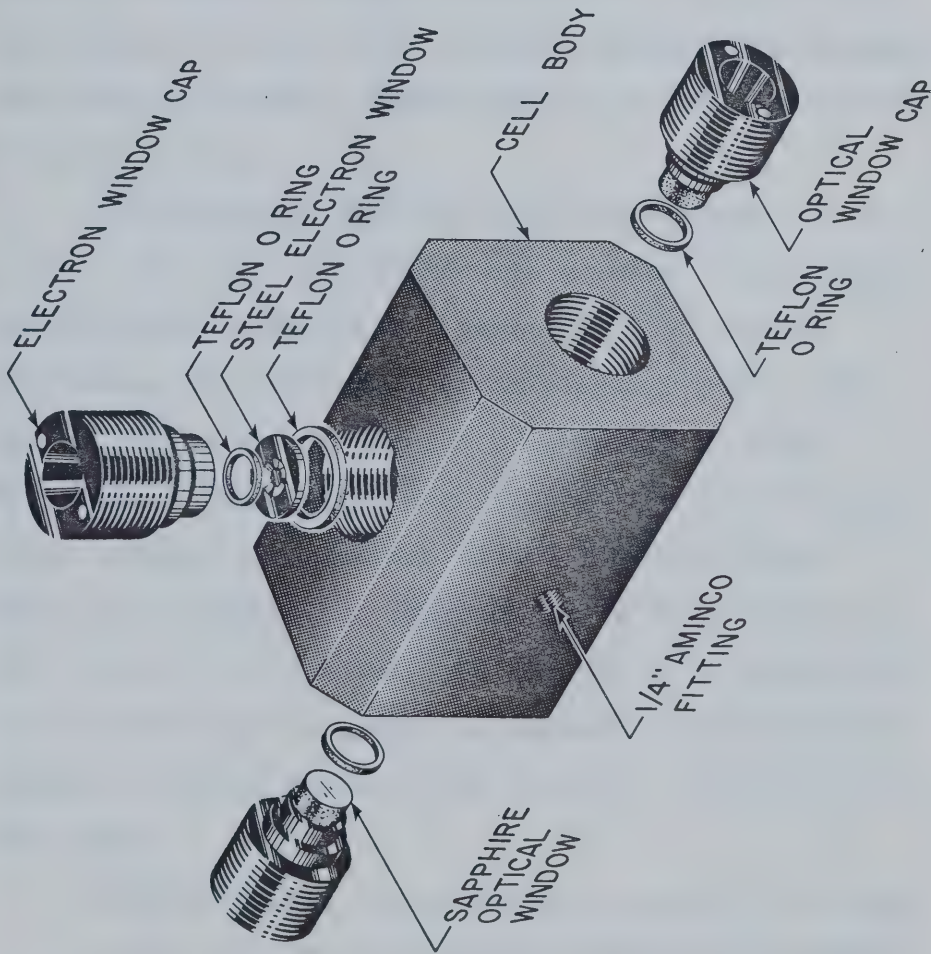


FIGURE II-2. The High Pressure Optical Cell

Maraging steel hardened to 57 Rockwell C. The 2 MeV electron beam penetrated a thickness of 0.028 inches of this steel, which withstood pressures of greater than three kilobars in tests. Electron windows of 0.032 inches thickness further attenuated the electron beam by a factor of two. Many pressure cycles work hardened the electron window, necessitating periodic replacement to avoid failure.

As protection against unexpected failure of the window, the cell was fitted with a rubber lined steel shutter which opened for a period of 1.25 seconds, bracketing the occurrence of an electron pulse. The rubber lining was to prevent ricocheting of metal particles. The shutter was fixed to the cell body and fully covered the electron window cap when closed. Power was necessary to overcome the spring tension on the solenoid and maintain the shutter in a closed position. There was therefore no magnetic field from the shutter solenoid while it was open for a fast absorption experiment.

Teflon O-rings (Crane Packing Company) were used to seal cell caps to the body and the electron window to the electron window cap. It was found that Buna N O-rings could not be used in contact with alcohol because of sample contamination. In some cases, Viton A O-rings could be used.

Analyzing light passed through 2.8 cm of solution. The thinned portion of the electron window was 0.90 cm in diameter. Only solution behind this thinned portion received radiation, making the effective light path 0.90 cm.

A small amount of Loc-Lube (Burrell Corporation) was used on the cap threads to prevent their fusing to the cell body under high pressure.

2. THE OPTICAL DETECTION SYSTEM

A schematic diagram of the path of the analyzing light is given in Figure II-3. The source was an Osram XBO 450 W xenon arc lamp contained in an Oriel Optics Corporation lamp housing (model C-60-50). A Perspex filter was usually placed in the lamp housing to filter out ultra-violet light. Power to the lamp was provided by the very stable SRL 40-50 Sorensen power supply obtained from Raytheon Company. Lamp noise was \pm 0.25% of the light output at 600 nm. At least one third of this noise was due to vibration caused by the cooling fan motor. A large part of the remainder was due to mirror vibration.

A light shutter protected the sample from unnecessary exposure. This was important for low temperature samples to prevent warming. The shutter could be remotely controlled manually or automatically. In automatic operation it opened for 1.25 seconds.

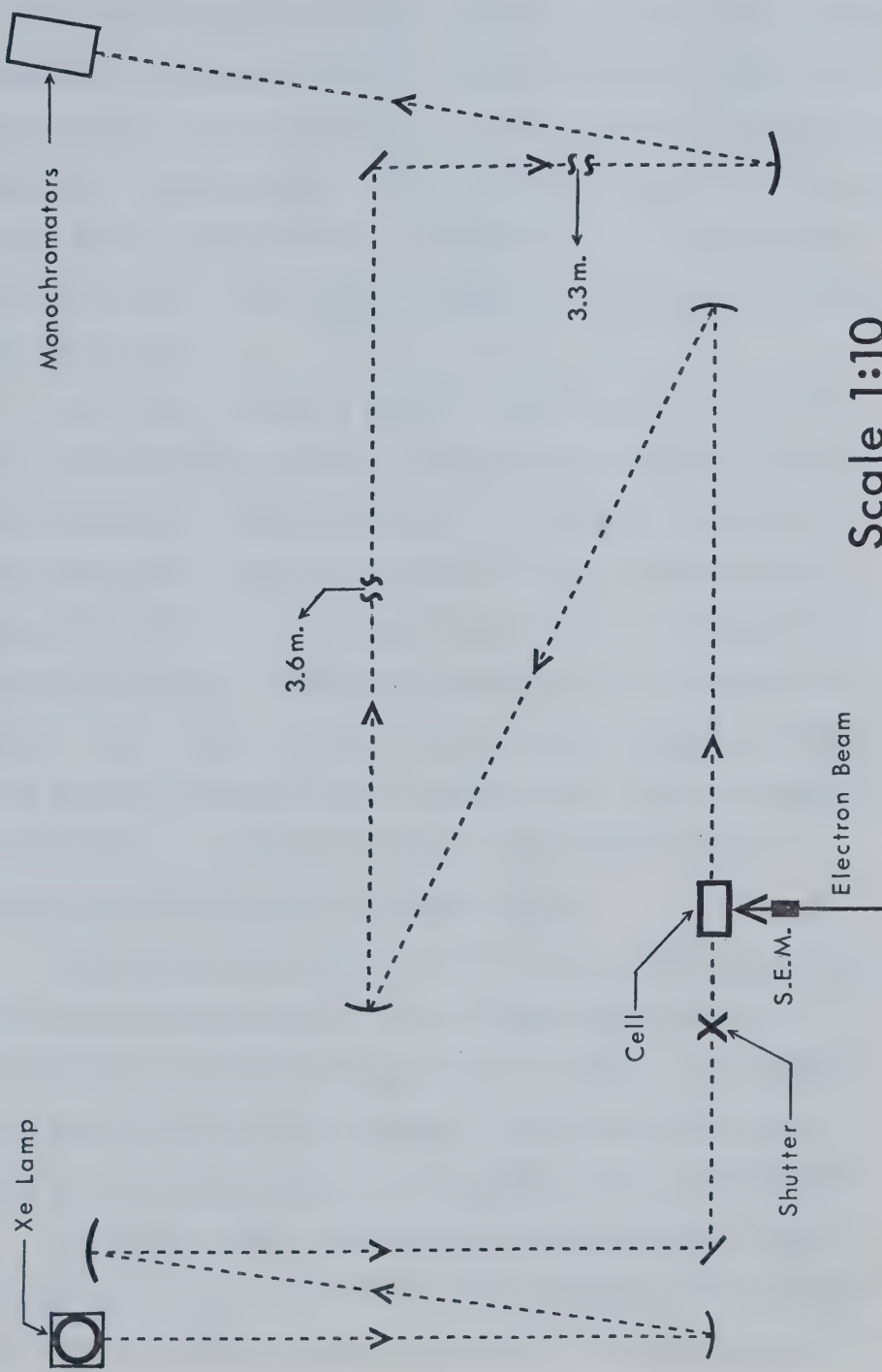


FIGURE II-3. The Optical Detection System

Front surface aluminum mirrors coated with silicone monoxide were used to direct the light beam, focus it at the centre of the irradiation cell, and then render it parallel. In this way the light was transported from the irradiation room through a hole in the 1.2 meter thick concrete wall. Total path length of the optical system was 15 meters.

The final concave mirror could be swung such that the light was focussed on either of two Bausch and Lomb monochromators (model 33-86-25). The one normally in use contained a number 33-86-02 grating (350-800 nm). Entrance and exit slits were set to give a bandpass of 10 nm at 500 nm. The grating scale was calibrated at 404.7, 435.8, 546.1 and 577.0 nm using a mercury lamp from Pen-ray Ultra Violet Products Inc. It was checked periodically at 632.8 nm with a He-Ne gas laser (University Laboratories, model 240).

Wavelength settings could be advanced either manually or automatically in preset increments using a Slow-Syn Synchronous/Stepping Motor (model TS25-1009) from Superior Electric Company. Wavelength was read from a digital display calibrated to the grating scale.

The photodiode detector and the amplifier were housed in a brass box which made a light tight seal to the exit slit of the monochromator. The SGD-444-2 photodiode was supplied by EG & G Incorporated, and

had a spectral range (10% points) from 350 nm to 1,130 nm. Maximum spectral response occurred at 900 nm where the sensitivity was typically $0.5 \mu\text{A}/\mu\text{W}$. Response was linear over seven decades of incident power.

Amplifier response from the absorption channel is illustrated in Figure II-4. Rise time (10-90%) of the detector and amplifier was 52 nanoseconds as shown in the inset to the figure. Rise time of the amplifier alone was 29 ns. Resistance gain of the absorption channel was $460 \text{ K}\Omega$.

The incident light channel measured d.c. light level and had a gain 11.1 times smaller than the absorption channel. This difference in gain is referred to as the amplifier factor. It was determined by measuring the simultaneous output from each channel of an input signal from a rapidly pulsing light emitting diode (Hewlett-Packard, model 5082-4400).

Incident light was recorded as a voltage on a Hewlett-Packard model 3440A digital voltmeter, and was typically from one to five volts. Absorption signals were recorded as voltages on an oscilloscope cathode ray tube (CRT). Tektronix 549, 7704 or 7623 oscilloscopes equipped with the appropriate plug-ins were used. Each CRT trace was photographed for later analysis using a Polaroid Model C12 camera and type 47 or 410 Polaroid Land film.

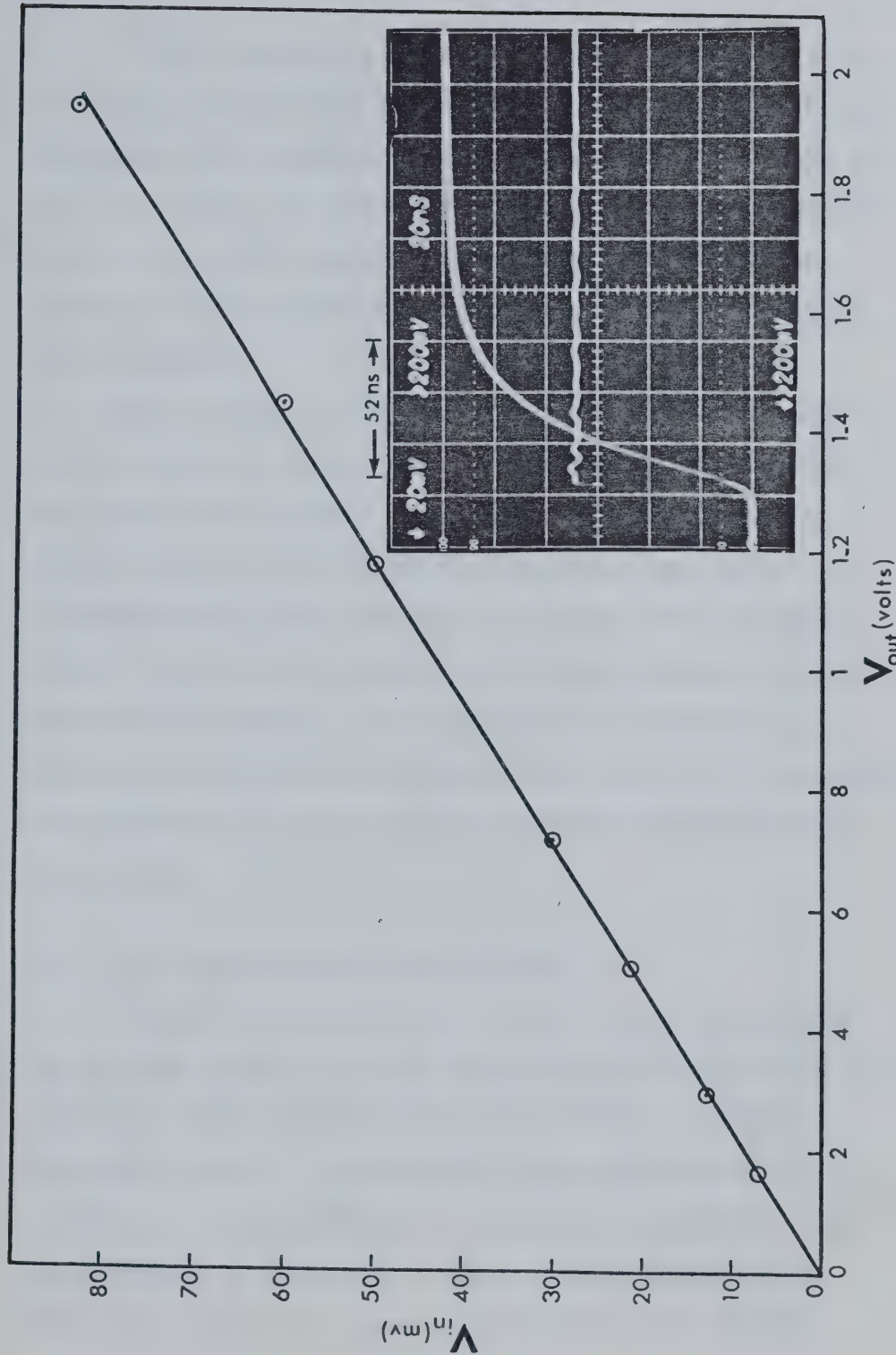


FIGURE III-4. The Amplifier Linearity and Rise Time

Rise time of the total measurement system was 70 ns. Use of the 5 MHz filter on the 7A13 plug-in of the Tektronix 7623 oscilloscope increased this rise time to 100 ns. Where the added rise time was not important the filter was used. Oscilloscope traces then had less noise, so the photographs could be analyzed more easily and accurately.

For in situ Fricke dosimetry, a different measurement system was used. The Perspex filter was removed from the lamp housing. The second monochromator was fitted with a 33-86-01 grating (180-400 nm) and a 1P28 photomultiplier (General Electric) with its amplifier. The response time of the 10 mM ferrous ion dosimeter was 3 seconds. The signal was recorded by a model 1062 instrument computer from Fabri-Tek Instruments Incorporated. Polaroid photographs of the CRT traces were taken.

3. THE TEMPERATURE CONTROL SYSTEM

Temperatures from 296K to 150K could be achieved by boiling liquid nitrogen at a controlled rate from a 50 litre, wide necked steel Dewar vessel (Sulfrian Cryogenics Inc.). A poly-vinyl chloride pipe (2.5 inches i.d.) extended to the bottom of the Dewar. It was notched at the base to allow liquid nitrogen to flow in, and it was fixed to a lid which fit snugly to the neck of the Dewar. The system could be filled

with liquid nitrogen while in use through a hole in the lid. A 1000 watt nichrome wire coil was attached inside the P.V.C. pipe about 7 cm from the bottom.

Cold nitrogen gas was transported to the sample box through one meter of brass pipe (0.5" i.d.). The pipe was insulated by a layer of sponge rubber tubing (0.625" i.d. x 0.5" wall) and a layer of Styrofoam 3 cm thick.

Temperatures from 296K to 370K were obtained using hot air from a modified laboratory heat gun (Master Appliance Corporation, Model HG-501L). Current to the element and the fan motor could be individually controlled. The fan speed was controlled by manually setting a Variac. Hot air travelled 45 cm through uninsulated brass tubing (0.5" i.d.) to the sample box.

Current to the nichrome element in the Dewar and the heat gun element was provided by an Ohmite "V.I." Variac (0-120 V, 25 amps) from Ohmite Manufacturing Company. It was controlled by a two mode controller from API Instruments Company. The voltage setting on the Variac depended on the temperature desired. Too high a setting would result in rapid cooling. The controller could not then respond fast enough, resulting in overcooling. Equilibration at a desired temperature could be achieved more rapidly with gradual cooling.

Optical cells were held snugly on three sides

by a one piece blackened-brass holder. A steel spring which assured accurate cell position formed the fourth side of the holder. An adjustable slit, usually set at 0.3 x 2.5 cm, was attached to the side of the holder.

The holder was fixed in a Styrofoam box of 12 x 12 x 27 cm outside and 7 x 7 x 17 cm inside dimensions. To minimize spreading of the electron beam the Styrofoam was thinned from the outside directly in front of the cell. Analyzing light entered and left the box through evacuated Suprasil quartz windows (2 x 2 cm) press fitted into the sides of the box. At temperatures below 240K it was necessary to blow dry air on the windows to keep the outside surface frost free.

Heating or cooling gas entered at the bottom of the box and was deflected to force it to circulate before leaving through a 30 cm high insulated chimney in the lid. Maximum temperature was limited to 370K because of distortion of the Styrofoam at higher temperatures.

Temperature measurements were made using copper-constantan thermocouples.¹³⁵ Initially they were calibrated in slush baths at 113 K (iso-pentane), 175K (methanol), 210K (chloroform), 250K (carbon tetrachloride), 273K (ice-water), and 371K (boiling water). Later, because of their reliability, thermocouples were only checked against each other at room temperature

and 273K.

Two thermocouples were attached to the brass cell holder and one to the cell using G.E. RTV silicone rubber adhesive. Miniature thermocouple connectors (Thermo Electric (Canada) Ltd.) were used to connect the thermocouples to the voltage measurement system. A millivolt potentiometer (Leeds and Northrup Co., Cat. No. 8686) provided sensitive voltage measurement.

Temperature equilibrium in the system was assumed to exist when all three thermocouples indicated the same ($\pm 1^{\circ}\text{C}$) for a period of five minutes. Once equilibrium was achieved the temperature could be maintained indefinitely.

The sample box was fitted with two pieces of square steel tubing ($0.5 \times 0.5 \times 4"$) in which samples could be placed for pre-cooling. The tubing protected the samples from radiation and the pre-cooling speeded return to temperature equilibrium after a sample change.

4. THE HIGH PRESSURE SYSTEM

Figure II-5 shows the high pressure system which was built for both direct and remote operation. The air driven fluid pump (Haskel Engineering and Supply Co., 600 to 1 pump ratio, 75,000 psi rated) was run

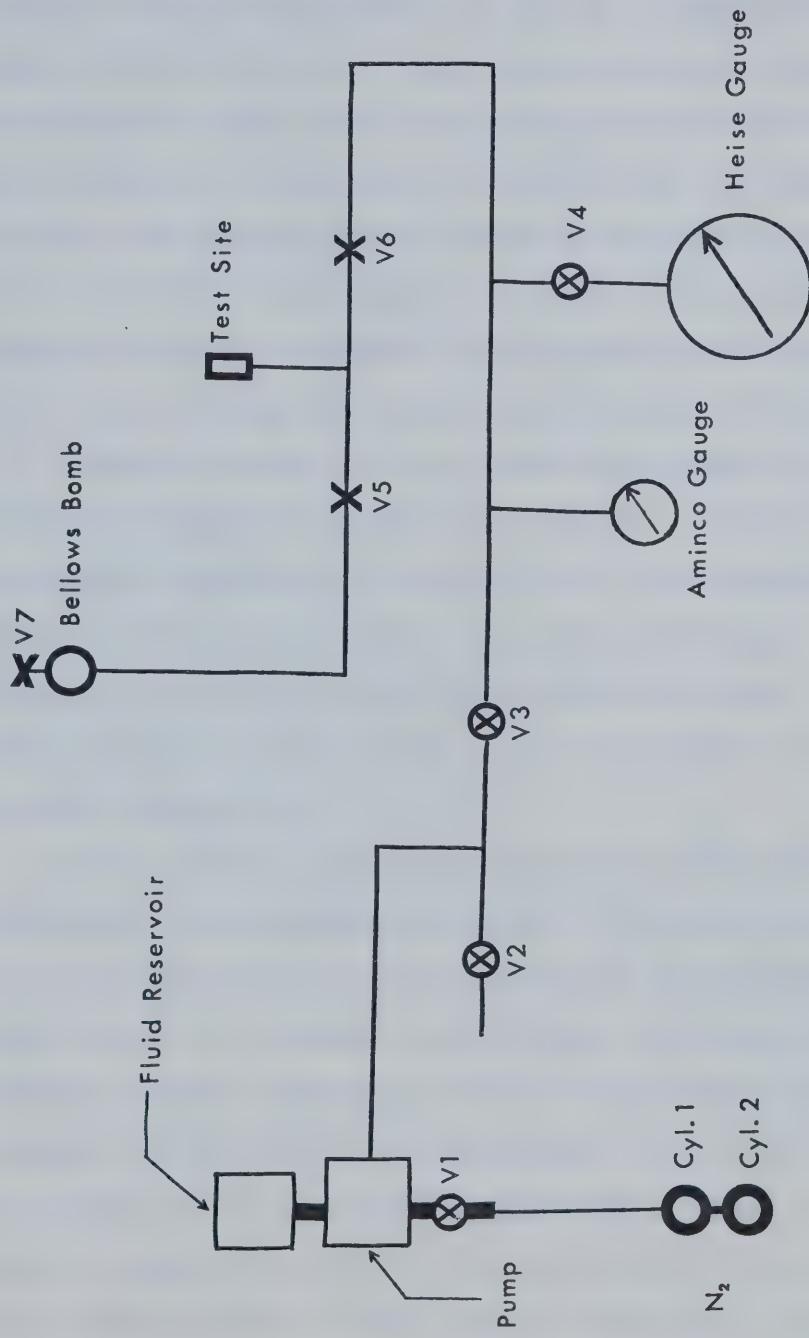


FIGURE II-5. The High Pressure System

on nitrogen gas (Liquid Carbonic Canadian Corporation).

Cylinder 1 was maintained at 60 psi by a regulated supply from cylinder 2. Smooth pump operation required this ballast volume, and restricting it to 60 psi ensured against pressurizing the system over 2.6 Kbar.

Gas flow for pump operation could be controlled remotely by a valve (VI) fitted with a Slow-Syn driving motor (Superior Electric Company). The pressurizing fluid was a low viscosity oil (Bayol 35, Imperial Oil Co.).

Manifold valves V2 to V7 were from American Instrument Company (100,000 psi, Cat. No. 44-19115) as were the associated fittings (1/4") and connecting tubing (316 Stainless Steel, 100,000 psi rating). Valves V2 to V4 were fitted with Slow-Syn motors. The system could be depressurized either manually at V7 or remotely through V2.

Obtaining the same pressures during different experiments was sometimes necessary. The pump could not usually be stopped in mid-stroke, so some pressure often had to be released. Due to the very small fluid volumes involved, opening a valve to atmosphere released pressure too quickly to be controlled. This problem was solved by use of a "controlled leak" which could be installed at V2. The leak was made from an Aminco high pressure union (Cat. No. 45-12957). A

short piece of 1/4" steel rod was prepared the same as high pressure tubing would be. A very shallow file mark was then made on the rod where it made the metal to metal seal with the union. Tightening the gland nut set the leak rate along the file mark.

A factory calibrated 100,000 psi Heise gauge was used to measure system pressure. The gauge was viewed on a closed circuit television monitor during remote operation. For pressure tests a more rugged 80,000 psi Aminco gauge was used. Access for pressure tests was provided between valves V5 and V6.

Isolation of the pressurizing fluid from sample solutions was accomplished using the bellows bomb shown in Figure II-6. The bomb was fabricated in the chemistry department workshop from Ultimo 200 steel, heat treated after machining and then pressure tested to 4.3 kb. The stainless steel metal bellows (Metal Bellows Corporation) was silver soldered to a hardened 416 S.S. plug. Bellows assemblies were leak tested under vacuum with a helium leak detector. The plug to bomb seal was made with a -218 Buna N O ring.

The bellows bomb was mounted directly above the high pressure cell, the cell and bellows assembly being joined by 15 cm of high pressure tubing.

Failure of the pressure system on the sample

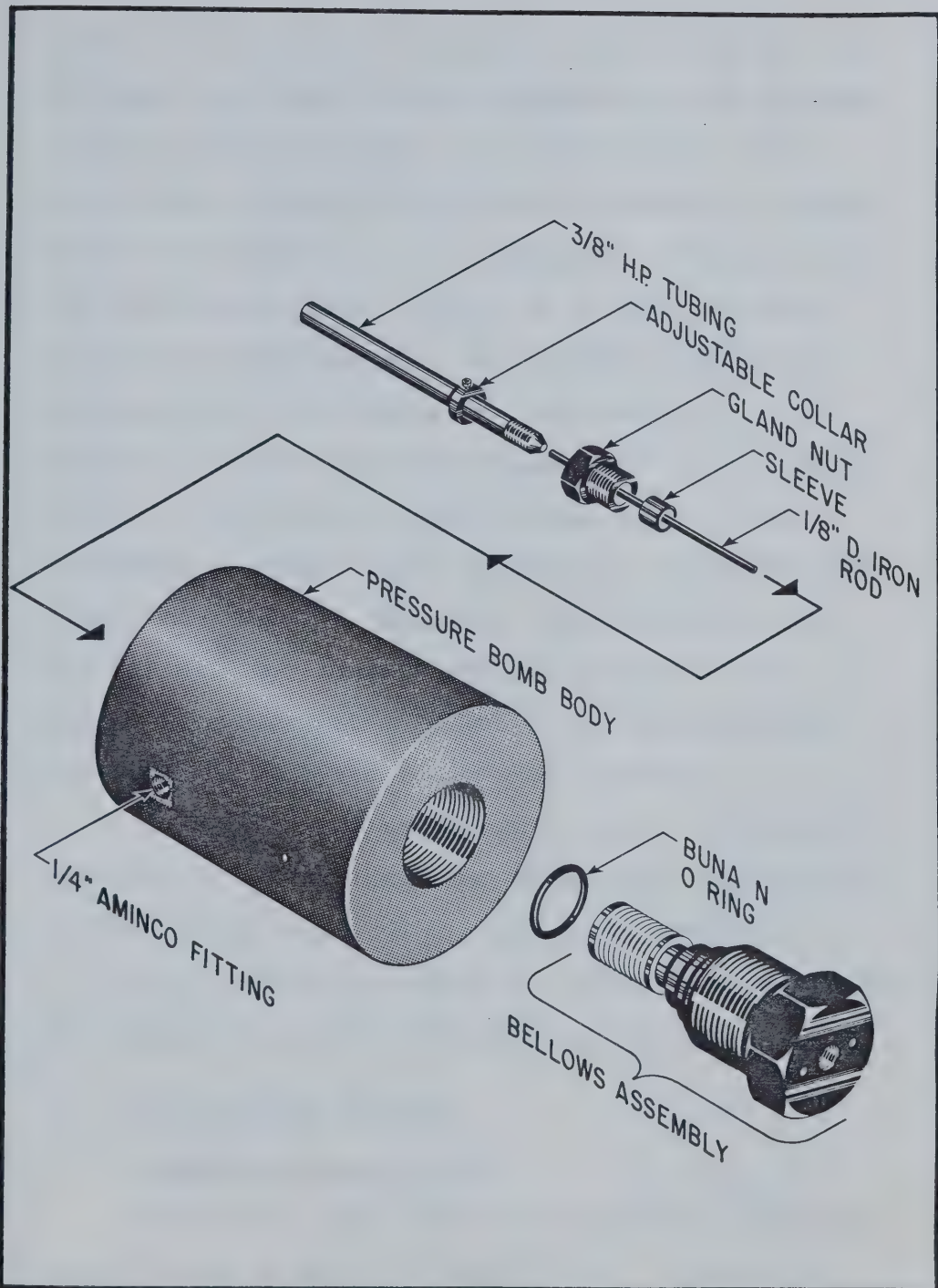


FIGURE II-6. The High Pressure Bomb and Bellows Position Indicator

side of the bellows or incomplete filling of the high pressure cell could result in destruction of the bellows by over-compression. To guard against this a device was designed to indicate the amount of compression of the bellows. The compression indicator used the inductance change created as an iron rod moved through the windings of a transformer to produce a deflection on a microammeter. The rod (1/8" x 6") rested on top of the bellows assembly, and could move freely up and down in the stainless steel barrel illustrated in Figure II-6. Electronic components were housed in two metal cabinets, one of which fit over the barrel. Moving this cabinet up and down the barrel by adjustment of a collar set the stroke of the iron rod into the transformer windings.

The indicating microammeter was in the second cabinet. It was set near the Heise gauge such that it could also be viewed on the television monitor.

The circuitry designed and built by the chemistry department electronics shop is shown in Figure II-7.

5. THE BUBBLING SYSTEMS

a. Samples in Quartz Cells

The U.H.P. Argon bubbling manifold for use with quartz cells is shown in Figure II-8. A regulator controlled argon pressure at 6 psi. Heavy wall rubber

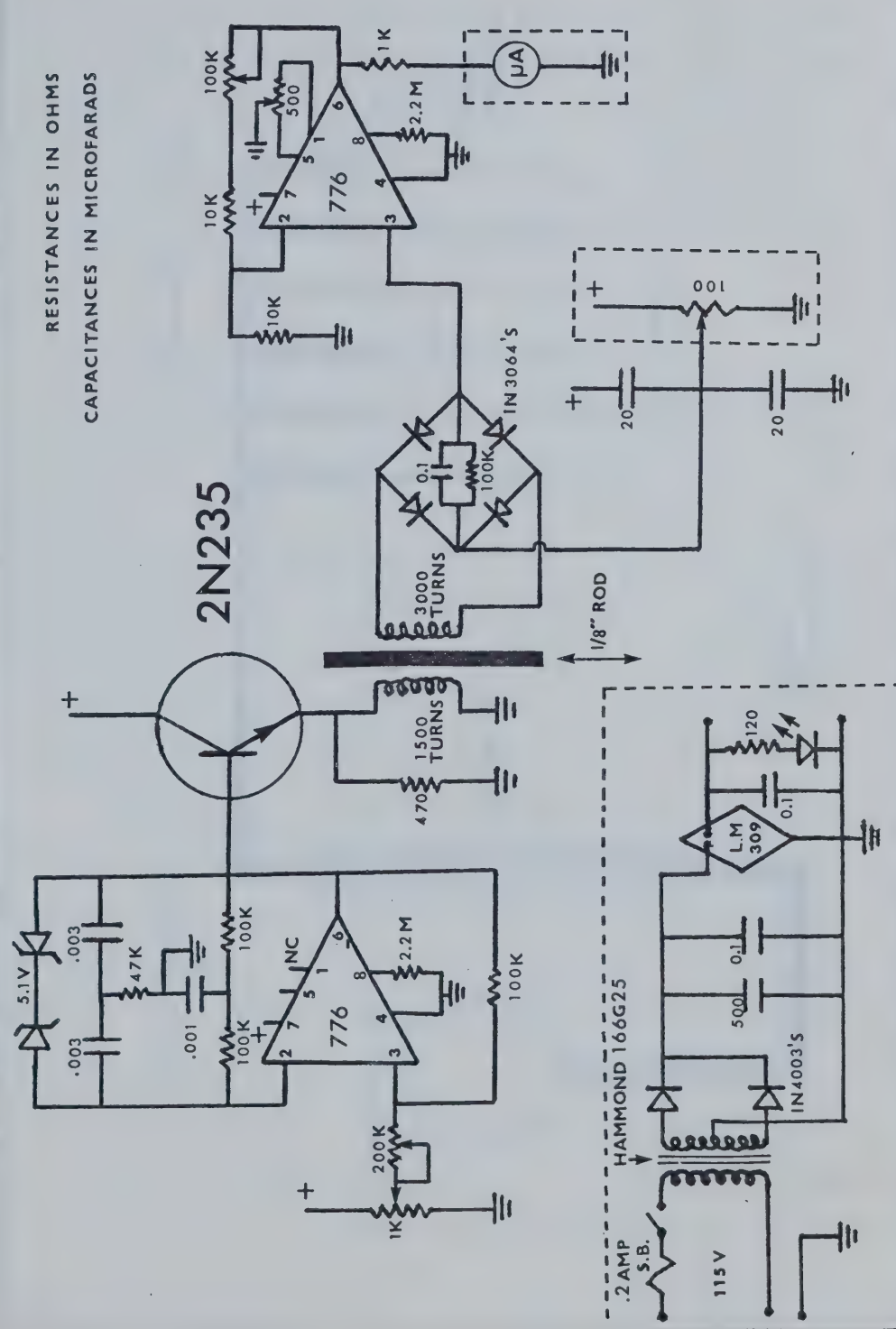


FIGURE II-7. The Bellows Position Indicator Circuit

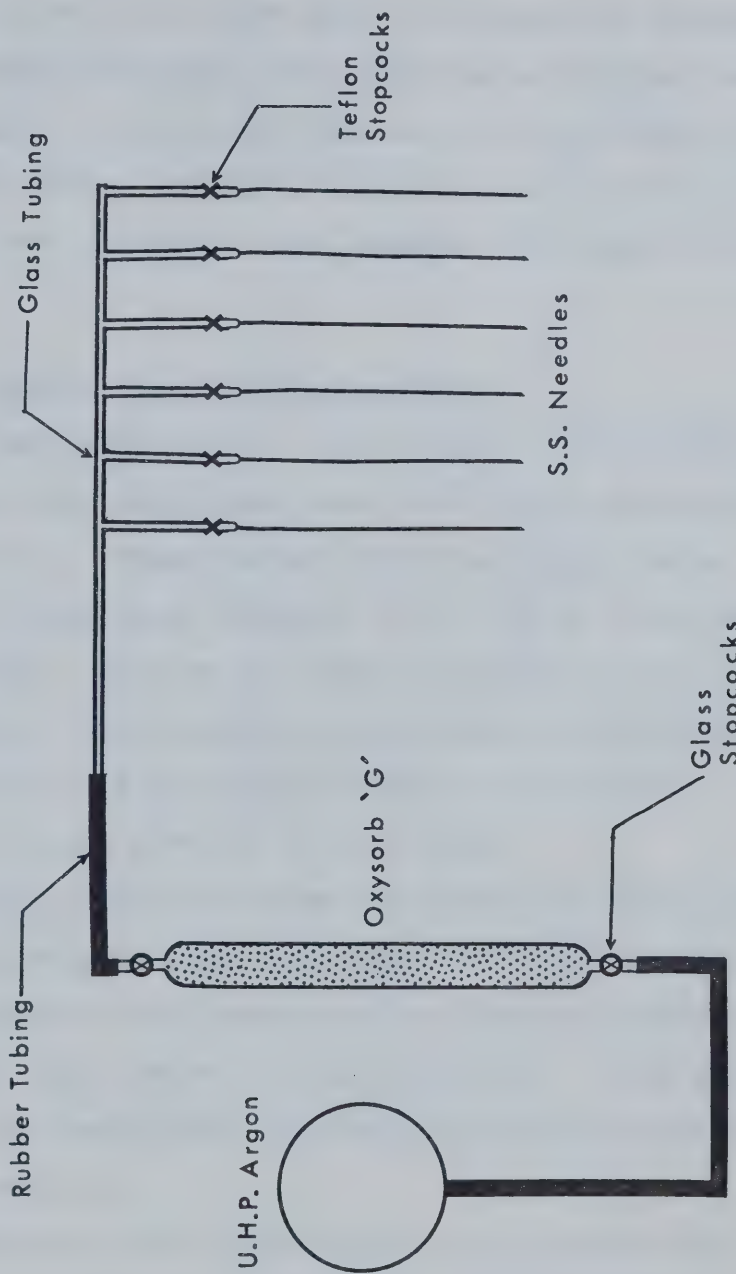


FIGURE II-8. The Sample Bubbler Manifold for Use with Quartz Cells

tubing (1/4" i.d. x 1/8" wall) connected the regulator to a column of Oxysorb "G" which removed oxygen from the argon. The main manifold was of Pyrex glass. Pyrex No. 7282 Teflon stopcocks controlled the gas flow through the stainless steel needles (8" long x 0.025" i.d.).

b. Samples for High Pressure Cell

Samples were U.H.P. argon bubbled and the high pressure cell was filled using the system depicted in Figure II-9. Tygon tubing (1/4") connected components from the argon cylinder to the 200 ml Pyrex sample reservoirs. Oxysorb "G" removed traces of oxygen from the argon. The reservoirs were filled through greaseless 35/25 ball and socket joints which could be tightly closed with No. 35 ball clamps.

During sample bubbling the system was maintained at the regulated supply pressure of 10 psi by throttling through Nupro needle valves (Nuclear Products Company, type B-4H-VT) on the reservoirs. Lead sheet (1/4") surrounded the reservoirs to protect samples from radiation.

Filling of the high pressure cell entailed the following sequence of operations. The Rotoflo TF2/13 valve (V3) and the Aminco high pressure valve were opened. Vacuum caused the cell bellows assembly and

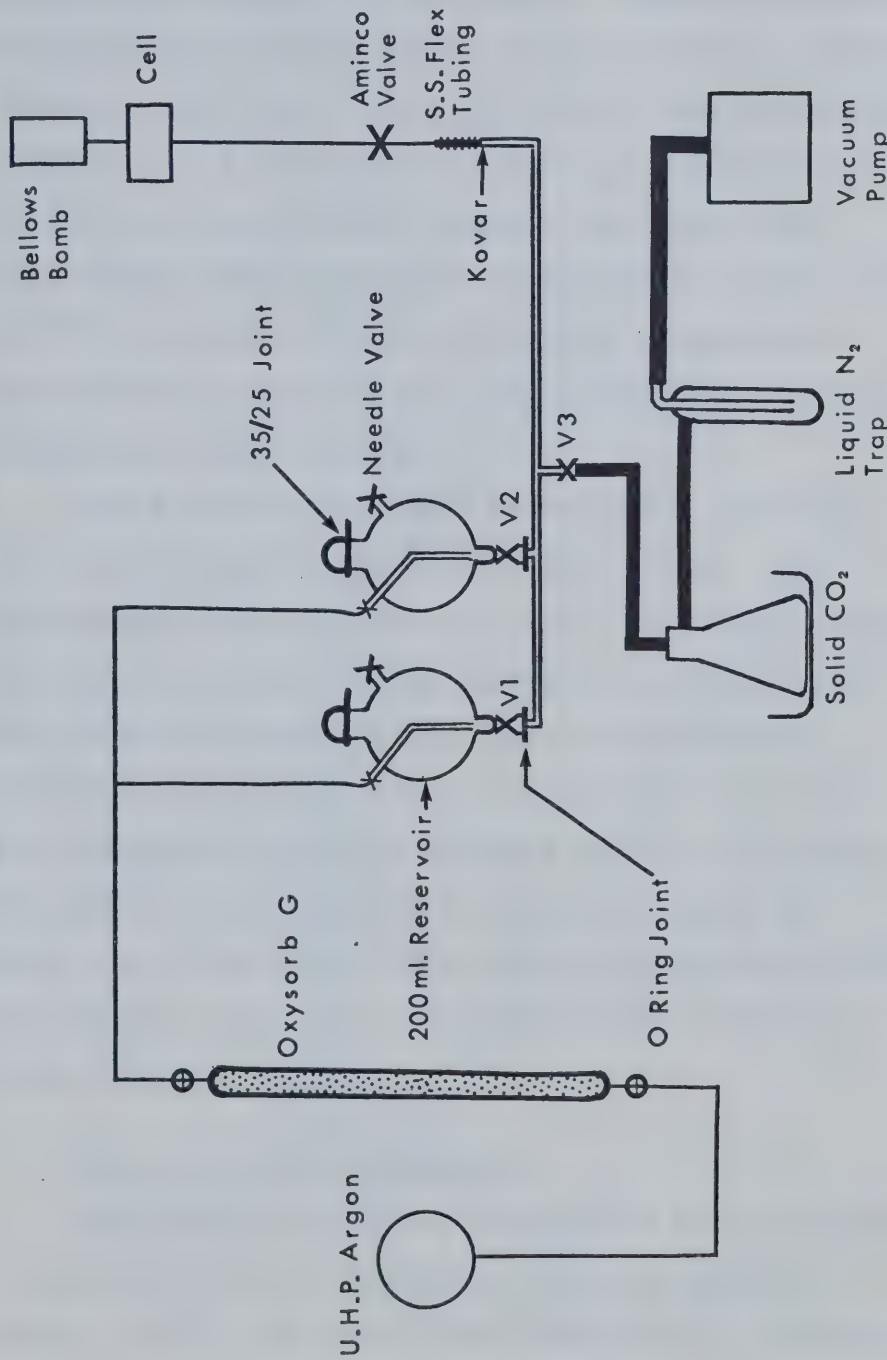


FIGURE II-9. The High Pressure Sample Preparation System

connecting tubing to be evacuated. Complete evacuation collapsed the bellows and was indicated by the bellows position indicator. Fluid drained from the system was trapped in a 2 litre flask placed in a styrofoam box filled with solid carbon dioxide. The Welch Duo-seal vacuum pump was further protected by a trap held at 77K by a Dewar of liquid nitrogen. Components from valve V3 to the vacuum pump were connected with heavy wall rubber tubing.

Valve V3 and the needle valve on the reservoir containing sample solution were then closed. The appropriate Rotoflo valve (V1 or V2) was opened slowly and sample solution flowed through Pyrex tubing, then high pressure tubing, to fill the cell and bellows assembly. Complete filling to a pressure of 10 psi was indicated by a fully extended bellows. The emptying sequence was repeated to flush the system and after the final filling the Aminco high pressure valve was closed. About 50 ml of solution was needed to flush and fill the cell.

c. The Gaseous Solute Bubbler

The apparatus used for preparation of stock solutions saturated with a gaseous solute is shown in Figure II-10. Gas entered the bubbler at V1 (Rotoflo TF2/13 valve). A fine porosity glass frit near the

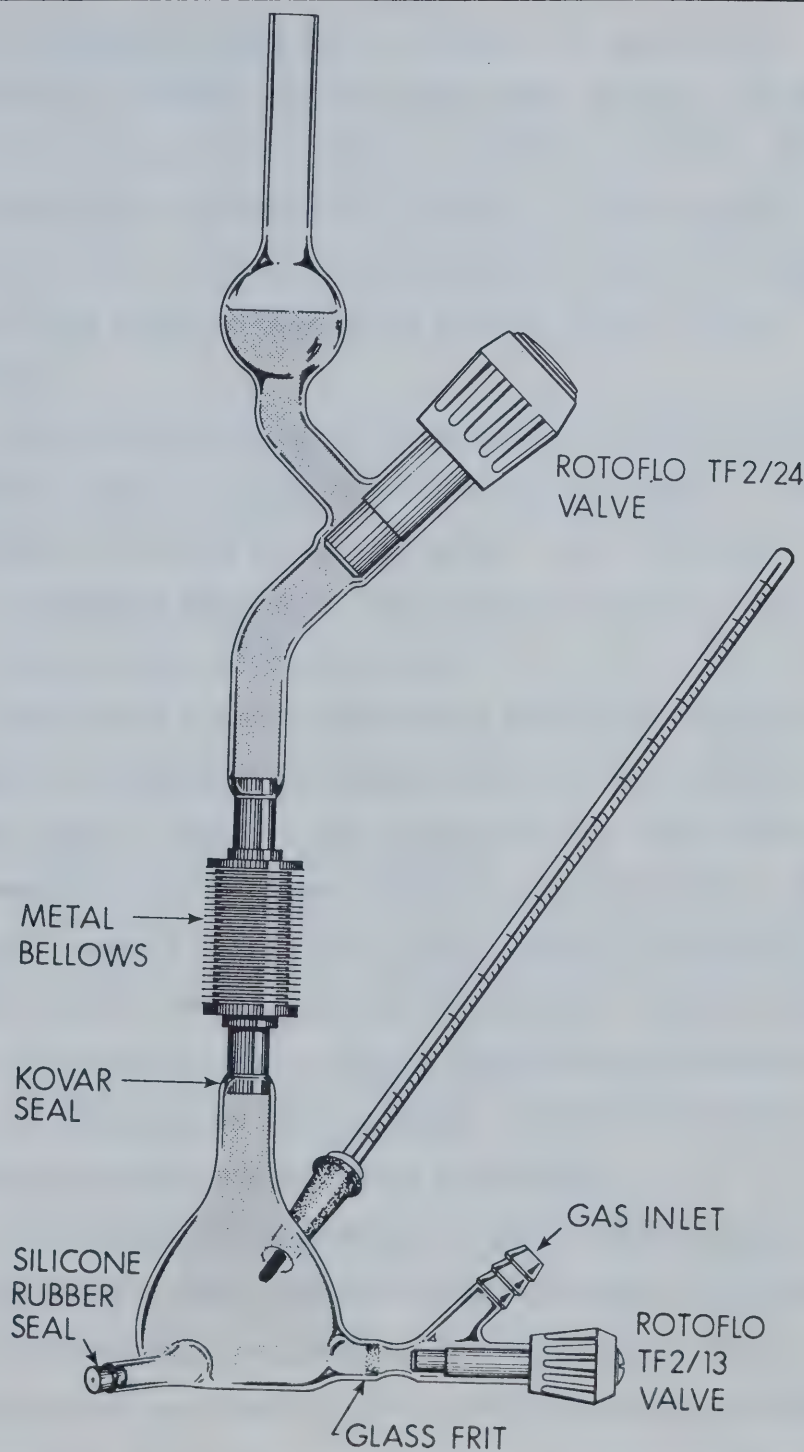


FIGURE III-10. The Gaseous Solute Stock Solution Preparation Apparatus

valve prevented fluid from escaping and gave finely divided gas bubbles for more efficient mixing. The gas flow rate was generally about 60 cm³ per minute. The solution was constantly stirred with a Teflon coated stirring bar. A mercury thermometer fitted the grease free 10/30 ground glass joint midway up the 100 ml bubbler.

Gases were usually pre-treated by bubbling twice through medium porosity fritted glass immersed in 200 ml flasks of triply distilled water. The "scrubbed" gas was passed through a trap held at 266K by an ice-salt bath to dry it before use.

To obtain a stock solution a microlitre syringe (Hamilton Company) was injected through the silicone rubber seal. Valve V1 was closed and all gas bubbles allowed to escape. Then valve V2 (Rotoflo TF2/24) was closed. Manual squeezing of the modified stainless steel bellows (Metal Bellows Corporation) forced solution into the syringe. It was withdrawn before pressure on the bellows was released. Valves V1 and V2 were then opened and bubbling continued.

This technique prevented solution degassing as would normally occur when filling a syringe. Samples of the stock solution were taken regularly in the same manner for immediate gas chromatographic analysis.

6. GAS CHROMATOGRAPHY

A Hewlett-Packard 5750 Research Chromatograph was used with thermal conductivity detection. The flow rate of helium carrier gas was 55-60 cm³ per minute. It was dried before use by passage through a 30 cm column packed with molecular sieves (Linde Company). The desiccant was periodically regenerated by removing it from the column and then heating it to 423K for several hours in an oven equipped with an exhaust fan.

a. Analysis of Water in Alcohols

The column used was stainless steel (1/8" x 6') packed with 10% by weight Carbowax 1540 on 30/60 mesh Chromosorb W (Waters Associates Ltd).

b. Analysis of Gaseous Solutes

The column used was copper (3/16" x 6') packed with 30/40 mesh silica gel (Fisher Scientific Company).

7. THE VAN DE GRAAFF ACCELERATOR

The source of high energy electrons was a Type AK 2.0 MeV van de Graaff Accelerator manufactured by High Voltage Engineering Corporation. The normal operating voltage of 1.87 MeV could be extended to 2.20 MeV when needed. The maximum peak current delivered during pulsed operation was 130 ma. Pulse lengths of 3, 10, 30, 100 nanoseconds and 1.0 microseconds were available, but only

the two longest pulses provided useful doses.

Variable millisecond and direct current operation were also possible. However, in these operational modes, serious heating of the 0.003" thick aluminum electron window (Figure II-11) could occur if too high a beam current were used. Failure of the window due to heat weakening would destroy the high vacuum ($\sim 2 \times 10^{-7}$ torr) inside the accelerator beam pipe. Serious damage to electronic components could also result. Beam current was therefore limited to 100 μ a during d.c. operation. Slightly higher currents could be used with millisecond pulses.

The entrance from the control room to the accelerator and target rooms was shielded by a concrete maze. Closing and locking the iron gate at the control room end of the maze sounded a warning buzzer for 15 s. Accelerator operation was possible only after cessation of the buzzer. Opening of the iron gate resulted in immediate shut-down of the van de Graaff generator.

Several methods could be used to monitor the steering and focussing of the electron beam. The method commonly used was to fix a piece of phosphorescent paper to the end of the accelerator beam pipe. The paper could be viewed on closed circuit television. Each pulse of electrons caused a visible glow where it struck the phosphor, enabling accurate steering and focussing by adjustment of current to electromagnets.

When equipment blocked visual observation, the beam could be steered by maximizing either the SEM dose (see page 68) or the absorption from a "dummy" sample.

Typical beam diameter at the electron window was 2.5 cm, with the most intense portion confined to an area of about 1 cm².

8. THE SECONDARY EMISSION MONITOR (SEM)

The relative dose for each electron pulse was indicated by a secondary emission monitor. The SEM consisted of three thin metal foils placed inside the accelerator beam pipe perpendicular to the path of the high energy electrons. As shown in Figure II-11, the SEM was positioned near to the electron window. This was to ensure that the beam monitored was as similar as possible to the beam striking a sample.

Aluminum (0.001" thick) was originally used for the foils. However, the emission characteristics changed with time, probably due to slow surface oxidation of the foils. The secondary emission was also found to depend on beam current density.

Use of Havar, a cobalt base high strength alloy, overcame these problems. It was obtained in very thin (0.0001") sheets from the Hamilton Watch Company, Precision Metals Division. The low average atomic number (about 27) of this material made it superior to gold

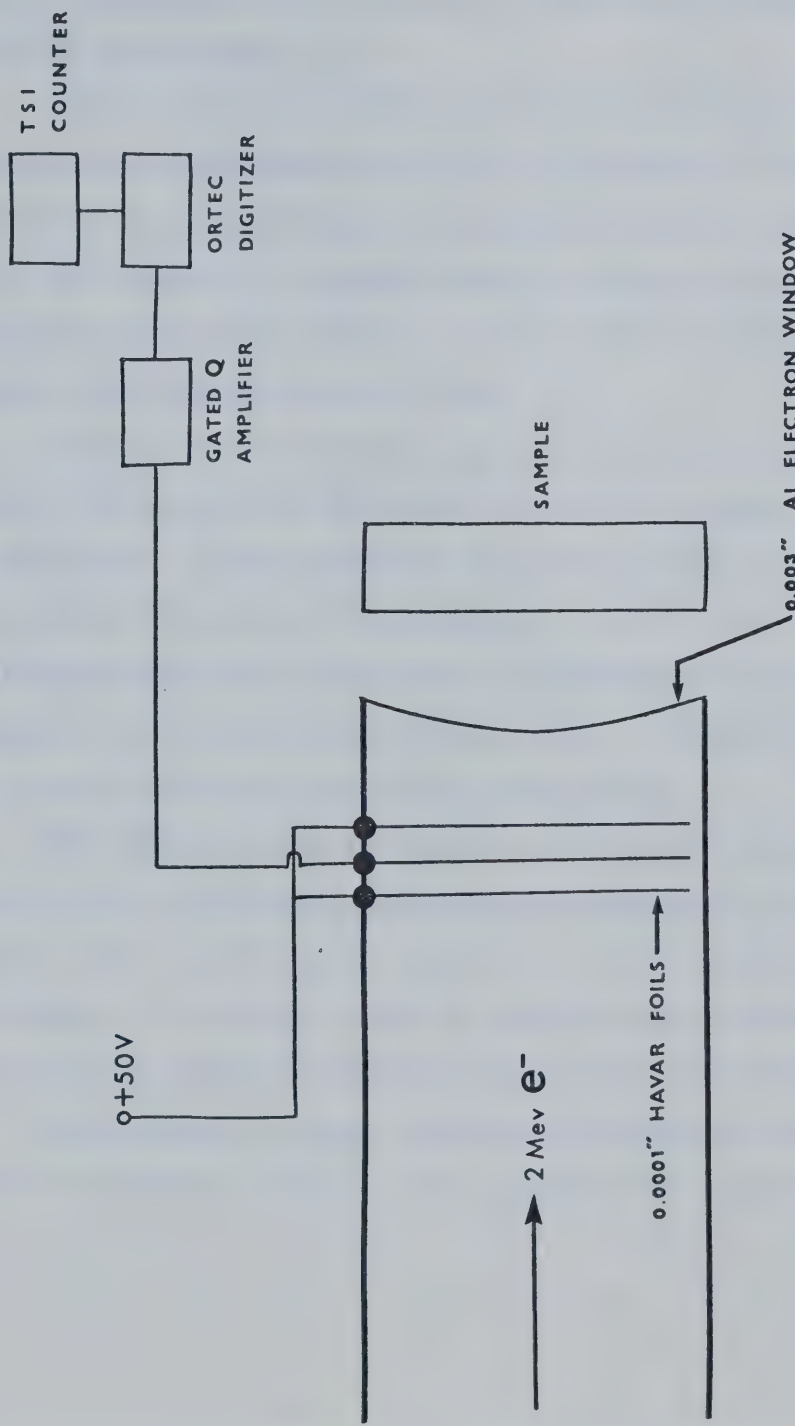


FIGURE II-11. The Secondary Emission Monitor (SEM)

(At.No. 79) because of less beam attenuation through electron scattering.

The 2" diameter foils were separated by 0.5 cm. The outer two were maintained at a potential of +50 volts. Passage of an electron pulse generated secondary electrons. The electrons ejected from the centre foil were collected by the outer foils, the net result being a current flow from the centre foil.

Current flow occurred only during a high energy electron pulse and was measured and held by a gated charge (Q) amplifier. This amplifier then fed current into an Ortec Model 439 current digitizer for 0.50 seconds. The digitized signal was displayed as picocoulombs of charge on channel A of a TSI Model 1535 counter. Channel B of the counter recorded cumulative sample dose.

The SEM dose for 1.0 and 0.1 μ s electron pulses was 4.45% of the primary electron dose measured as a current from a gold target fixed to the beam pipe electron window. The ratio of SEM to target dose could be varied +7% by changing beam steering and/or focussing.

Actinometry in situ was used to calibrate the SEM as a secondary dosimeter as explained on page 95.

C. TECHNIQUES1. SAMPLE PREPARATION

Quartz cells and other glassware were cleaned by performing the following sequence of operations. First the vessel was rinsed twice with absolute ethanol. While the surface was still alcohol wetted, concentrated nitric acid was added. The resulting exothermic reaction caused the acid to boil vigorously. Acid was then removed by rinsing many times with triply distilled water and the glassware was dried at 388K in a clean oven reserved for that purpose. Just before use it was rinsed twice with the appropriate solvent or solution.

Metal apparatus, including syringe needles, were washed first with hexane to remove oil and grease, then with soap and hot water. They were finally rinsed many times with triply distilled water and oven dried. Before use they were rinsed several times with the solvent being used.

a. Samples in Type (a) Cells

Stock solutions were prepared in either 50 or 100 ml Pyrex volumetric flasks. Solid solutes were weighed in the flask on an analytical balance. Liquid solutes were added by microlitre syringe (10, 50 or 100 μ l). The exception was perchloric acid, which was weighed to avoid contact with metal. Dilution of the acid was done

at 195K to avoid decomposition of the alcohol solvent.

Samples were prepared by syringe addition of stock solution to solvent in a clean cell. For samples containing a high enough solute concentration the stock solution was the pure solute. Samples were de-aerated by bubbling for at least 20 minutes with U.H.P. argon at a rate of about 25 cm^3 per minute, and then sealed by closing the stopcock.

b. Samples in Type (b) Cells

These samples were prepared in the manner described in a, but were sealed after bubbling as illustrated in Figure II-12. Step 1 took place at room temperature. The syringe needle was then withdrawn to just above the liquid as shown in step 2 and the argon flow rate was increased somewhat. The cell was placed in a Dewar flask filled with finely ground solid carbon dioxide and cooled to 195K. Heating the thinned portion of the tubing with a flame flushed volatile substances from the glass wall. The syringe needle was then further withdrawn as shown in step 3, and the seal was made as rapidly as possible. This method was used for all samples in alcohols at low temperature. A given sample gave the same electron lifetime at room temperature whether sealed in this way or by a stopcock.

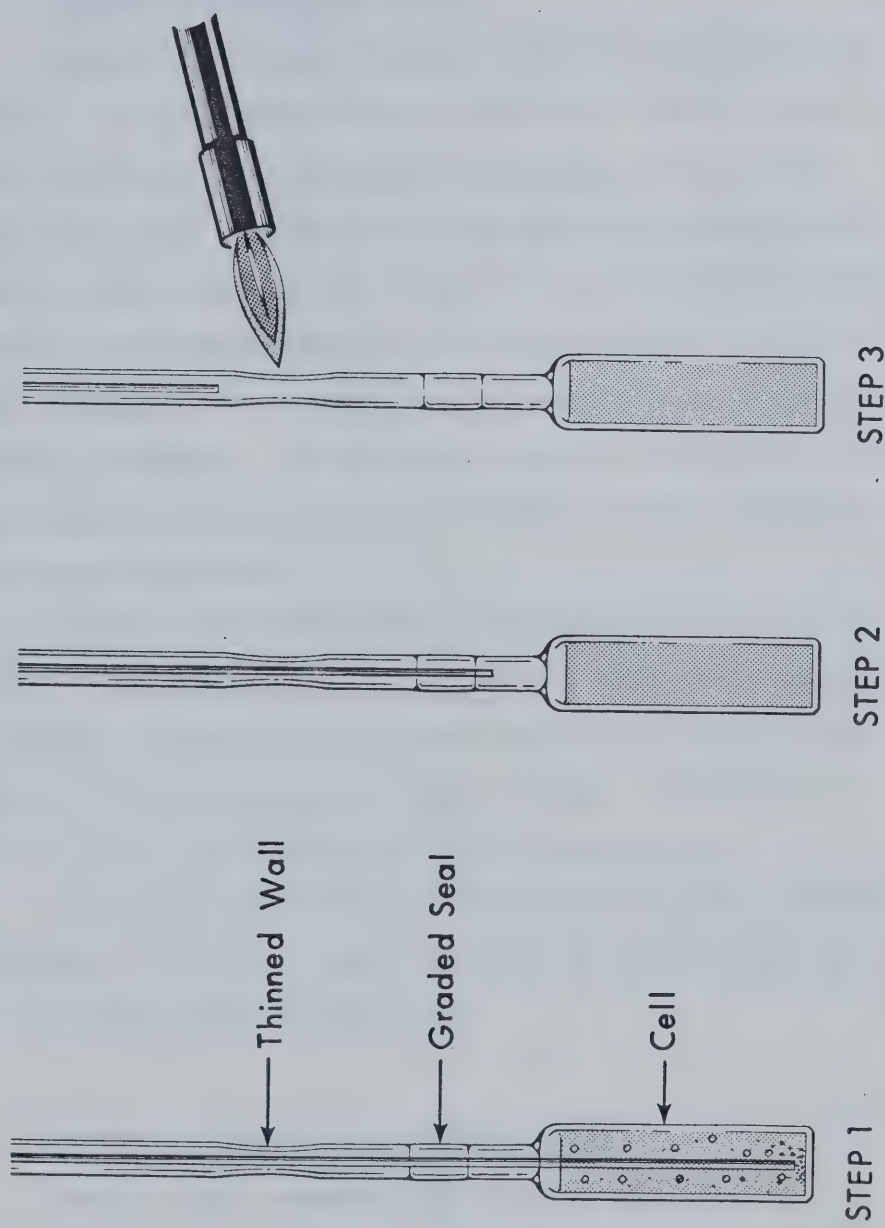


FIGURE 11-12. The Sealing Technique for Type (b) Cells.

c. Samples in Type (c) Cells

Sample cells were filled to above the valve with solvent and deoxygenated with argon at a rate of about 40 cm^3 per minute for at least 30 minutes. The syringe needle was then withdrawn to just above the valve seat, and the valve was closed. This left no gas volume in the sample. Only when injections of stock solution of $>50 \mu\text{l}$ were necessary was a small gas volume left in the cell to prevent breakage. The solvated electron lifetime could be determined in the pure solvent before syringe addition of the solute solution.

Solute and solvent were thoroughly mixed after an injection by repeatedly inverting the cell while shaking it gently. This action allowed the Teflon coated stirring bar to travel back and forth between the bottom of the cell and the valve seat (see Figure II-12).

The injection technique was improved until several injections of U.H.P. argon resulted in no decrease in the solvated electron half-life.

d. Samples in the High Pressure Cell

Samples were prepared by syringe addition of stock solution to solvent in a 50 or 100 ml volumetric flask. After thorough mixing the solution was put in the 200 ml Pyrex sample reservoir (Figure II-9) and bubbled with U.H.P. argon at a rate of at least 40 cm^3

per minute for 30 minutes or more.

Subsequent handling of the sample is explained on page 60.

e. Samples Containing Sodium Alkoxide

Freshly cut and cleaned sodium metal was washed with n-hexane, then dried in a stream of U.H.P. argon before it was added to the alcohol solvent. This solvent was then used for sample preparation in the normal manner.

The approximate concentration of sodium alkoxide was determined by titration to the bromothymol blue end point using standardized aqueous HCl.

2. GAS CHROMATOGRAPHY

a. Analysis of Water in Alcohols

A column oven temperature of 351K gave good separation of water from methanol or ethanol. Retention times for methanol and ethanol were 20 s and 26 s respectively. The retention time for water was 90 s.

Calibration solutions of 1, 0.5, 0.2, 0.1 and 0.05 volume percent water were made by syringe addition of water to the appropriate absolute alcohol.

Water peaks were broad with long following tails. This made determination of peak area difficult. Calibration peaks were therefore compared visually with those

obtained from sample injections. By adjusting the sample injection volume to obtain a peak of similar area to a calibration peak, the unknown water content could be approximated.

The column retained a small amount of water permanently at 351K. It was therefore necessary to condition it by injecting a small amount (several μ l) of water at the beginning of each run.

b. Analysis of Gaseous Solutes

The column conditions were varied to suit individual gases being analyzed, as is given in Table II-1. Solvent retention times were much longer than those for the gaseous solutes. To speed elution of the solvent, the column oven temperature was increased to more than 500K after appearance of the solute peak.

Calibration for each gas was done under conditions identical to those used during analysis. The required gas was contained in a Pyrex bulb of about 20 cm^3 volume. A silicone rubber seal and a Rotoflo valve formed a "Y" on the bulb. While filling the bulb, the valve was open and gas was flushed through a syringe needle inserted to the bottom of the bulb through the rubber seal. After thorough flushing the valve was closed and the bulb filled to greater than atmospheric pressure.

Gas tight 10 or 25 μ l syringes (Unimetrics Universal Corporation, 1000 Series) were used to withdraw gas

TABLE II-1Column Conditions for Gaseous Solutes Analysis

Solute	Column Oven ($\pm 1^{\circ}\text{K}$)	Retention Time ($\pm 2\text{s}$)
1,3 Butadiene	486	87
Carbon dioxide	423	33
Ethylene	423	39
Ethyne (acetylene)	422	50
Nitrous oxide	368	75
Oxygen	368	17
Sulphur hexafluoride	368	70
	423	32

from the bulb and inject it onto the chromatograph column. As shown in Figure II-13, plots of recorder peak height versus injection volume were linear.

For 1,3-butadiene the peak area was plotted against injection volume. This was because the half-width of peaks from gaseous and solution injections were different.

Small air peaks from calibration injections were sometimes encountered. It was difficult to eliminate the air. Calibration for air was therefore done, and the air peak corrected for on gaseous solute calibration plots. This procedure resulted in a zero intercept on the plots.

3. SODIUM-POTASSIUM ALLOY PREPARATION

Sodium-potassium alloys containing between about 10 and 50 percent sodium by weight are liquid at room temperature.¹³⁶ These alloys are superior to either pure metal in providing reducing media for chemical purifications. The major reason is that with stirring, a fresh metal surface is constantly exposed.

Alloy was prepared in the Pyrex apparatus depicted in Figure II-14. The volume of the reservoir was chosen to suit the amount of solvent to be purified, but was generally greater than 100 cm³. The Hoke valve had a stainless steel body and a Teflon seat. The stirring bar was Teflon coated. A series of constrictions formed

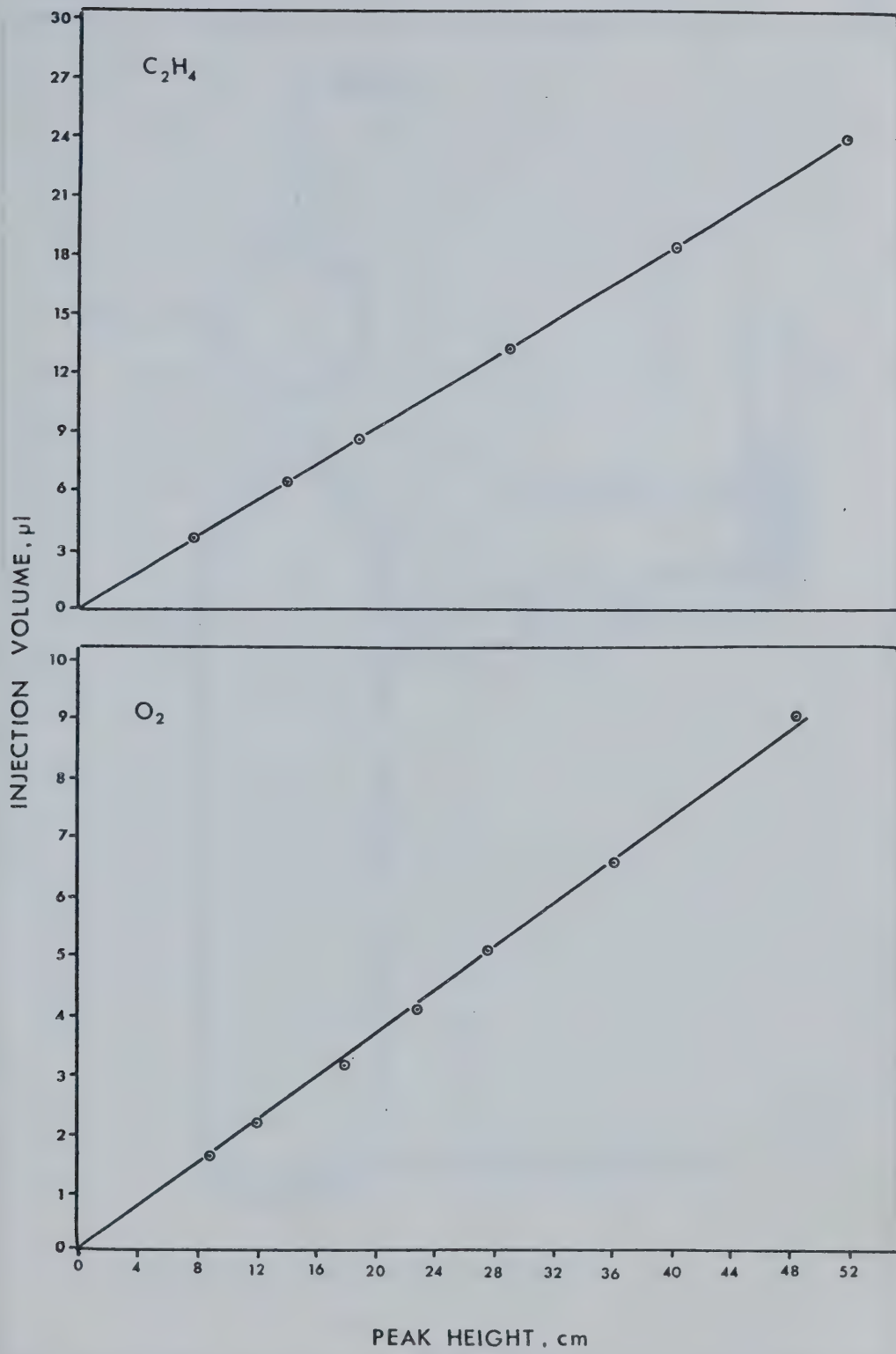


FIGURE II-13. Gas Chromatograph Calibration Plots

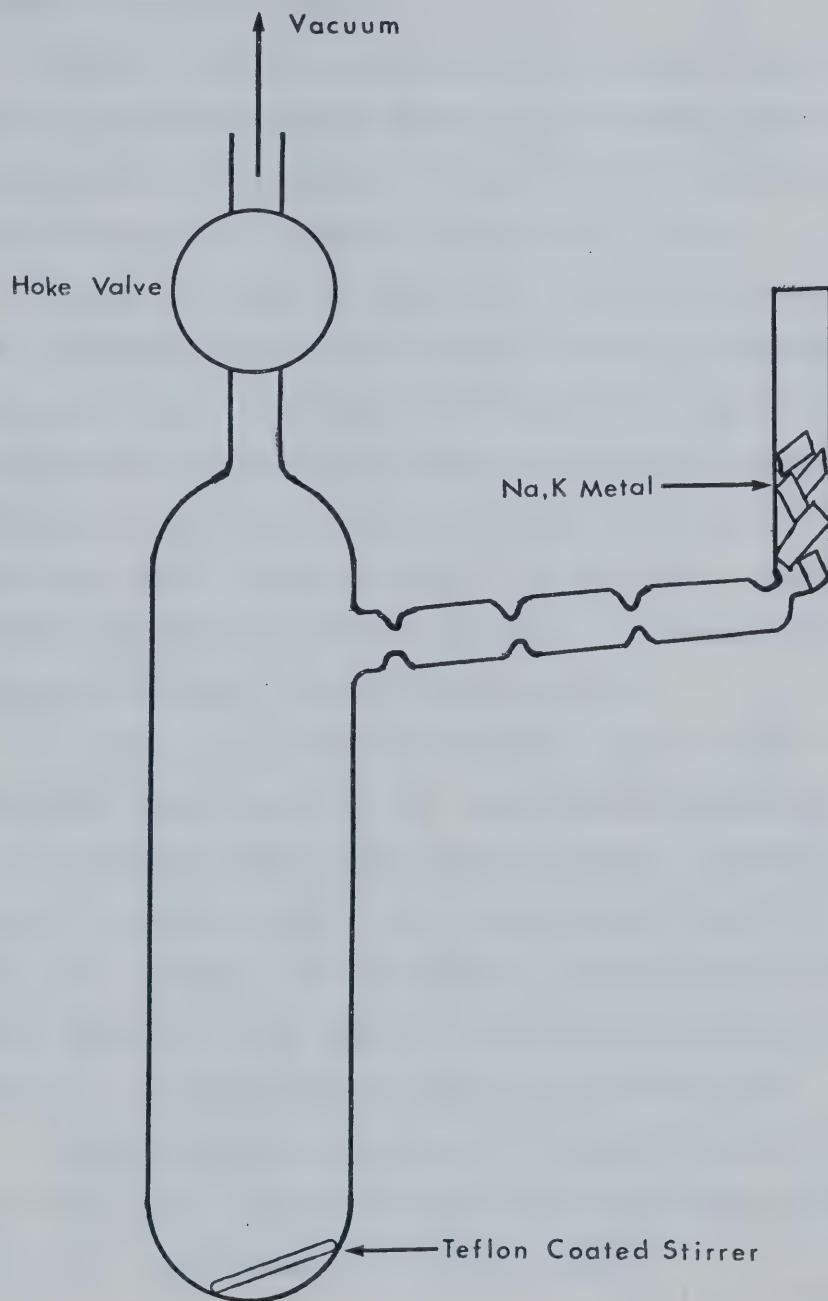


FIGURE II-14. The Na-K Alloy Preparation Apparatus

"cells" along the sidearm.

Small cubes of freshly cut and cleaned metal were placed in the sidearm as shown in the figure. The tube was then carefully sealed off with a flame and the system evacuated to a pressure of $< 1 \times 10^{-6}$ torr.

After closing the Hoke valve, heat was applied with a modest flame to the tubing containing the metal. When the alloy flowed into the first cell, the first constriction was sealed off and the used tubing was discarded. Alloy was then distilled from one cell to the next, each time sealing off the used cell, until it flowed into the reservoir. The Hoke valve was then reopened to remove any volatile material.

A Dewar of liquid nitrogen was used to lower the reservoir temperature to 77K, and then the material to be purified was distilled onto the alloy. Before removing the Dewar from around the reservoir the Hoke valve was closed. If upon warming to room temperature there appeared to be appreciable reaction occurring, the valve was periodically opened to remove gases.

After stirring overnight the treated material was distilled under vacuum at 77K into 10 cm³ Pyrex bulbs, which were then sealed off with a flame.

4. ANALYSIS OF POLAROID PHOTOGRAPHS

Typical photographs taken of the CRT of the

Tektronix 7623 oscilloscope are shown in Figure II-15. Each picture was taken after a 100 ns pulse at a sweep speed (horizontal scale) of 1.0 μ s/cm. The vertical scale is in volts/cm and is proportional to absorbance. For i and ii the vertical scale is 0.05 and 0.1 volts/cm respectively.

It should be noted that the actual CRT trace was photoreduced by a factor of 1.28. This factor has no effect so long as one main graticle division is allowed to represent 1.0 cm when making measurements.

a. Analysis of the Kinetics from Photograph i

Photograph i in Figure II-15 shows the first-order decay of the solvated electron absorption at 600 nm in ethanol at 297K. The solvated electron half-life was normally determined directly from such photographs. First, a best-fit line was drawn through the noise on both the baseline and the decay curve. Then the vertical distance between the curve and the baseline was taken using calipers. This distance was usually measured along the second vertical graticle line following the end of the electron pulse. Using a graticle line as reference, the calipers were then closed to one half the distance first measured. With one caliper point on the baseline, the other point was used to scratch a mark half way between the curve and the baseline. This mark was

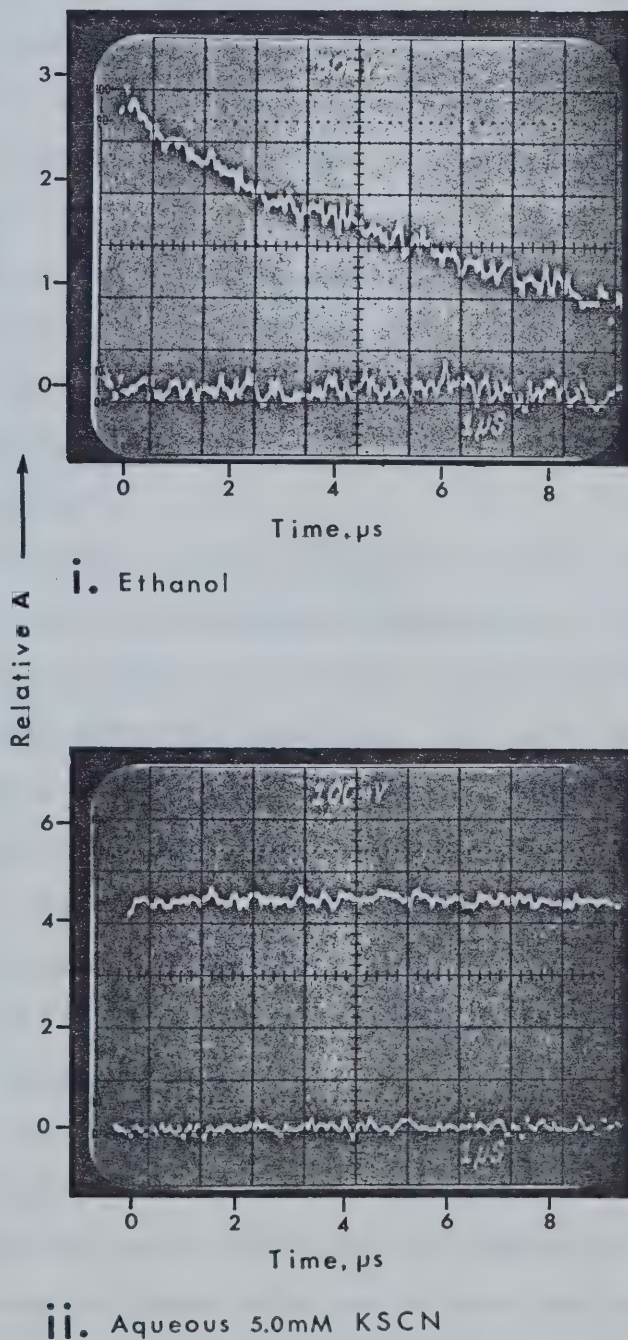


FIGURE II-15. Typical Oscilloscope Trace Photographs

checked by measuring the distance from it to the curve with the same caliper setting. The distance from this mark to the point where a horizontal straight line intersected the curve represented the half-life. This direct reading method yielded a solvated electron half-life ($t_{1/2}$) of 6.1 μ s in photograph i. Plots of the log of relative absorbance against time from the end of the electron pulse were sometimes made. Such a plot from data on photograph i is shown in Figure II-16. After the first microsecond the plot is linear, indicating first-order kinetics.

The half life of solvated electrons is the time required for the absorbance to decrease by a factor of two from any point on the linear position of the plot. This method gives the same half life as is quoted above.

As is the case in the figure, plots were sometimes initially non-linear. This could be due to either the noise in the trace or a contribution from a faster reaction or both. Therefore the first centimeter or so of the trace was ignored when analyzing kinetics by the direct reading method.

In low temperature alcohols there was a large contribution of an initial faster first order reaction. This contribution increased as the temperature decreased. Photographs for these experiments were analyzed by

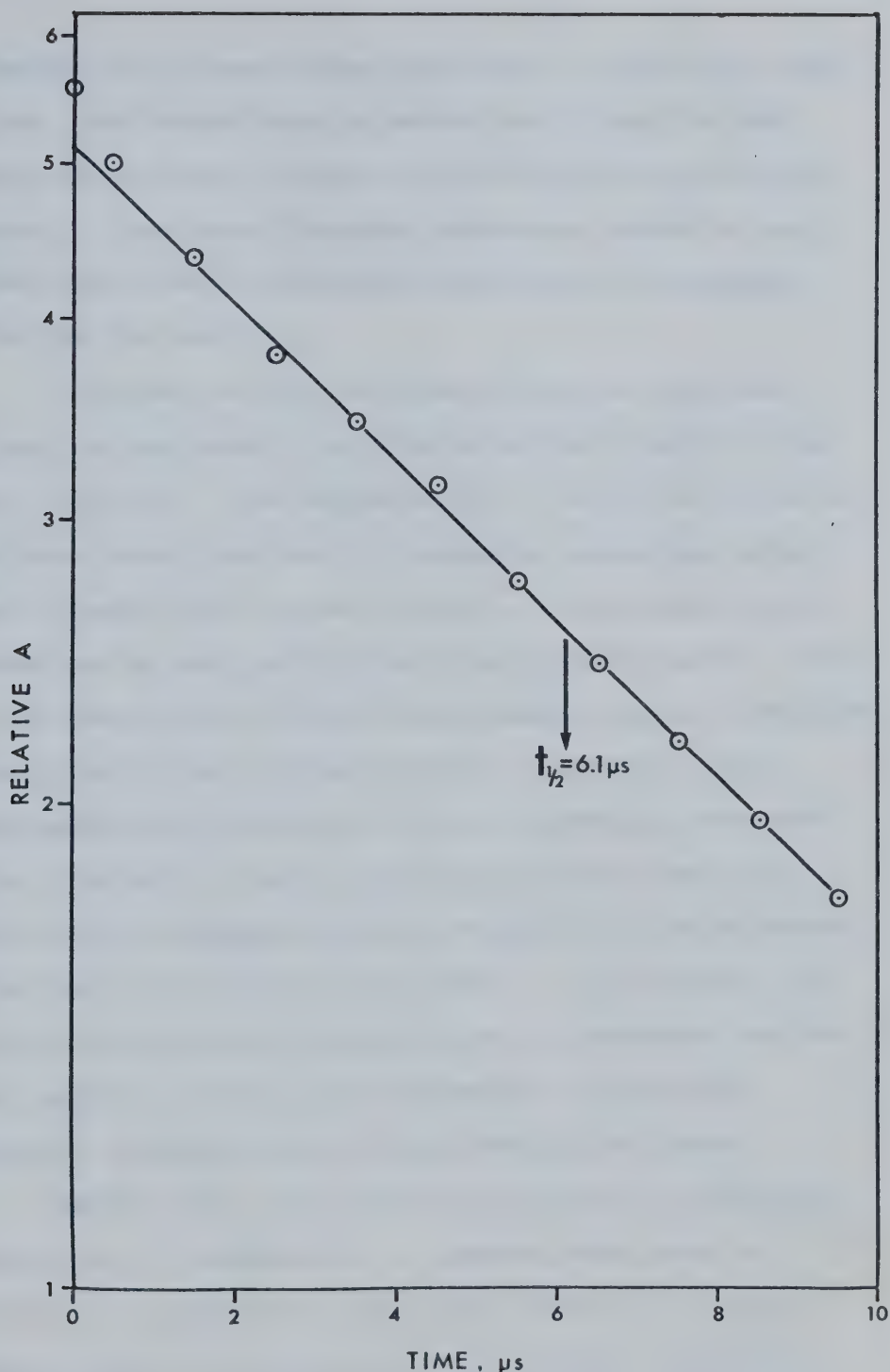


FIGURE II-16. The First Order Decay of Solvated Electrons in Ethanol

extending the slower decay curve back to the end of the pulse. The direct reading method could then be used. First order plots indicated that this method was satisfactory. The faster decaying absorbance could be analyzed approximately using the extension of the slower decay as the baseline.

A minimum of three concentrations of scavenger molecules were used in the determination of second order rate constants. The concentration of solvated electrons was much lower than that of scavenger molecules, resulting in pseudo first order kinetics. Photographs could therefore be analyzed by the direct reading method. Plots of the pseudo first order rate constant against scavenger concentration had a slope equal to the second order scavenging rate constant. The zero scavenger concentration intercept of such a plot should have given the first order decomposition rate constant of the solvated electron in the solvent being used. If it did not, an error in the plotted concentration of scavenger was the most probable reason. The direction of the error assisted in determining and correcting the cause.

Second order rate constants obtained at different conditions of temperature or pressure were used to determine the Arrhenius activation energy or the activation volume for the reaction of scavenger molecules

with solvated electrons. Activation energies were calculated from the slope of a plot of the log of the rate constant against the reciprocal of the absolute temperature. Activation volumes were calculated from the slope of a plot of the log of the rate constant against the pressure.

b. Analysis of Optical Absorption From Photograph i

Absorbance could be determined at any time along the solvated electron decay curve by substitution in the following formula.

$$A = \frac{D_o}{D} \log_{10} \left[I_o / \left(I_o - \frac{I_t}{F} \right) \right] \quad (1)$$

A is absorbance at time t after the beginning of the electron pulse.

D_o/D is a dose normalization factor where D is the SEM dose and D_o is an average dose, usually chosen to be 1.0 ncoul. from the SEM.

I_o is the incident analyzing light in volts

I_t is the absorbed light in volts at time t .

F is the amplifier factor which is the ratio of the amplification of the absorbed light to the incident analyzing light.

Calculations of absorbance for the purpose of spectrum plotting were done using (1) in a simple computer program. Normally, t equalled the length of the

electron pulse.

When the solvated electron lifetime was short there was significant decay in the absorbance during the pulse. This was particularly true for 1.0 μ s pulses. A correction for this decay was applied where necessary using (2).

$$A_o = A_{t_p} \left\{ \frac{t_{1/2}}{0.69t_p} \left[1 - \exp(-0.69t_p/t_{1/2}) \right] \right\}^{-1} \quad (2)$$

A_o is the absorbance at t_p corrected for decay during the pulse.

$t_{1/2}$ is the solvated electron decay half-life.

t_p is the electron pulse length.

Analysis of a minimum of ten photographs, each taken of an experiment at a different wavelength, was necessary to plot a solvated electron optical absorption spectrum. The spectra were always broad. It was often difficult to determine the wavelength of maximum absorbance by inspection. To remove bias a geometric method was used. A minimum of three lines were drawn on a spectrum parallel with the abscissa (wavelength scale). A mark was made on each line half way between the points where the line crossed the shoulders of the spectrum. A line joining these points intersected the spectrum at λ_{max} . The method is illustrated in Figure

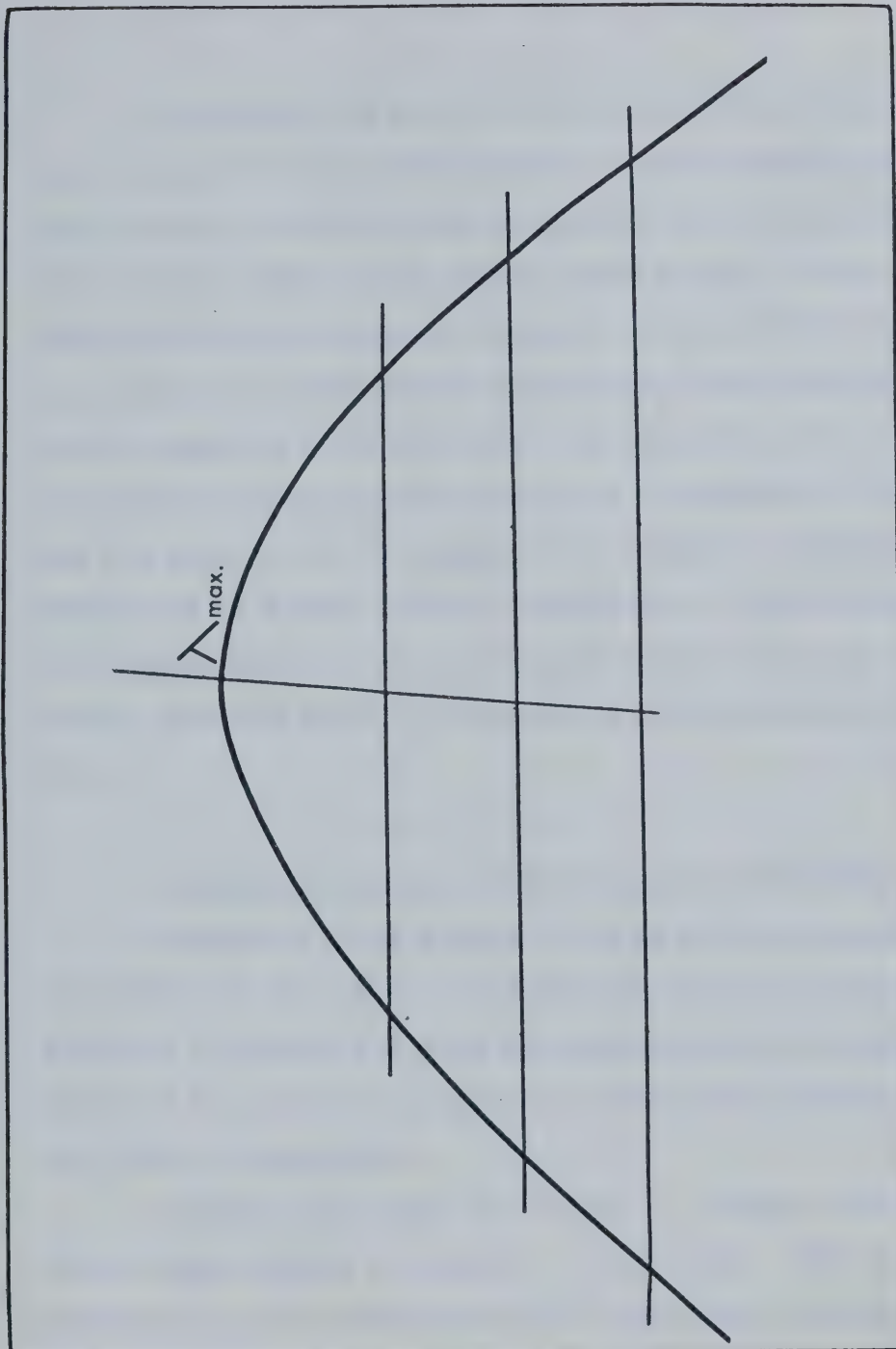


FIGURE II-17 The Geometric Method of Determining λ_{max}

In ethanol the build up of radiolysis products which react with solvated electrons spoiled samples. To avoid errors from this source, samples were usually used for less than ten pulses before being changed. Also, spectra were determined by a method which detected changes in a sample or experimental conditions. Wavelength was first varied in 20 nm increments in one direction, then in the reverse direction with the first increment of 10 nm, and the rest 20 nm. If there was no change in experimental conditions or sample purity, the points at intermediate wavelengths should fall on the same smooth curve as those points obtained prior to reversal of the direction of the scan.

c. Analysis of Optical Absorption from Photograph ii

Photograph ii in Figure II-15 is of the optical absorption at 478 nm in a 5.0 mM KSCN aqueous dosimeter solution following a 0.1 μ s electron pulse. At a sweep speed of 1.0 μ s/cm there is very little decay evident in the $(SCN)_2^-$ absorption.

Calipers were used to measure I_t between straight lines drawn through the noise on each trace. The absorbance was calculated using (1). The dose received by the sample could then be calculated.

D. TIMING OF A FAST ABSORPTION EXPERIMENT

Several highly coordinated measurements were necessary to conduct a successful fast absorption experiment. The electronic system most used evolved to the point where a properly prepared experiment could be largely conducted by pushing one button. The timing of events initiated by this button is illustrated in Figure II-18. Since the duration of events differ by up to six orders of magnitude, their widths in the figure could not be drawn to scale.

Assuming all preparation was complete, including settings on the Tektronix 7623 fast storage oscilloscope, an experiment proceeded as follows. Initially the remote erase cleared the oscilloscope CRT and Channel A of the TSI Counter. At the same time the light shutter, and if applicable, the high pressure cell electron window shutter, were opened. Also, the request for an experiment was added to the total of previous requests for a particular sample. This electron pulse count was registered on a Hewlett-Packard 5245L Electronic Counter.

After 1.2 s, at point A on the figure, the main sweep was enabled. To improve reproducibility the main sweep gate always triggered from a point on the power line signal which had positive level and positive

Remote Erase

Lamp Shutter
High Pressure Cell Shutter

Erase Previous Dose



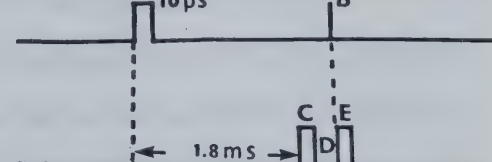
Main Sweep Gate



Fire Van de Graaff



Delayed Sweep Gate



Delayed Sweep Holdoff



Gate to SEM



Hold Incident Light



Sample Incident Light



FIGURE II-18. The Timing Sequence of an Absorption Experiment

slope. This point was chosen to obtain the longest possible low light-noise region for the experiment. Reasons for the importance of the analyzing light amplitude remaining constant during an experiment are given later.

The first event in the main sweep was a 10 μ s pulse to fire the van de Graaff accelerator. A high energy electron pulse, indicated by B, occurred about 1.8 ms later. There was an uncertainty in the time a beam pulse would occur. The 10 to 50 μ s uncertainty (D) was called beam "jitter" and was caused by the irreproducible closing of a mechanical relay.

The signal to sweep the baseline for the absorption trace came from the delayed sweep gate at point C. It was swept at the same speed as set for the corresponding absorption decay curve. After sweeping the baseline there was a 5 μ s delayed sweep holdoff. This time was needed to allow the system to settle.

Passage of the electron pulse through a toroid located part way down the accelerator beam pipe supplied a fast pulse. This pulse was used to trigger an oscilloscope sweep to record the absorption. Point E on the figure represents this sweep. Again, as for C, it was followed by a 5 μ s delayed sweep holdoff.

The SEM was monitored from the beginning of a baseline sweep up to the end of the absorption sweep.

Thus any current from the SEM due to passage of high energy electrons was measured during the entire experiment and recorded.

The incident analyzing light was sampled at the same time as a baseline was swept. It then had to be held for at least 500 ms while the H.P. 3440 A digital voltmeter responded. Actual sampling of the incident light took a further 60 ms. This was the time required for the DVM to digitize the analog signal.

Beam "jitter" was a complicating factor, particularly in obtaining an accurate baseline. It was important to have the baseline written as close in time to the absorption as possible. This was because any change in the analyzing light amplitude between sweeps C and E would result in an erroneous baseline. Any adjustment made in the delay time preceding sweep C was therefore quite critical. If the baseline were swept too early it could be incorrect. If it were swept too late the absorption signal would be either missed completely (if the electron pulse occurred during the delayed sweep holdoff) or it would appear during the baseline sweep. The slower the sweep speed, the greater the possibility became that there would be delay problems. The system was in fact limited to a slowest horizontal sweep of 2 μ s/cm.

Modification of the system would allow use of

slower sweeps. This was necessary only for samples having a solvated electron half life greater than about 15 μ s. The method used was to deliberately sweep the baseline late. The electron pulse would thus occur during sweep C, producing a short leading baseline, then the absorption trace. However, even with this technique, for speeds of 10 μ s/cm or slower there was a significant chance for error due to changes in analyzing light during the absorption trace.

When the automatic sequence of events was complete, the manual sequence began. First the CRT trace was photographed and the oscilloscope settings were recorded. Then the pulse number, SEM dose, incident light, temperature, monochromator wavelength and other pertinent data were recorded.

Occasionally an experiment was not completely successful. Reasons for this could be incorrect oscilloscope settings, missed baseline, missed dose record, noise in the trace, or any of many other problems. After attempting to correct a problem the experiment would be repeated. Some samples, especially pure ethanol, were spoiled by build up of radiolysis products making it necessary to limit repeats of experiments to a minimum number of times. This was a major reason for keeping a record of the number of electron pulses a sample received.

At the conclusion of experiments on a particular

sample, the electron pulse count and accumulated SEM dose on Channel B of the TSI counter were erased manually.

E. IRRADIATION AND DOSIMETRY

1. IRRADIATION

For irradiation of samples in quartz cells 1.87 MeV electron pulses of 1.0 or 0.10 μ s duration were used. These pulses normally gave doses of about 9×10^{16} (~ 2 ncoul SEM) or 3×10^{16} eV/g (~ 0.6 ncoul SEM) respectively. The beam current could be adjusted to give a maximum dose of about 3×10^{17} eV/g for a 1.0 μ s pulse and a minimum dose of about 1×10^{16} eV/g for a 0.1 μ s pulse. Overlap in the dose delivered by pulses of different width could not normally be obtained.

An accelerator voltage of 2.2 MeV was used for irradiation of samples in the steel high pressure cell. The higher voltage and 1.0 μ s pulses were needed to obtain a dose of 5×10^{16} eV/g. This dose was deposited in the sample behind the thinned portion of the steel electron window. The thinned portion had a diameter of 0.9 cm.

2. DOSIMETRY

The dose delivered in each electron pulse was monitored by the secondary emission monitor (SEM). The SEM was calibrated to the dose received by a sample

using in situ actinometry.

Routine actinometry used the optical absorption produced in oxygen-saturated 0.2 or 0.5 mM KSCN aqueous solutions. The molar absorptivity, ϵ , (molar extinction coefficient) used was 7600 $M^{-1} cm^{-1}$ for $(SCN)_2^-$ at 478 nm. This value was chosen after performing experiments to resolve confusion in the literature.^{43,137-139} The wavelength of maximum absorbance ($\lambda_{max} = 478 \pm 4$ nm) and the absorbance were independent of temperature from 293 to 332K.⁶⁵ All dosimetry was done in this region. It was assumed that $G(OH)_{bulk} = 2.9$.^{8,17}

The dose in eV/g was calculated from the absorbance measured from photographs of the type shown in Figure II-15, ii.

$$D = \frac{A \cdot N_O}{\epsilon \cdot G(OH) \cdot b \cdot \rho \cdot 10} \text{ eV/g} \quad (3)$$

where A = absorbance

N_O = Avagadro's number

ϵ = molar absorptivity = 7600 $M^{-1} cm^{-1}$

$G(OH)$ = Number of OH radicals scavenged by SCN^- for each 100 eV of dose absorbed

b = path length of analyzing light

ρ = density of absorber.

The aqueous KSCN dosimeter was also compared to the Fricke dosimeter (ferrous \longrightarrow ferric ion) as reported in the results section.

F. DIELECTRIC CONSTANT (ϵ) AND DENSITY (ρ)

1. THE EFFECT OF TEMPERATURE

Changing temperature changes the density (ρ) of methanol and ethanol. This effect required adjustment of absorbed dose and solute concentration which had been determined for room temperature. The adjustment routine was simplified using a plot of ρ_{293}/ρ_T as shown in Figure II-19. Values for absorbed dose or solute concentration were multiplied by the factor ρ_{293}/ρ_T , where T was the experimental temperature in $^{\circ}\text{K}$. The factor was calculated from data in the literature.¹⁴⁰

The effect of temperature on the static dielectric constant (ϵ) is given in Figure II-20. Data from ref. 141 was used between 298 and 500K. From 323 to 120K, data from ref. 142 was used.

2. THE EFFECT OF PRESSURE

The effect of pressure on the ratio ρ_p/ρ_o is the same for methanol and ethanol, as illustrated in Figure II-21. ρ_o is the density at 1 bar and ρ_p is the density at the pressure of the experiment. The points were

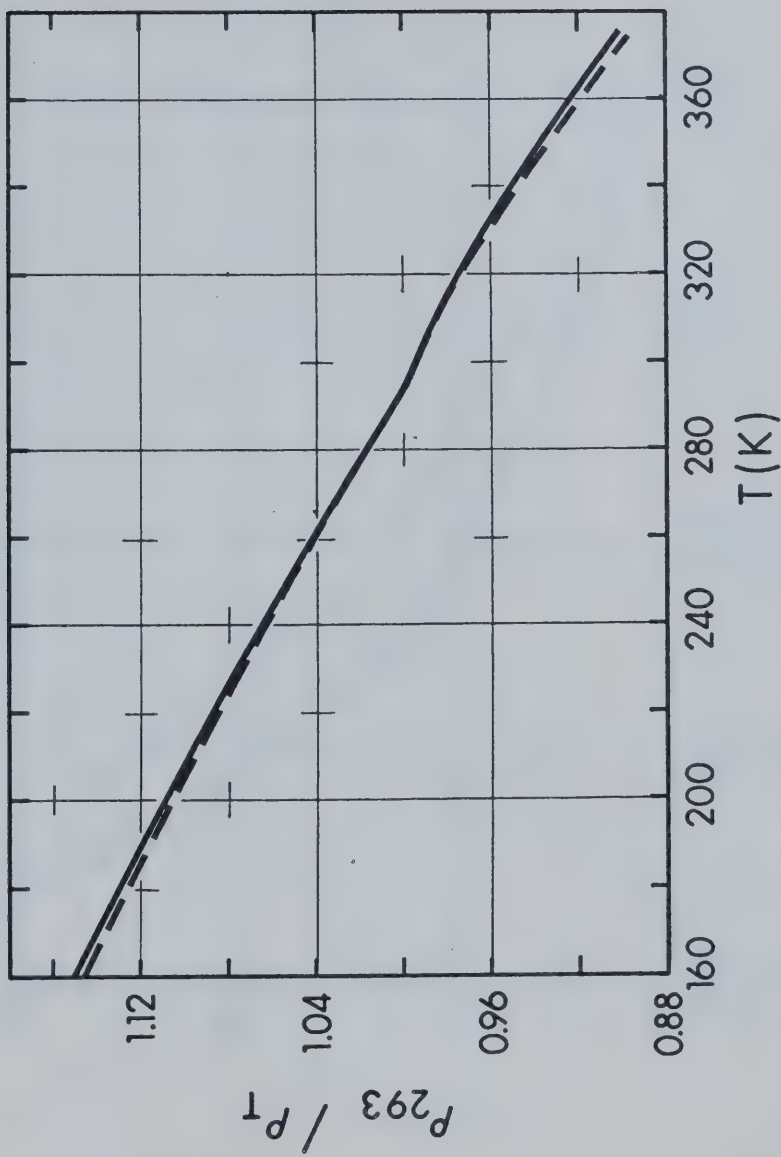


FIGURE III-19. The Effect of Temperature on the Density. 140

—, Methanol; —, Ethanol.

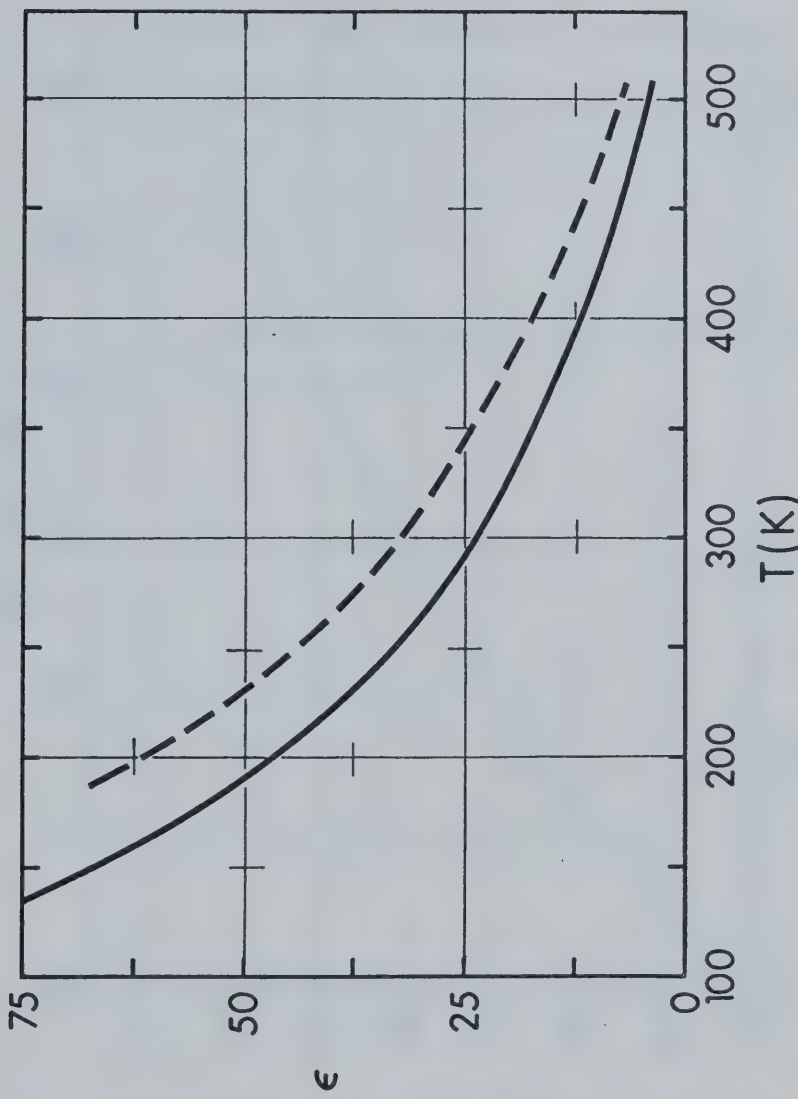


FIGURE II-20. The Effect of Temperature on the Static Dielectric Constant. 141,142 -----, Methanol; ——, Ethanol.

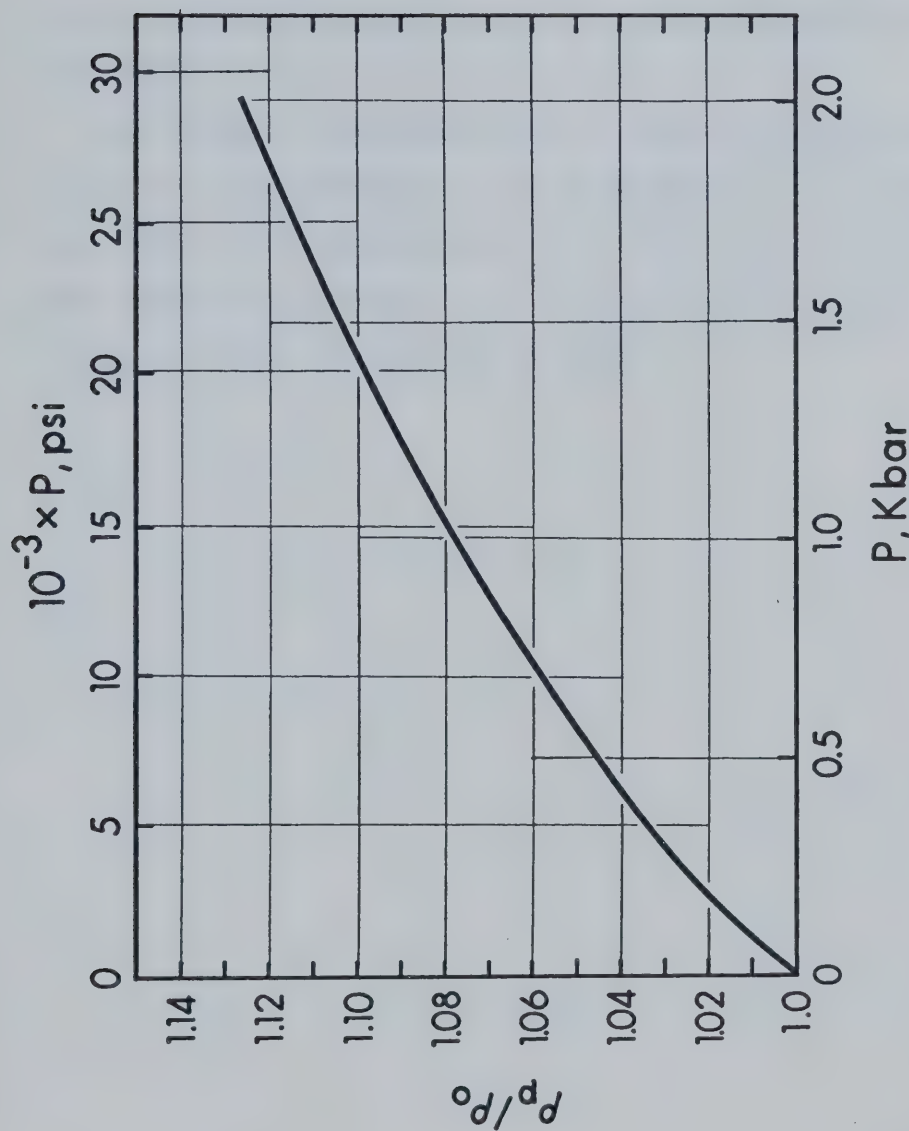


FIGURE III-21. The Effect of Pressure on the Density of Methanol and Ethanol. 143

calculated from data given in ref. 143. Multiplying the absorbed dose or concentration determined at 1 bar by ρ_p/ρ_o adjusted for the change in solvent density with pressure.

The effect of pressure on ϵ is given in Figure II-22. There is some conflict in the literature ^{144,145} about the effect of pressure on ϵ . The data from ref. 145 was chosen because the 1 bar values agreed well with those of refs. 141 and 142 at 293K.

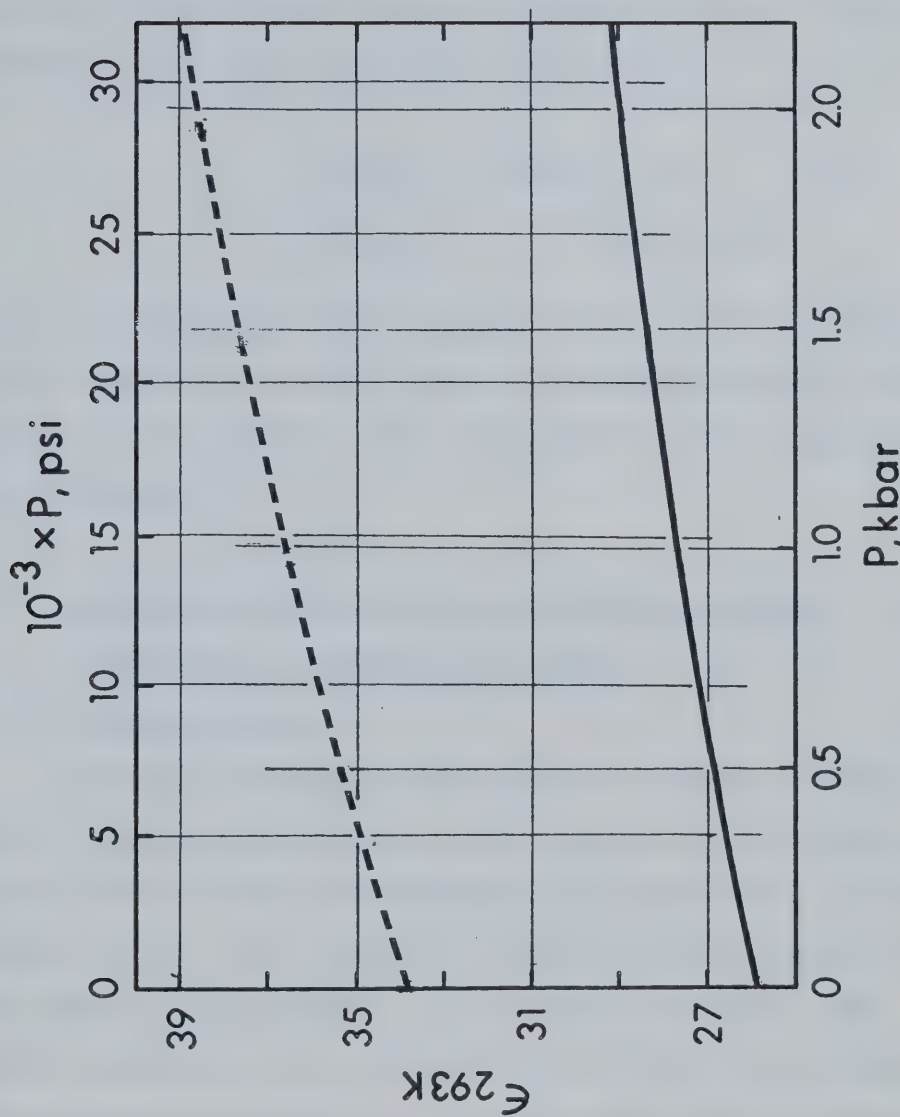


FIGURE III-22. The Effect of Pressure on the Dielectric Constant. 145 ———, Methanol; ——, Ethanol

R E S U L T S

Throughout the results section, there will be reference to the two main types of reactions of e_s^- investigated in this work. These are (4) and (5).



k_4 is a first order rate constant for the decomposition of e_s^- and has units s^{-1} . k_5 is a second order rate constant for the reaction of a scavenger (S) with e_s^- , and has units of $M^{-1} s^{-1}$.

A. SOLVATED ELECTRON OPTICAL ABSORPTION SPECTRA

1. THE EFFECT OF TEMPERATURE CHANGE

a. Neutral Ethanol

Spectra measured in pure neutral ethanol at temperatures from near its freezing point to near its boiling point (155 to 343K) are presented in Figure III-1. The absorbance (A) was calculated from measurements made at the end of 1.0 μs pulses of 1.87 MeV electrons. The pulse length (0.1 or 1.0 μs) had no effect on the energy of maximum absorbance (E_{\max}) or the peak width at half height ($W_{\frac{1}{2}}$) of a spectrum. The maximum absorbance (A_{\max}) per unit dose was lower for 1.0 μs pulses than for 0.1 μs pulses, especially at high temperature. This

was due to more decay occurring during the longer pulse as the solvated electron (e_s^-) lifetime became shorter.

The values of E_{\max} , $W_{\frac{1}{2}}$ and the wavelength at which A_{\max} occurred (λ_{\max}) are listed in Table III-1. There is good agreement with values obtained previously at 195 and $\sim 298K$.⁶⁷ Similar data obtained in neutral methanol^{65,67} are also tabulated for comparison.

In order to determine $W_{\frac{1}{2}}$ from the spectra in Figure III-1, extrapolation of the curves was necessary. This extrapolation was made assuming a bell shaped absorption on a wave length (λ) plot. Extrapolation of the high energy portion (short λ) would introduce a larger possible error in $W_{\frac{1}{2}}$ than would extrapolation of the low energy (long λ) portion of a spectrum. Fortunately only a short extrapolation was usually necessary to determine the half-height on the high energy side. $W_{\frac{1}{2}}$ increased slightly with increasing temperature.

The room temperature spectrum generally agrees well in shape and position with that determined by others.^{64, 67, 71} There is no indication of structural features recently reported.¹⁴⁶ A careful re-determination of the spectrum by Gavalas and Dorfman⁷¹ also failed to show any resolvable structure.

At lower temperatures an initial fast decay component of the absorption became increasingly apparent. This "spike" was due to absorption by solvated electrons

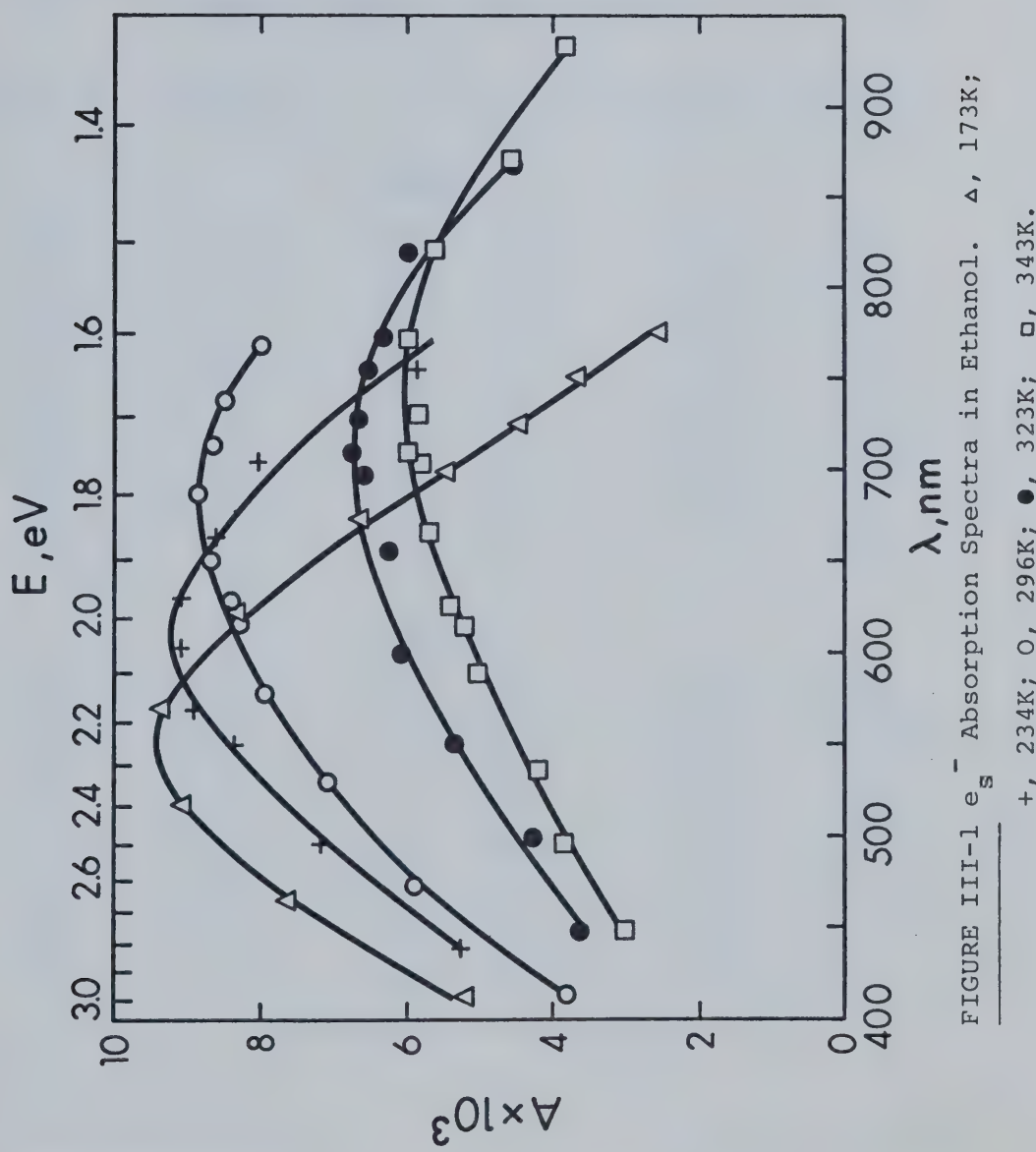


FIGURE III-1 e^- Absorption Spectra in Ethanol. Δ , 173K;

+, 234K; ○, 296K; ●, 323K; □, 343K.

TABLE III-1

Solvated Electron Optical Absorption Properties

Neutral Ethanol and Methanol^a

T, \pm 2K	ρ , g/cm ³ ^b	ϵ ^c	λ_{max} , nm ^d	E_{max} , eV	$W_{1/2}$, eV
<u>Ethanol</u>					
155	0.908	64.5	545	2.27	~1.3
173	0.892	56.2	555	2.23	1.4
(195) ^e	0.871	48.1	(582)	(2.13)	(1.4)
234	0.836	37.0	610	2.03	1.4
296	0.780	24.5	688	1.80	1.4
(~298)	0.778	24.2	(700)	(1.77)	(1.55)
323	0.755	20.8	715	1.73	1.5
343	0.737	18.4	745	1.66	1.5
<u>Methanol</u>					
183	0.888	69.0	557	2.22	1.1
(195)	0.879	63.8	(565)	(2.20)	(1.26)
243	0.836	45.3	600	2.07	1.3
294	0.792	33.5	635	1.95	1.3
(~298)	0.788	32.7	(630)	(1.97)	(1.29)
320	0.767	29.0	651	1.90	
336	0.752	26.5	675	1.84	
358	0.729	23.3	710	1.75	

^a Reference 65.^b From Figure II-19.^c From Figure II-20.^d Mean deviation \pm 1%.^e Values in brackets are from reference 67.

that rapidly undergo geminate neutralization.³⁰ They may be called geminate ions and are designated ($e_{s,\text{gem}}^-$). To obtain the spectrum of only solvated electron free ions ($e_{s,\text{fi}}^-$) the slow decay portion was extrapolated back to the end of the pulse. First order plots including the extrapolation were linear. On the time scale of the present work, there would be no effect on the E_{max} or $W_{\frac{1}{2}}$ of the low temperature spectrum if the absorption due to $e_{s,\text{gem}}^-$ was included. This is shown in Figure III-2 using the e_s^- spectrum in neutral ethanol at 166K. The curve through the circles is the total A at the end of a 0.10 μs pulse. The curve through the triangles is the A 4 μs after the end of the pulse. Here most of the $e_{s,\text{gem}}^-$ absorption has decayed. ($t_{\frac{1}{2}} \leq 1 \mu\text{s}$). The lowest curve, through the squares, is the difference between the first two. It is enriched in A due to $e_{s,\text{gem}}^-$ and has λ_{max} of $570 \pm 20 \text{ nm}$. For the total e_s^- and the $e_{s,\text{fi}}^-$ spectrum, λ_{max} is $565 \pm 5 \text{ nm}$. The shape of the spectrum is also independent of time, within experimental error. A short extrapolation on the high energy side enables determination of $W_{\frac{1}{2}}$'s of 0, 1.30 eV; Δ , 1.25 eV; and \square , 1.27 eV.

The only effect of including the "spike" in plotting a spectrum of e_s^- in low temperature alcohols is to increase A proportionally at all wavelengths. This would not be the case at shorter times. At ns times

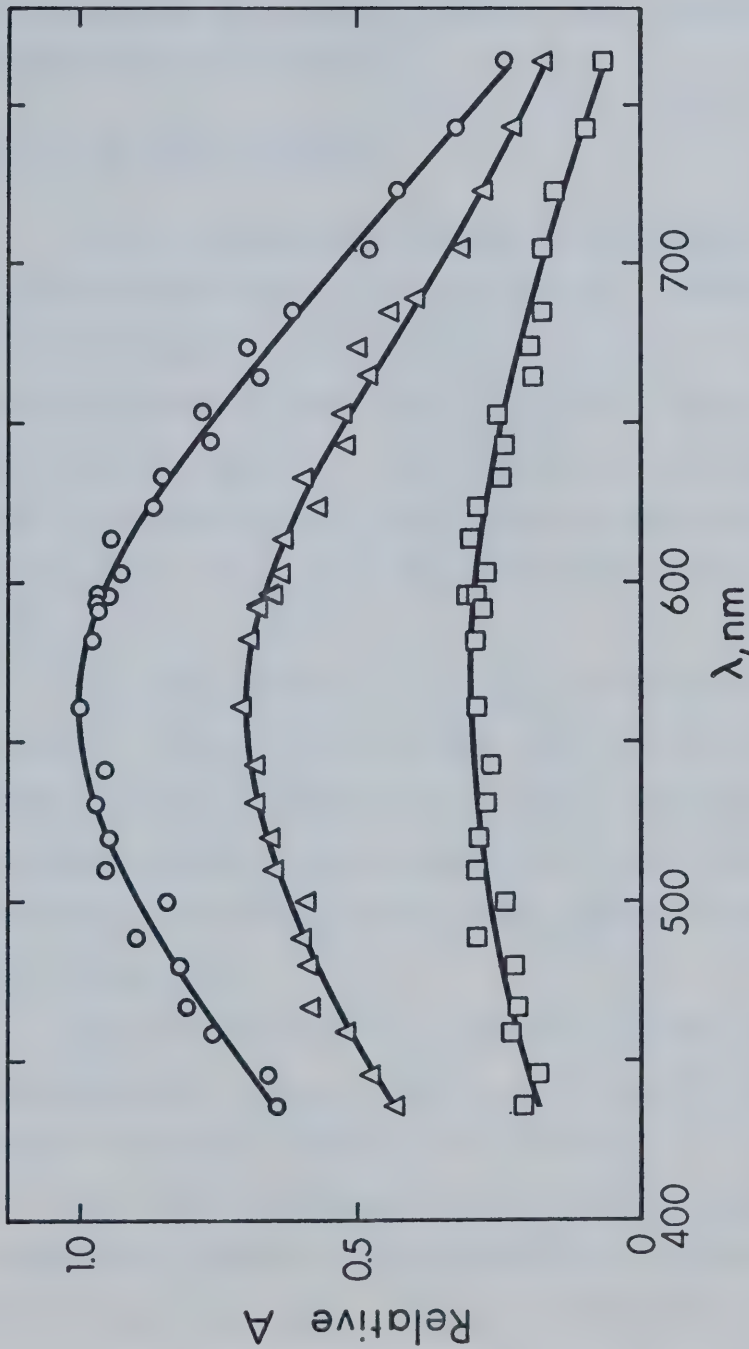


FIGURE III-2.

Time Dependent Shape of Solvated Electron Spectrum in Ethanol at 166K. O, A at $t = 0$; Δ, A at $t = 4 \mu s$; \square, A at $t = 0$, $- A$ at $t = 4 \mu s$. A in arbitrary units.

the spectrum E_{max} and $W_{1/2}$ are very time dependent in low temperature alcohols.³⁰⁻³²

b. \sim mM KOH in Ethanol

The e_s^- absorption spectra in irradiated \sim 1 mM KOH in ethanol are given in Figure III-3. The absorbance is that obtained for a SEM dose of 1.5 ncoul. The A was not corrected for decay in the pulse or change in dose with solvent density. This results in a natural vertical staggering of the spectra for minimum overlap. This would have no effect on the properties listed in Table III-2.

The 230K spectrum has a low A relative to the others. The e_s^- half life was also low (\sim 16 μ s) which indicates the presence of an electron scavenging impurity, probably oxygen. The A would be the only spectral property affected so long as the impurity concentration did not change.

The 168K spectrum includes the "spike" due to absorption by $e_{s,gem}^-$. The $e_{s,fi}^-$ spectrum had 26% lower A, but was otherwise identical.

$W_{1/2}$'s were not determined for spectra taken at high temperature because of the need for a long extrapolation on the low energy side. The $W_{1/2}$ of the room temperature spectrum is only approximate for the same reason.

The addition of \sim 1 mM KOH had no effect on E_{max}

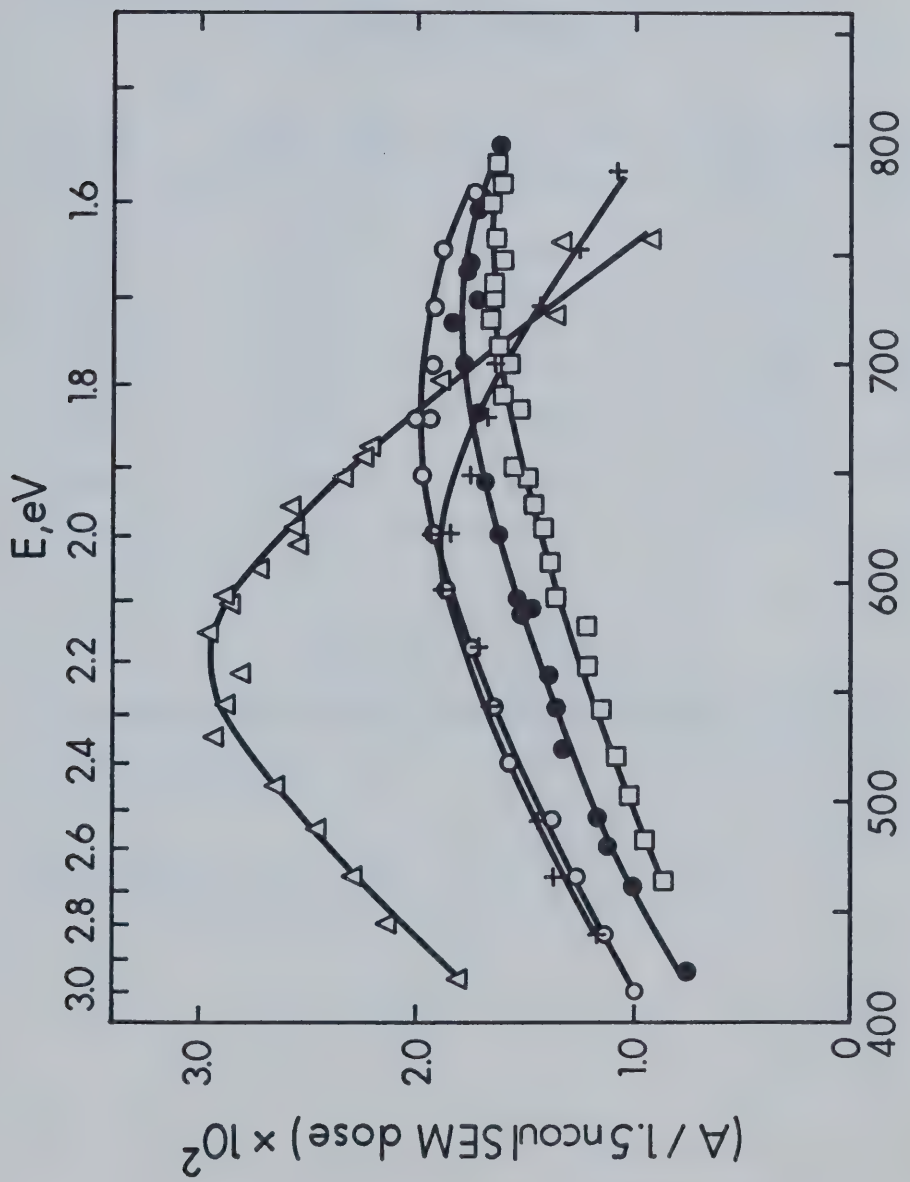


FIGURE III-3. e_s^- Absorption Spectra in ~ 1 mM KOH in Ethanol. Δ , 168K; \circ , 230K; \bullet , 294K; \square , 344K.

TABLE III-2Solvated Electron Optical Absorption Properties~1 mM KOH in Ethanol

T, \pm 2K	[KOH], mM ^a	λ_{max} , nm ^b	E_{max} , ev	$W_{1/2}$, ev
168	1.15	560	2.21	1.3
230	1.25	610	2.03	1.4 ₅
294	1.16	680	1.82	~1.6
324	0.98	720	1.72	
344	0.95	750	1.65	

^aBase concentration has been corrected for change in solvent density.

^b Mean deviation \pm 1%.

or $W_{\frac{1}{2}}$ of the e_s^- spectrum. It did increase A by about 30% at room temperature. This was due to base removing impurity which would normally react with e_s^- .

c. The Effect of Temperature on E_{\max} and $G_{fi} \cdot \epsilon_{\lambda_{\max}}$

The effect of temperature on E_{\max} of the e_s^- absorption in ethanol is shown in Figure III-4. Values plotted are taken from Tables III-1 and III-2. The temperature coefficient of the energy of maximum absorbance (dE_{\max}/dT) is -3.2×10^{-3} ev/deg in both neutral and mM basic ethanol. An earlier report gave $dE_{\max}/dT = -3.4 \times 10^{-3}$ ev/deg, ⁶⁴ determined from measurements at 195 and ~ 298 K.

Values of $G_{fi} \cdot \epsilon_{\lambda_{\max}}$ in neutral and mM basic ethanol are presented in Figure III-5 and Table III-3. The units of $G_{fi} \cdot \epsilon_{\lambda_{\max}}$ are (electrons $\ell/100$ ev mol cm). Only absorption due to $e_{s,fi}^-$ is included. An adjustment for change in absorbed dose for changing solvent density has been applied. Dose determination was based on the 2 mM aqueous KSCN actinometer using $G(OH) = 2.9$ and $\epsilon_{478}((SCN)^{2-}) = 7600 \text{ M}^{-1} \text{ cm}^{-1}$.

Where necessary, a correction was also applied for decay during the pulse using (2). The correction at room temperature, where $t_{\frac{1}{2}}$ of e_s^- was typically 4 μ s for a 1.0 μ s pulse, results in an increase in A of 9%. At low temperature the correction would be much less than 1% and was not made.

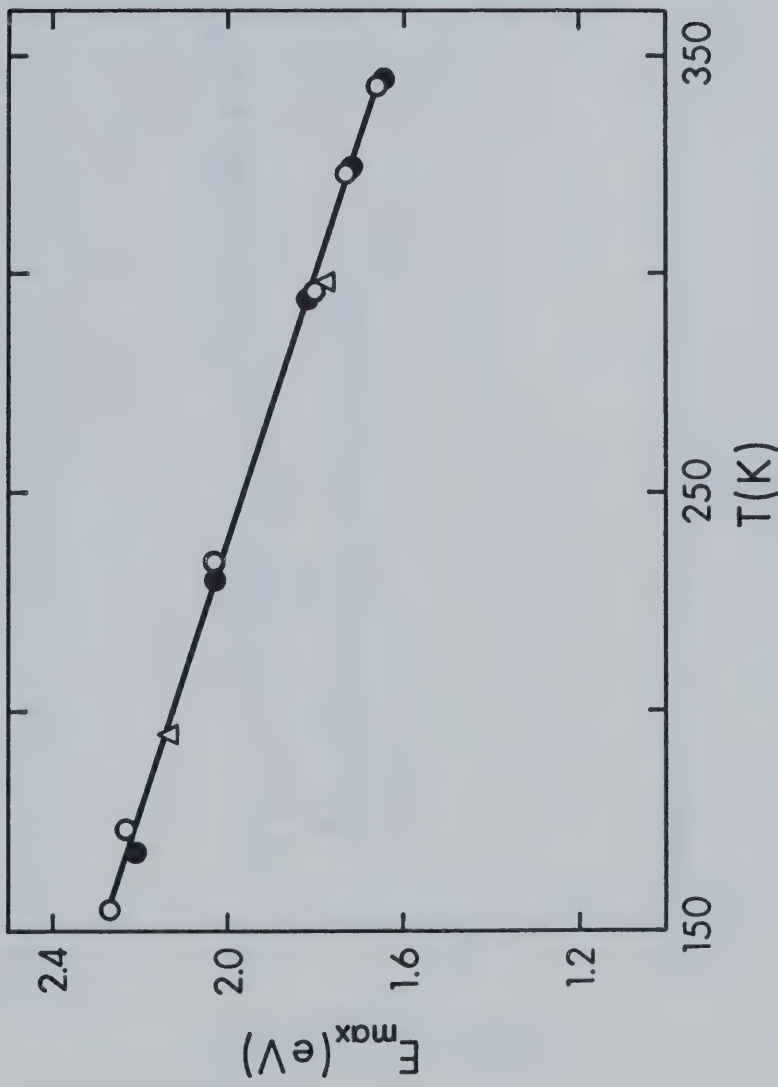


FIGURE III-4. Temperature Dependence of E_{\max} for e_s^- Absorption in Ethanol. ○, Neutral; ●, ~mM KOH; △, Reference 67

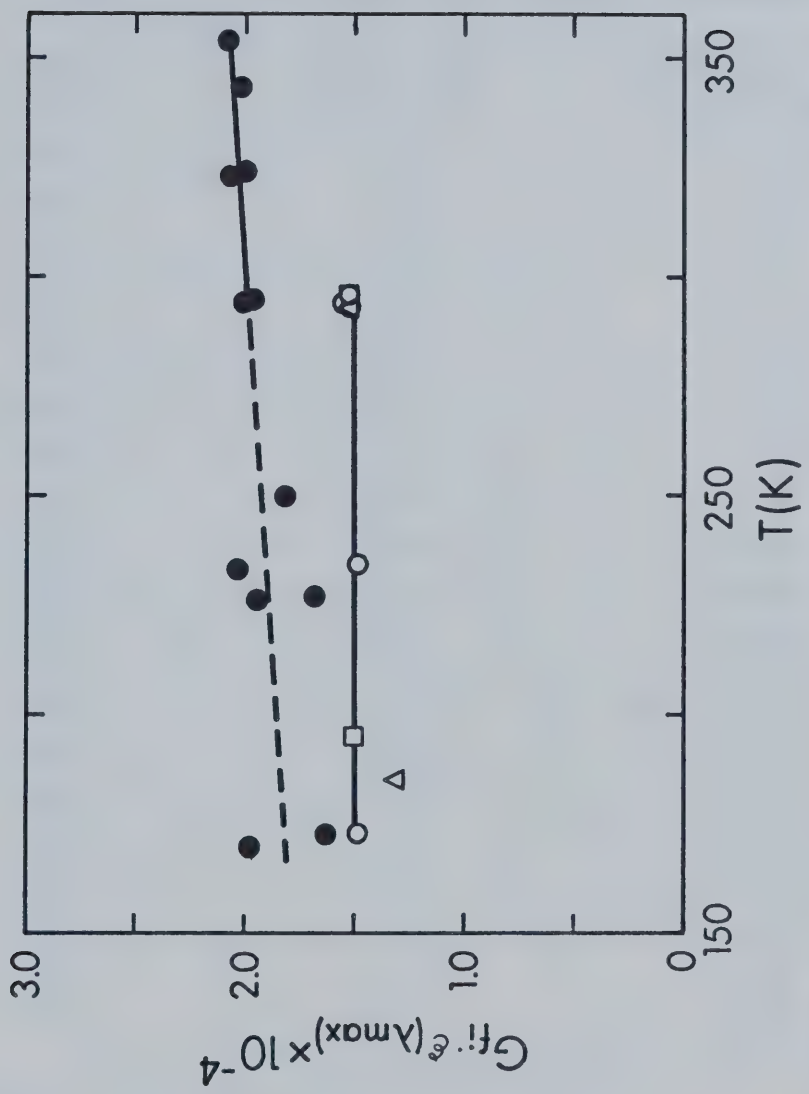


FIGURE III-5. Temperature Dependence of $G_{fi} \epsilon_{\lambda} \max$ in Ethanol.

\circ , Neutral; \bullet , \sim mM KOH; \square , Reference 67; Δ , Reference 31.

TABLE III-3

$G_{fi} \cdot \epsilon_{\lambda_{max}}$ in Neutral and $\sim \text{mM}$ KOH in Ethanol ^a		
T (K)	[KOH], mM^b	$10^4 \cdot G_{fi} \cdot \epsilon_{\lambda_{max}}^c$
~298	0.0	1.52 ^d
296	0.0	1.52
294	0.0	1.55
293	0.0	1.52
293	0.0	1.52 ^e
234	0.0	1.48
195	0.0	1.52 ^d
185	0.0	1.31 ^e
173	0.0	1.48
344	0.94	2.02
324	0.97	2.00
295	1.0	1.96
233	1.07	2.03
170	1.15	1.98
354	1.40	2.09
323	1.46	2.07
294	1.5	2.01
250	1.58	1.82
227	1.63	1.68
226	1.63	1.94
173	1.72	1.63

^a Both 1.0 and 0.1 μs pulses were used.

^b Corrected for solvent density.

^c Units of (electrons $\ell/100 \text{ eV mol cm}$).

^d Reference 67, normalized at room temperature to value from this work.

^e Reference 31.

$G_{fi} \cdot \epsilon_{\lambda_{max}}$ is independent of temperature in neutral ethanol. It increases slightly with increasing temperature in $\sim M$ basic ethanol. The value is always lower in neutral than in basic solution. The trends are the same in methanol.⁶⁵

2. THE EFFECT OF KOH CONCENTRATION

Absorption spectra for e_s^- in ethanol at $294 \pm 1K$ are given as a function of KOH concentration in Figures III-6 and III-7. The spectral properties are summarized in Table III-4. In order to calculate A it was necessary to know the solvent density. For 1.0 M KOH in ethanol a density of 0.842 gm/cm^3 was determined. Densities of other concentrations were found by interpolation between this and the pure solvent density.

The value of E_{max} was not affected by increasing base concentration. This has also been noted where the ethanol was made basic by the reaction with sodium metal.⁶⁹

A_{max} increased with increasing KOH concentration due to increasing yield of $e_{s,fi}^-$.

The spectrum shape, as indicated by $W_{1/2}$, appeared to be slightly base dependent. The narrowing at the highest base concentrations may have been partly due to the effect of water. The KOH used was about 15% water by

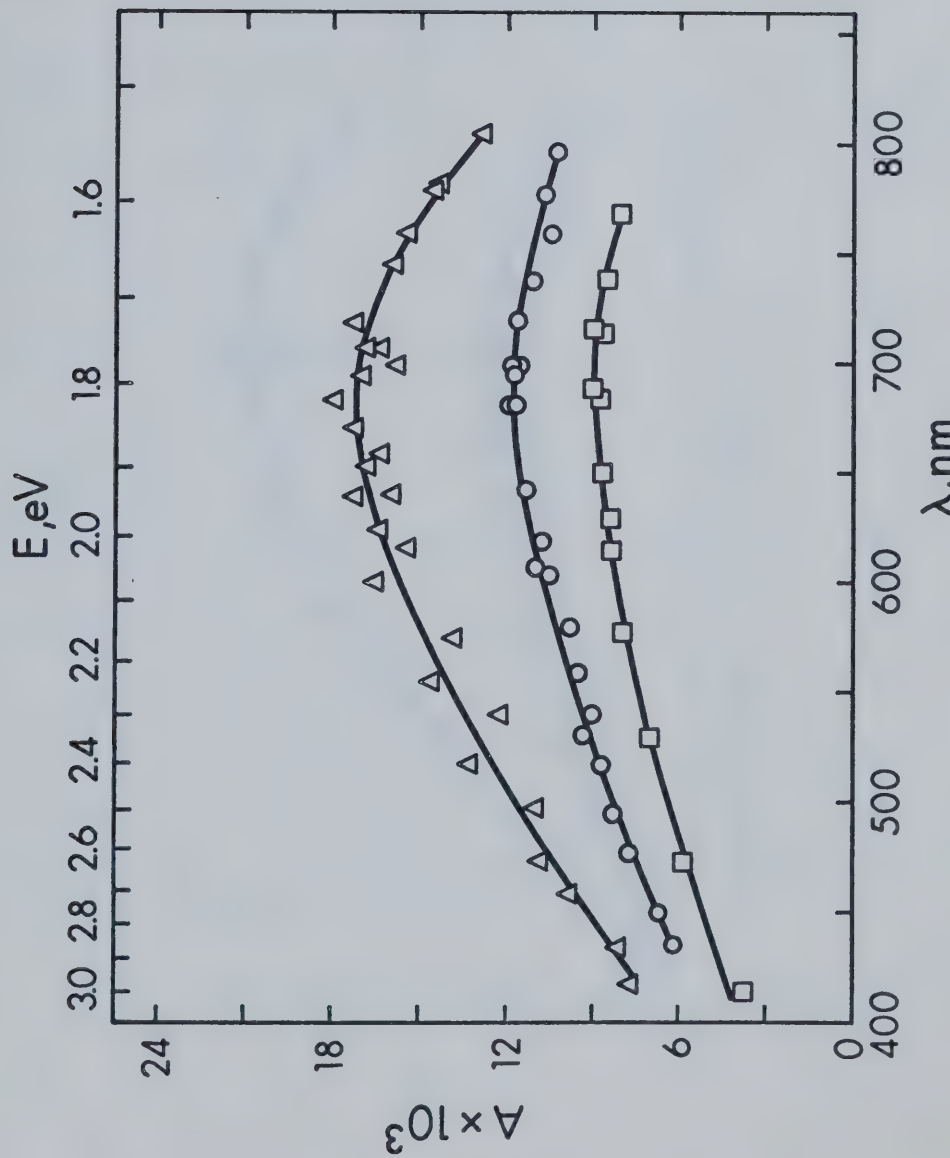


FIGURE III-6. e_s^- Absorption Spectra in Ethanol. $294 \pm 1\text{K}.$

Δ , 0.096 M KOH; \circ , 0.0011 M KOH; \square , neutral.

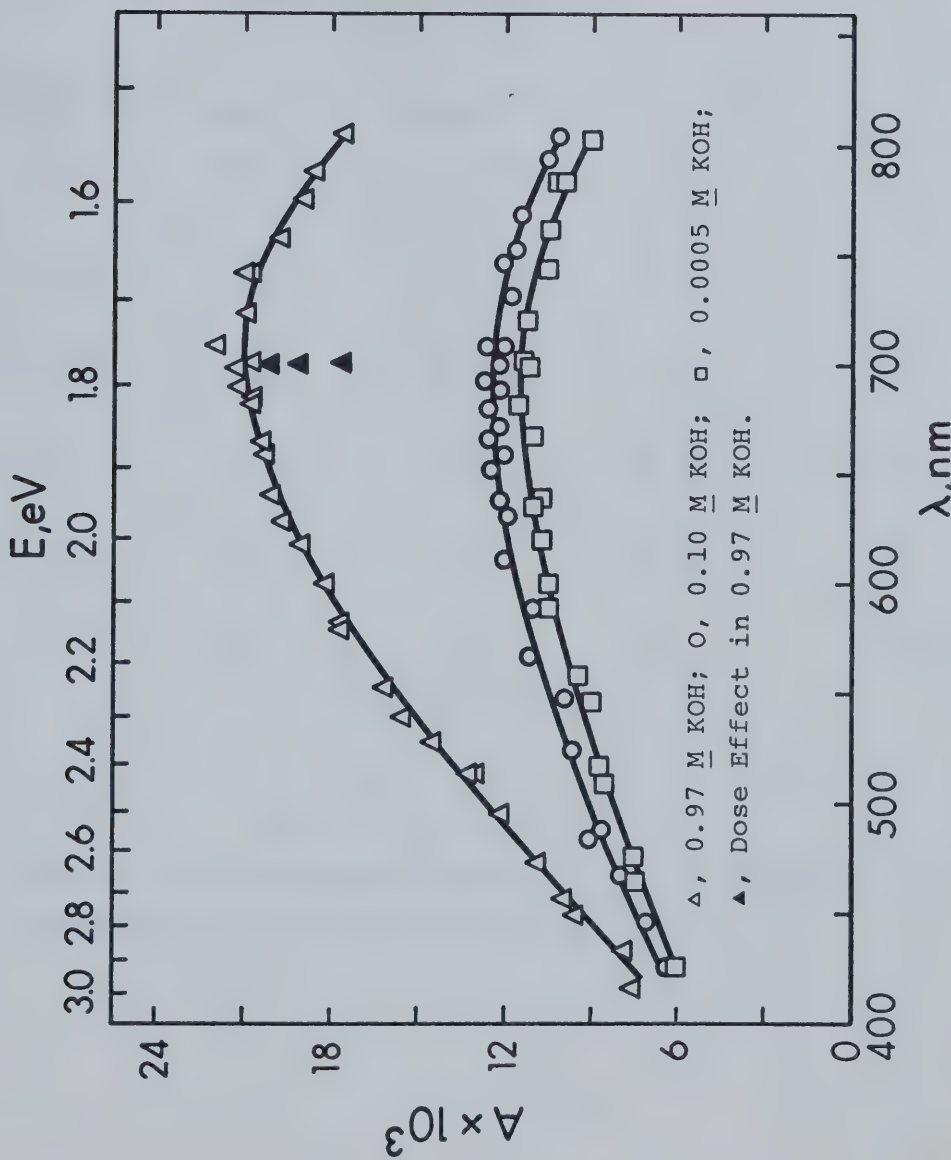


FIGURE III-7. e_s^- Absorption Spectra in Ethanol. $294 \pm 1\text{K}$.

TABLE III-4

Solvated Electron Optical Absorption Properties inBasic Ethanol, 294 \pm 1K

[KOH], M	λ_{max} , nm	E_{max} , eV	$A_{\text{max}} \cdot 10^3$	$W_{\frac{1}{2}}$, eV
0	690	1.80	8.87	1.4 ₇
0.0005	695	1.78	11.48	1.6 ₃
0.0011	690	1.80	11.70	1.5 ₆
0.010	685	1.81	12.45	1.6 ₇
0.096	684	1.81	17.25	1.4 ₂
0.97	705	1.76	21.0	1.25 ^a
Ave. 1.79 \pm 0.1				

^a Average from two spectra taken at widely separated times and different solution preparations.

weight. Thus a solution 1.0 M in KOH was at least 0.5 M in water. $W_{\frac{1}{2}}$ is much more dependent on the water content in ethanol-water mixtures than a direct relation to the mole fraction would predict.⁶⁷ The value of $W_{\frac{1}{2}}$ for the e_s^- spectrum in pure water is 0.885 eV⁶³ compared to 1.5 eV in pure alcohol. For spectra in ethanol-water solutions, $W_{\frac{1}{2}}$ is less than 1.0 eV for mixtures of greater than 0.25 mole fraction of water.⁶⁷

The effect of dose was much less in basic ethanol than in the pure neutral alcohol. A_{\max} had not changed after 500 1.0 μ s pulses in 0.97 M KOH. The solid triangles in Figure III-7 show the decrease in A due to 1,500, 3,000 and 6,000 pulses of 1.0 μ s duration.

3. THE EFFECT OF IMPURITIES THAT SCAVENGE e_s^-

Spectra taken in ethanol with added impurity are given in Figure III-8. The spectrum in 4.7×10^{-5} M H_2SO_4 solution was the same in shape ($W_{\frac{1}{2}} = 1.5$ eV) and position ($\lambda_{\max} = 690$ nm) as that in pure ethanol.

The spectrum in 1.9×10^{-4} M acetone solution had a shoulder near 540 nm. A shoulder in this region was found previously in unpurified ethanol.^{68,147} This shoulder was not found when purified ethanol was used.⁶⁴ At 1.0 μ s after the end of the pulse the spectrum appeared slightly time dependent between 530 and 630 nm. At 570 nm the absorption was about 7% greater than

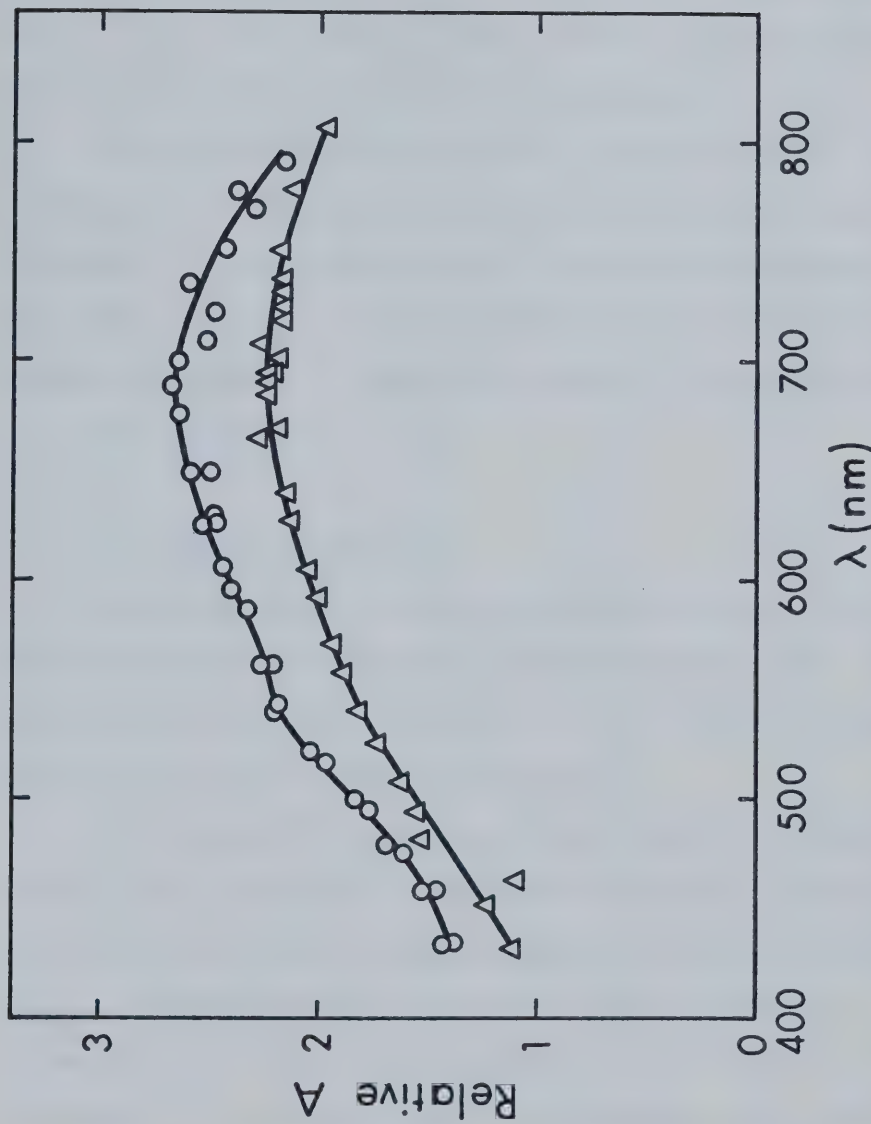


FIGURE III-8. The Effect of Scavenger on the Solvated Electron Spectrum in Ethanol. O, 1.9×10^{-4} M Acetone, 295K; Δ , 4.7×10^{-5} M Sulfuric Acid, 297K.

would be expected from assuming the absorption to decay at the same rate as at λ_{\max} . Due to the short lifetime of e_s^- ($t_{1/2} = 0.7 \mu s$) in this solution, time dependence at longer times could not be determined.

It was attempted to obtain a spectrum in a 1 mM acetone in ethanol solution to see if the shoulder was enhanced. The spectrum had a lot of scatter because the very short $t_{1/2}$ (~ 160 ns) made reading of the photographs difficult. There was, however, no evidence of a larger shoulder.

4. THE EFFECT OF PRESSURE

Solvated electron absorption spectra measured in pure methanol and ethanol at pressures of 1 bar, 1 kb and 2 kb are given in Figures III-9 and III-10. Electron pulses of 1.0 μs duration were used.

The values of λ_{\max} , E_{\max} and $W_{1/2}$ are listed in Table III-5. Within experimental error the 1 bar results are the same as those obtained in quartz cells. E_{\max} variation with pressure in ethanol compares favorably with that found previously in 5 mM NaOH solution.¹¹⁵ The shift due to pressure in E_{\max} and λ_{\max} was 0.10 eV and -30 nm per kilobar in methanol. In ethanol the shift was 0.075 eV and -25 nm per kilobar.

The $W_{1/2}$ increased with pressure in both alcohols

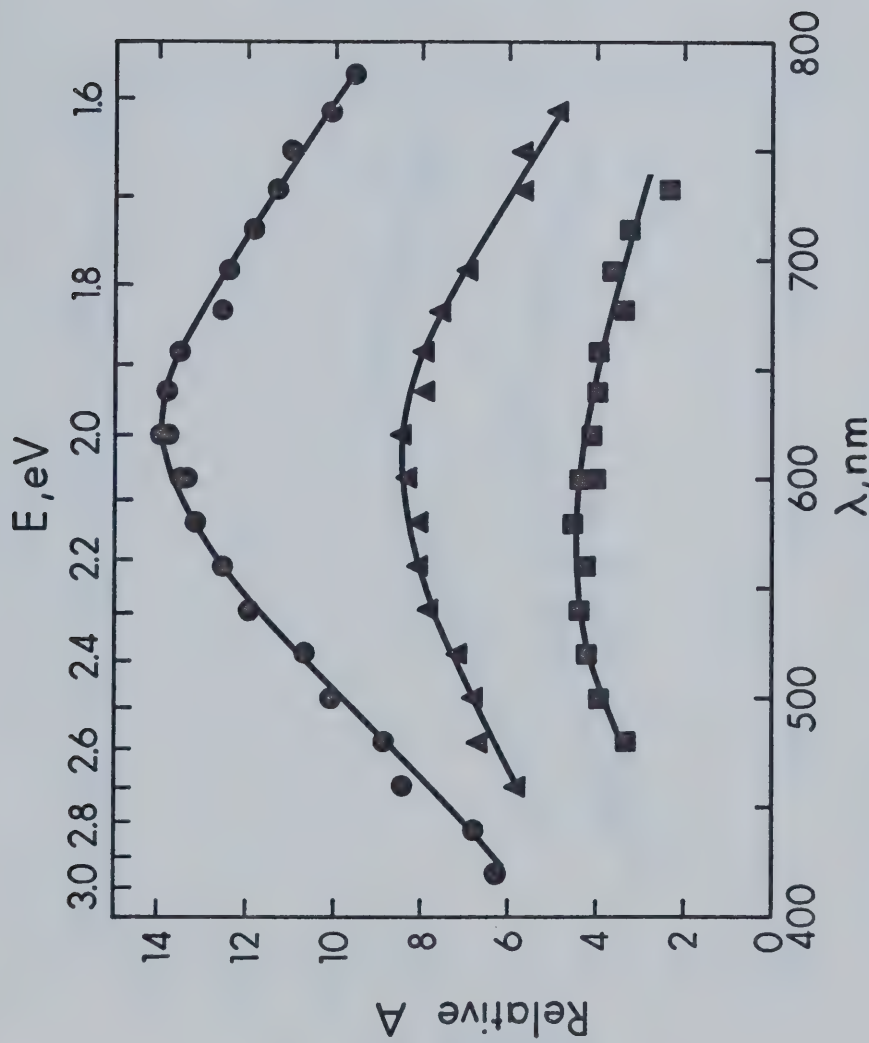


FIGURE III-9. e_s^- Absorption Spectra in Methanol.

●, 1 bar; ▲, 1 kb; ■, 2 kb. 295 \pm 1K.

A in arbitrary units.

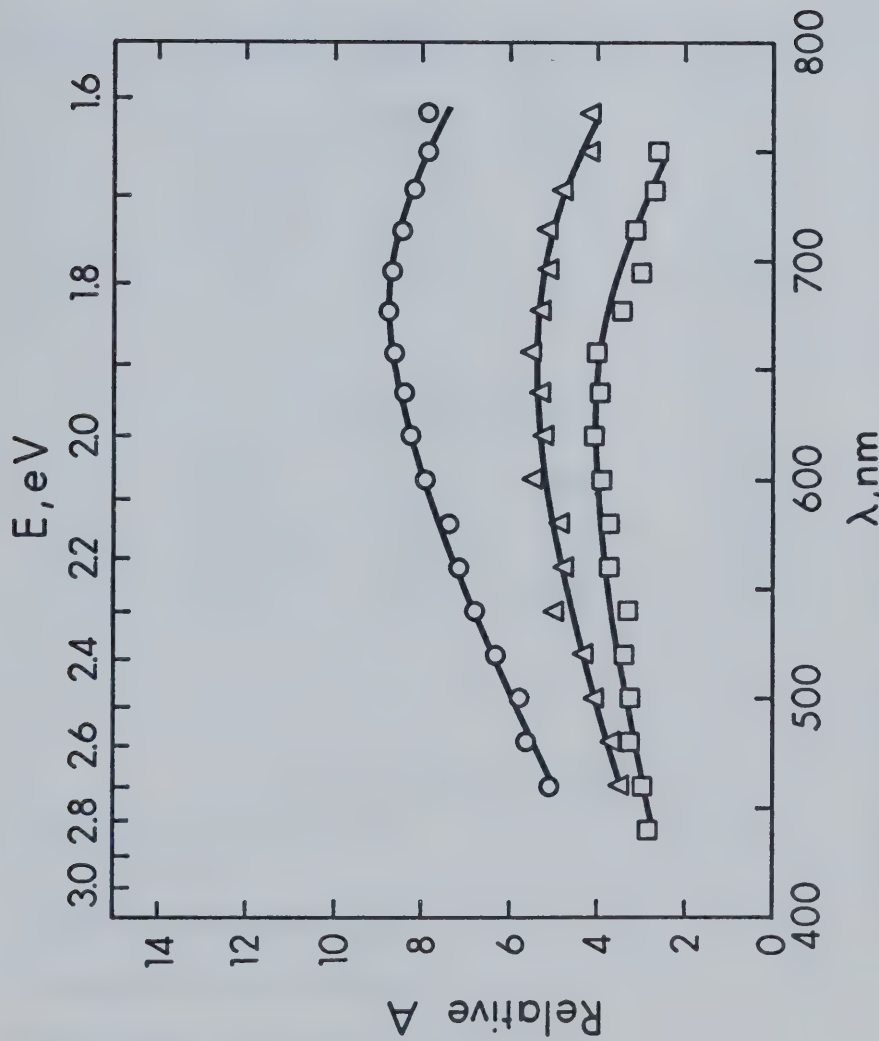


FIGURE III-10. e_s - Absorption Spectra in Ethanol.

\circ , 1 bar; \triangle , 2 kb; \square , 2 kb.

294 ± 1 K. A in arbitrary units.

TABLE III-5

Pressure Effects on the Solvated Electron OpticalAbsorption Spectrum

P (bars) ^a	ρ (g/cm ³) ^b	ϵ_{293K}^c	λ_{max} (nm) ^d	E_{max} (eV)	$W_{1/2}$, (eV)
<u>Methanol, 295K</u>					
1	.791	33.8	630	1.97	1.3 ₆
1k	.850	36.6	610	2.03	1.4 ₅
2k	.895	38.6	570	2.17	
<u>Ethanol, 294K</u>					
1	0.789	25.8	680	1.82	1.4
1k	0.849	27.6	660	1.88	1.5
2k	0.888	28.9	630	1.97	1.7

^a Pressure read to \pm 4%.

^b Determined from Figure II-21.

^c Determined from Figure II-22.

^d Wavelength deviation may be \pm 1%.

as has been found in water.^{115,118}

The A decreased with increasing pressure. The spectra have been corrected for decay during the pulse. They have also been adjusted for change in absorbed dose with increasing solvent density. This adjustment was made assuming all of the solution analyzed to be penetrated by the electron beam. It resulted in a decrease in A of 7.5% at 1 kb and 12.5% at 2 kb. However, as shown below, this correction would be in the wrong direction if 2.2 MeV electrons did not penetrate all of the solution sampled by the analyzing light.

The effect of increasing electron beam energy on relative A of e_s^- in methanol is shown in Figure III-11. The electron pulses were 1.0 μ s in duration. The temperature was 296 \pm 1K. The relative A plotted was for λ_{max} , and was determined from short scans of the top of the spectrum at each pressure and beam energy. A correction for decay during the pulse was applied. It varied from an 18% increase in relative A at 1 bar to a 51% increase at 2 kb.

Adjustment for increased absorbed dose with increased solvent density was only applied at 2.32 and 2.255 MeV. Leveling off of the A between these energies indicated all of the solution volume analyzed was being penetrated by the electron beam.

A cross section of the volume of solution analyzed

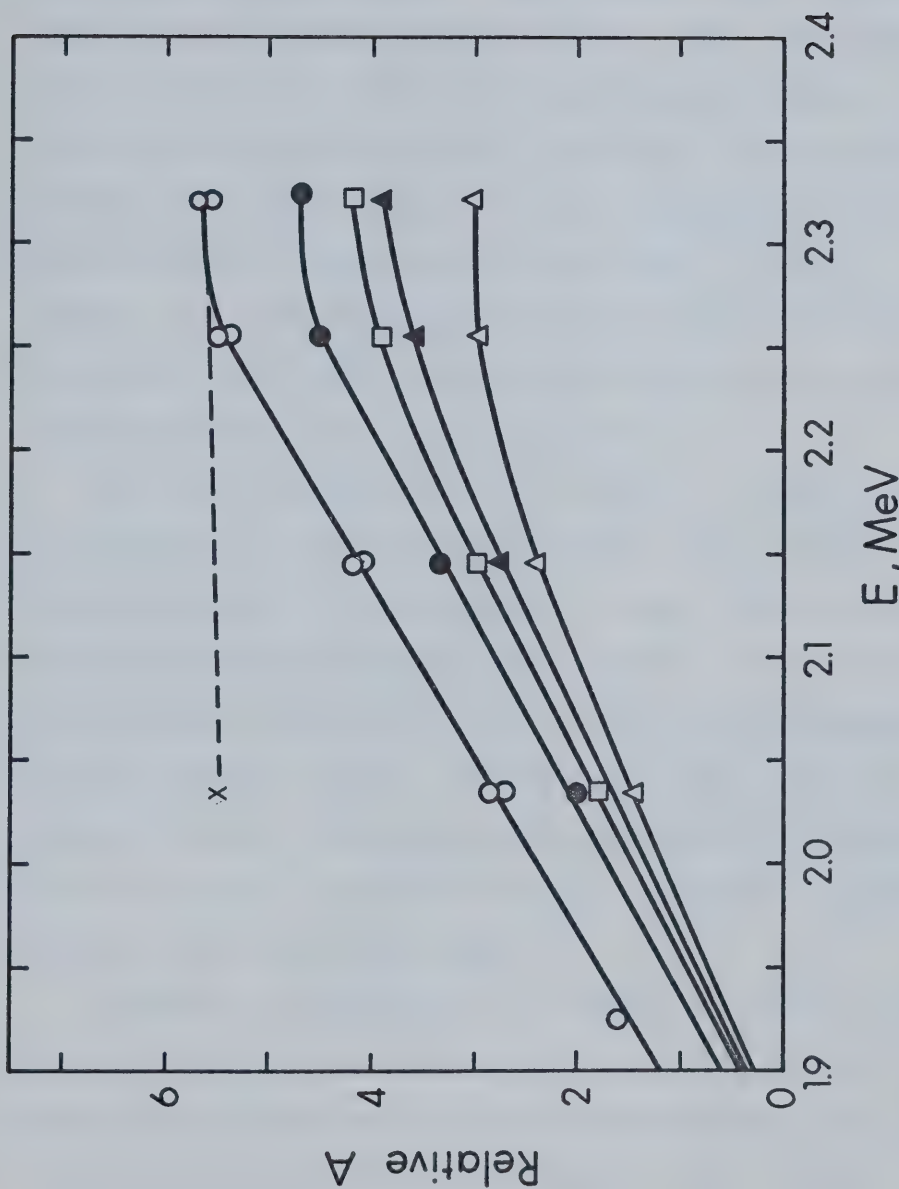


FIGURE III-11. Relative A in Methanol as a Function of Electron Beam Energy. O, 1 bar; ●, 0.55 kb; □, 1.03 kb; ▲, 1.52 kb; △, 2.07 kb; X, 1 bar corrected. 296K. A in arbitrary units.

is given in Figure III-12. The circular area indicates the 6.35 mm diameter analyzing light beam. The edges of this beam were cut off by the monochromator slits. This is approximately indicated by the dashed lines on the figure. The exact manner in which the analyzed light was affected by the slits was not known. It was assumed that 1 mm from each edge of the beam was lost. The area of the circle between the dashed lines is then a cross section of the analyzed volume.

At beam energies below 2.25 MeV all of the dose was deposited in the solution between the electron window and the back of the analyzed volume. The effect of increasing solvent density with pressure would be to increase that amount of the total dose being absorbed by the solution between the electron window and the analyzed volume. Correction for this would increase the relative A , in contrast to the case where the entire analyzed area was penetrated.

Accurate allowance for the change in A with solvent density could not be made in this case, due largely to insufficient knowledge of the distance between the electron window and analyzed volume. This distance increased with pressure in an unknown manner due to compression of the Teflon O ring and slight outward bowing of the steel window.

At a single pressure, A decreased with decreasing

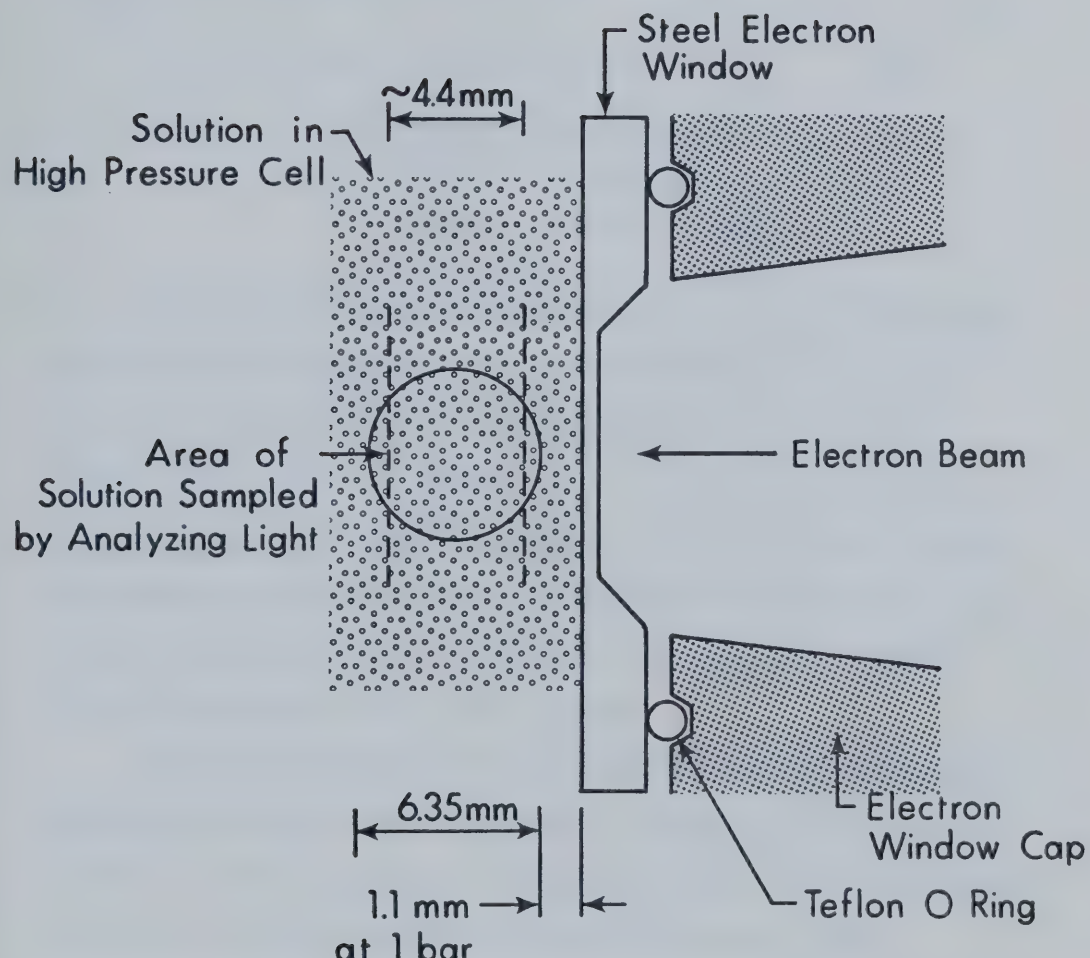


FIGURE III-12. Diagram Showing Area of Solution Sampled by Analyzing Light Beam.

beam energy. This was largely the result of less penetration of the solution by the electron beam.

$$R = 0.543E - 0.160 \quad (6)^3$$

R = range of electrons in
gms/cm² of aluminum

E = electron energy in MeV.

Using (6) it was calculated that a 2.035 MeV electron beam would penetrate 4.68 mm of methanol at 1 bar ($\rho = 0.79 \text{ gm/cm}^3$) after passing through the 0.71 mm thick steel electron window ($\rho = 8.1 \text{ gm/cm}^3$). The distance between the electron window and the analyzed volume was about 2.1 mm at 1 bar. Therefore electrons did not penetrate more than 2.58 mm into the analyzed volume.

This is just over half way across.

A similar calculation for 2.32 MeV electrons showed they penetrated 6.64 mm beyond the electron window, or at least 0.1 mm beyond the analyzed volume. The concentration of absorbing species, averaged over the whole analyzed volume, would therefore be about twice as great for a 2.32 MeV as for a 2.035 MeV electron pulse.

Correcting the relative A in Figure III-11 for the lower penetration at lower energies at all pressures, as well as for change in solvent density at high pressures, would tend to give nearly horizontal line plots. This is indicated by the x and the dashed line

in Figure III-11.

There is a monotonic decrease in A with increasing pressure even when all necessary adjustments are applied. The decrease in A_{\max} at a beam energy of 2.32 MeV is plotted in Figure III-13, and indicates $dA_{\max}/dP = -25\%$ per kb in methanol.

5. THE EFFECT OF PULSE DOSE ON ABSORBANCE

The effect of pulse dose on A in neutral and 1.1 mM KOH in ethanol solution is given in Figure III-14. All points have been corrected for decay during the pulse. For both the neutral and basic solutions, there was a linear relation between A and pulse dose. The A in the 1.1 mM basic solution was 26% greater than that in neutral ethanol.

For pulse doses greater than about 3 ncoul from the SEM, there was increased scatter, especially in the neutral alcohol. Pulse doses of greater than 2.0 ncoul were not normally used in quartz cells.

6. THE EFFECT OF ADDED WATER

As is indicated in Figure III-15, there was a large initial increase in A of e_s^- in ethanol when a small amount of water was added. Further addition of water resulted in A increasing linearly with the weight percent of water added.

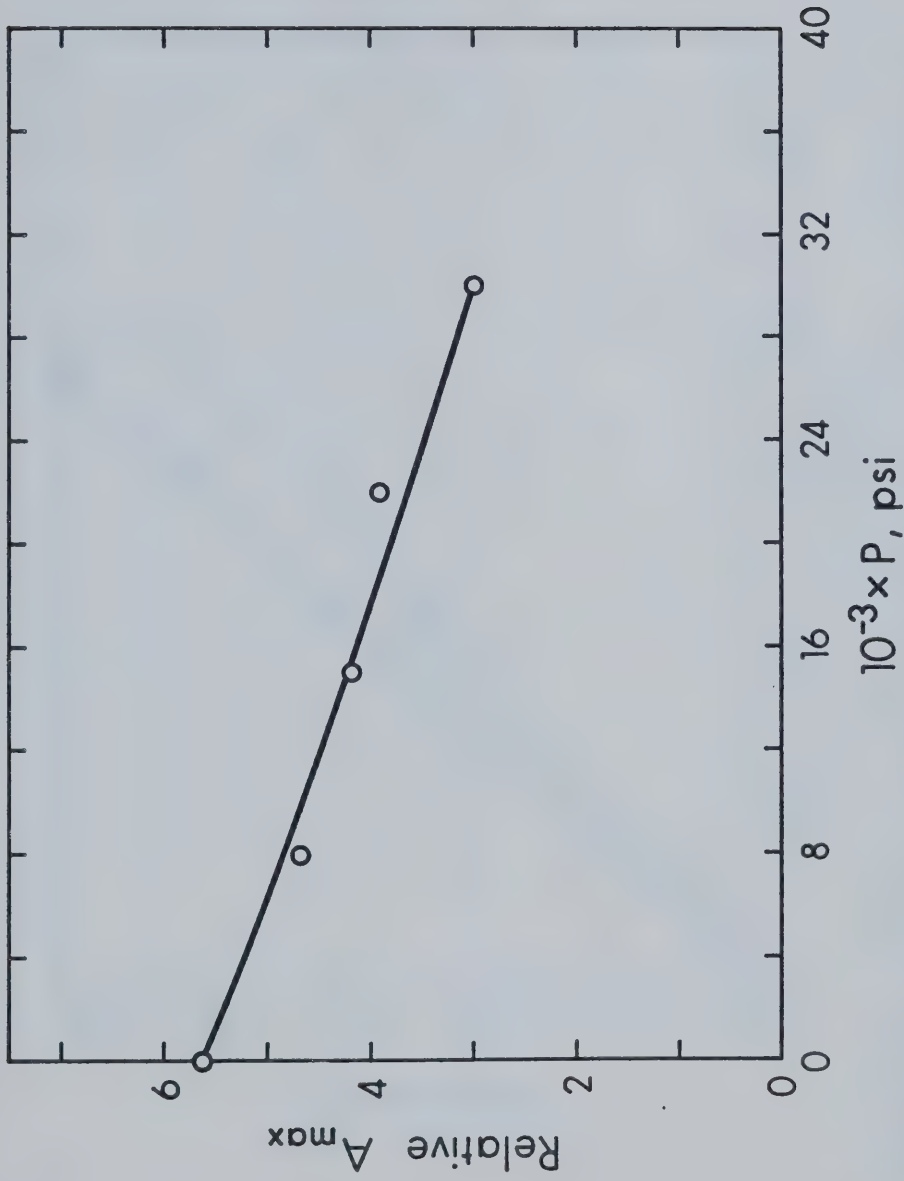


FIGURE III-13. The Decrease in A_{max} in Methanol with Increasing Pressure.
2.32 MeV Electron Pulses of $1.0 \mu\text{s}$ Duration. A in
arbitrary units

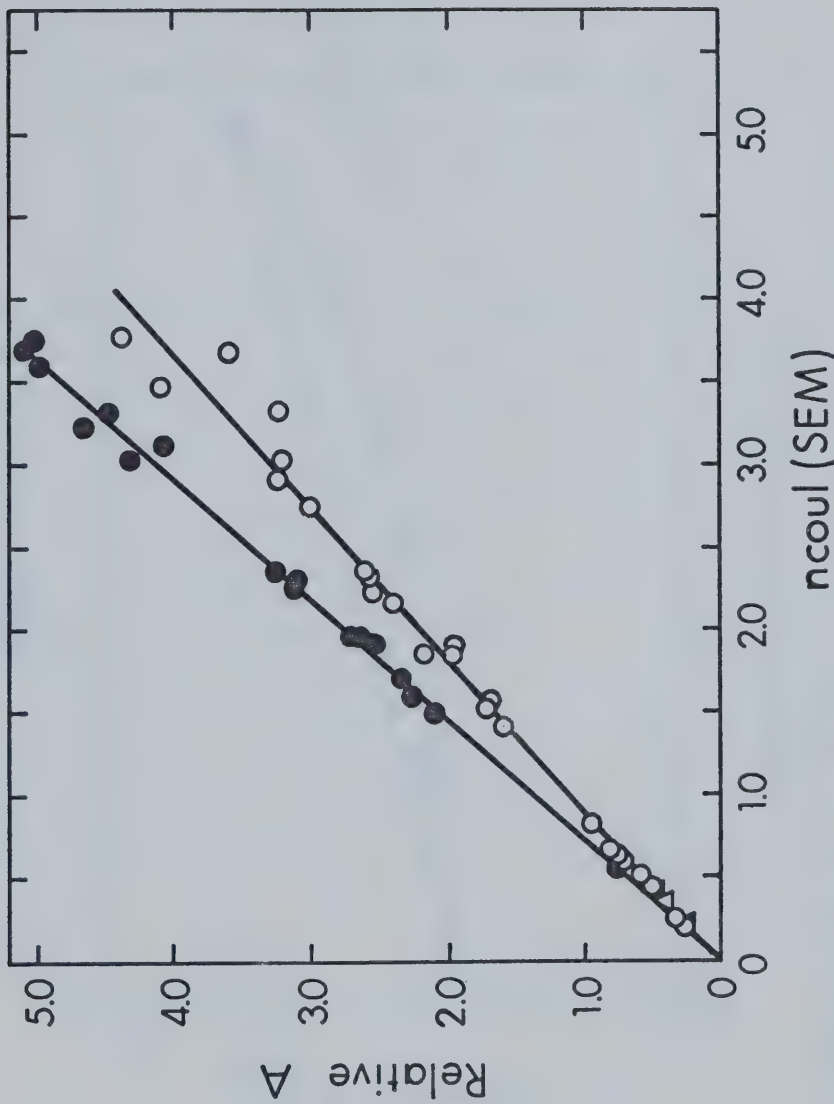


FIGURE III-14. The Effect of Pulse Dose on the A of e^- in Ethanol. 0, 1.0 μs Pulse, Neutral; ●, 1.0 μs Pulse, 1.1 mM KOH; ▲, 0.1 μs Pulse, 1.1 M KOH; △, 0.1 μs Pulse, Neutral. A in arbitrary units.

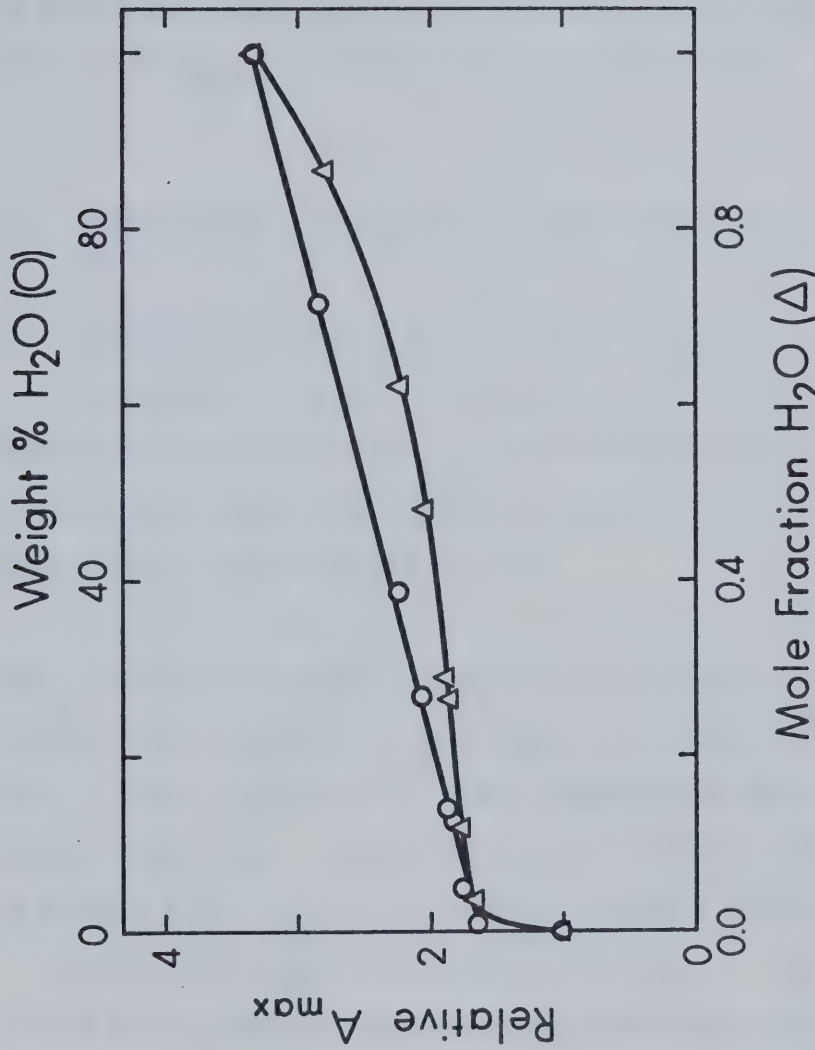


FIGURE III-15. The Effect of Water on the Δ_{\max} of e_s^- in Ethanol. $296 \pm 1\text{K}$.
690 nm. $1.0 \mu\text{s}$ Pulses. A in arbitrary units.

A is proportional to the product $G\cdot\epsilon$, so that

$A_{H_2O}/A_{EtOH} = G\cdot\epsilon_{H_2O}/G\cdot\epsilon_{EtOH}$. From the figure, the ratio of A_{max} in water to A_{max} in ethanol is 3.30. This ratio is about 5% lower than that obtained from published values of $G\cdot\epsilon_{max}$ in water⁶³ and ethanol.^{64,65}

B. TEMPERATURE EFFECTS ON e_s^- REACTION KINETICS

1. NEUTRAL AND $\sim 1mM$ KOH SOLUTIONS OF ETHANOL

Arrhenius activation energy (E_a) plots for the decomposition reaction of $e_{s,fi}^-$ in neutral and $\sim 1 \text{ mM}$ KOH solutions of ethanol are given in Figure III-16. The temperature range was 350 to 166K.

For both neutral and basic ethanol, the plotted data resulted in curves, indicating non-Arrhenius behavior. The value of k_4 was higher in neutral ethanol than in basic solution at every temperature when 1.0 μs pulses were used. Results in neutral ethanol from 0.1 μs pulses fell nearly on the basic ethanol curve.

The high temperature region ($10^3/T \approx 2.8$ to 3.6) of the basic ethanol plot was approximately linear and indicated an E_a of 4.8 kcal mol⁻¹. In the neutral alcohol there was curvature in this region. The best fit linear plot gave an E_a of 4.0 kcal mol⁻¹. At lower temperatures there was considerable curvature. However,

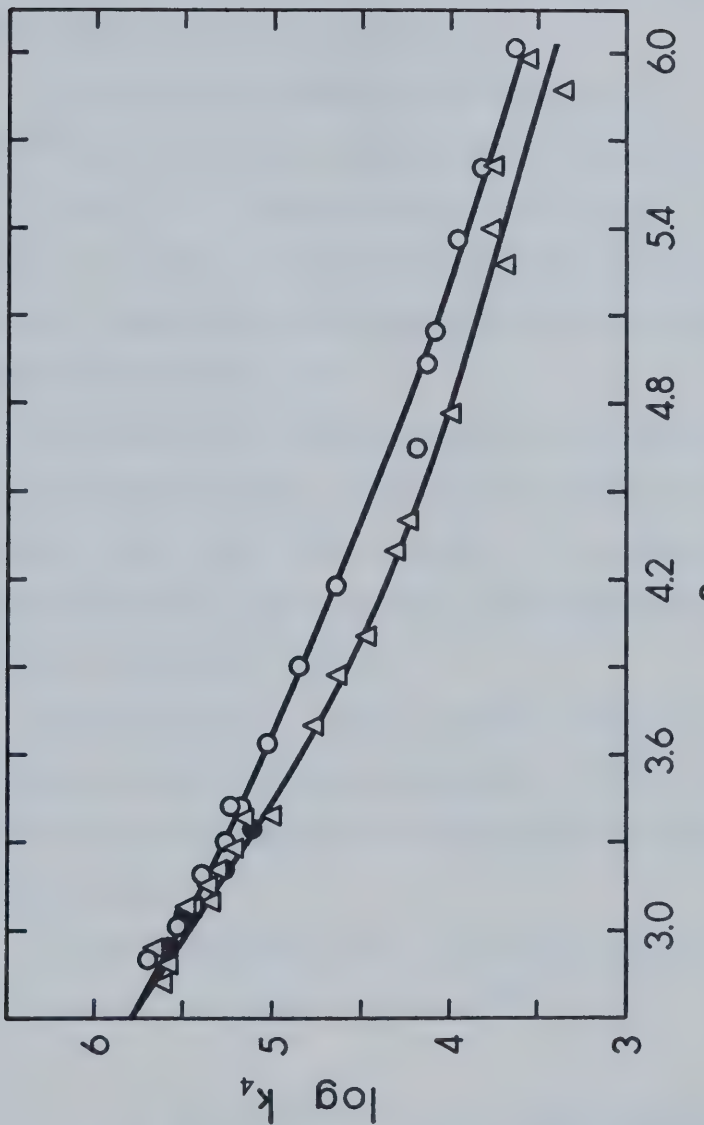


FIGURE III-16.

E_a Plots for e_s^- Decomposition Reaction in EtoH. \circ , $1.0 \mu s$ Pulse, Neutral EtoH; \bullet , $0.1 \mu s$ Pulse, Neutral EtoH; Δ , $1.0 \mu s$ Pulse, \sim mM Basic EtoH.

assuming a linear plot between 238 and 167K ($10^3/T = 4.2$ to 6.0) gave an E_a of 2.5 kcal mol $^{-1}$ for both the basic and the neutral alcohol.

For the basic solution to have an $E_a = 4.8$ kcal mol $^{-1}$ over the whole temperature range would require a $t_{1/2}$ for e_s^- of greater than 3 ms at 166K. This is nearly an order of magnitude greater than $t_{1/2}$'s observed at this temperature, as indicated by the values in Tables III-6 and III-7.

The detection system could not be used to measure ms half-lives because of changes in analyzing light intensity over such a time period. As explained on page 93 this problem was an important consideration for $t_{1/2}$'s greater than about 100 μ s.

Reaction of e_s^- with impurity could be responsible for part of the observed curvature. Since addition of base did not decrease the curvature, the impurity could not be acid.

Similar curvature has been observed in E_a plots in neutral and basic methanol.¹⁴⁸

2. E_a FOR THE REACTION OF e_s^- WITH SCAVENGERS IN
METHANOL AND ETHANOL.

Reaction rate constants for (5) were found by plotting the pseudo-first order rate constant against the concentration of scavenger (S). The slope gave the

TABLE III-6

The Effect of Temperature on the e_s^- Decomposition Reaction

<u>Neutral Ethanol</u>				
<u>T, \pm 2K</u>	<u>$10^3/T(K)$</u>	<u>$t_{1/2}, \mu s^a$</u>	<u>k_4, s^{-1}</u>	<u>$\log k_4$</u>
167	5.99	156	4.4×10^3	3.65
178	5.62	105	6.6×10^3	3.82
186	5.38	79	8.8×10^3	3.94
198	5.05	56	1.2×10^4	4.08
203	4.93	52	1.2×10^4	4.11
239	4.18	16	4.3×10^4	4.63
258	3.88	9.5	7.3×10^4	4.86
275	3.64	6.4	1.1×10^5	5.04
293	3.41	4.2	$1.6_5 \times 10^5$	5.22
293	3.41	4.7	1.5×10^5	5.18
303	3.30	3.8	1.8×10^5	5.26
313	3.19	2.9	2.4×10^5	5.38
331	3.02	2.05	3.4×10^5	5.53
345	2.90	1.4	$4.9_5 \times 10^5$	5.69
296	3.38	5.4 ^b	1.3×10^5	5.11
313	3.19	3.7 ^b	1.9×10^5	5.29
328	3.05	2.3 ^b	3.0×10^5	5.48
340	2.94	1.8 ^b	$3.8_5 \times 10^5$	5.59

^a \pm 5% for $t_{1/2} < 50 \mu s$. Error may be larger for longer $t_{1/2}$.^b 0.1 μs pulses. Other data obtained using 1.0 μs pulses.

TABLE III-7

The Effect of Temperature on the e_s^- Decomposition Reaction

T, \pm 2K	$\sim 1 \text{ mM KOH}$ in Ethanol			
	$10^3/T(\text{K})$	$t_{1/2}, \text{ s}^a$	$k_4, \text{ s}^{-1}$	$\log k_4$
167	5.99	190	$3.6_5 \times 10^3$	3.56
170	5.88	307	2.3×10^3	3.36
178	5.62	128	5.4×10^3	3.73
185	5.40	116	6.0×10^3	3.78
189	5.29	150	4.6×10^3	3.66
210	4.77	73.5	9.5×10^3	3.98
227	4.41	42	$1.6_5 \times 10^4$	4.22
230	4.35	35	2.0×10^4	4.30
250	4.00	26.5	2.6×10^4	4.42
259	3.86	16.8	4.1×10^4	4.62
271	3.69	11.6	6.0×10^4	4.78
294	3.40	5.6	1.2×10^5	5.08
295	3.39	7.4	9.4×10^4	4.97
305	3.28	4.15	1.7×10^5	5.23
312	3.21	3.35	2.1×10^5	5.32
318	3.14	3.05	2.3×10^5	5.36
320	3.13	2.6	2.7×10^5	5.43
323	3.10	3.3	2.1×10^5	5.32
325	3.08	2.3	3.0×10^5	5.48
325	3.08	2.45	2.8×10^5	5.45
340	2.94	1.5	4.6×10^5	5.66
346	2.89	1.8	$3.8_5 \times 10^5$	5.59
354	2.82	1.75	4.0×10^5	5.60

^a $\pm 5\%$ for $t_{1/2} < 50 \mu\text{s}$. Error may be larger for longer $t_{1/2}$.

second order rate constant for the scavenging reaction. A minimum of three concentrations of S were used at each temperature. The molar concentrations were adjusted for change in solvent density with temperature.

Samples were prepared by syringe addition of a stock solution to a known volume of solvent in a quartz cell. Samples were de-oxygenated by bubbling with UHP argon. Cells were sealed after bubbling by one of the methods explained in II-C-1, a and b. Electron pulses of 0.1 μ s duration and 1.87 MeV energy were used.

Most points were calculated from the average results of three experiments. Results obtained in the solvents methanol and ethanol are indicated by closed and open points, respectively.

a. Acetone ($(CH_3)_2CO$) as e_s^- Scavenger

The plots used to determine k_5 as a function of temperature are presented in Figure III-17, A, B, C, D, E and F. The plot for E_a is given in Figure III-17G. Rate constants calculated from the data in Figures II-17 A to E are presented in Table III-8. The rate constant at 295K in methanol is $4.3 \times 10^9 \text{ M}^{-1} \text{ s}^{-1}$. This is higher than the $2.5 \times 10^9 \text{ M}^{-1} \text{ s}^{-1}$ reported by Pikaev et. al.¹⁴⁹ at room temperature. However, it is in good agreement with the values of 4.2 and $4.0 \times 10^9 \text{ M}^{-1} \text{ s}^{-1}$ found by Jha¹⁴⁸ and Robinson, respectively,

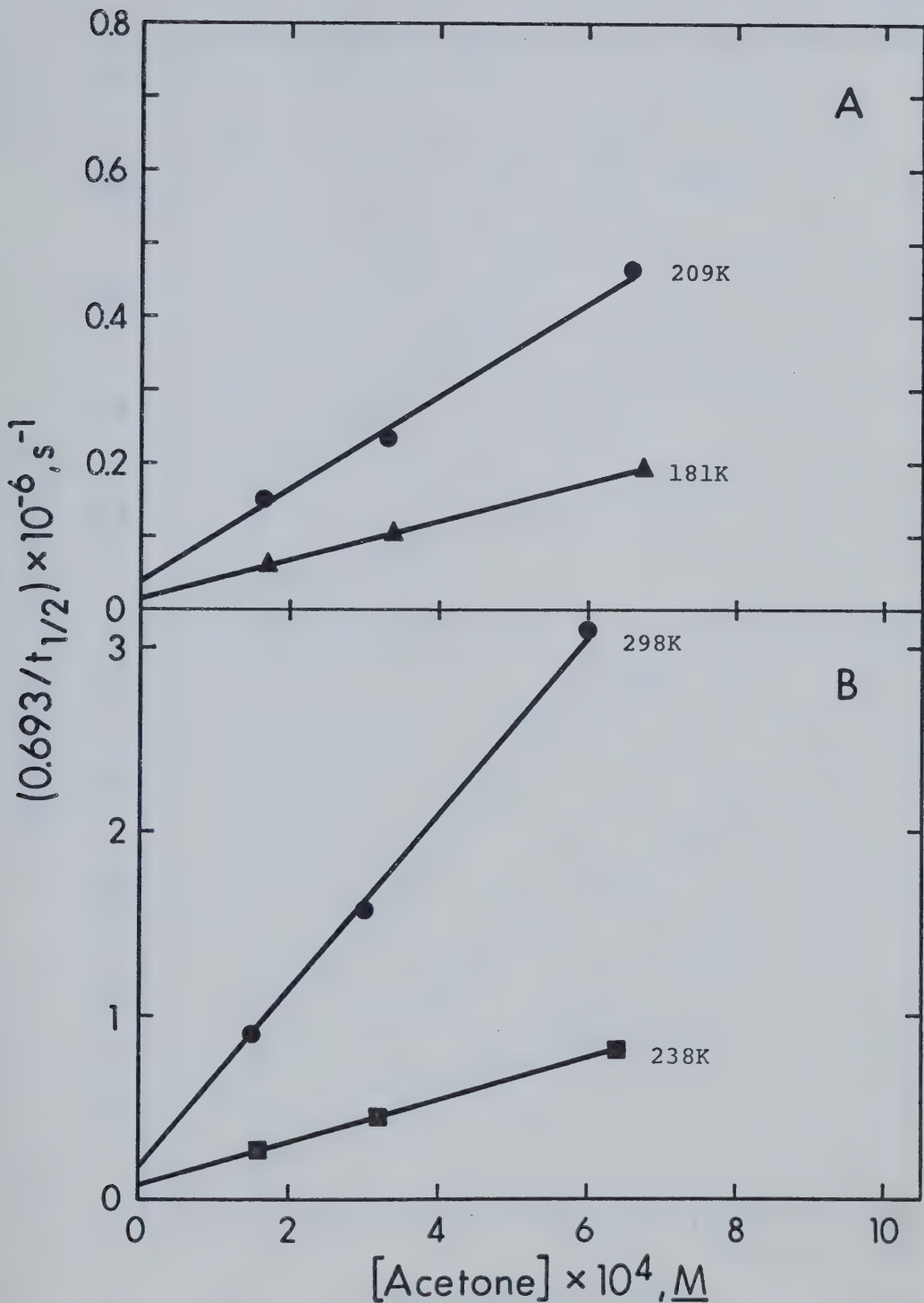


FIGURE III-17 A, B. The Effect of T on $e_s^- + \text{Acetone}$
(EtOH, Open Points; MeOH, Closed Points)

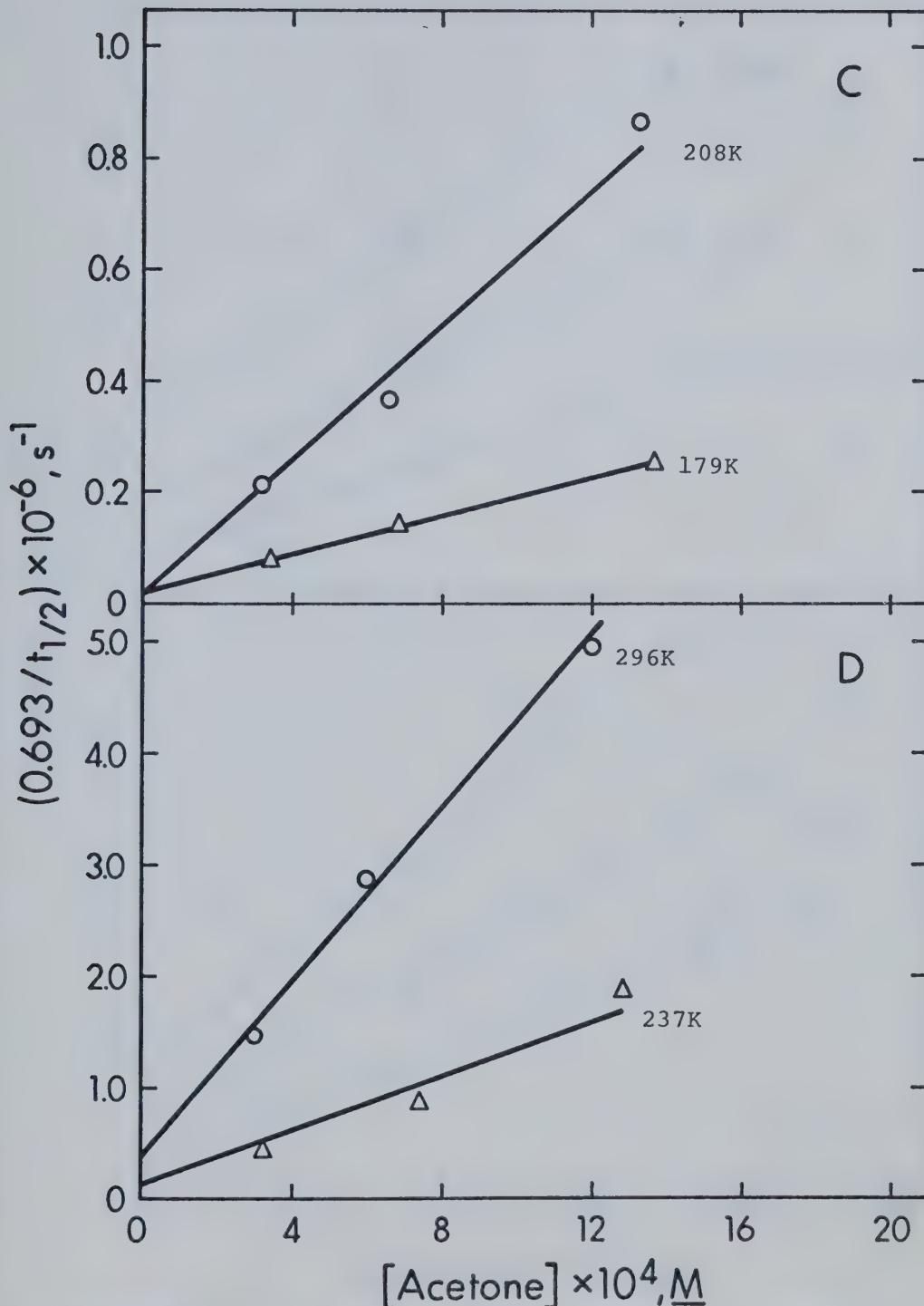


FIGURE III-17 C, D. The Effect of T on $e_s^- + Acetone$
(EtOH, Open Points; MeOH, Closed Points)

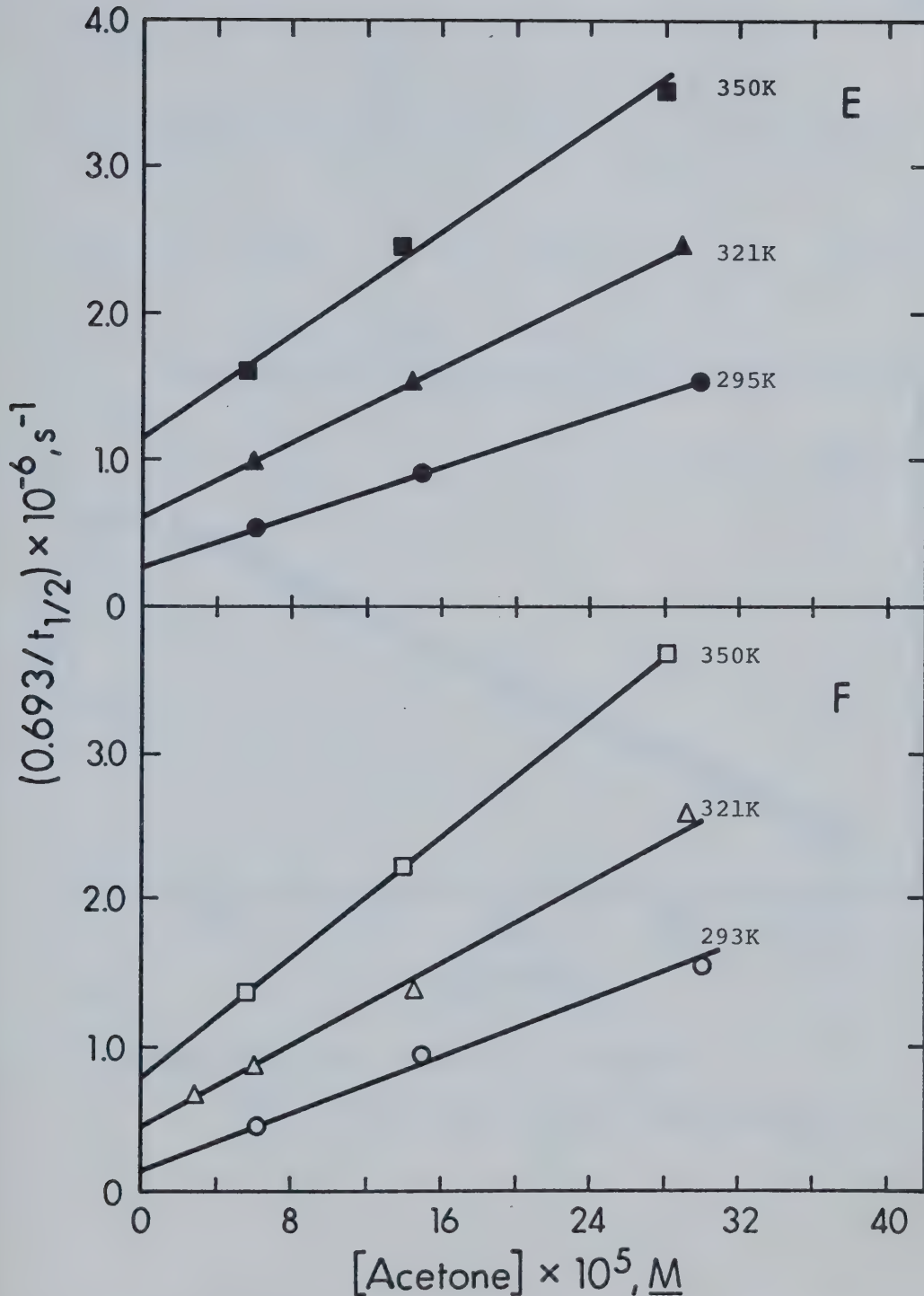


FIGURE III-17, E, F. The Effect of T on ϵ_s + Acetone
(EtOH, Open Points; MeOH, Closed Points)

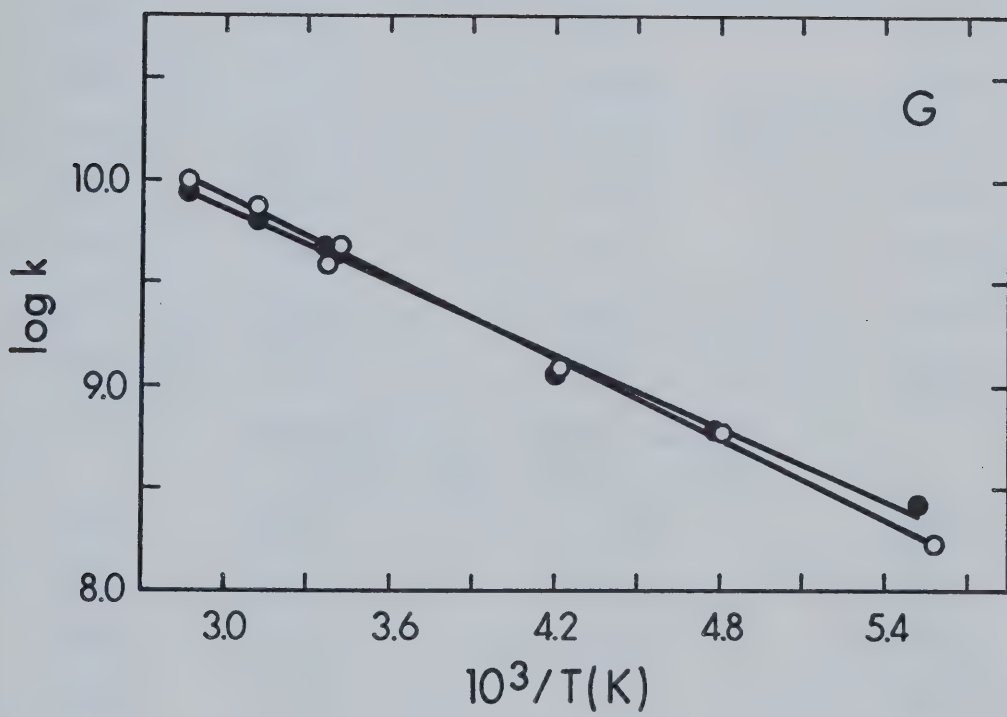


FIGURE III-17 G. E_a for $e_s^- + \text{Acetone}$
(EtOH, Open Points; MeOH, Closed Points)

TABLE III-8

The k 's and E_a 's for the Reaction of e_s^- with Acetone

<u>T, \pm 1K</u>	<u>$10^3/T$</u>	<u>$10^{-9} \times k_5^a, M^{-1}s^{-1}$</u>	<u>$\log k_5$</u>
Methanol, $E_a = 2.74$ kcal mol $^{-1}$			
181	5.52	0.27	8.43
209	4.78	0.63 ₅	8.80
238	4.20	1.1 ₅	9.06
295	3.39	4.3	9.63
298	3.36	4.8	9.68
321	3.12	6.3	9.80
350	2.86	8.7	9.94
Ethanol, $E_a = 3.0$ kcal mol $^{-1}$			
179	5.59	.17	8.23
208	4.81	.61	8.79
237	4.22	1.2	9.08
293	3.41	4.9	9.69
296	3.38	3.9	9.59
321	3.12	7.1	9.85
360	2.86	10.0	10.00

^a Error may be \pm 5%.

at 295K. The latter value is reported in this work.

b. Nitrobenzene ($C_6H_5NO_2$) as the e_s^- Scavenger

The results are presented in Figure III-18 A, B, C and D, and in Table III-9.

The E_a 's in methanol and ethanol are $3.0 \text{ kcal mol}^{-1}$, but at any given temperature, the reaction occurs faster in methanol than in ethanol.

Results from separate preparation of solute and solvent at similar temperatures (291 and 295K) gave good agreement.

c. Naphthalene ($C_{10}H_8$) as the e_s^- Scavenger

The data used to determine the second order scavenging rate constants are depicted in Figure III-19 A, B and C. The plot used to obtain E_a is given in Figure III-19 D, and the data are summarized in Table III-10.

As was the case for nitrobenzene, the E_a for the scavenging reaction did not depend on the solvent used, although the reaction proceeded faster in methanol than in ethanol at all temperatures.

A value of k_5 of $2 \times 10^9 \text{ M}^{-1} \text{ s}^{-1}$ in methanol¹⁵⁰ at 293K is in satisfactory agreement with values reported here. Similarly, values of 5.4 and $4.5 \times 10^9 \text{ M}^{-1} \text{ s}^{-1}$ for k_5 in ethanol^{89,44} at $295 \pm 1\text{K}$ are only slightly higher than the $4.24 \times 10^9 \text{ M}^{-1} \text{ s}^{-1}$ found at 294K in this work.

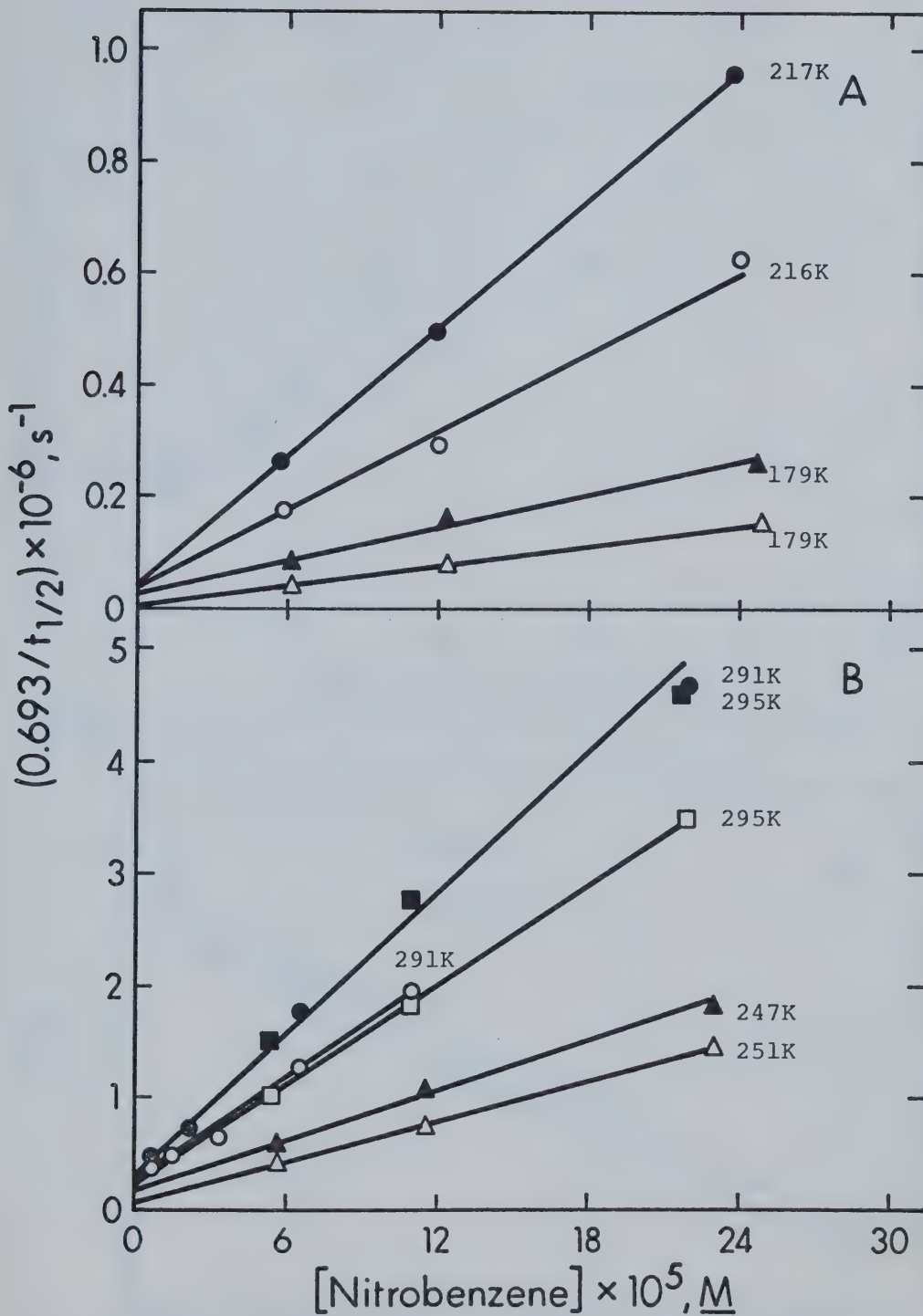


FIGURE III-18 A, B. The Effect of T on $e_s^- + \text{Nitrobenzene}$ (EtOH, Open Points; MeOH, Closed Points)

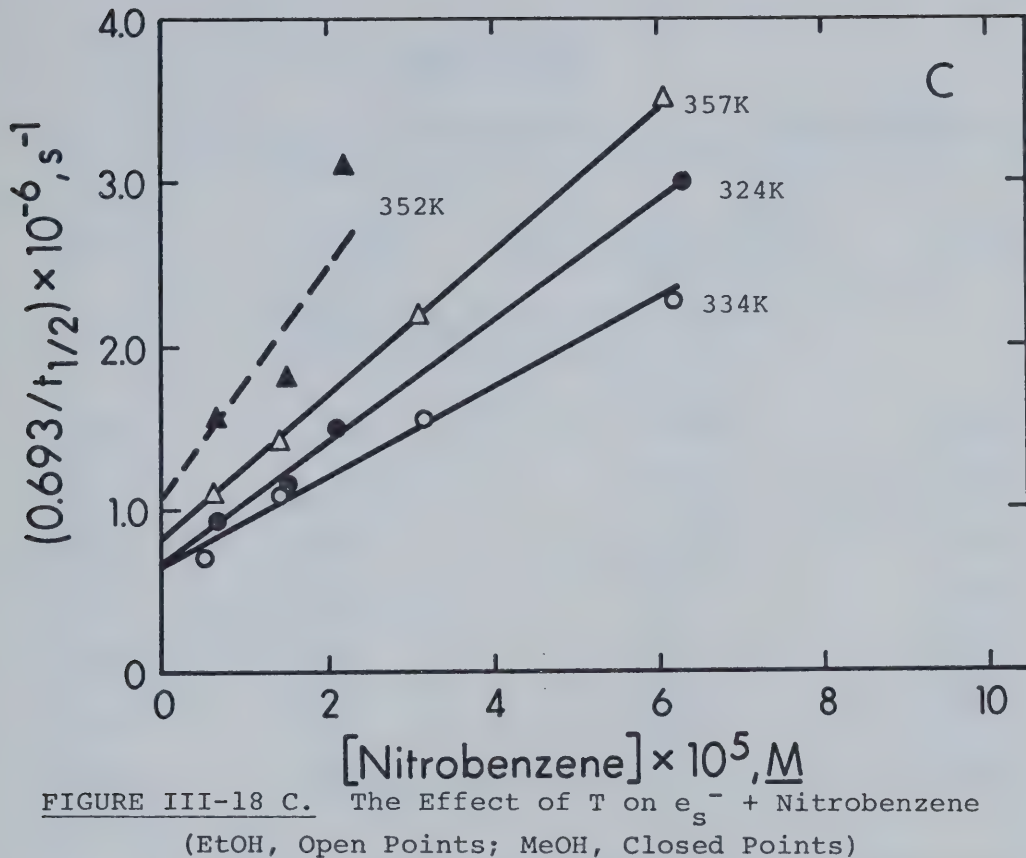


FIGURE III-18 C. The Effect of T on $e_s^- + \text{Nitrobenzene}$ (EtOH, Open Points; MeOH, Closed Points)

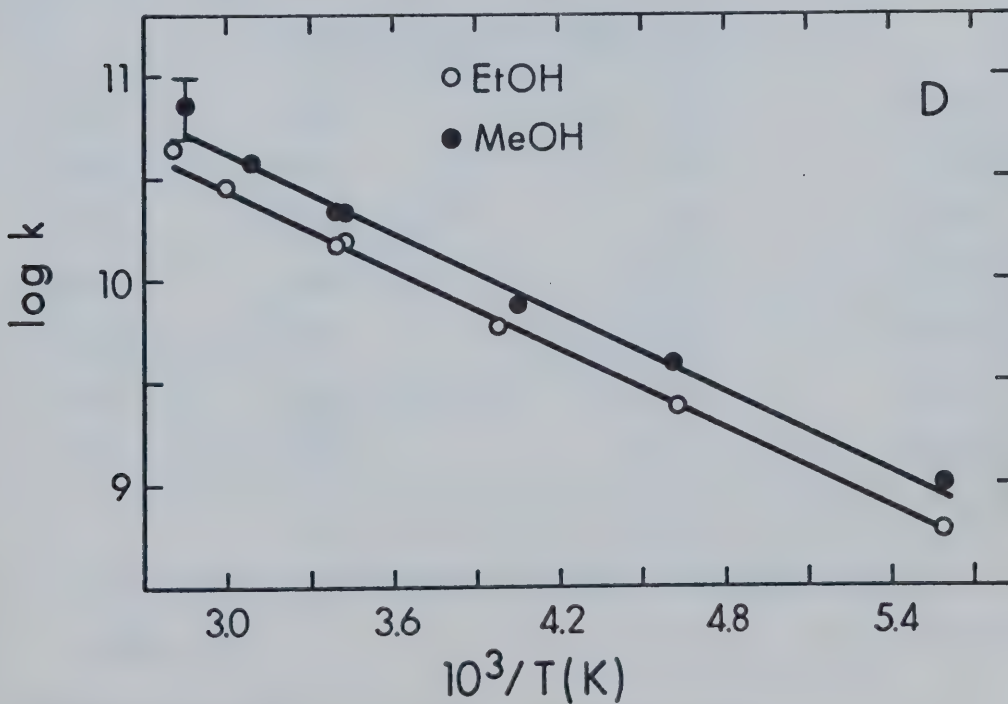


FIGURE III-18 D. E_a for $e_s^- + \text{Nitrobenzene}$

TABLE III-9

The k's and E_a 's for the Reaction of e_s^- with Nitrobenzene

$T, \pm 1K$	$10^3/T(K)$	$10^{-10} \times k_5^a, M^{-1}s^{-1}$	$\log k_5$
Methanol, $E_a = 3.0 \text{ kcal mol}^{-1}$			
179	5.59	0.10	9.00
217	4.61	0.39	9.59
247	4.05	.74	9.87
291	3.44	2.1	10.32
295	3.39	2.1	10.32
324	3.09	3.7	10.57
352	2.84	~ 7.3	10.86
Ethanol, $E_a = 3.0 \text{ kcal mol}^{-1}$			
179	5.59	.059	8.77
216	4.63	.24	9.38
251	3.98	.59	9.77
291	3.44	1.5_3	10.18
295	3.39	1.4_8	10.17
334	2.99	2.8	10.45
357	2.80	4.4	10.64

^a Error may be $\pm 5\%$, except for $T > 295K$, where it is $\pm 10\%$.

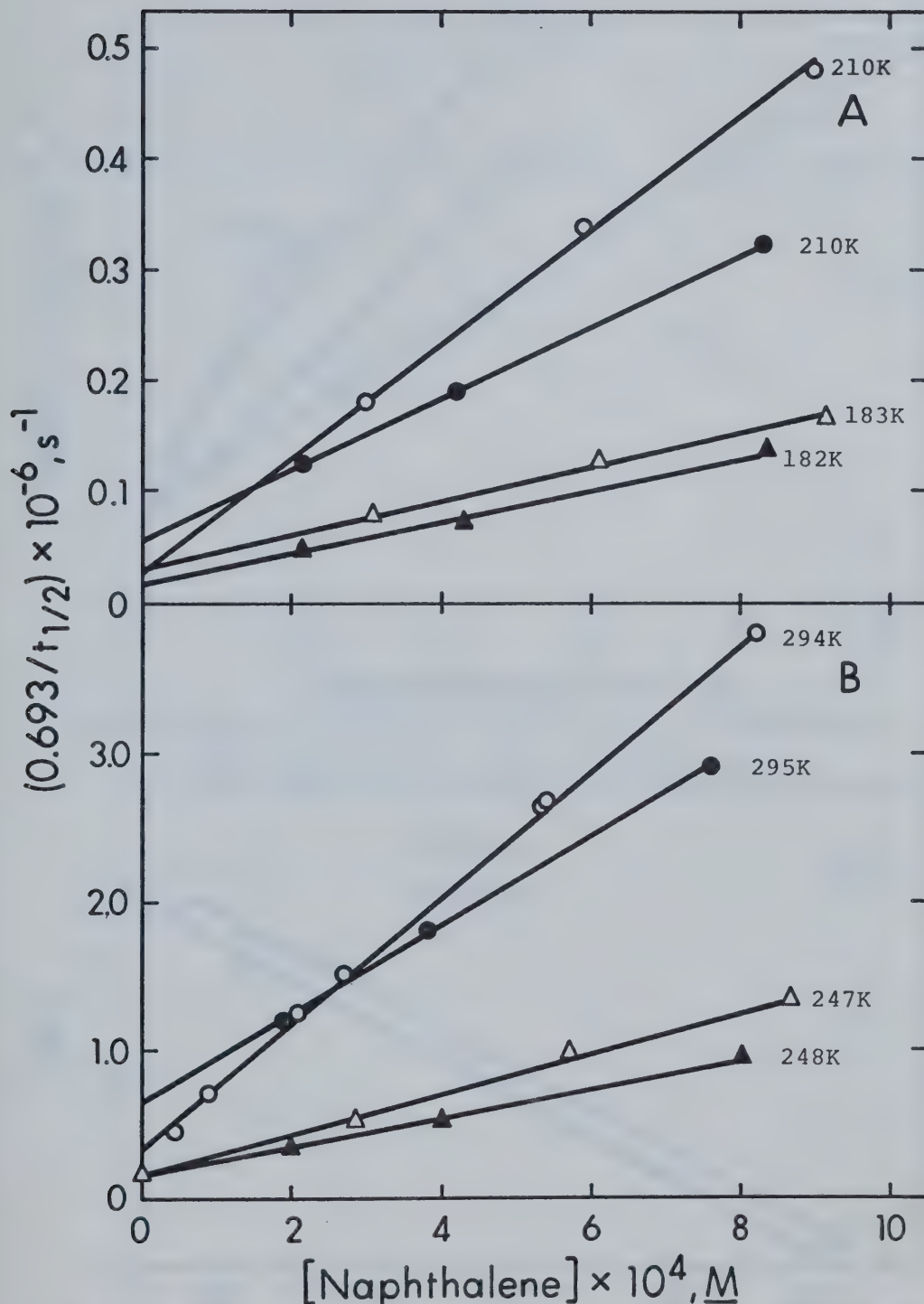


FIGURE III-19 A, B. The Effect of T on $e_s^- + \text{Naphthalene}$
(EtOH, Open Points; MeOH, Closed Points)

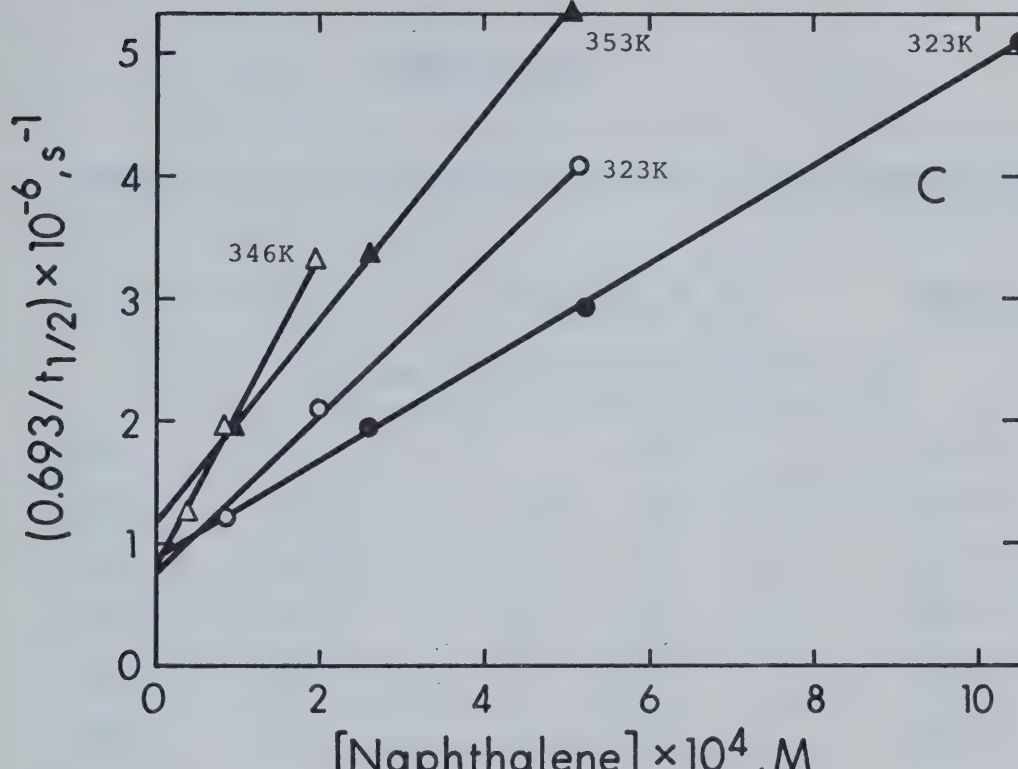


FIGURE III-19 C. The Effect of T on $e_s^- +$ Naphthalene
(EtOH, Open Points; MeOH, Closed Points)

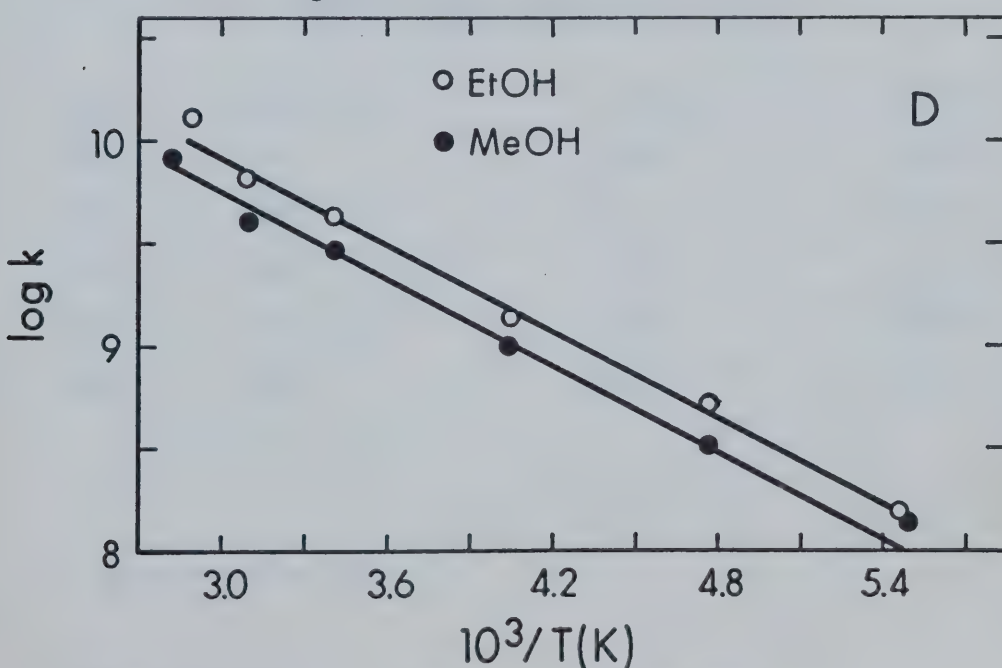


FIGURE III-19 D. E_a for $e_s^- +$ Naphthalene

TABLE III-10

The k 's and E_a 's for the Reaction of e_s^- with Naphthalene

$T, \pm 1K$	$10^{3}/T$	$10^{-9} \times k_5^a, M^{-1}s^{-1}$	$\log k_5$
Methanol, $E_a = 3.24$ kcal mol $^{-1}$			
182	5.49	.14	8.15
210	4.76	.32	8.51
248	4.03	.99	9.00
295	3.39	3.0	9.48
323	3.10	4.0	9.60
353	2.83	8.4	9.92
Ethanol, $E_a = 3.24$ kcal mol $^{-1}$			
183	5.46	.15 ₅	8.19
210	4.76	.52	8.72
247	4.05	1.4	9.15
294	3.40	4.2 ₄	9.63
323	3.10	6.5	9.81
346	2.89	12.8	10.11

^a Error may be $\pm 5\%$.

d. Perchloric Acid (HClO_4) as the e_s^- Scavenger

The results for acid scavenging of e_s^- in methanol and ethanol are presented in Figure III-20 A and B. The rate constant data used to determine E_a from Figure III-20 C is compiled in Table III-11.

Considerable difficulty was experienced in the acid kinetics work because of adsorption of H^+ onto the walls of the quartz optical cells. This resulted in intercepts on the "wrong axis" in some cases.⁸⁸ At temperatures above 295K, curvature was evident in plots of $0.693/t_{\frac{1}{2}}$ versus $[\text{H}^+]$, making determination of the rate constant impossible. At higher temperature, reaction of the acid with the solvent could occur. The direction of the curvature was consistent with removal of acid from solution by reaction.

The values reported for k_5 at room temperature in methanol 87,88,92,147 and ethanol 44,68,88,89,92,93,147 differ by about a factor of three. The most recent pulse radiolysis results⁸⁸ agree well with those obtained by conductivity measurements⁹² and calculated diffusion controlled values.⁸⁸ The 296K values reported here are 12% and 10% lower in methanol and ethanol, respectively, than those calculated for a diffusion controlled reaction. The value recommended by Baxendale⁴⁷ in methanol is $5.6 \pm 0.8 \times 10^{10} \text{ M}^{-1} \text{ s}^{-1}$, in good agreement with the result of this work.

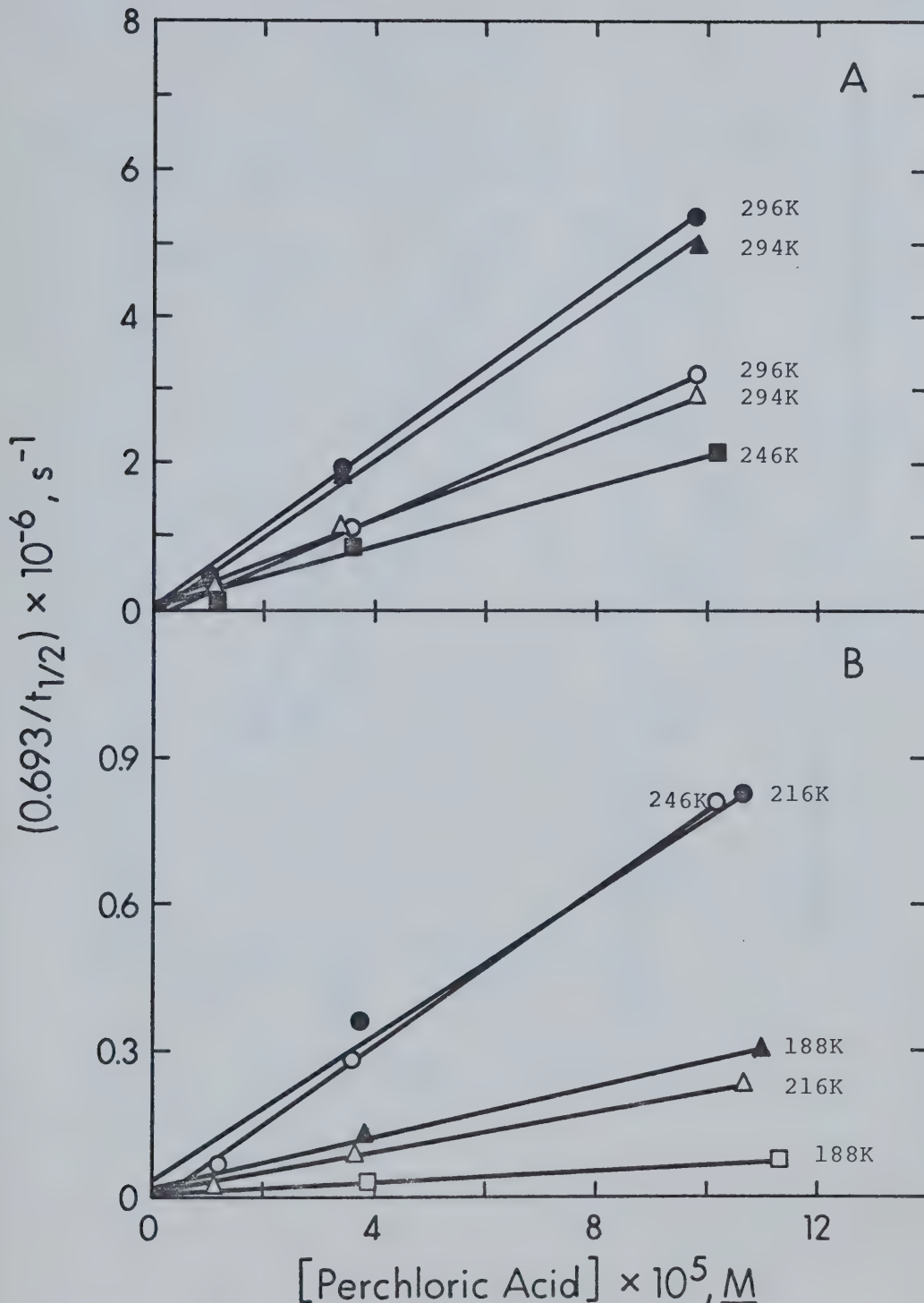


FIGURE III-20 A,B. The Effect of T on $e_s^- + H_s^+$
(EtOH, Open Points; MeOH, Closed Points)

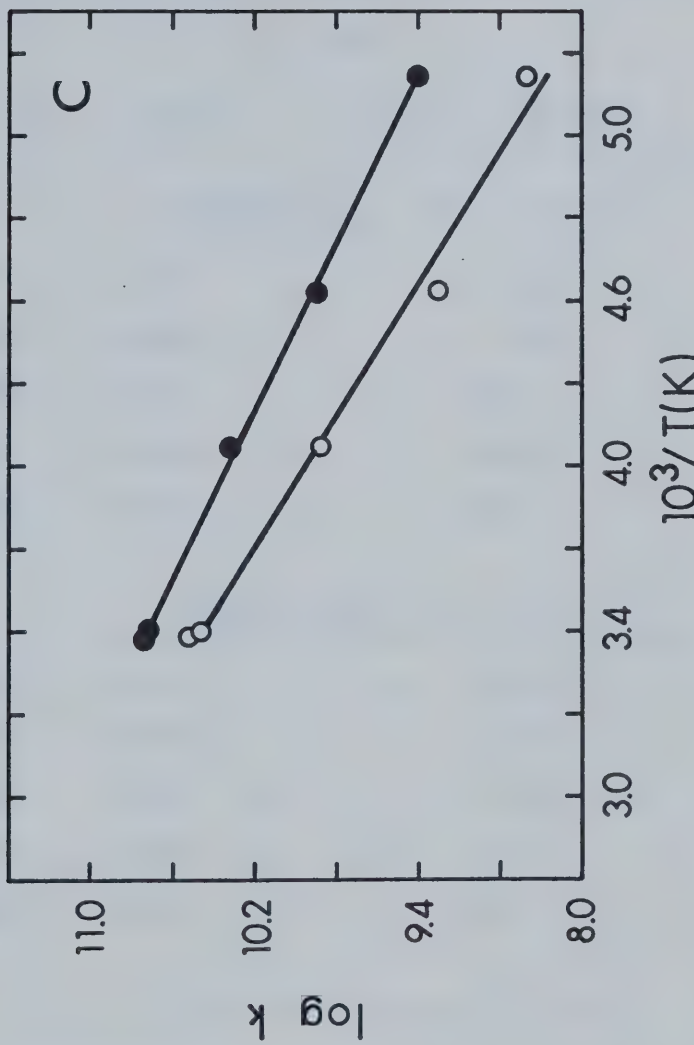


FIGURE III-20 C. E_a for $e_s^- + H_s^+$
(EtOH, Open Points; MeOH, Closed Points)

TABLE III-11

The k 's and E_a 's for the Reaction of e_s^- with Perchloric

Acid

<u>T, \pm 1K</u>	<u>$10^3/T$</u>	<u>$10^{-10} \times k_5^a, M^{-1} s^{-1}$</u>	<u>$\log k_5$</u>
<u>Methanol, $E_a = 3.2 \text{ kcal mol}^{-1}$</u>			
188	5.32	.25 ₅	9.41
216	4.63	.75	9.88
246	4.07	2.1	10.32
294	3.40	5.2 ₄	10.72
296	3.38	5.5	10.74
<u>Ethanol, $E_a = 4.0 \text{ kcal mol}^{-1}$</u>			
188	5.32	0.075 ^b	8.88
216	4.63	.20 ^b	9.30
246	4.07	.78 ^b	9.89
294	3.40	2.9	10.46
296	3.38	3.3	10.52

^a Error may be \pm 15%.

^b Results from 2 acid concentrations.

Low values result when water is an impurity, due to a decrease in the diffusion coefficient of solvated protons. 88, 92, 151, 152

e. Benzene (C_6H_6) as the e_s^- Scavenger

The results are shown in Figure III-21 A, B, C, D and E, and in Table III-12.

Benzene is a poor scavenger of electrons. The room temperature rate is four to five orders of magnitude lower than for acid or other efficient scavengers. If there were from 0.01 to 0.001 mole % of impurity in the benzene, which scavenged electrons at a diffusion controlled rate, it could account for all of the observed decrease in the e_s^- lifetime. There are two facts which indicate that this is not the case. One is that E_a in both methanol and ethanol was found to be about 6 kcal mol^{-1} , or nearly twice that for the faster scavenger reactions. The other is that there was a much larger effect of solvent on the benzene + e_s^- rate than there was for the faster reactions. For example, at 295K, $k_5(EtOH)/k_5(MeOH) = 5.3$ for benzene + e_s^- . The same factor is 0.6 for acid + e_s^- , and 0.7 for nitrobenzene + e_s^- .

Calculated rate constants from competition kinetics are $5 \times 10^6 \underline{M}^{-1} s^{-1}$ 153 and $2 \times 10^7 \underline{M}^{-1} s^{-1}$ 154 in ethanol and methanol at room temperature. These values

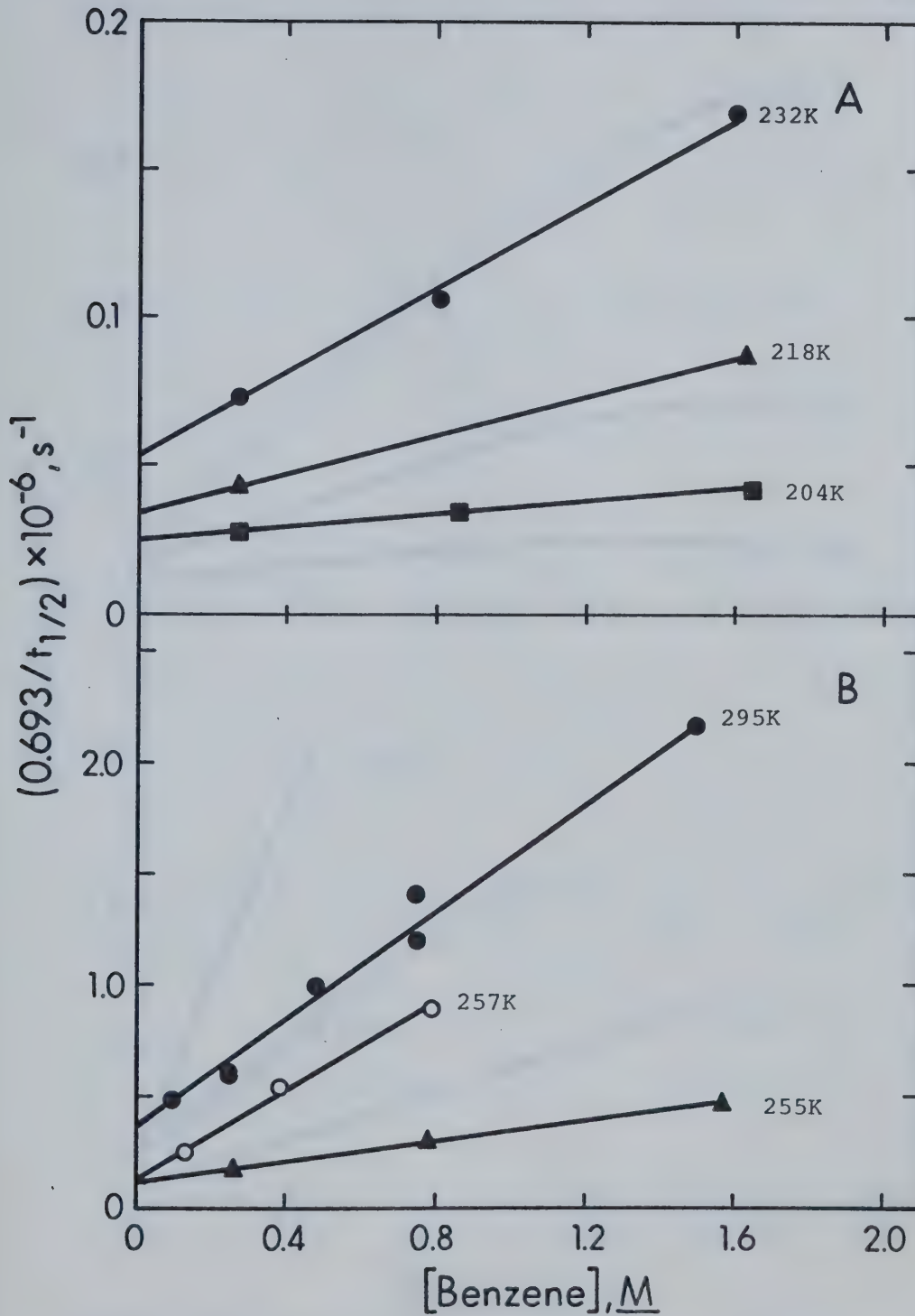


FIGURE III-21 A, B. The Effects of T on $e_s^- + \text{Benzene}$ (EtOH, Open Points; MeOH, Closed Points)

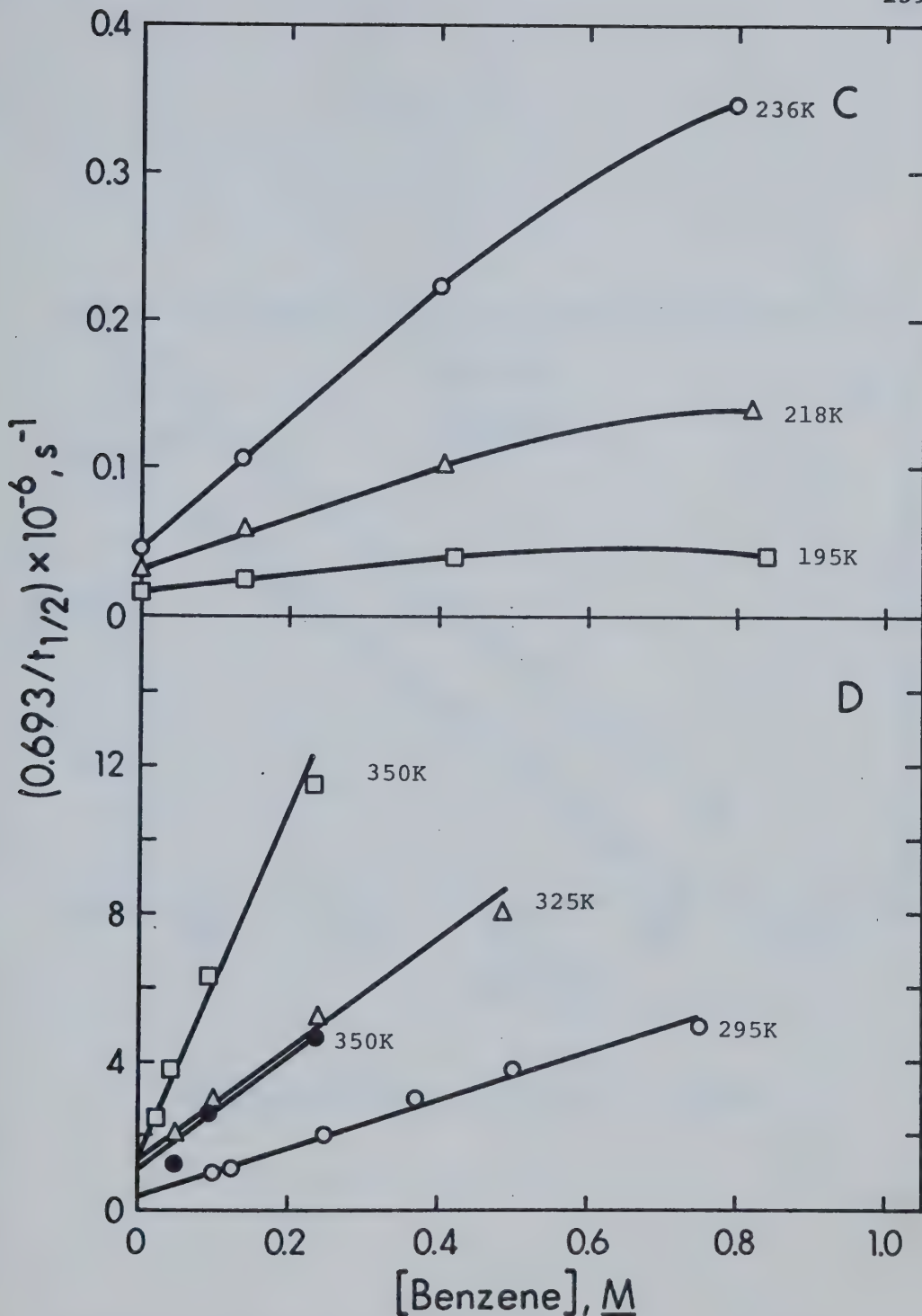


FIGURE III-21 C, D. The Effects of T on $e_s^- + Benzene$
(EtOH, Open Points; MeOH, Closed Points)

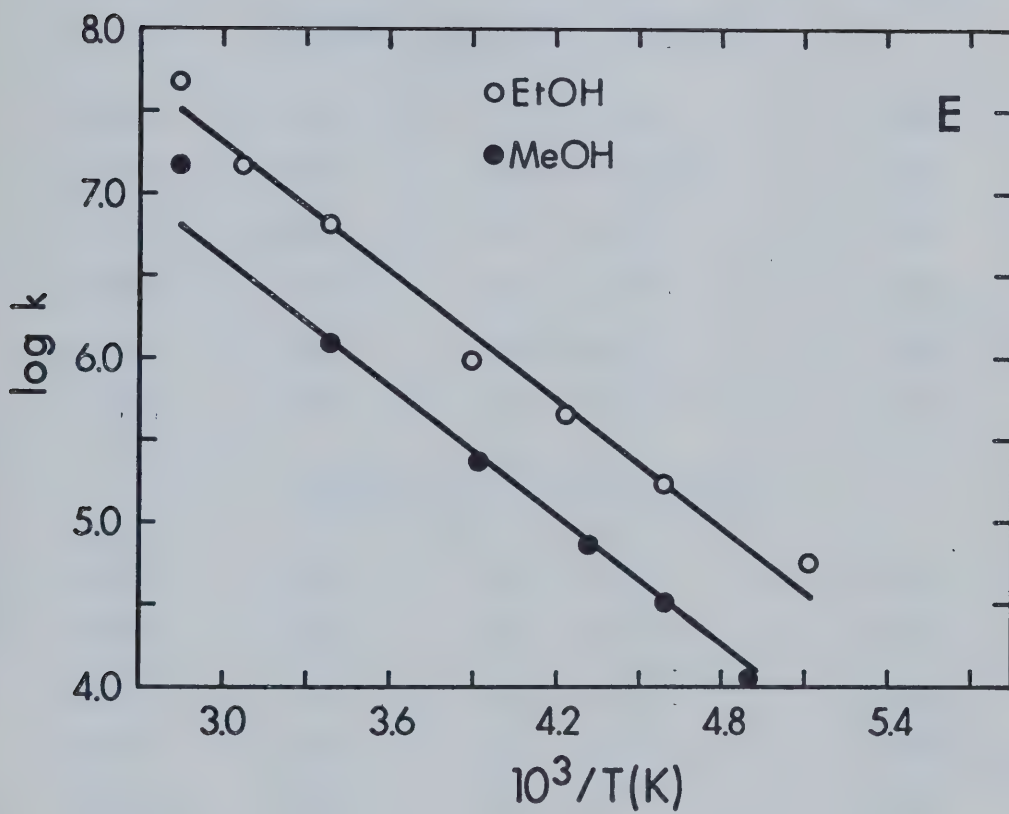


FIGURE III-21 E. E_a for $e_s^- + \text{Benzene}$

TABLE III-12

The k 's and E_a 's for the Reaction of e_s^- with Benzene

$T, \pm 1K$	$10^3/T(K)$	$k_5^a, M^{-1} s^{-1}$	$\log k_5$
Methanol, $E_a = 6.4 \text{ kcal mol}^{-1}$			
204	4.90	1.1×10^4	4.04
218	4.59	3.3×10^4 b	4.52
232	4.31	7.2×10^4	4.86
255	3.92	2.3×10^5	5.36
295	3.90	1.2×10^6	6.08
350	2.86	1.5×10^7	7.18
Ethanol, $E_a = 6.0 \text{ kcal mol}^{-1}$			
195	5.13	5.5×10^4 c	4.74
218	4.59	1.7×10^5 c	5.23
236	4.24	4.4×10^5 c	5.64
257	3.89	9.8×10^5	5.99
295	3.90	6.4×10^6 d	6.81
325	3.08	1.5×10^7	7.18
350	2.86	4.6×10^7	7.66

^a Error may be $\pm 10\%$.

^b Determined from two benzene concentrations.

^c Rate constants determined from linear portion.

^d Separate preparation of solute and solvent gave same result.

are relative to assumed values of $k(e_s^- \rightarrow RO_s^- + H) = 1 \times 10^5 \text{ s}^{-1}$ and $k(e_s^- + \text{impurity})[\text{impurity}] = 5 \times 10^4 \text{ s}^{-1}$ for the former, and $k(e_s^- + N_2O \rightarrow \cdot) = 8.7 \times 10^9 \text{ M}^{-1} \text{ s}^{-1}$ for the latter case. The value in ethanol agrees well with that presented here, but the methanol value is high. A similar high value of $1.8 \times 10^8 \text{ M}^{-1} \text{ s}^{-1}$ was reported (assuming $k(e_s^- + N_2O \rightarrow \cdot) = 8.7 \times 10^9 \text{ M}^{-1} \text{ s}^{-1}$) in n-propanol.¹⁵⁵ Use of impure benzene is the most probable reason for obtaining apparently high k_5 's.

The low temperature portion of this work required careful attention to the possibility of benzene freezing out of solution. Sample cells were sealed at 195K for low temperature irradiation. Several samples which were greater than 1 M in benzene were observed to have crystals in them at this temperature. These samples were warmed and mixed well before use. They were not used below 204K. No solid benzene could be seen in the samples at this temperature. However, the freezing out of benzene is probably responsible for the curvature at high benzene concentration in Figure III-21-C.

This is further support for the contention that impurity was not responsible for the observed decrease in $t_{1/2}$ for e_s^- . If it were impurity alone, freezing out of benzene would not affect $t_{1/2}$.

f. Phenol (C_6H_5OH) as the e_s^- Scavenger

The results depicted in Figure III-22 A, B, C, D, E and F are tabulated in Table III-13.

Phenol is also a relatively poor electron scavenger. The same difficulty in establishing solute purity encountered with benzene also applied here. Use of arguments similar to those used with benzene may imply that the observed rate was not due to impurity reactions.

However, the E_a 's of 4.5 and 4.4 kcal mol⁻¹ in methanol and ethanol are between those found for benzene and those found for efficient scavengers. The room temperature rate is faster for phenol than for benzene by a factor of 5 in methanol and 7 in ethanol. It is therefore not possible to rule out some contribution of an impurity reacting with e_s^- .

A likely impurity in phenol is benzoquinone, which should scavenge e_s^- efficiently. It should also react with alkali metal more rapidly than does phenol. It was therefore attempted to purify phenol by treatment in vacuum with Na-K alloy, followed by sublimation off the resulting salt. Phenol treated in this manner apparently increased slightly the scavenging rate in ethanol at room temperature. The data are included in Table III-13.

However, the treated phenol gave a k_5 lower than

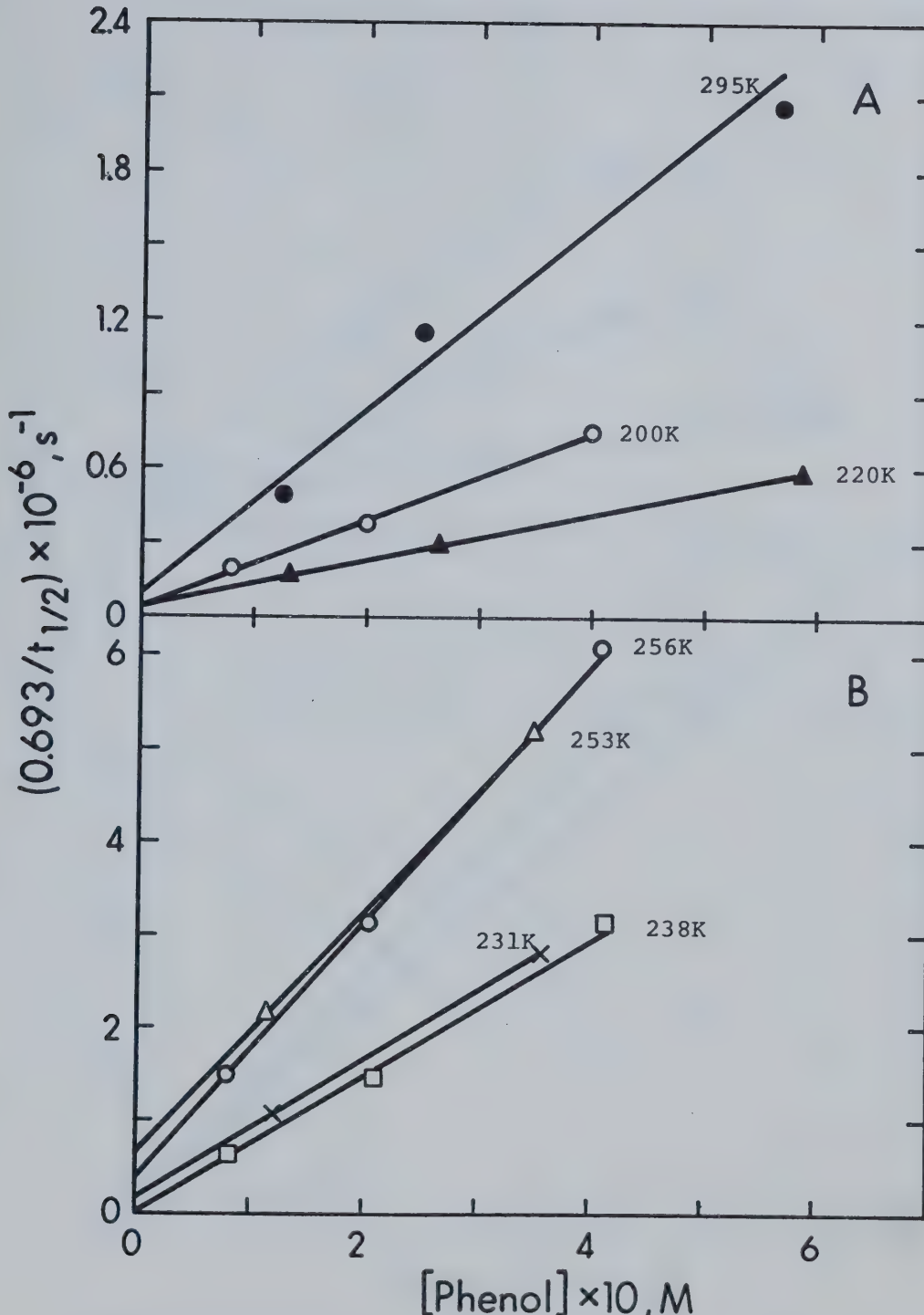


FIGURE III-22 A, B. The Effect of T on $e_s^- + \text{Phenol}$
(EtOH, Open Points; MeOH, Closed Points)

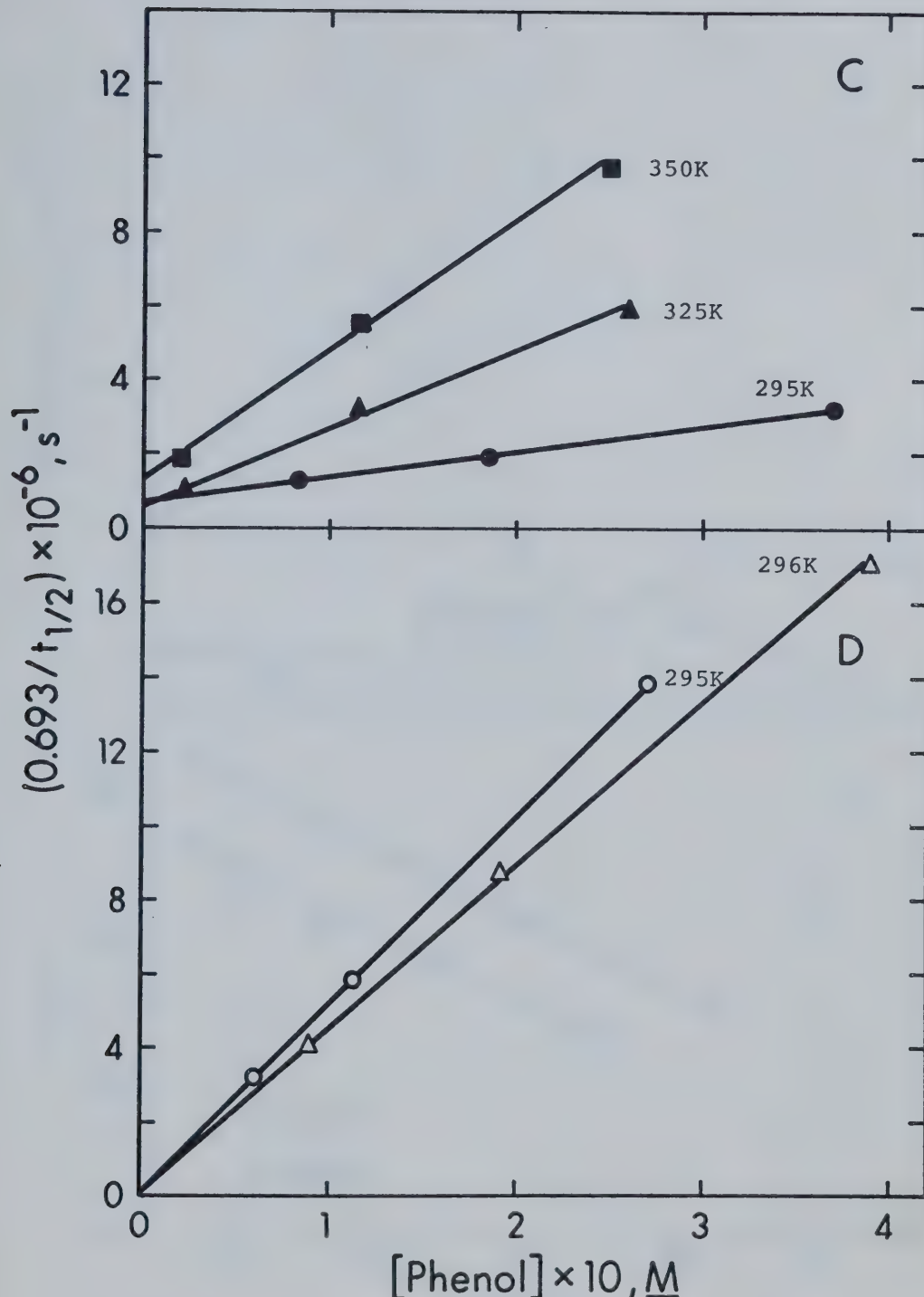


FIGURE III- 22 C,D. The Effect of T on $e_s^- + \text{Phenol}$
(EtOH, Open Points; MeOH, Closed Points)

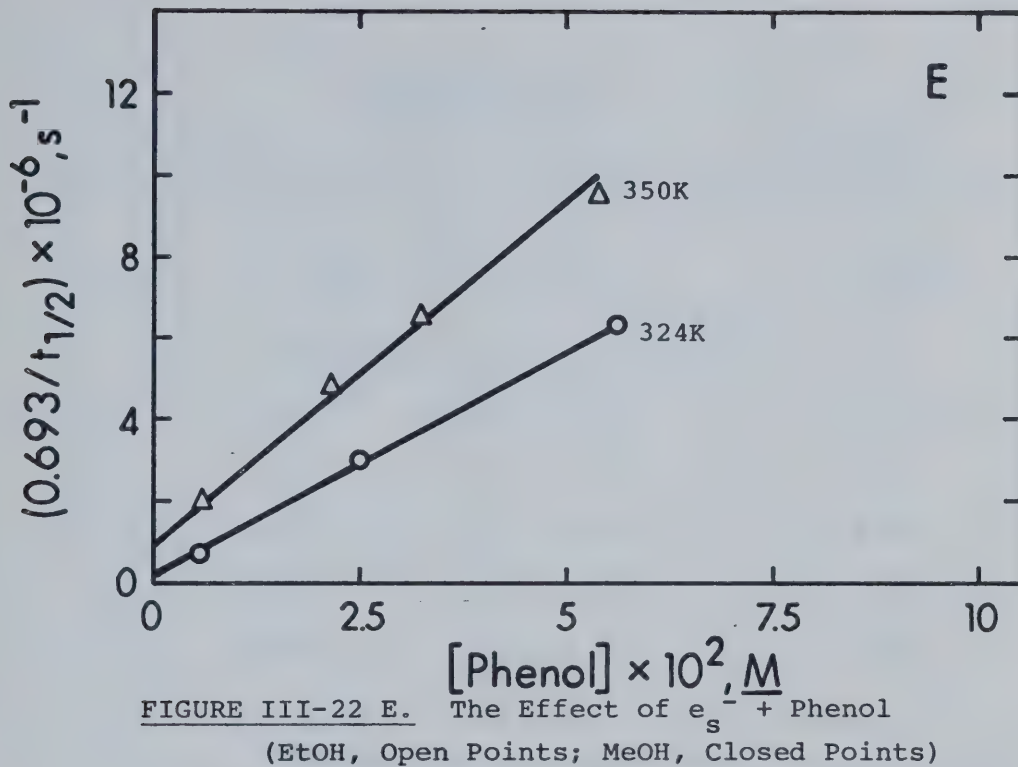


FIGURE III-22 E. The Effect of $e_s^- + \text{Phenol}$
(EtOH, Open Points; MeOH, Closed Points)

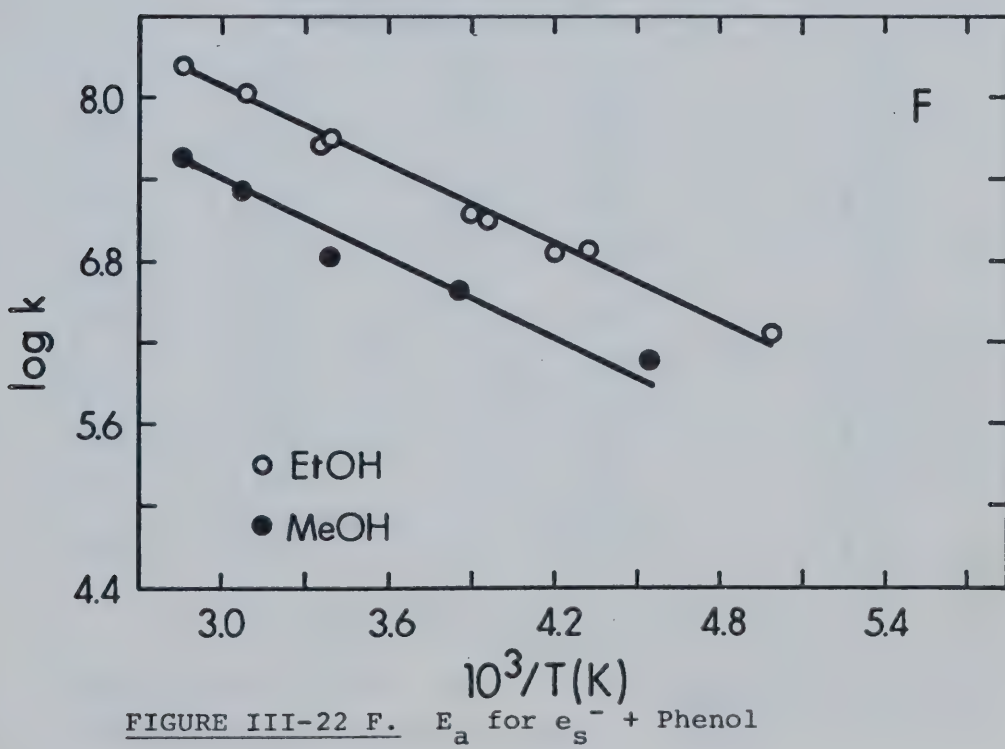


FIGURE III-22 F. E_a for $e_s^- + \text{Phenol}$

TABLE III-13

The k 's and E_a 's for the Reaction of e_s^- with Phenol

$T, \pm 1K$	$10^3/T(K)$	$k_5^a, M^{-1} s^{-1}$	$\log k_5$
Methanol, $E_a = 4.5 \text{ kcal mol}^{-1}$			
220	4.55	9.3×10^5	5.97
259	3.86	3.7×10^6	6.57
295	3.39	$6.7 \times 10^6^b$	6.83
325	3.08	2.1×10^7	7.33
350	2.86	$3.5_5 \times 10^7$	7.55
Ethanol, $E_a = 4.4 \text{ kcal mol}^{-1}$			
200	5.00	1.8×10^6	6.26
231	4.33	$7.4 \times 10^6^c$	6.87
238	4.20	7.3×10^6	6.86
253	3.95	$1.3 \times 10^7^c$	7.10
256	3.90	1.4×10^7	7.14
295	3.39	$5.0_5 \times 10^7^b$	7.70
296	3.38	4.4×10^7	7.64
324	3.09	1.1×10^8	8.04
350	2.86	1.7×10^8	8.23

^a Error may be $\pm 10\%$.^c Determined from two concentrations of phenol^b Phenol treated with Na-K alloy.

expected at 295K in methanol. This is evident in that $\log k_5$ falls below the line on the E_a plot at this temperature. From the E_a plot, the expected k_5 at 295K would be $1 \times 10^7 \text{ M}^{-1} \text{ s}^{-1}$. This was the value found at 295K using untreated phenol.¹⁴⁸ It therefore appears as though the Na-K alloy treatment had no effect on the purity of the phenol within the error of the experiment.

C. PRESSURE EFFECTS ON e_s^- REACTION KINETICS

The effect of pressure (P) on the rate of the e_s^- reaction with a solvent or a solute is of particular interest. Any change in rate with P can be related to a change in volume between the reactants in their initial state and in their transition state.^{1b,127,156} This volume change is called the activation volume (ΔV^\ddagger), and is the sum of the volume changes resulting from both electrostriction, and physical rearrangement of the reactants.

Second order rate constants were determined from slopes of plots of the pseudo first order rate constant versus the solute concentration. From 4 to 15 concentrations of solute were used to determine a k_5 at each pressure.

The value of ΔV^\ddagger was calculated from plots of $\log k$ versus P, using (7).

$$\Delta V^\ddagger = - \frac{2.303RT(\log k_a/k_b)_T}{P_b - P_a} \quad (7)$$

ΔV^\ddagger has units of $\text{cm}^3 \text{ mol}^{-1}$

R is the gas constant

T is the temperature in degrees K

k_a is the rate constant at pressure P_a

k_b is the rate constant at pressure P_b

When $T = 295\text{K}$ and $(P_b - P_a) = 2 \text{ kb}$ ($2.9 \times 10^4 \text{ psi}$), then

(7) reduces to (8).

$$\Delta V^\ddagger = -28.3 (\log k_b/k_a)_T. \quad (8)$$

Pulses of 2.2 MeV electrons of 1.0 μs duration were used throughout the high pressure work.

Some of the results presented for the solvent methanol are from data obtained by M. G. Robinson.¹⁵⁷ They are included for completeness and for comparison between the solvents methanol and ethanol.

1. THE EFFECT OF PRESSURE ON THE e_s^- DECOMPOSITION REACTION

a. Pure neutral methanol and ethanol

The effect of pressure on the reaction of e_s^- with methanol or ethanol is illustrated by the results in Figure III-23 and Table III-14.

Methanol used for this study was treated by the

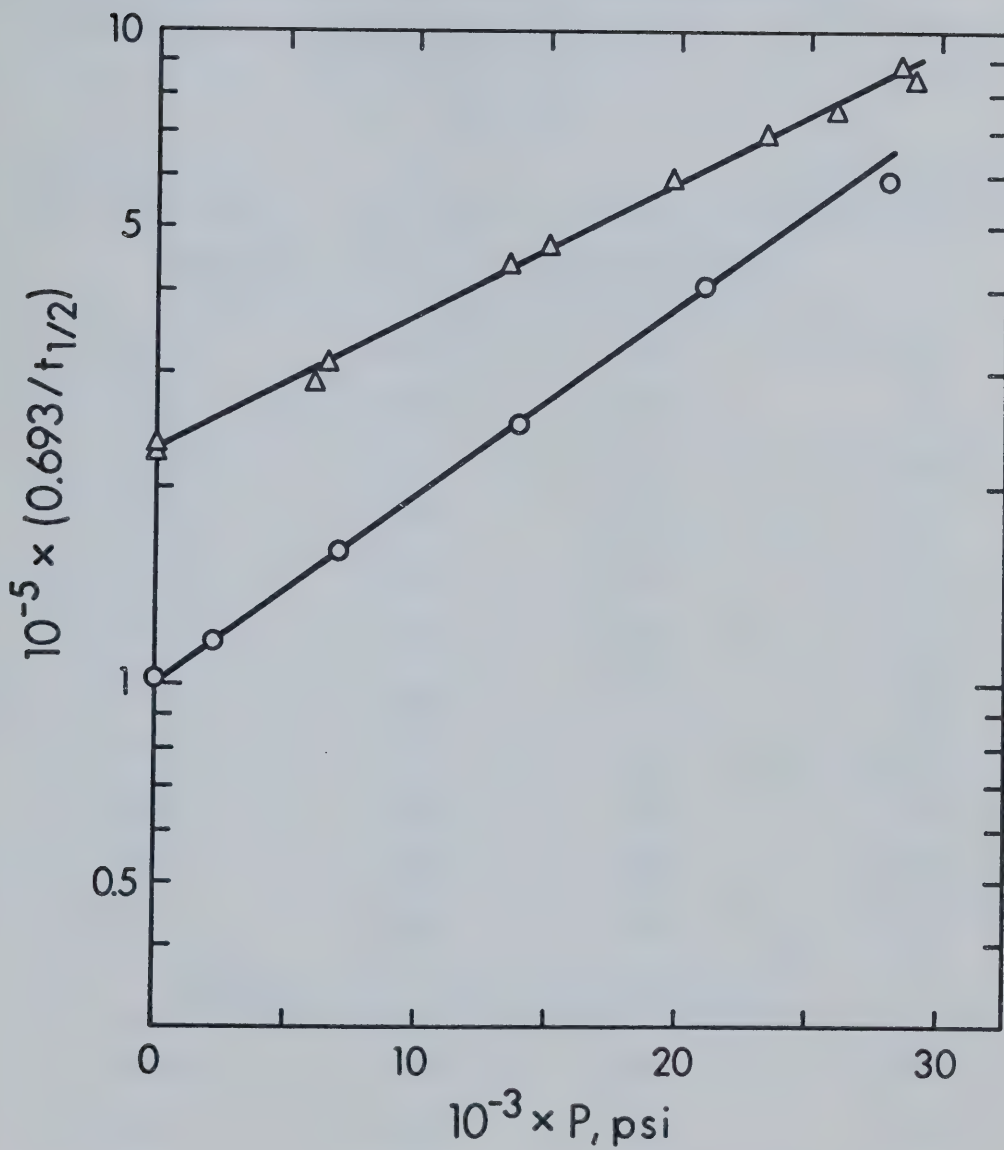


FIGURE III-23. ΔV^\ddagger for the e_s^- Decomposition Reaction
in MeOH (Δ) or EtOH (\circ). $295 \pm 1\text{K}$.

TABLE III-14

The Effect of Pressure on e_s^- Decomposition in

Methanol and Ethanol

T = 295 \pm 1K

$10^{-3} \times P^a, \text{psi}$	P, kb	$t_{1/2}, \mu\text{s}$	$10^{-5} \times k_4^b, \text{s}^{-1}$
Methanol, $\Delta V^\ddagger = -16.7 \pm 0.5 \text{ cm}^3 \text{ mol}^{-1}$			
0.014	0.001	3.0	2.3
0.014	0.001	3.1	2.2
6.0	0.41	2.4	2.9
6.5	0.45	2.2 ₅	3.1
13.5	0.93	1.6	4.3
15.0	1.03	1.5	4.6
19.8	1.36	1.2	5.8
23.3	1.61	1.0	6.9
26.0	1.79	0.92	7.5
28.5	1.96	0.79	8.8
29.0	2.00	0.83	8.3
Ethanol, $\Delta V^\ddagger = -23.4 \pm 0.5 \text{ cm}^3 \text{ mol}^{-1}$			
0.014	0.001	6.8	1.0
2.35	0.16	6.0	1.1 ₅
7.0	0.48	4.3	1.6
13.8	0.95	2.7	2.6
21.0	1.45	1.7	4.1
28.0	1.93	1.2	5.8

^a \pm 200 psi for P > 1 bar.^b Error may be \pm 5%

Na-NaBH₄ purification method.

Values for ΔV^\ddagger are -23.4 and -16.7 cm³ mol⁻¹ in ethanol and methanol, respectively. These may be compared to $\Delta V^\ddagger = -14.3$ cm³ mol⁻¹ found for e_s⁻ decomposition ¹²³ in water.

b. The effect of base on ΔV^\ddagger of e_s⁻ decomposition

The results for methanol and ethanol are given in Figures III-24 and III-25, respectively. The data are summarized in Tables III-15 and III-16.

Solutions were made basic by addition of translucent KOH pellets which were free of carbonate spots. As KOH concentration was increased in methanol, ΔV^\ddagger became more negative. In ethanol, the addition of base caused ΔV^\ddagger to be initially less negative, then more negative again as the base concentration increased. The $t_{1/2}$ of e_s⁻ was similarly affected in this study, first decreasing, and then increasing as the base concentration was increased. This may be interpreted in terms of the amount of impurity present, although it is not understood how addition of more base could overcome the impurity introduced at low base concentration. The lower the contribution of reaction (5), the more negative ΔV^\ddagger would be.

A value of -16 cm³ mol⁻¹ in ethanol containing ~5 mM NaOH has been reported.¹¹⁵ The more negative values reported here indicate that the ethanol used in this work was of higher purity.

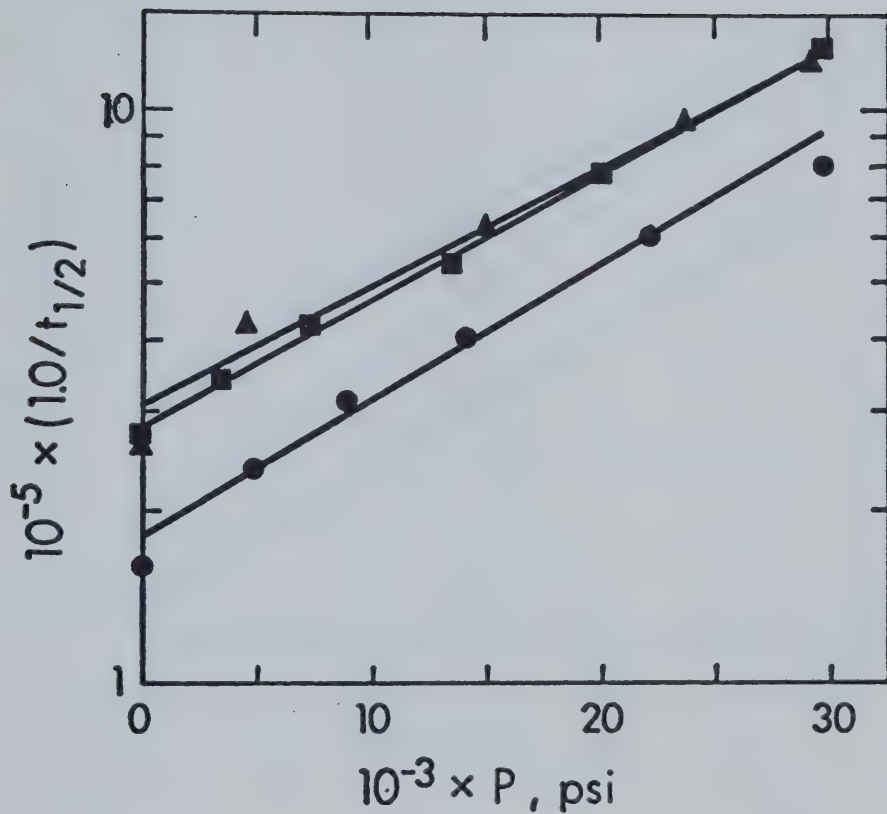


FIGURE III-24. The Effect of $[\text{KOH}]$ on ΔV^{\ddagger} of e_s^-

Decomposition in Methanol. $295 \pm 1\text{K}$.

▲, 0.021 M; ■, 0.069 M; ●, 0.90 M.

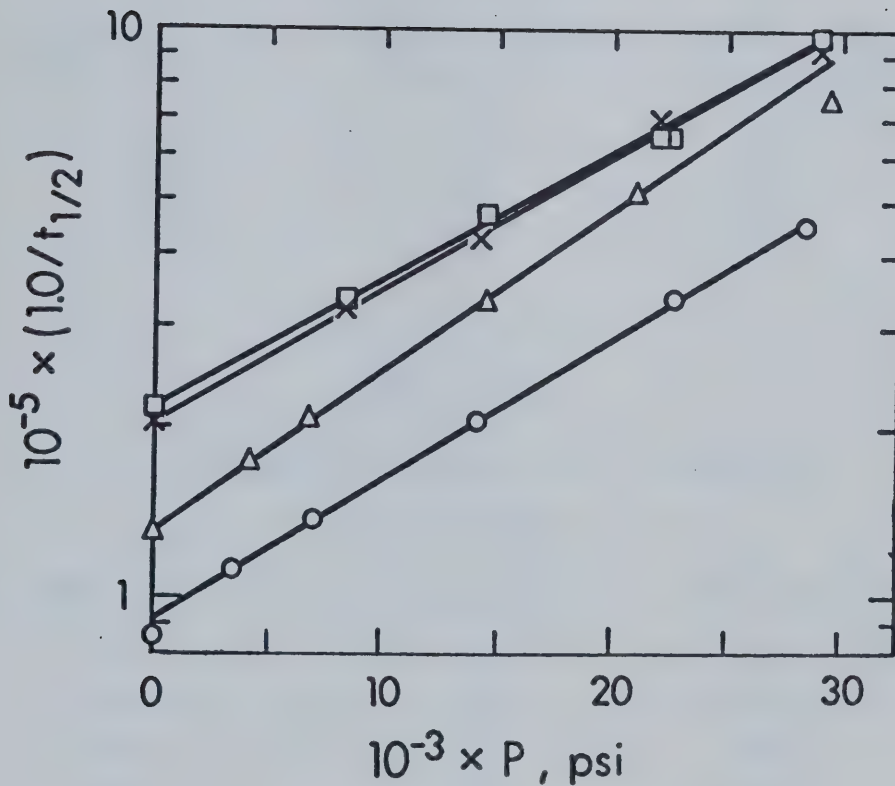


FIGURE III-25. The Effect of [KOH] on ΔV^{\ddagger} of e_s^- Decomposition in Ethanol. $295 \pm 1\text{K}$. \times , 0.001 M ;
 \square , 0.005 M ; \triangle , 0.013 M .
 \circ , 0.98 M

TABLE III-15

The Effect of Base on ΔV^\ddagger in Methanol¹⁵⁷

$[KOH]^a, M$	$T = 295 \pm 1K$		$\Delta V^\ddagger c, \text{cm}^3 \text{mol}^{-1}$
	$10^{-5} \times k_4, \text{b s}^{-1}$		
0	2.3		-16.7 \pm 0.5
0.021	1.8		-17.0
0.069	1.9		-18.1
0.90	1.1		-19.4

TABLE III-16

The Effect of Base on ΔV^\ddagger in Ethanol

$[KOH]^a, M$	$T = 295 \pm 1K$		$\Delta V^\ddagger c, \text{cm}^3 \text{mol}^{-1}$
	$10^{-5} \times k_4, \text{b s}^{-1}$		
0	1.0		-23.4 \pm 0.5
0.001	1.4		-18.6
0.005	1.5		-18.3
0.013	0.9		-23.1
0.98	0.6		-20.3

^a Concentration at 1 bar.^b Rate constant for e_s^- decay at 1 bar.^c Error may be $\pm 1.0 \text{ cm}^3 \text{mol}^{-1}$ for basic solutions.

c. The effect of water on ΔV^\ddagger of e_s^- decomposition in
ethanol.

Results are presented in Figure III-26 and Table III-17 for the effect on ΔV^\ddagger of adding water to ethanol. There was a monotonic decrease in $|\Delta V^\ddagger|$ as the water concentration increased.

The ΔV^\ddagger obtained in pure ethanol agrees well with that given in Figure III-23. Within experimental error, there was no change in ΔV^\ddagger for up to 3.0 M H_2O added. However, $t_{1/2}$ for e_s^- was increased at all pressures and curvature developed at low pressure, after 0.5 M water was added.

For "pure" (55.6 M) water, $\Delta V^\ddagger = +0.8 \text{ cm}^3 \text{ mol}^{-1}$. This compares well with values found by pulse radiolysis for diffusion controlled reactions of e_s^- in water with a variety of scavengers ¹¹⁹, and may be attributed to reaction with impurities in the water.

2. THE EFFECT OF PRESSURE ON THE SCAVENGING OF e_s^-

The effect of pressure on the reaction rate of e_s^- with scavenging solutes (5) was determined in the solvents methanol and ethanol. Nine compounds were used as solutes in ethanol. Of these, only acid was not also used in methanol.

Scavenger species were chosen to include a wide range of reaction rate constants. Results are reported

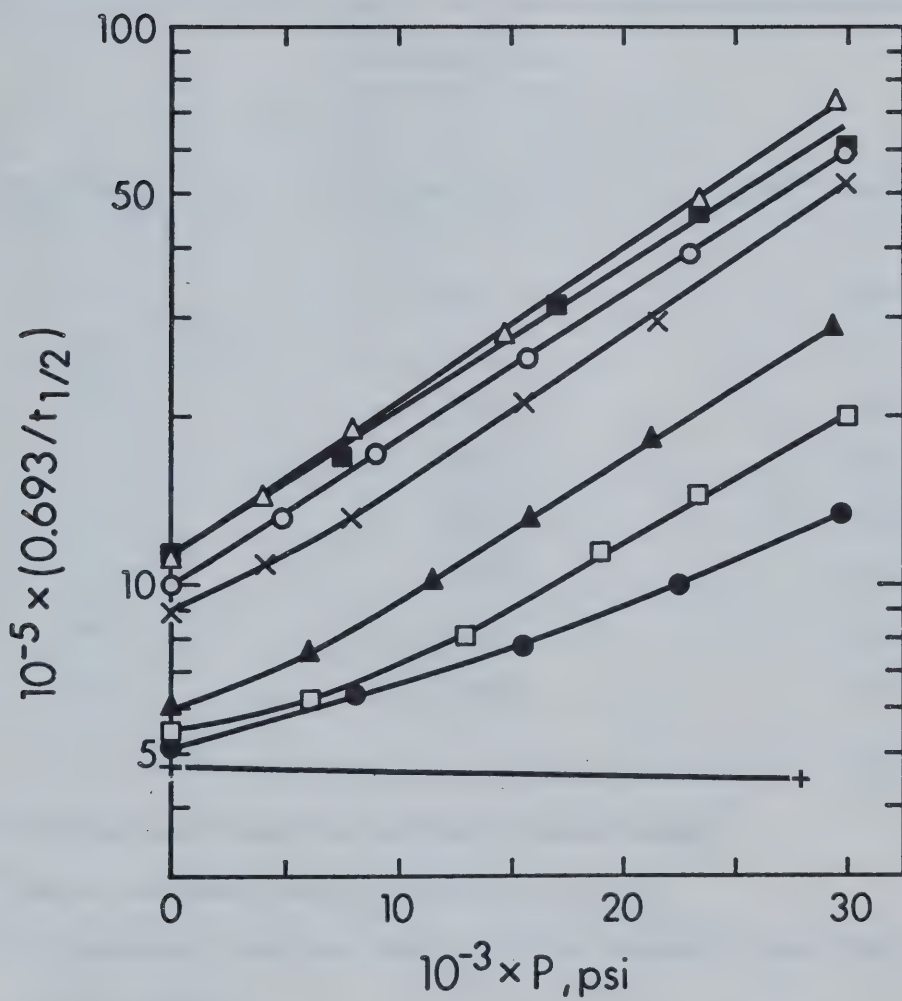


FIGURE III-26. The Effect of $[\text{H}_2\text{O}]$ on ΔV^\ddagger of e_s^- Decomposition in Ethanol. Δ , 0.0 M;
 ■, 0.1 M; ○, 0.5 M; X, 1.0 M; ▲, 3.0 M;
 □, 5.0 M; ●, 10.0 M; +, 55.6 M.

TABLE III-17

The Effect of H_2O on ΔV^\ddagger of e_s^- Decomposition in Ethanol $T = 295 \pm 1K$

$[H_2O]^a, M$	$10^{-5} \times k_4^b, s^{-1}$	$\Delta V^\ddagger c, cm^3 mol^{-1}$
0.0	1.1	-22.6
0.1	1.1	-21.3
0.5	1.0	-21.2
1.0	0.89	-22.3
3.0	0.61	-20.8
5.0	0.55	-19.3
10.0	0.52	-13.5
55.6	0.48	+ 0.8 ^d

^a Calculated from the volume % water added.^b Rate constant for e_s^- decay at 1 bar.^c Calculated from the slope of the longest linear portion of the plot.^d Average value between 0 and 2 kbar.

roughly in the order of decreasing ΔV^\ddagger , with data from both solvents presented together for a particular scavenger.

a. Naphthalene ($C_{10}H_8$) as e_s^- scavenger

The results are presented in Figure III-27 A, B, C and D for methanol as solvent, and Figure III-28 A, B, C and D for ethanol as solvent. Rate constants at different pressures are summarized in Table III-18.

The k_5 's at 1 bar are a factor of 1.41 higher in both solvents than those determined in quartz cells. Separate stock solutions of naphthalene in methanol and ethanol were used. Therefore the most likely reason for the higher k_5 's was impurity in the naphthalene used in preparation of the stock solution.

In spite of the scatter on the ΔV^\ddagger plot in methanol, it was evident that ΔV^\ddagger is positive in sign.

b. Acetonitrile (CH_3CN) as e_s^- scavenger

The results are presented in Figure III-29 A, B, C and D and in Figure III-30 A, B, C and D for the solvents methanol and ethanol, respectively. The k_5 's and ΔV^\ddagger 's are compiled in Table III-19.

Acetonitrile does not scavenge electrons at a diffusion controlled rate. Its purity must therefore be established to ensure that there was not appreciable

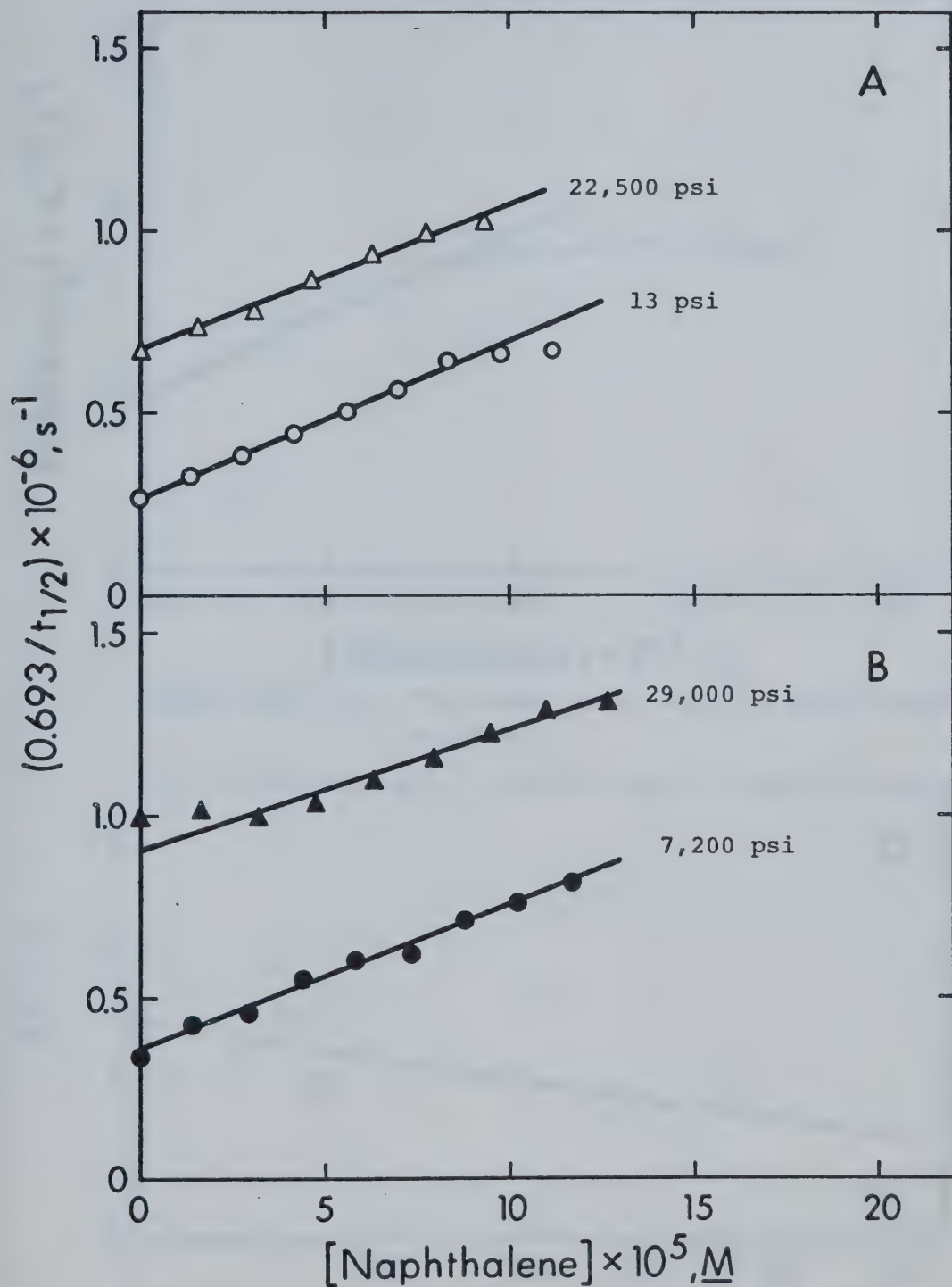


FIGURE III-27 A,B. The Effect of P on $e_s^- +$ Naphthalene in MeOH.

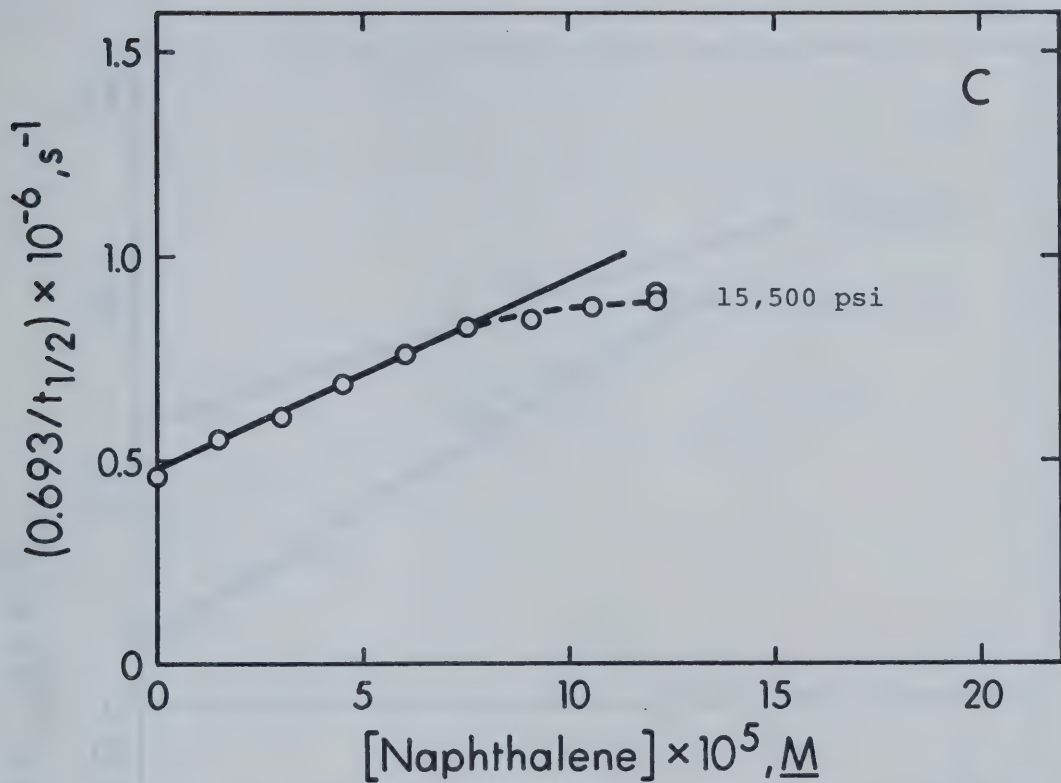


FIGURE III-27 C. The Effect of P on $e_s^- + \text{Naphthalene}$ in MeOH.

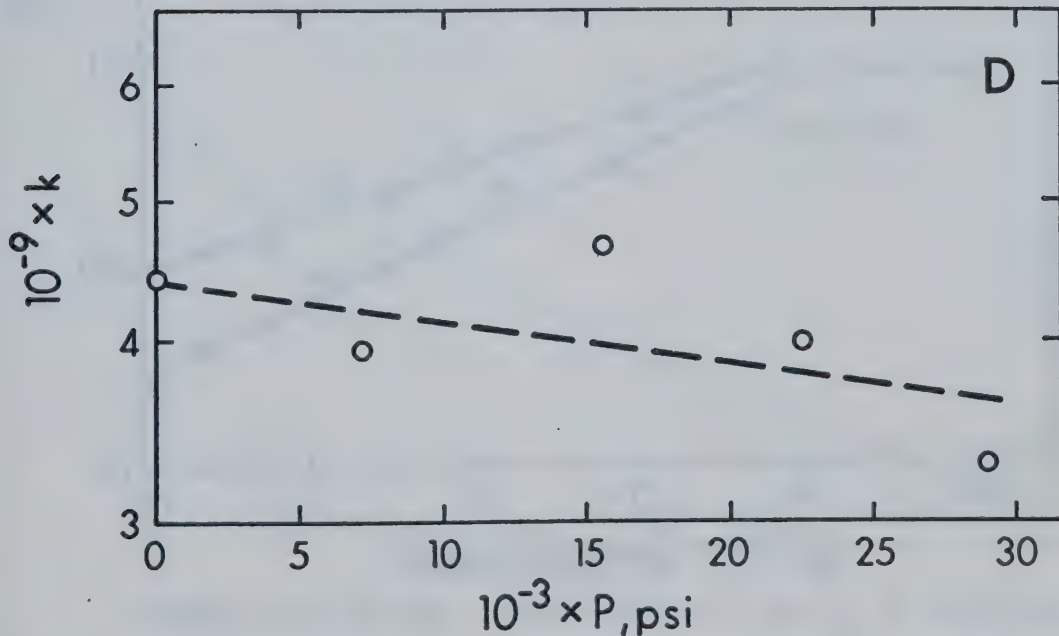


FIGURE III-27 D. ΔV^\ddagger for $e_s^- + \text{Naphthalene}$ in MeOH.

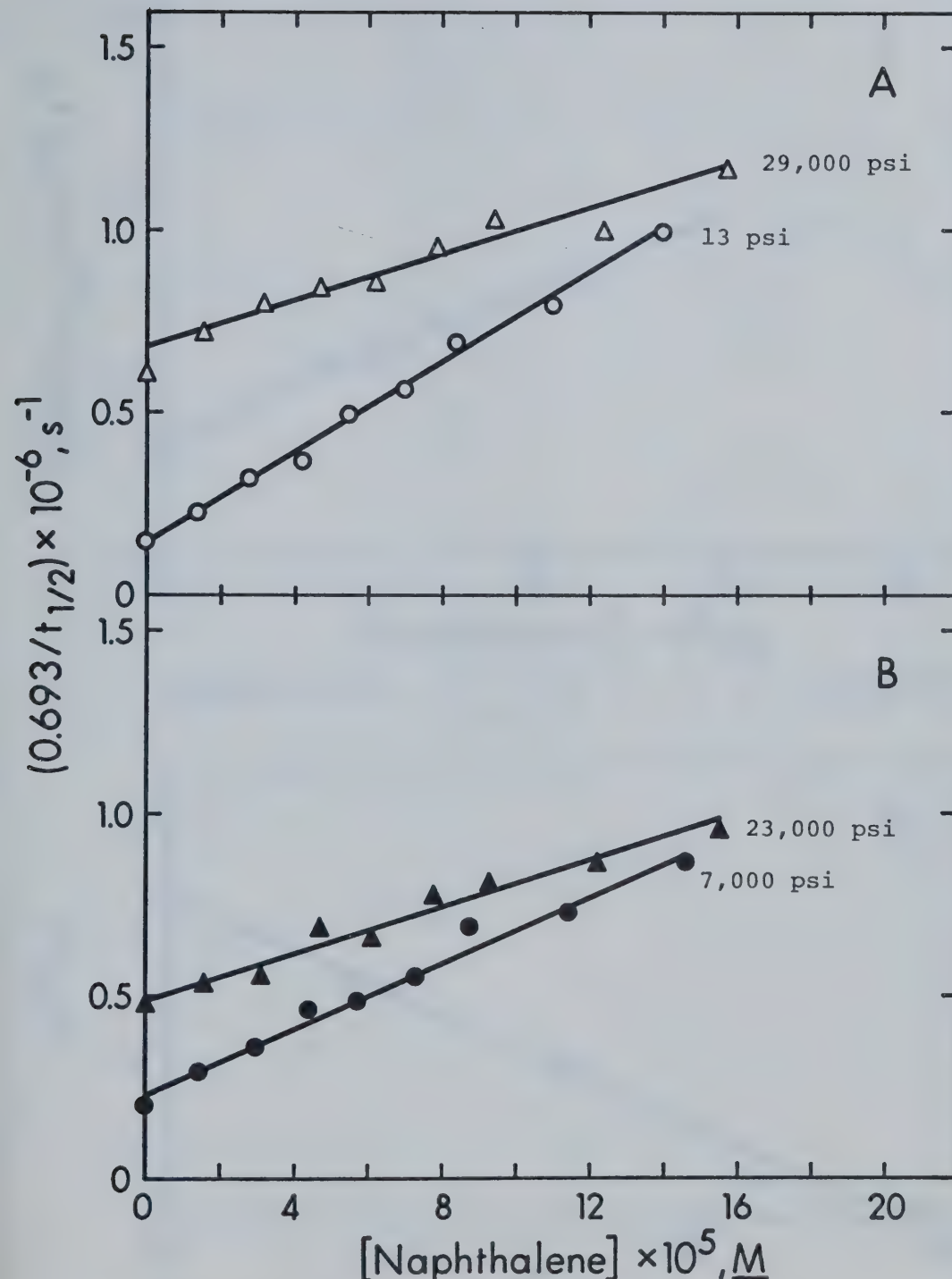


FIGURE III- 28 A,B. The Effect of P on $e_s^- + \text{naphthalene}$ in EtOH.

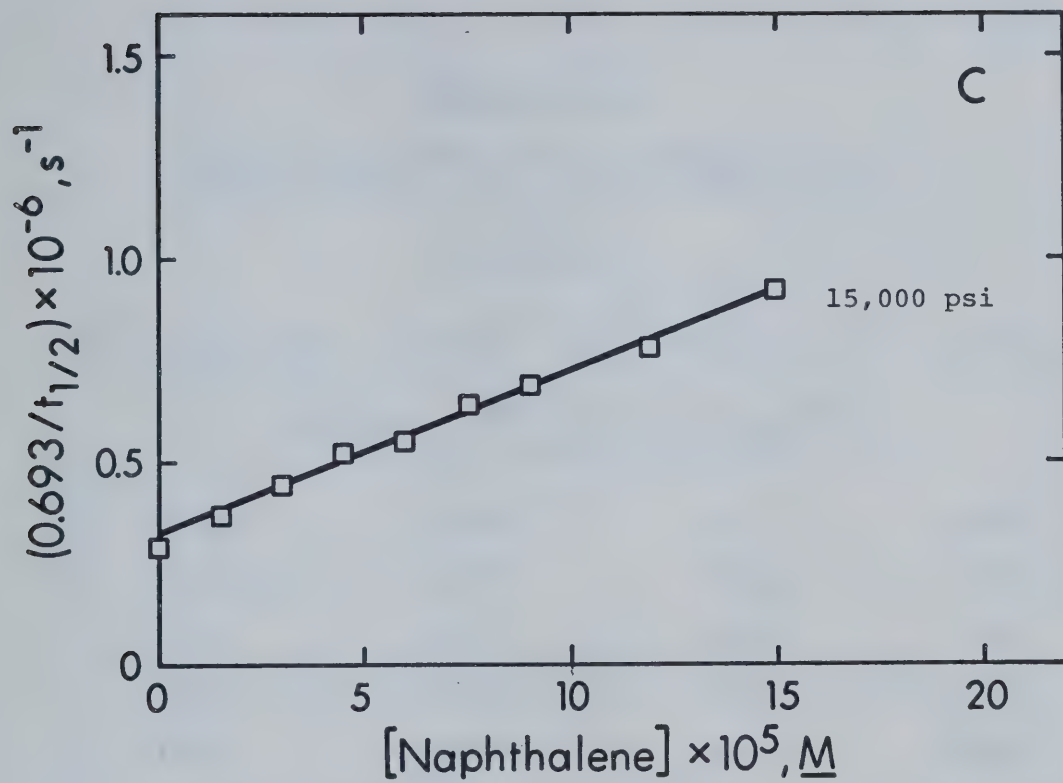


FIGURE III-28 C. The Effect of P on $e_s^- +$ Naphthalene in EtOH.

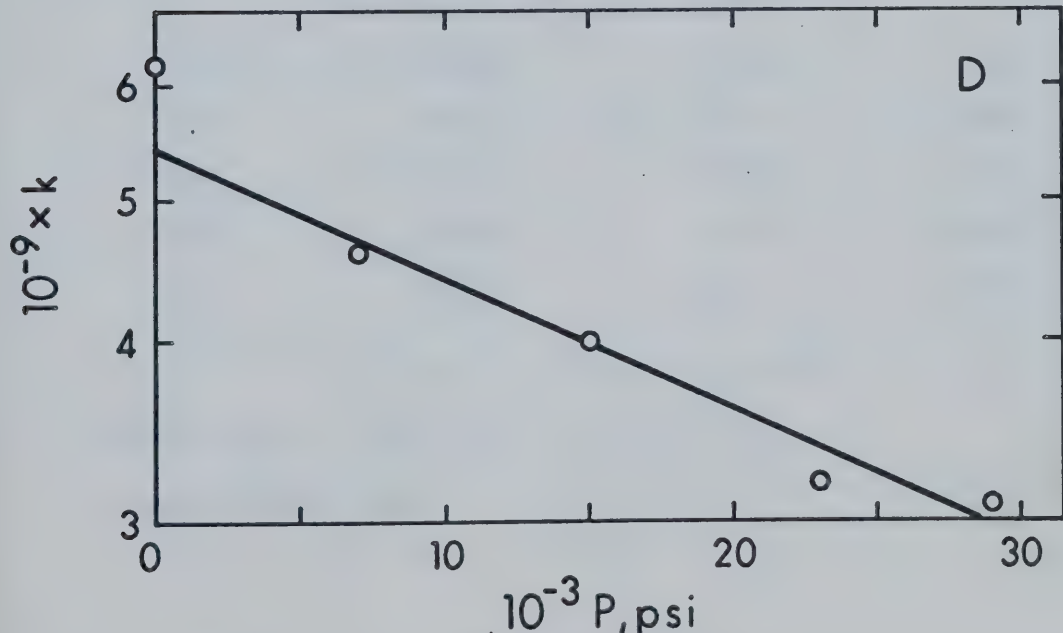


FIGURE III-28 D. ΔV^\ddagger for $e_s^- +$ Naphthalene in EtOH.

TABLE III-18

The k 's and ΔV^\ddagger 's for $e^-_s +$ Naphthalene $T = 295 \pm 1K$

$10^{-3} \times P^a, \text{ psi}$	$P, \text{ kb}$	$10^{-9} \times k_5^b, \text{ M}^{-1} \text{ s}^{-1}$	$\log k_5$
Methanol, $\Delta V^\ddagger = 2 \pm 1 \text{ cm}^3 \text{ mol}^{-1}$			
0.013	0.001	4.4	9.64
7.2	0.50	3.9 ₅	9.60
15.5	1.07	4.6 ₅	9.67
22.5	1.55	4.0	9.60
29.0	2.00	3.3	9.52
Ethanol, $\Delta V^\ddagger = 7.3 \pm 1 \text{ cm}^3 \text{ mol}^{-1}$			
0.013	0.001	6.2	9.79
7.0	0.48	4.6	9.66
15.0	1.03	4.0	9.60
23.0	1.58	3.2	9.51
29.0	2.00	3.1	9.49

^a Error may be $\pm 3\%$.^b Error may be $\pm 5\%$.

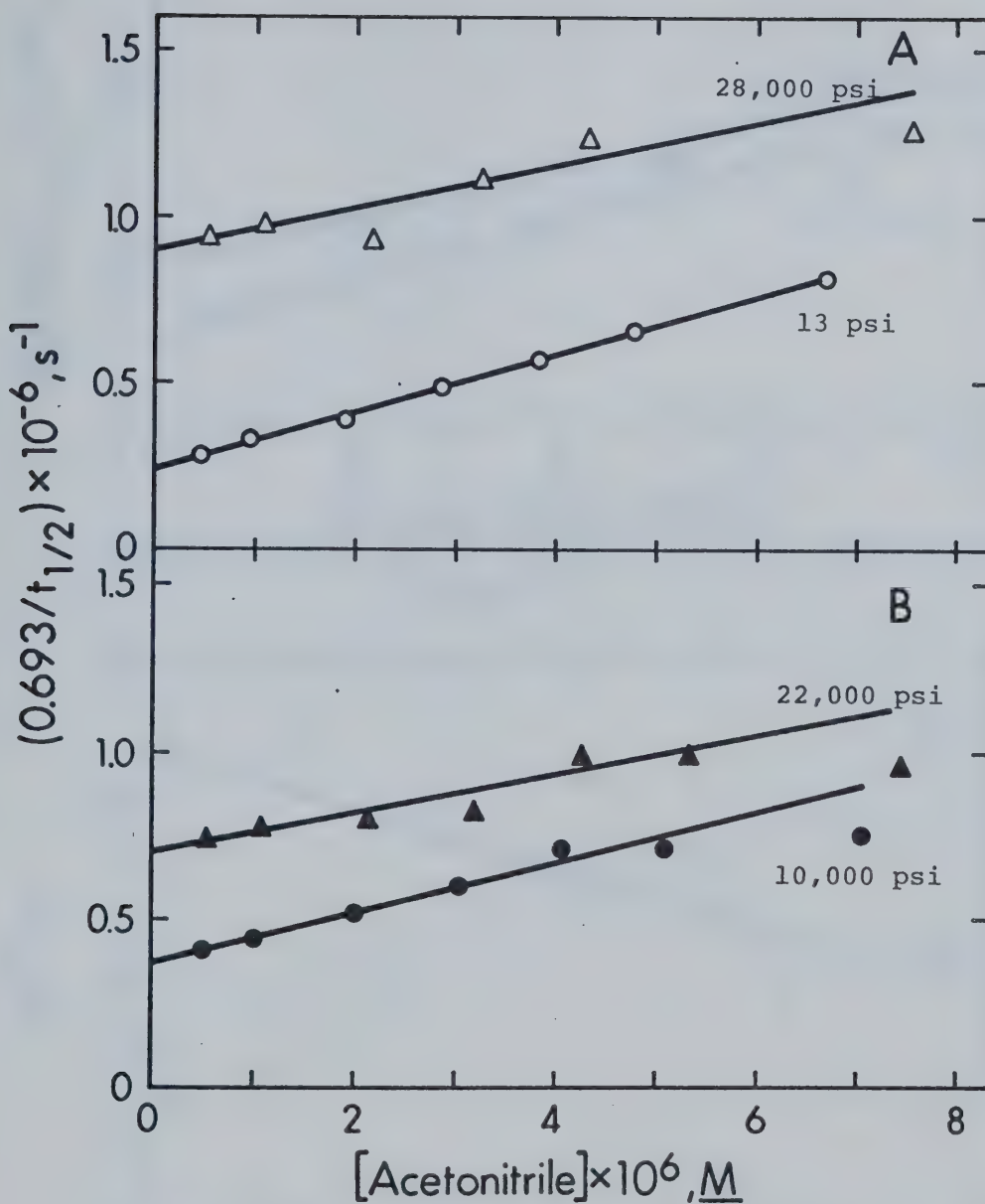


FIGURE III-29 A,B. The Effect of P on $e^- + Acetonitrile$ in MeOH.

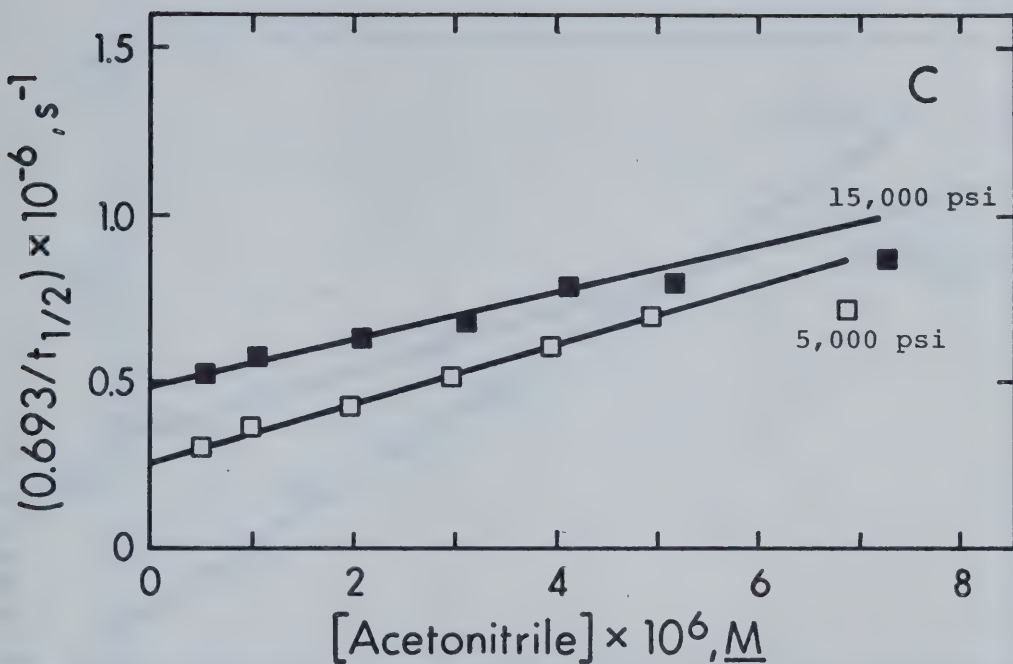


FIGURE III-29 C. The Effect of P on e_s^- + Acetonitrile in MeOH.¹⁵⁷

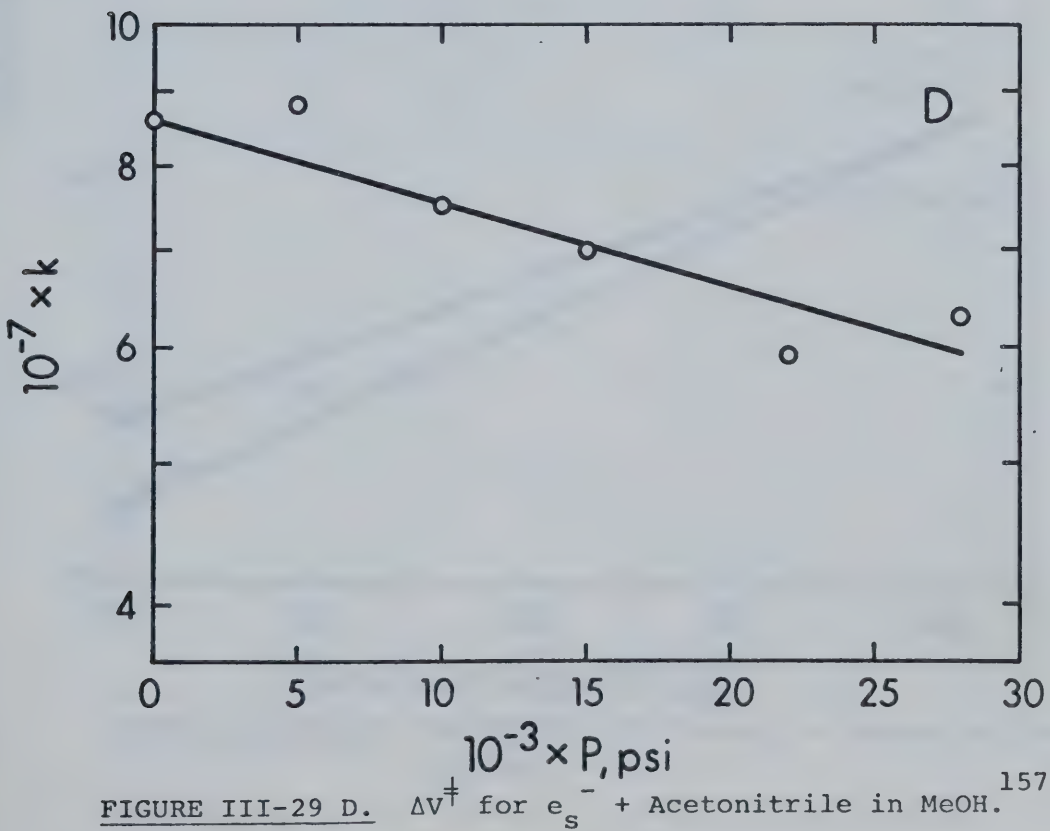


FIGURE III-29 D. ΔV^\ddagger for e_s^- + Acetonitrile in MeOH.¹⁵⁷

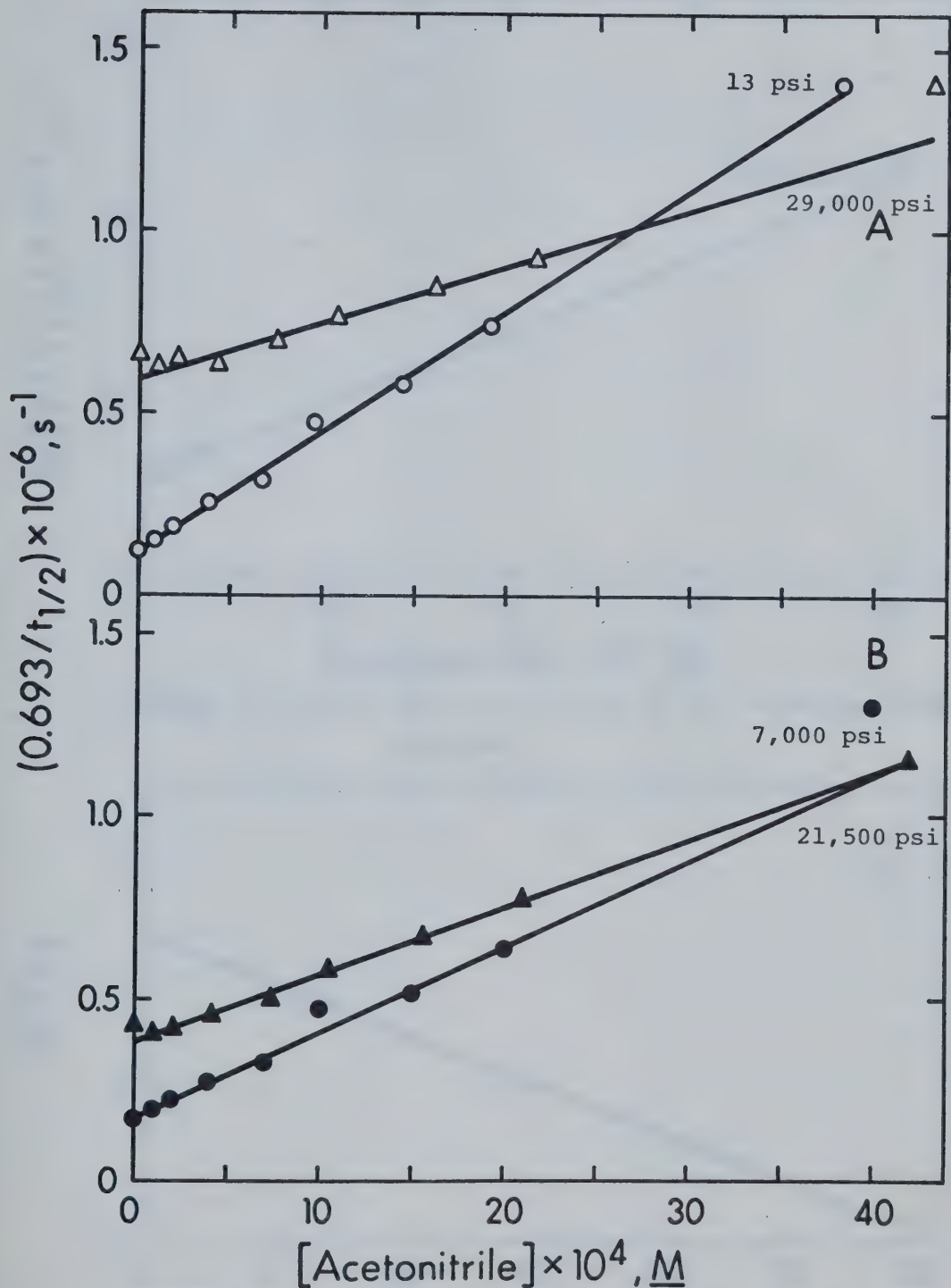


FIGURE III-30 A, B. The Effect of P on $e_s^- + \text{Acetonitrile}$ in EtOH.

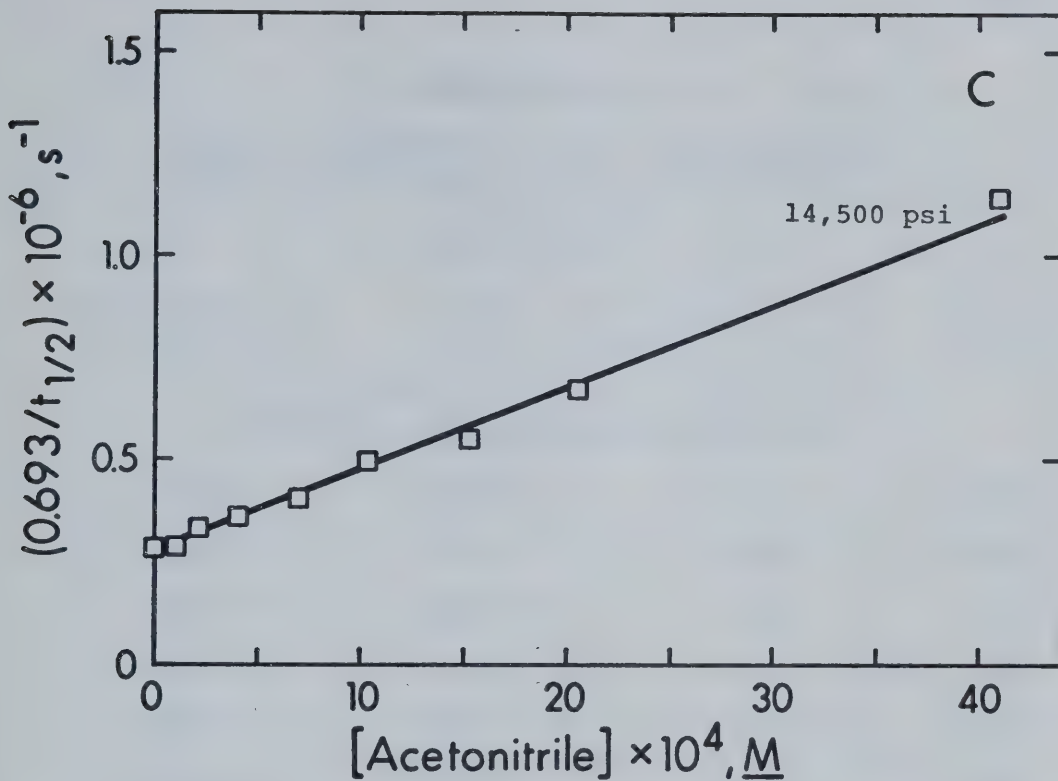


FIGURE III-30 C. The Effect of P on $e_s^- + \text{Acetonitrile}$ in EtOH.

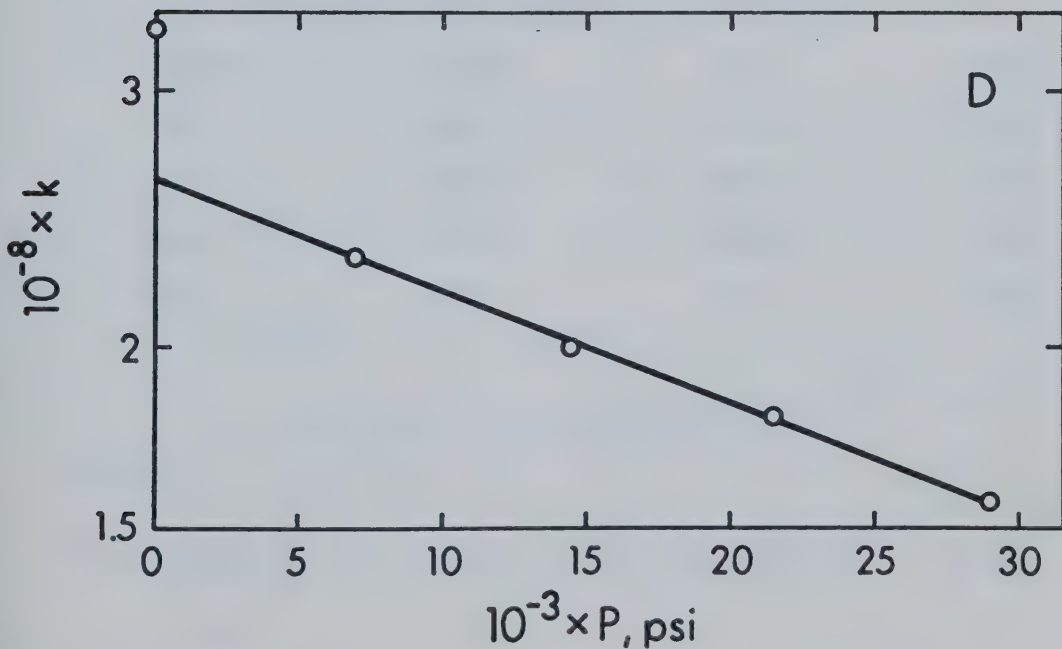


FIGURE III-30 D. ΔV^\ddagger for $e_s^- + \text{Acetonitrile}$ in EtOH.

TABLE III-19

The k 's and ΔV^\ddagger 's for $e_s^- + \text{Acetonitrile}$ $T = 295 \pm 1\text{K}$

$10^{-3} \times P^a, \text{ psi}$	$P, \text{ kb}$	$10^{-7} \times k_5^b, \text{ M}^{-1} \text{ s}^{-1}$	$\log k_5$
Methanol 157 , $\Delta V^\ddagger = 4.7 \pm 1.3 \text{ cm}^3 \text{ mol}^{-1}$			
0.013	0.001	8.6	7.93
5.0	0.34	8.8	7.94
10.0	0.69	7.5	7.88
15.0	1.03	7.0	7.85
22.0	1.52	5.9	7.77
28.0	1.93	6.3	7.80
Ethanol, $\Delta V^\ddagger = 6.3 \pm 0.2 \text{ cm}^3 \text{ mol}^{-1}$			
0.013	0.001	33.0	8.52
7.0	0.48	23.0	8.36
14.5	1.00	20.0	8.30
21.5	1.48	18.2	8.26
29.0	2.00	15.7	8.20

^a Error may be $\pm 3\%$.^b Error may be $\pm 5\%$ for $P \leq 1 \text{ kb}$ and $\pm 15\%$ for $P > 1 \text{ kb}$.

reaction of e_s^- with an unknown impurity. The MC/B spectroscopic grade CH_3CN used has been reported to be of very high purity ¹⁵⁸, the major impurity being water (0.04%). Water would not affect the results at this concentration.

The U.V. optical absorption cutoff was at ~190 nm for the CH_3CN used. Addition of 0.15 mole % CH_2CHCN (acrylonitrile) increased the U.V. cutoff to 220 nm. The maximum concentration of acrylonitrile originally present was therefore << 0.15 mole %.

In ethanol, k_5 for acrylonitrile is $7 \times 10^9 \text{ M}^{-1} \text{ s}^{-1}$ (determined from only one CH_2CHCN concentration). This is only about 20 times greater than k_5 found for CH_3CN in ethanol. For the observed rate to have been due to acrylonitrile would have required it to be 5 mole % of the CH_3CN used. It was not.

Other possible impurities in acetonitrile are benzene, ammonia, acetic acid, and unsaturated nitriles.¹⁵⁹ None were in high enough concentration to affect the results.

As noted for benzene and phenol, a value of the ratio $k_5(\text{EtOH})/k_5(\text{MeOH}) > 1$ is not indicative of a fast scavenger. For acetonitrile the ratio at 1 bar is 3.8.

c. Perchloric acid (HClO_4) as e_s^- scavenger

The data are given in Figure III-31 A, B, C and D.

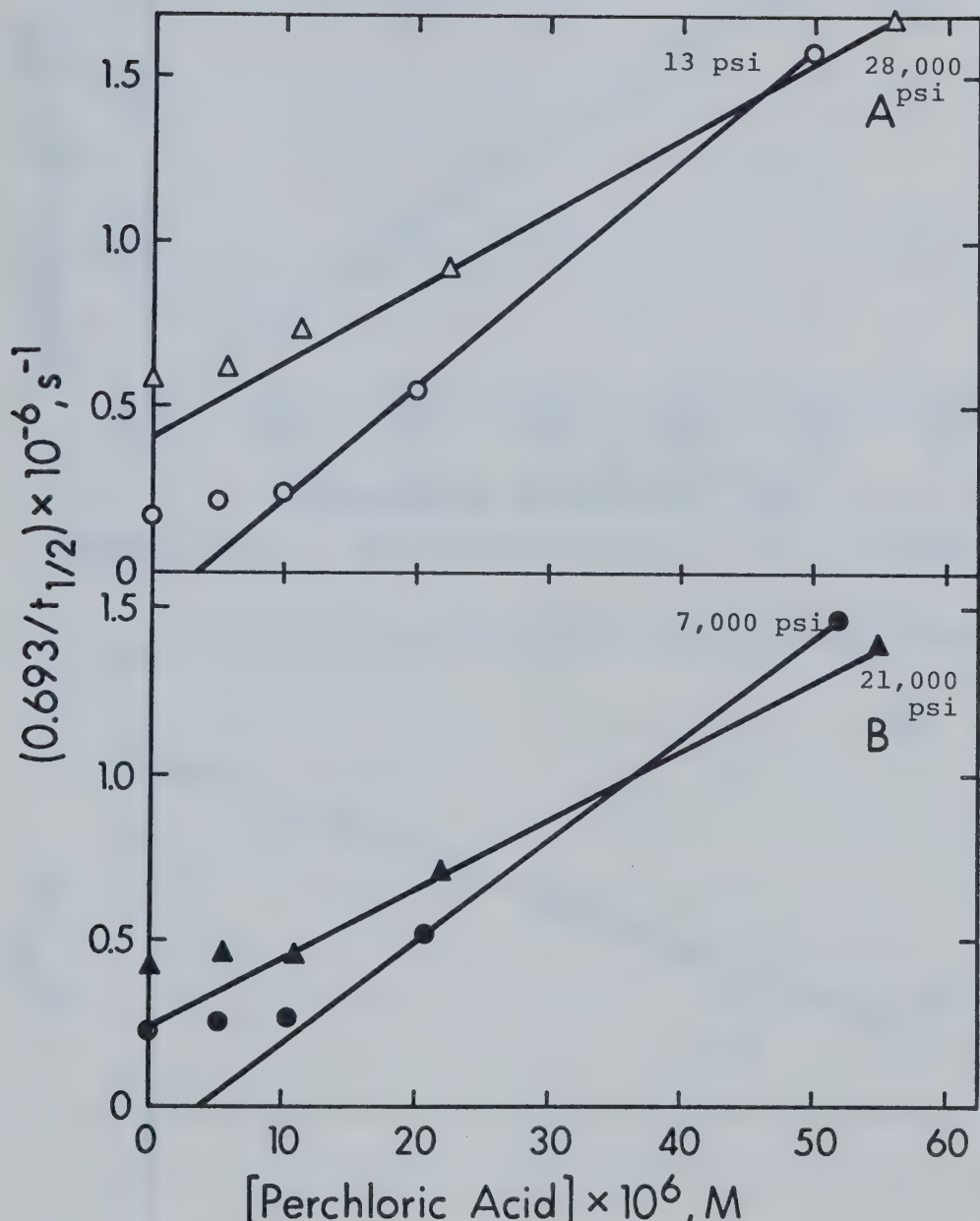


FIGURE III-31 A,B. The Effect of P on $e_s^- + H_s^+$ in EtOH.

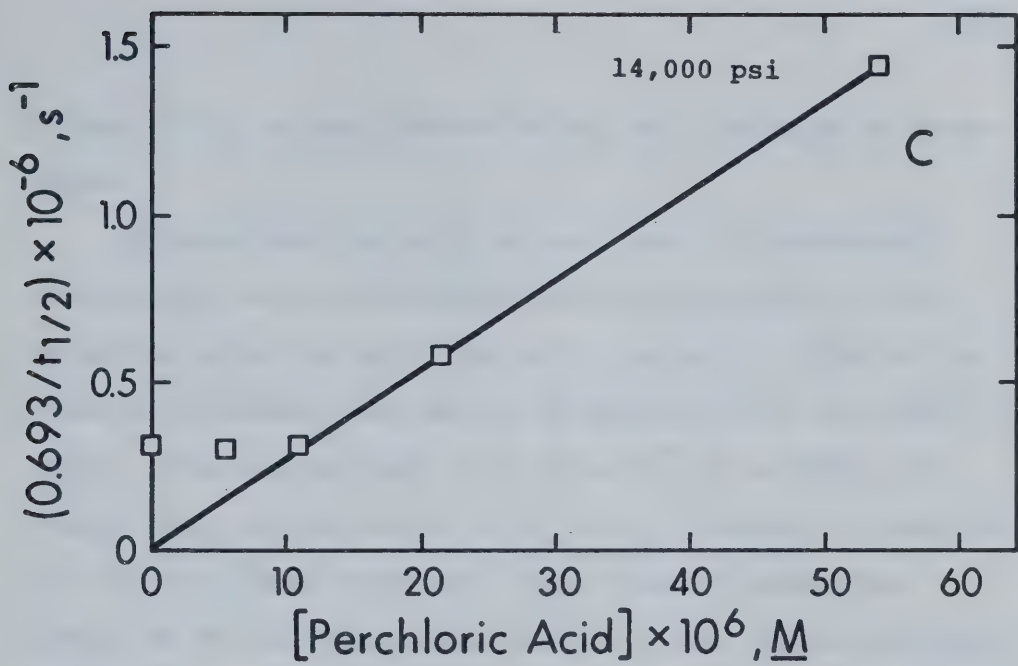


FIGURE III-31 C. The Effect of P on $e_s^- + H_s^+$ in EtOH.

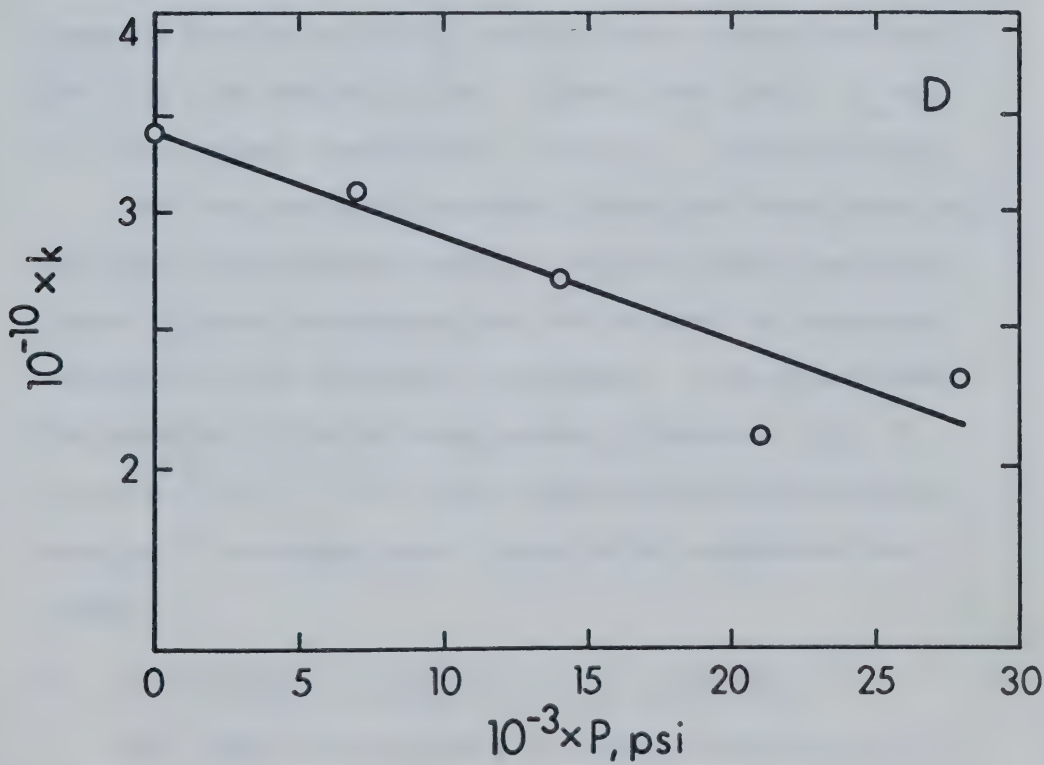


FIGURE III-31 D. ΔV^\ddagger for $e_s^- + H_s^+$ in EtOH.

Table III-20 gives a record of k_5 as a function of pressure.

Ethanol was the only solvent used. Considerable difficulty was encountered with acid adsorbing on, or reacting with, the metal walls of the cell. This is the reason for some plots having an intercept on the wrong axis. The samples made 5 or 10×10^{-6} M in HClO_4 produced very little change in $t_{\frac{1}{2}}$ of e_s^- because of removal of the acid from solution. This removal could have occurred at the Pyrex glass walls of the sample bubblers also.

Even higher acid concentrations could be largely removed from solution by cycling the pressure between 1 bar and 2 kb several times. After each cycle, $t_{\frac{1}{2}}$ for e_s^- was longer, indicating a lower H_s^+ concentration.

For the results presented, readings were taken only on the first pressure cycle. Even so, only the two or three highest concentrations can be used to determine values of k_5 at different pressures. This introduces the possibility of a large error. However, a k_5 of $3.4 \times 10^{10} \text{ M}^{-1} \text{ s}^{-1}$ at 1 bar agrees well with previous results⁸⁸ obtained over a much wider concentration range.

d. Nitrobenzene ($\text{C}_6\text{H}_5\text{NO}_2$) as e_s^- scavenger

The data are presented in Figures III-32 A, B, C

TABLE III-20

The k 's and ΔV^\ddagger 's for $e_s^- + H_s^+$

$T = 295 \pm 1K$

$10^{-3} \times P^a$, psi	P, kb	$10^{-10} \times k_5, \frac{M}{M} s^{-1}$	$\log k_5$
Ethanol, $\Delta V^\ddagger = 5.9 \pm 1 \text{ cm}^3 \text{ mol}^{-1}$			
0.013	0.001	3.4 ^b	10.53
7.0	0.48	3.1	10.49
14.0	0.96	2.7	10.43
21.0	1.45	2.1	10.32
28.0	1.93	2.3	10.36

^a Error may be $\pm 3\%$.

^b $3.6 \times 10^{10} \frac{M}{M} s^{-1}$ in quartz cells.

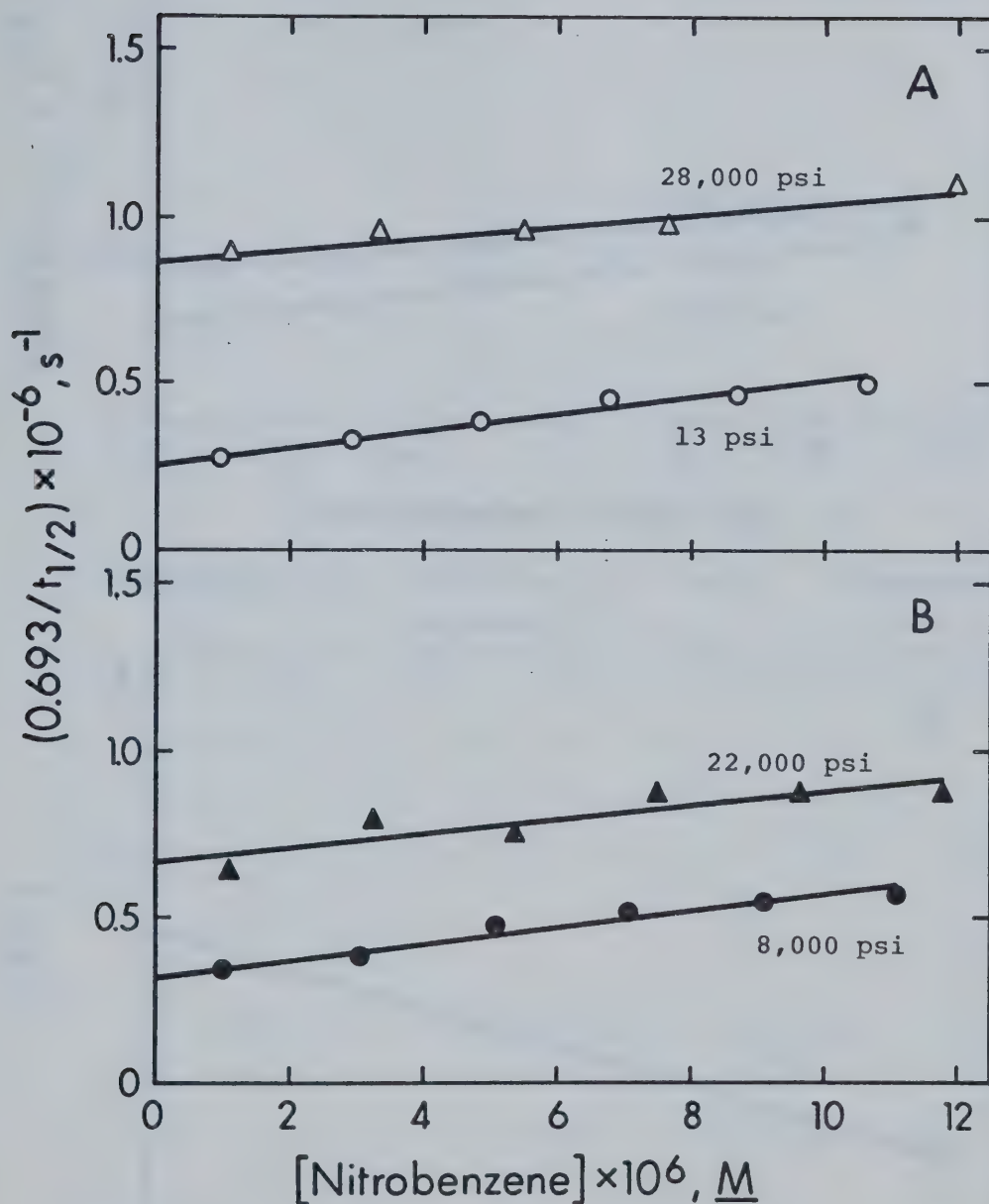


FIGURE III-32 A,B. The Effect of P on $e_s^- + \text{nitrobenzene}$ in MeOH .¹⁵⁷

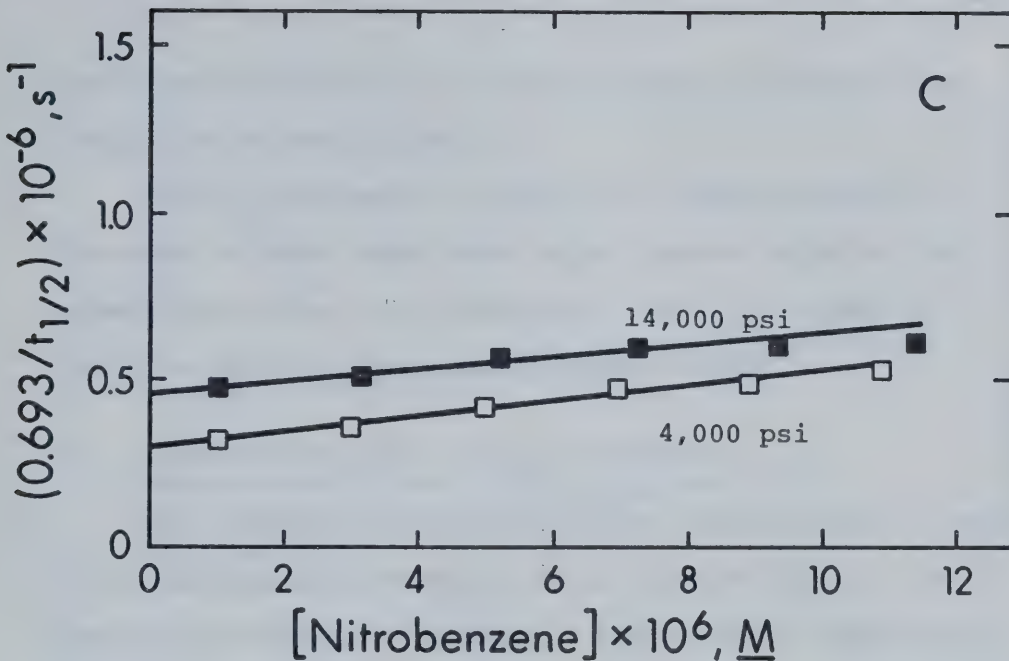


FIGURE III-32 C. The Effect of P on $e_s^- +$ Nitrobenzene in MeOH.¹⁵⁷

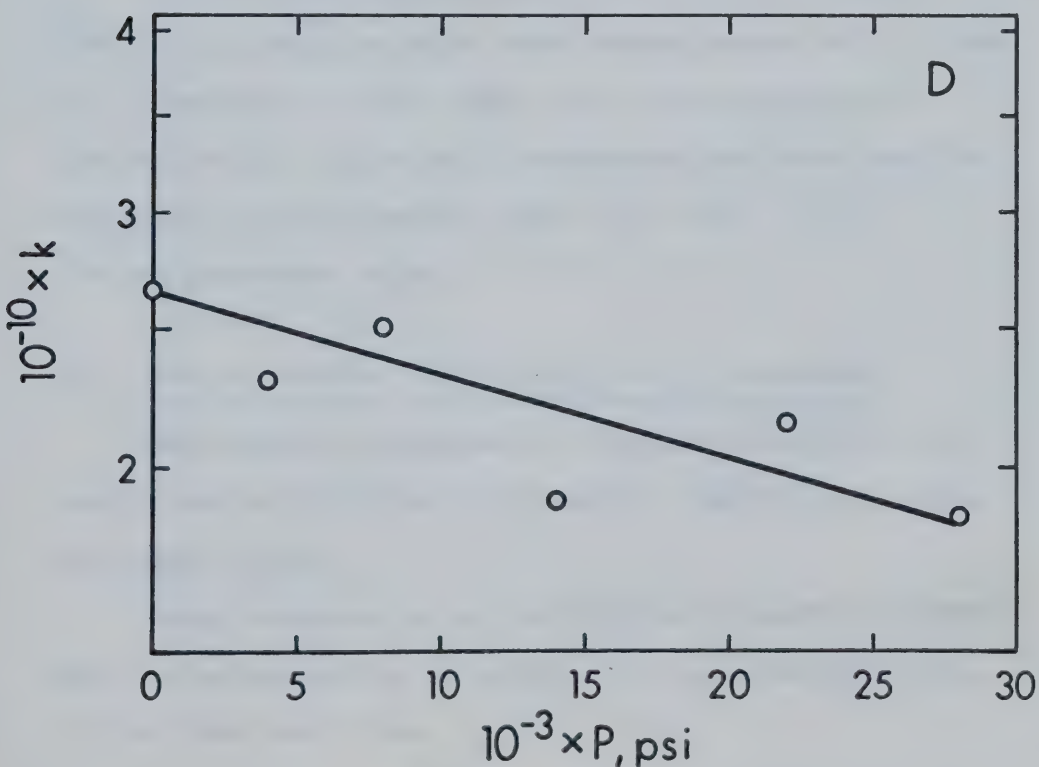


FIGURE III-32 D. ΔV^\ddagger for $e_s^- +$ Nitrobenzene in MeOH.¹⁵⁷

and D and III-33 A, B, C and D. The k_5 's and ΔV^\ddagger are tabulated in Table III-21.

The k_5 obtained in ethanol at 1 bar and 295K is the same as that found when using quartz cells at the same temperature. For methanol, the k_5 is higher by 20% than that found when using quartz cells.

e. Acetone ($(CH_3)_2CO$) as e_s^- scavenger

The results are given in Figure III-34 A, B, C and D for methanol as solvent, and in Figure III-35 A, B, C and D for ethanol as solvent. Table III-22 summarizes the k_5 's and ΔV^\ddagger 's obtained.

Within experimental error, the k_5 at 1 bar and 295K is the same as that found using quartz cells. The k_5 in methanol is 20% lower than that determined in quartz cells. Since more concentrations were used for the work in the pressure cell, $k_5 = 4.0 \times 10^9 \text{ M}^{-1} \text{ s}^{-1}$ is the preferred value.

f. Ethyl acetate ($CH_3CO_2C_2H_5$) as e_s^- scavenger

The results are shown in Figures III-36 A, B, C and D and in III-37 A, B, C and D. The k's are given in Table III-23.

Ethyl acetate is not an efficient electron scavenger. The ratio of k_5 in ethanol to k_5 in methanol is 2.4 at 295K and 1 bar.

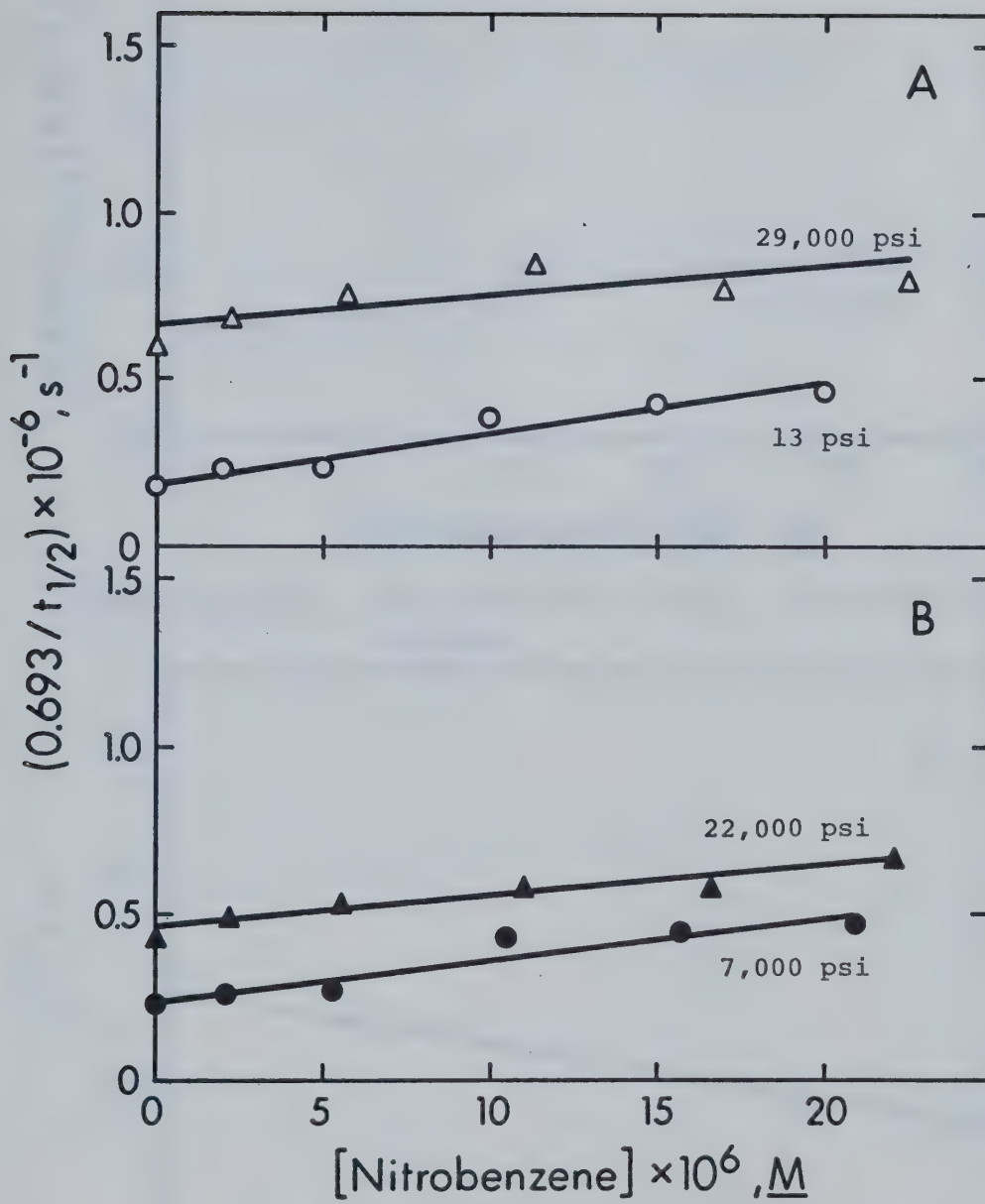


FIGURE III-33 A, B. The Effect of P on $e_s^- + \text{Nitrobenzene}$ in EtOH.

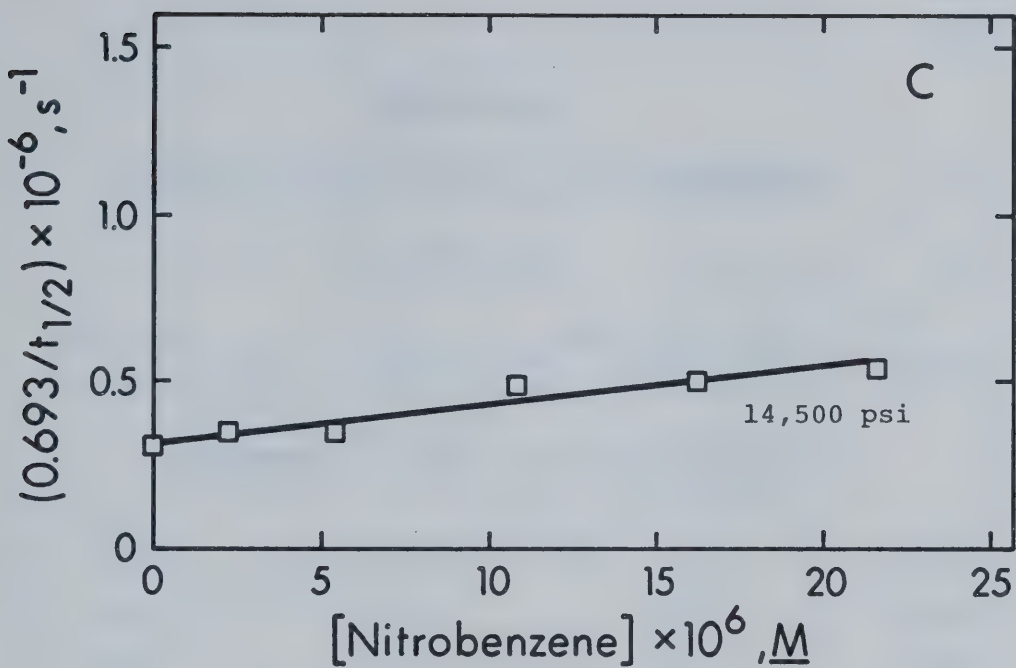


FIGURE III-33 C. The Effect of P on $e_s^- + \text{Nitrobenzene}$ in EtOH.

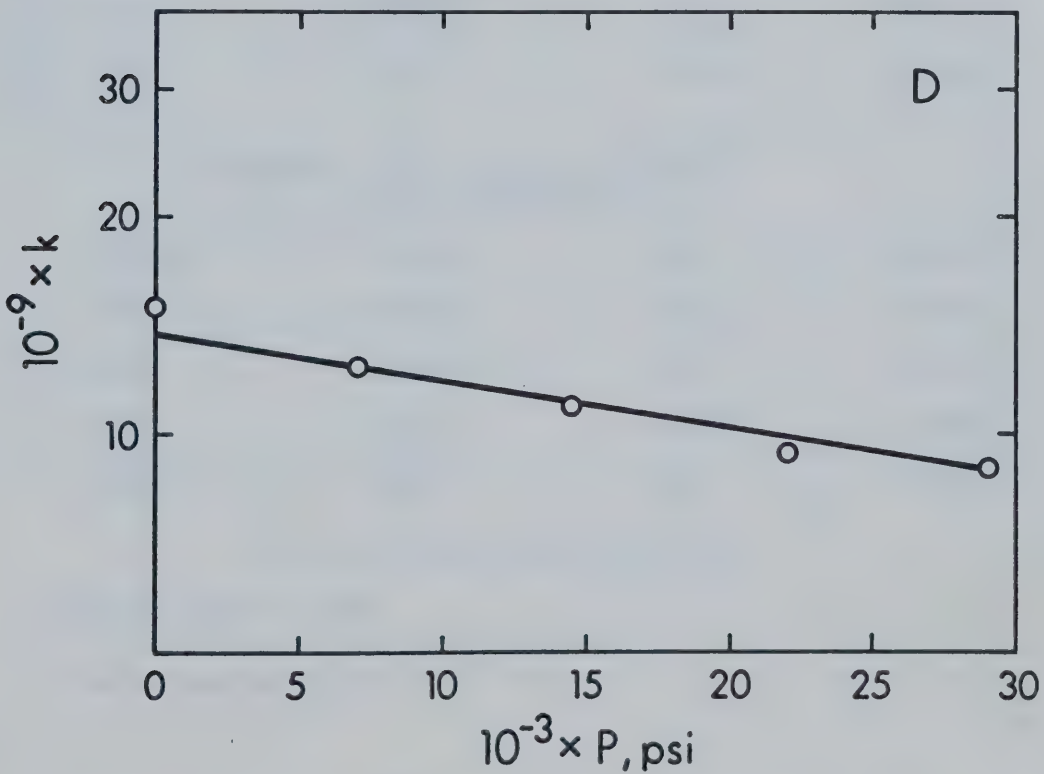


FIGURE III-33 D. ΔV^\ddagger for $e_s^- + \text{Nitrobenzene}$ in EtOH.

TABLE III-21

The k 's and ΔV^\ddagger 's for $e_s^- +$ Nitrobenzene $T = 295 \pm 1K$

$10^{-3} \times P^a, \text{ psi}$	$P, \text{ kb}$	$10^{-10} \times k_5^b, \text{ M}^{-1} \text{ s}^{-1}$	$\log k_5$
-----------------------------------	-----------------	--	------------

Methanol 157 , $\Delta V^\ddagger = 4.7 \pm 1.4 \text{ cm}^3 \text{ mol}^{-1}$			
---	--	--	--

0.013	0.001	2.6_5	10.42
4.0	0.28	2.3	10.36
8.0	0.55	2.5	10.40
14.0	0.96	1.9	10.28
22.0	1.52	2.1_5	10.33
28.0	1.93	1.8_5	10.27

Ethanol, $\Delta V^\ddagger = 5.2 \pm 1 \text{ cm}^3 \text{ mol}^{-1}$			
--	--	--	--

0.013	0.001	1.5	10.18
7.0	0.48	1.2_5	10.97
14.5	1.00	1.1	10.41
22.0	1.52	0.95	9.98
29.0	2.00	~ 0.9	9.95

^a Error may be $\pm 3\%$.

^b Error may be $\pm 10\%$.

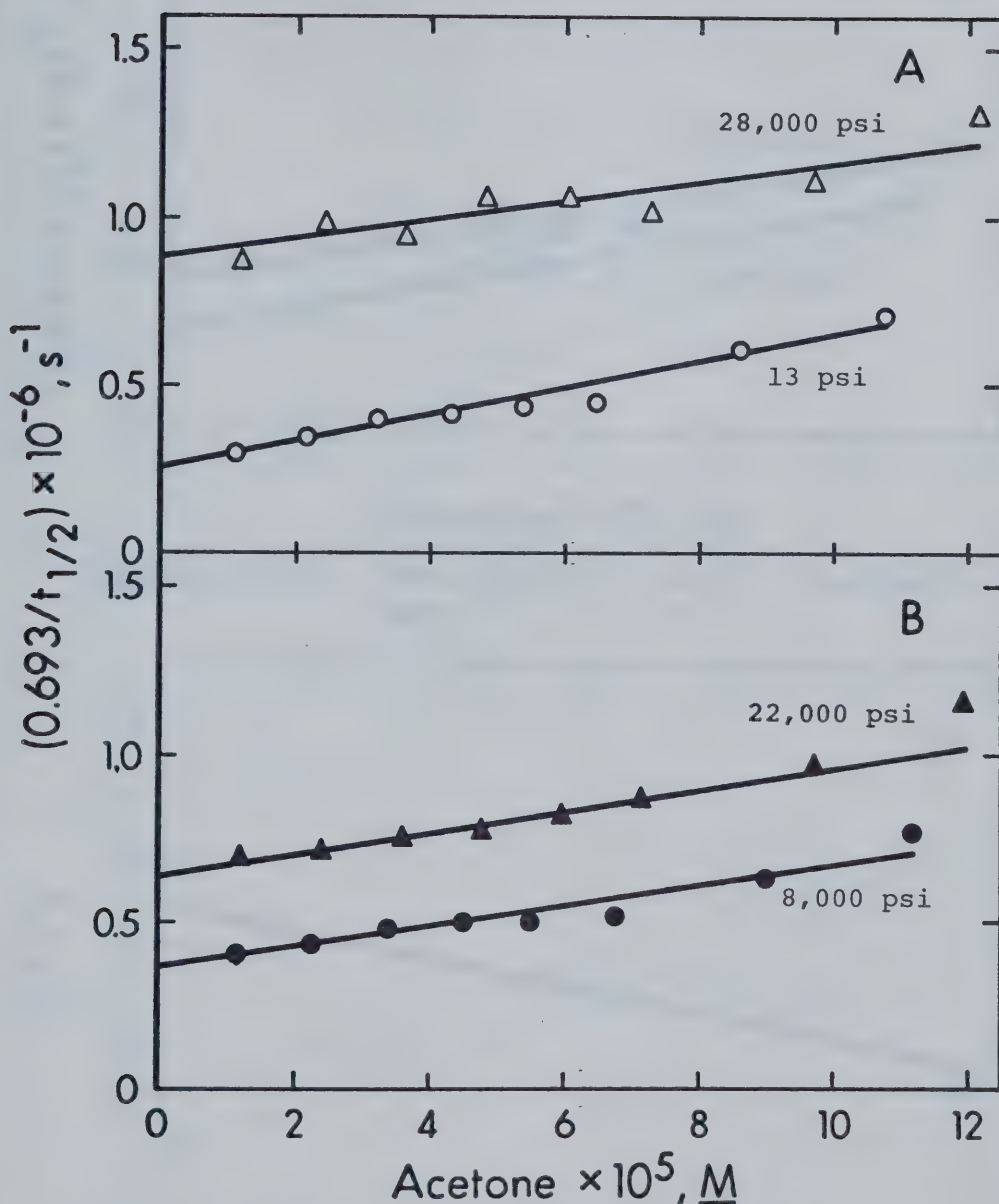


FIGURE III-34 A,B. The Effect of P on $e_s^- + \text{Acetone}$ in MeOH .

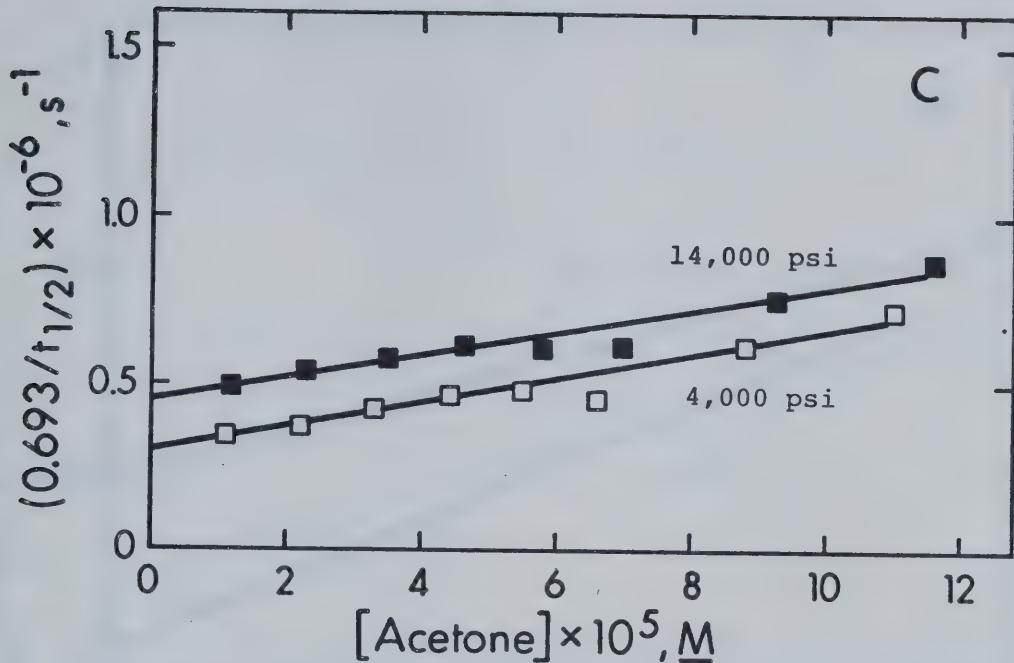


FIGURE III-34 C. The Effect of P on $e_s^- + \text{Acetone}$ in MeOH .

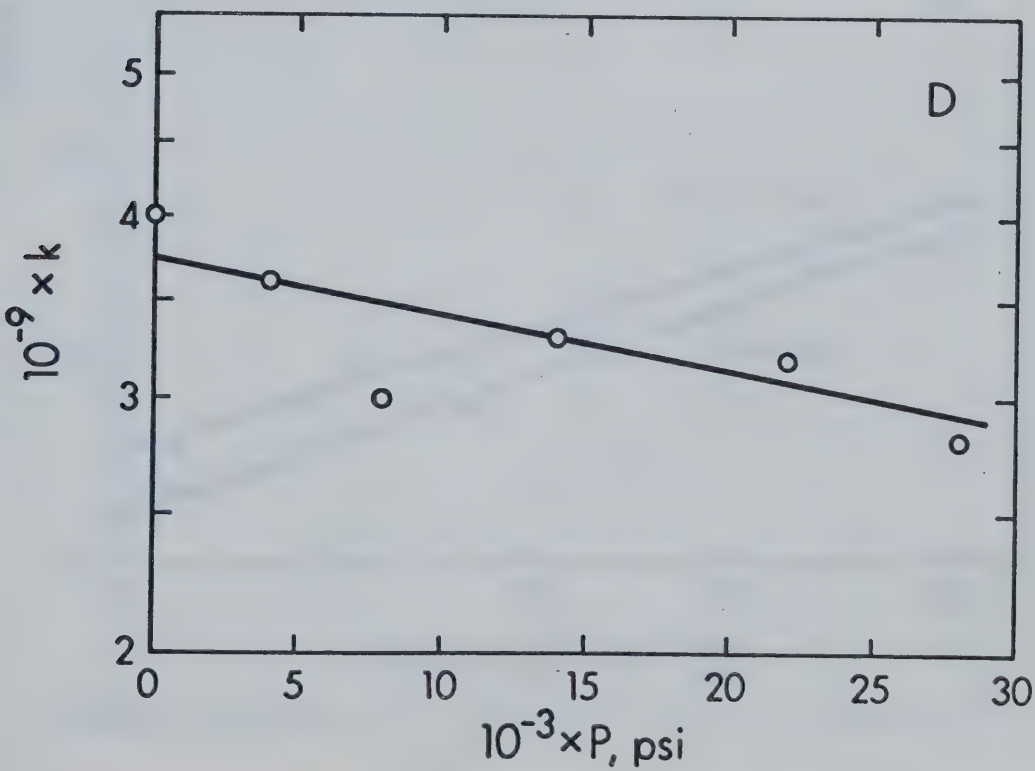


FIGURE III- 34 D. ΔV^\ddagger for $e_s^- + \text{Acetone}$ in MeOH .

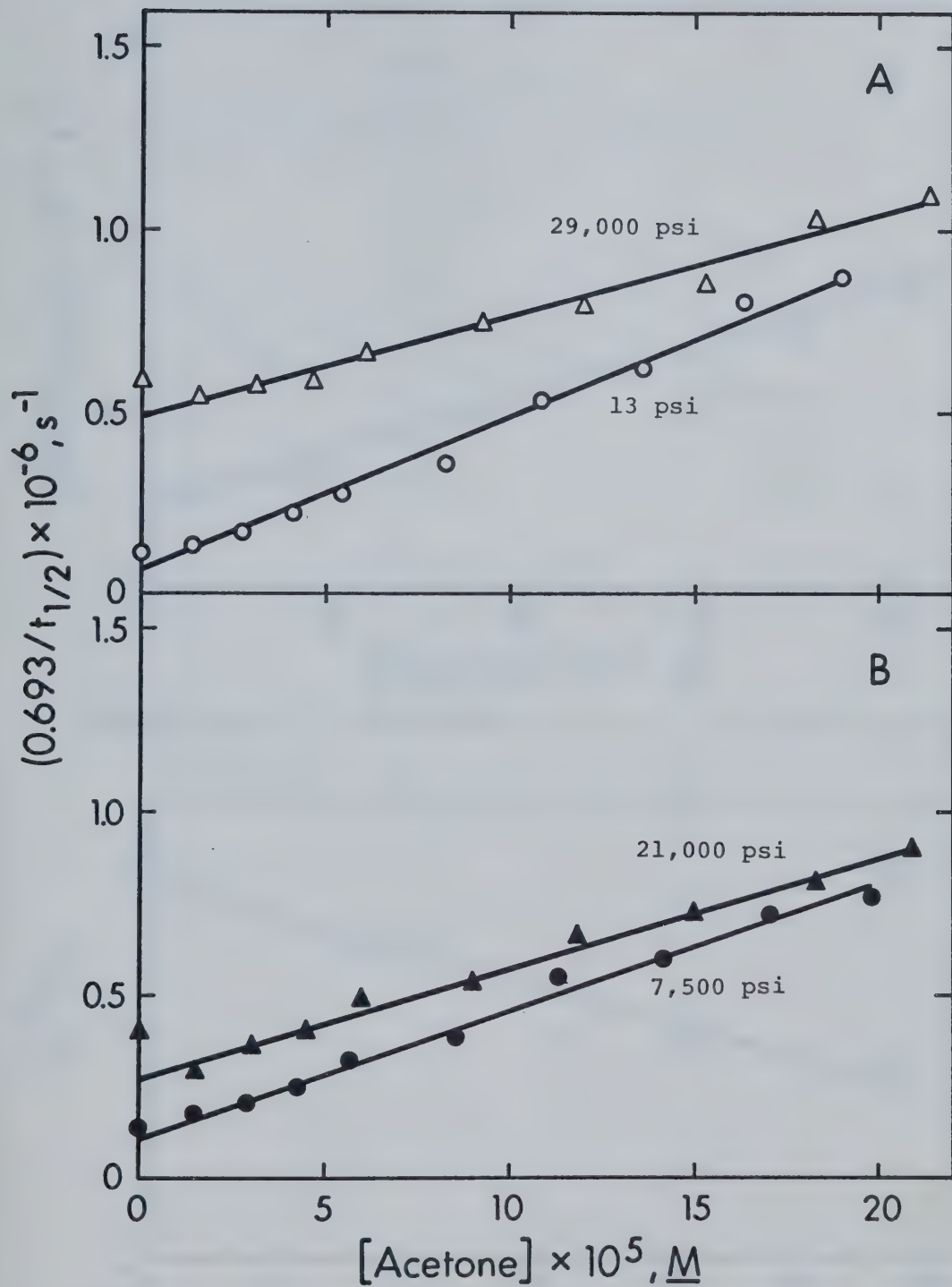


FIGURE III-35 A,B. The Effect of P on $e_s^- + \text{Acetone}$ in EtOH.

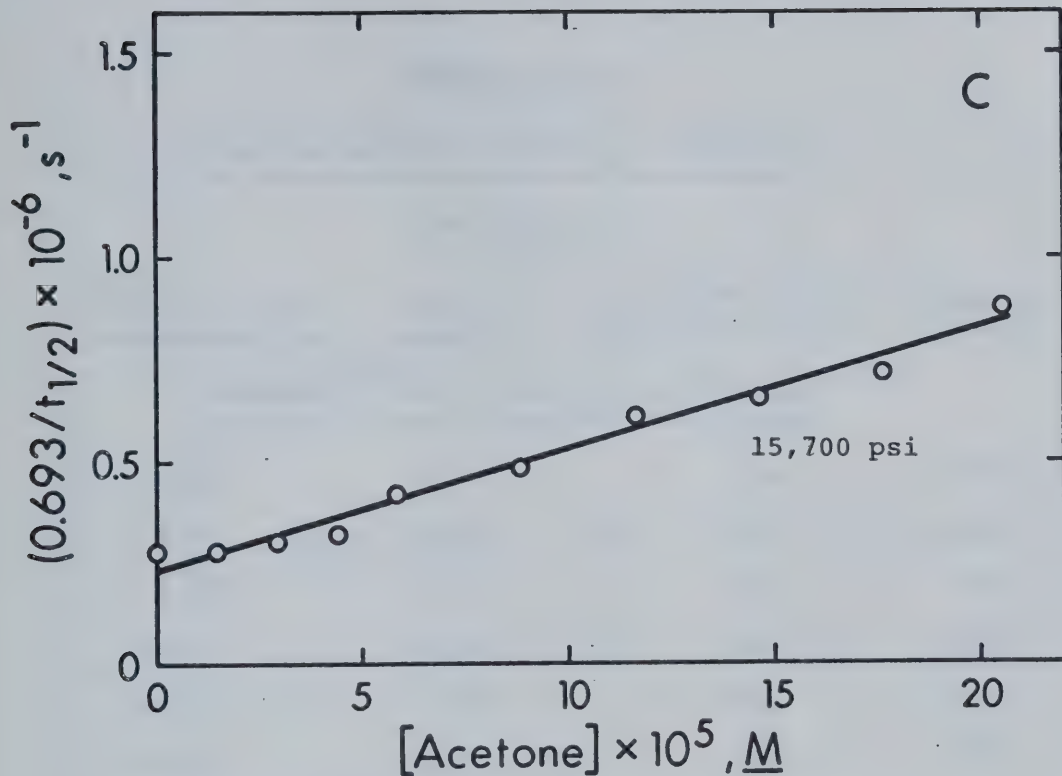


FIGURE III-35 C. The Effect of P on $e_s^- + \text{Acetone}$ in EtOH.

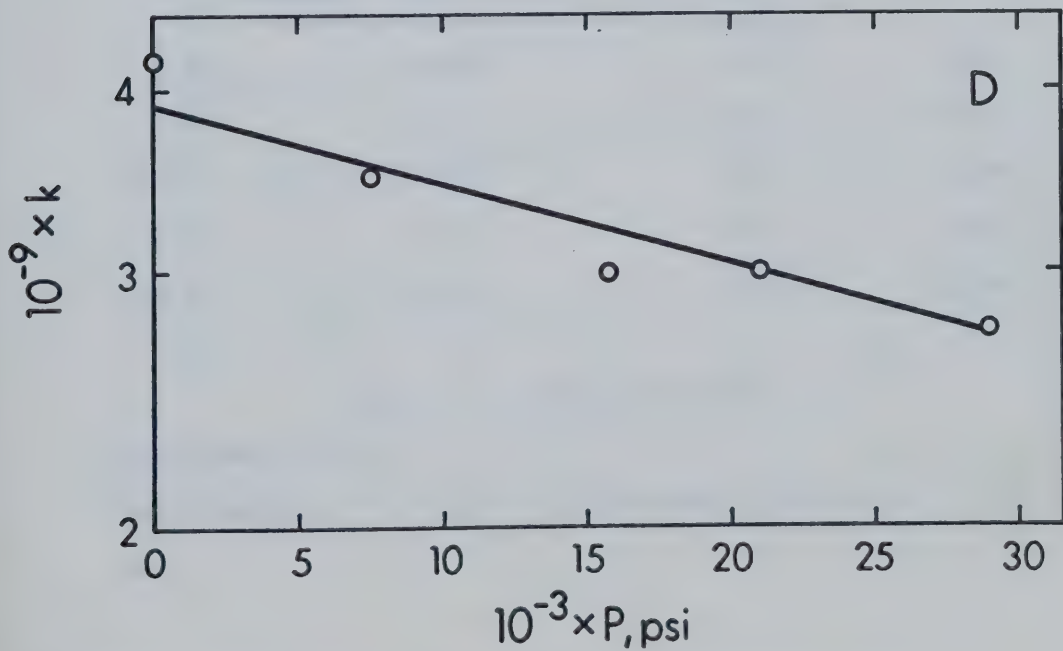


FIGURE III-35 D. ΔV^\ddagger for $e_s^- + \text{Acetone}$ in EtOH.

TABLE III-22

The k 's and ΔV^\ddagger 's for $e_s^- + \text{Acetone}$ $T = 295 \pm 1\text{K}$

$10^{-3} \times P^a, \text{ psi}$	$P, \text{ kb}$	$10^{-9} \times k_5^b, \text{ M}^{-1} \text{s}^{-1}$	$\log k_5$
-----------------------------------	-----------------	--	------------

Methanol¹⁵⁷, $\Delta V^\ddagger = 3.1 \pm 1.5 \text{ cm}^3 \text{ mol}^{-1}$

0.013	0.001	4.0	9.60
4.0	0.28	3.6	9.56
8.0	0.55	3.0	9.48
14.0	0.96	3.3	9.52
22.0	1.52	3.2	9.51
28.0	1.93	2.8	9.45

Ethanol, $\Delta V^\ddagger = 4.4 \pm 1 \text{ cm}^3 \text{ mol}^{-1}$

0.013	0.001	4.2	9.62
7.5	0.52	3.5	9.54
15.7	1.08	3.0	9.48
21.0	1.45	3.0	9.48
29.0	2.00	2.7 ₅	9.44

^a Error may be $\pm 3\%$.^b Error may be $\pm 5\%$ at $P < 1.5 \text{ kb}$ and $\pm 10\%$ for $P > 1.5 \text{ kb}$.

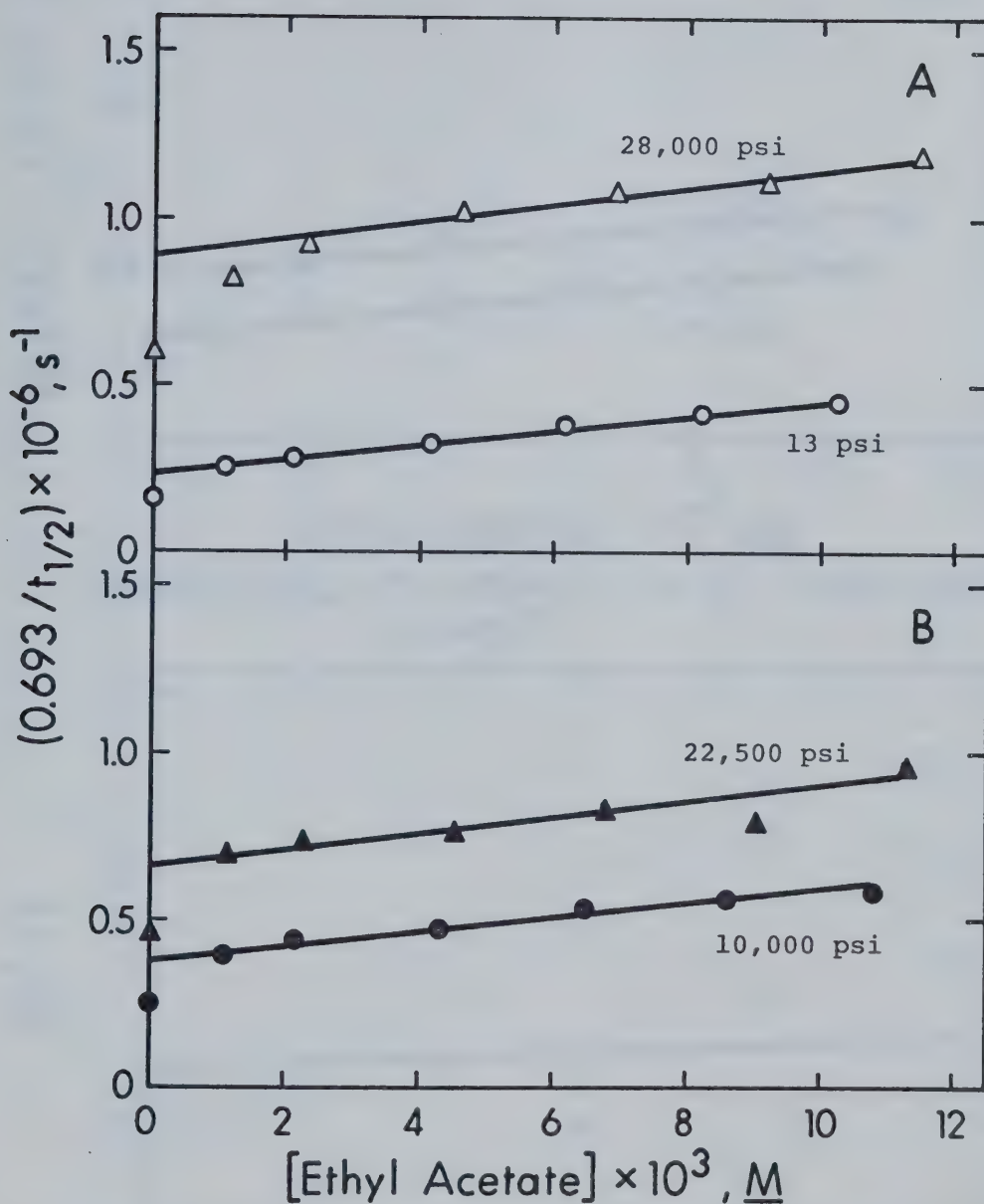


FIGURE III-36 A,B. The Effect of P on e_s^- + Ethyl Acetate in MeOH.

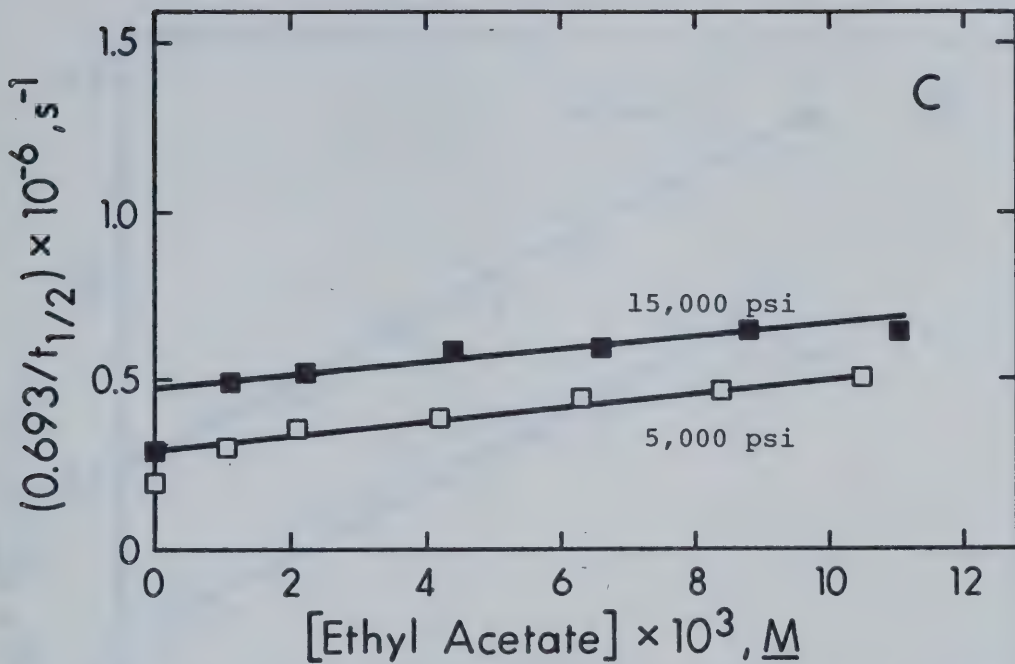


FIGURE III-36 C. The Effect of P on e_s^- + Ethyl Acetate in MeOH. ¹⁵⁷

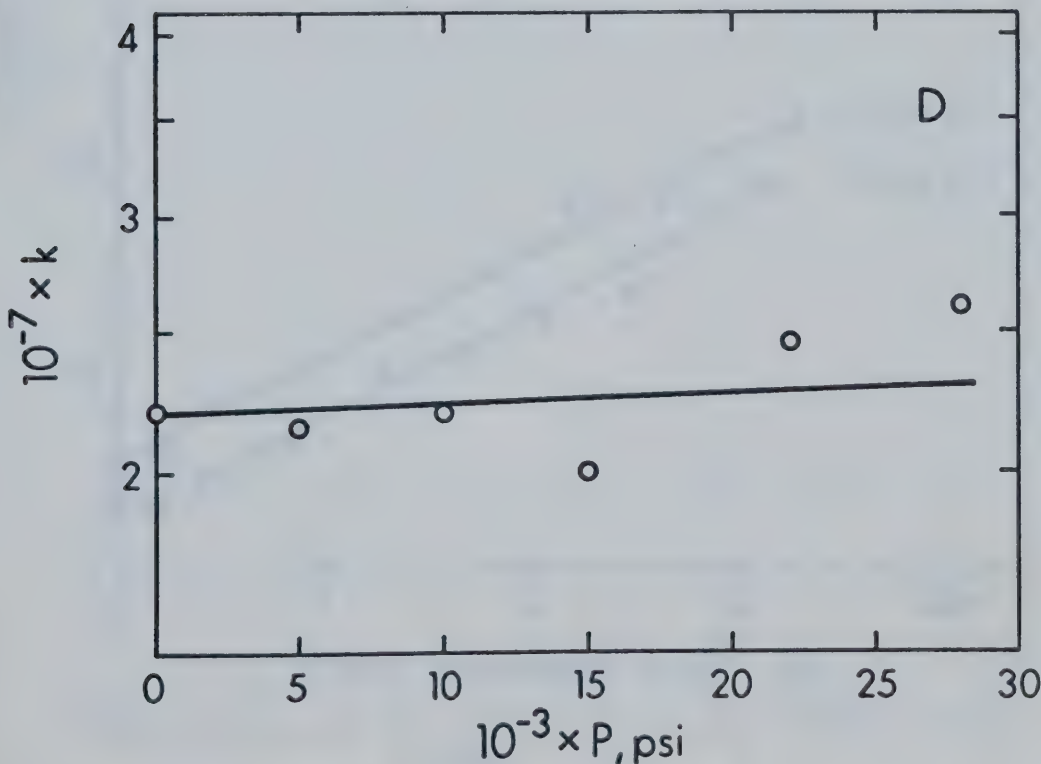


FIGURE III-36 D. ΔV^\ddagger for e_s^- + Ethyl Acetate in MeOH. ¹⁵⁷

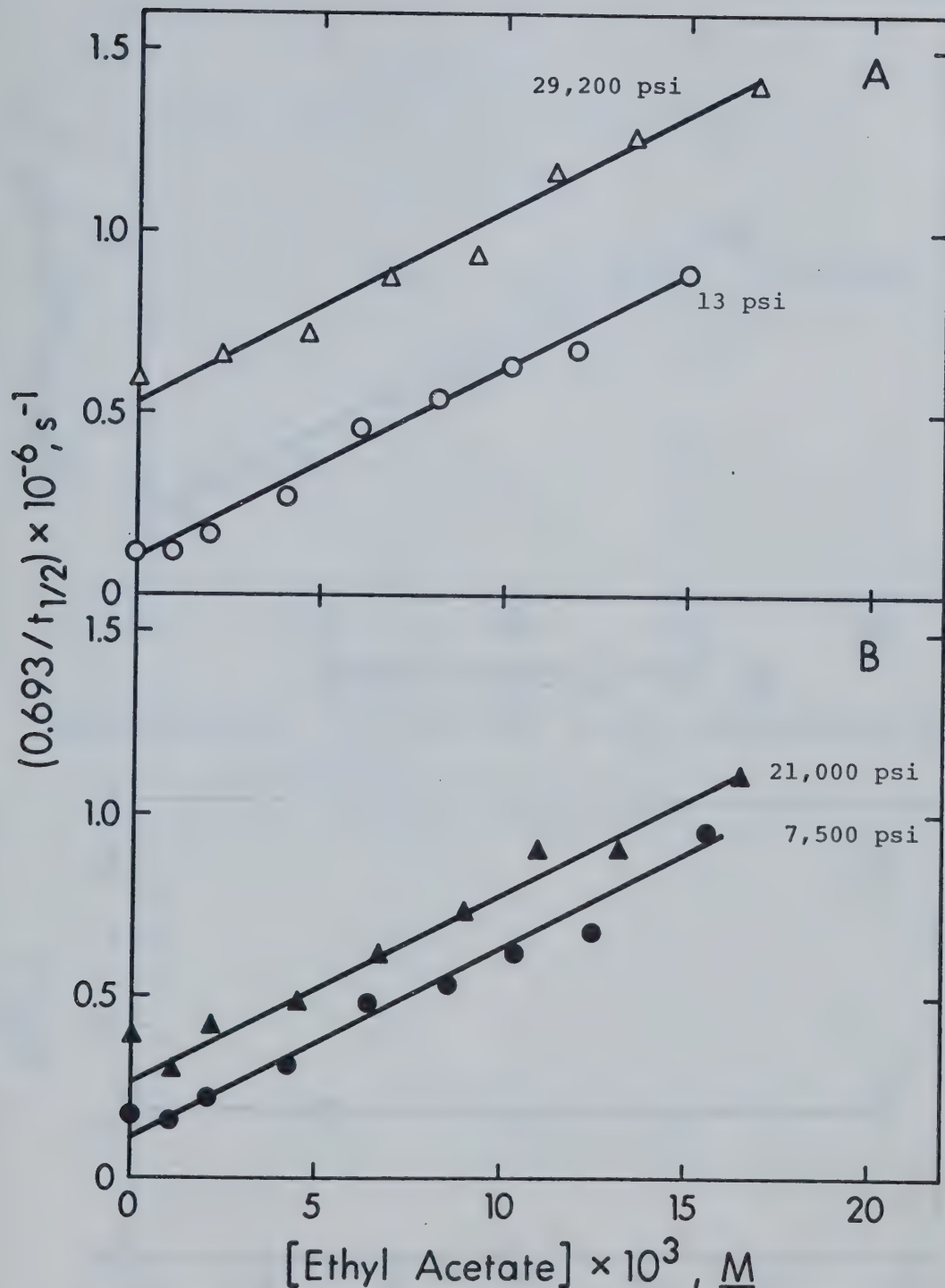


FIGURE III-37 A,B. The Effect of P on $e_s^- +$ Ethyl Acetate in EtOH.

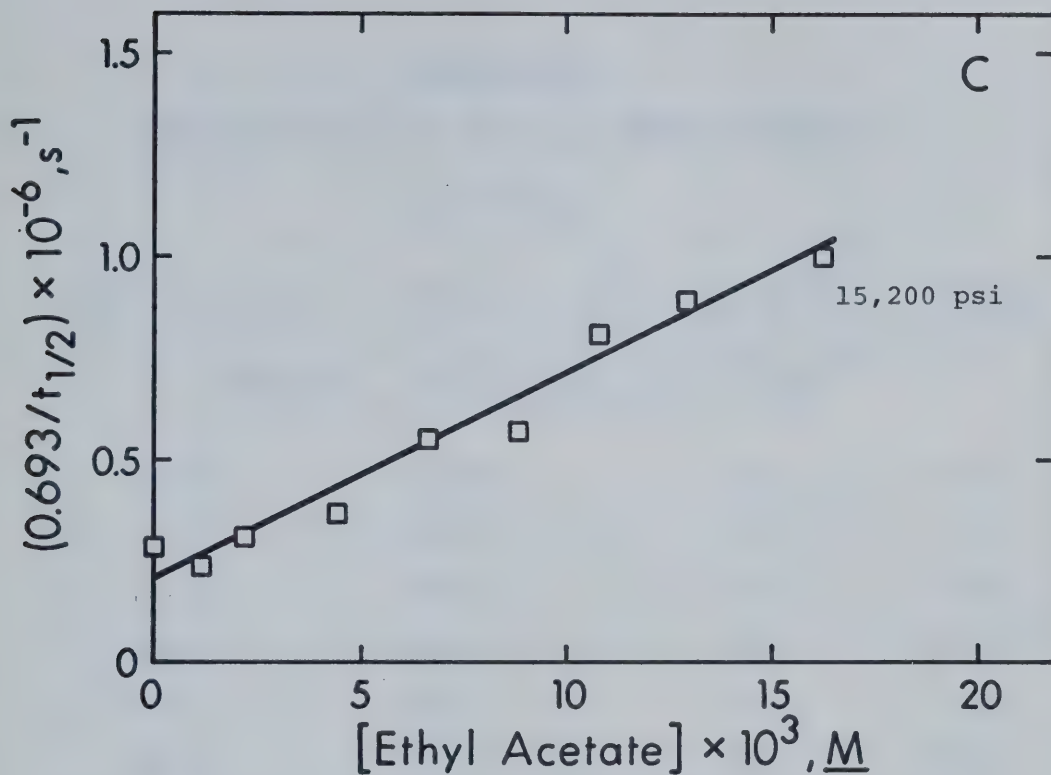


FIGURE III-37 C. The effect of P on $e_s^- +$ Ethyl Acetate in EtOH.

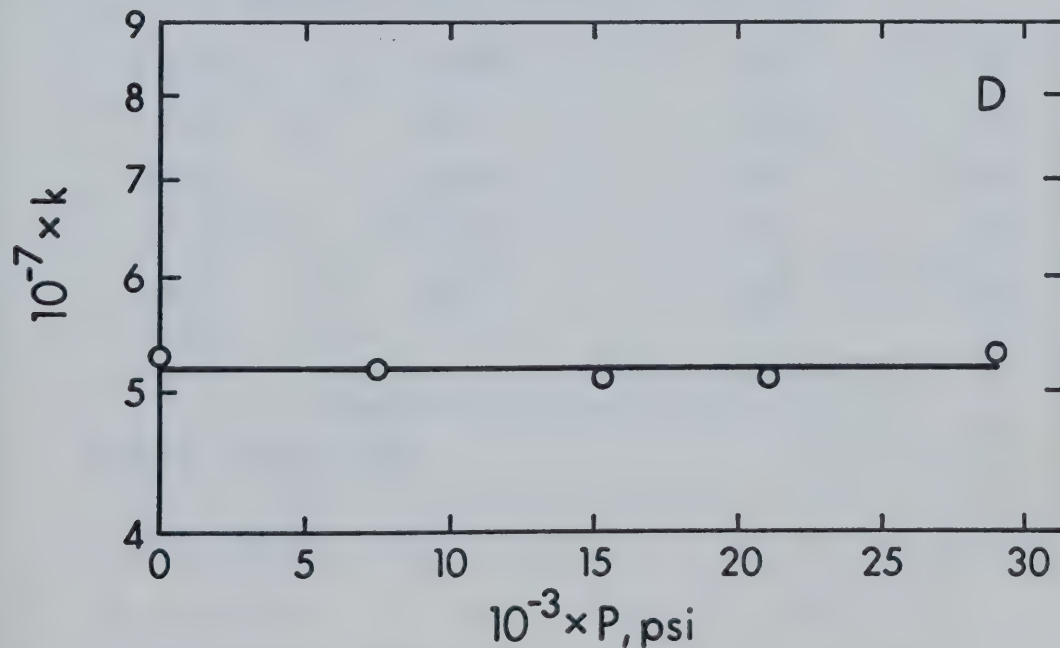


FIGURE III-37 D. ΔV^\ddagger for $e_s^- +$ Ethyl Acetate in EtOH.

TABLE III-23

The k 's and ΔV^\ddagger 's for $e_s^- +$ Ethyl Acetate $T = 295 \pm 1K$

$10^{-3} \times P^a, \text{psi}$	P, kb	$10^{-7} \times k_5^b, \text{M}^{-1} \text{s}^{-1}$	$\log k_5$
Methanol, $\Delta V^\ddagger = -0.6 \pm 1.5 \text{ cm}^3 \text{ mol}^{-1}$			

0.013	0.001	2.2	7.34
5.0	0.34	2.1 ₅	7.33
10.0	0.69	2.2	7.34
15.0	1.03	2.0	7.30
22.5	1.55	2.4 ₅	7.39
28.0	1.93	2.6	7.41

Ethanol, $\Delta V^\ddagger = 0.0 \pm 0.5 \text{ cm}^3 \text{ mol}^{-1}$

0.013	0.001	5.3	7.72
7.5	0.52	5.2	7.72
15.2	1.05	5.1	7.71
21.0	1.45	5.1	7.71
29.2	2.01	5.3	7.72

^a Error may be $\pm 3\%$.^b Error may be $\pm 10\%$.

For reaction of ethyl acetate with e_s^- in water, k_5 is less than $10^7 \text{ M}^{-1} \text{ s}^{-1}$.⁴⁹ The same authors reported $k < 10^7 \text{ M}^{-1} \text{ s}^{-1}$ for $e_s^- +$ phenol in water. Similarly, for the same alcohol, k_5 's for the e_s^- reaction with phenol and ethyl acetate are comparable. For both scavengers, k_5 increases on going from water to methanol to ethanol as the solvent.

g. Cadmium Chloride (CdCl_2) as e_s^- scavenger

The results are given in Figure III-38 A, B, C and D and in Figure III-39 A, B, C and D. They are summarized in Table III-24.

The Cd^{+2} ion is an efficient electron scavenger, having $k_5 = 5.2 \times 10^{10} \text{ M}^{-1} \text{ s}^{-1}$ for reaction with e_s^- in water¹⁶⁰ at room temperature. The value $k_5 \approx 2 \times 10^{10} \text{ M}^{-1} \text{ s}^{-1}$ in methanol is much larger than the $k_5 \approx 3.8 \times 10^9 \text{ M}^{-1} \text{ s}^{-1}$ in ethanol. This is explained on page 329.

h. Toluene ($\text{C}_6\text{H}_5\text{CH}_3$) as e_s^- scavenger

The results obtained in methanol are presented in Figure III-40 A, B, C and D and in Table III-25. In ethanol, toluene not treated with Na-K alloy was used as well as the normally purified toluene. Results for the latter are given in Figure III-41 A, B, C and D. For the untreated toluene in ethanol, results are given in Figure III-42 A, B, C and D. The rate constants as

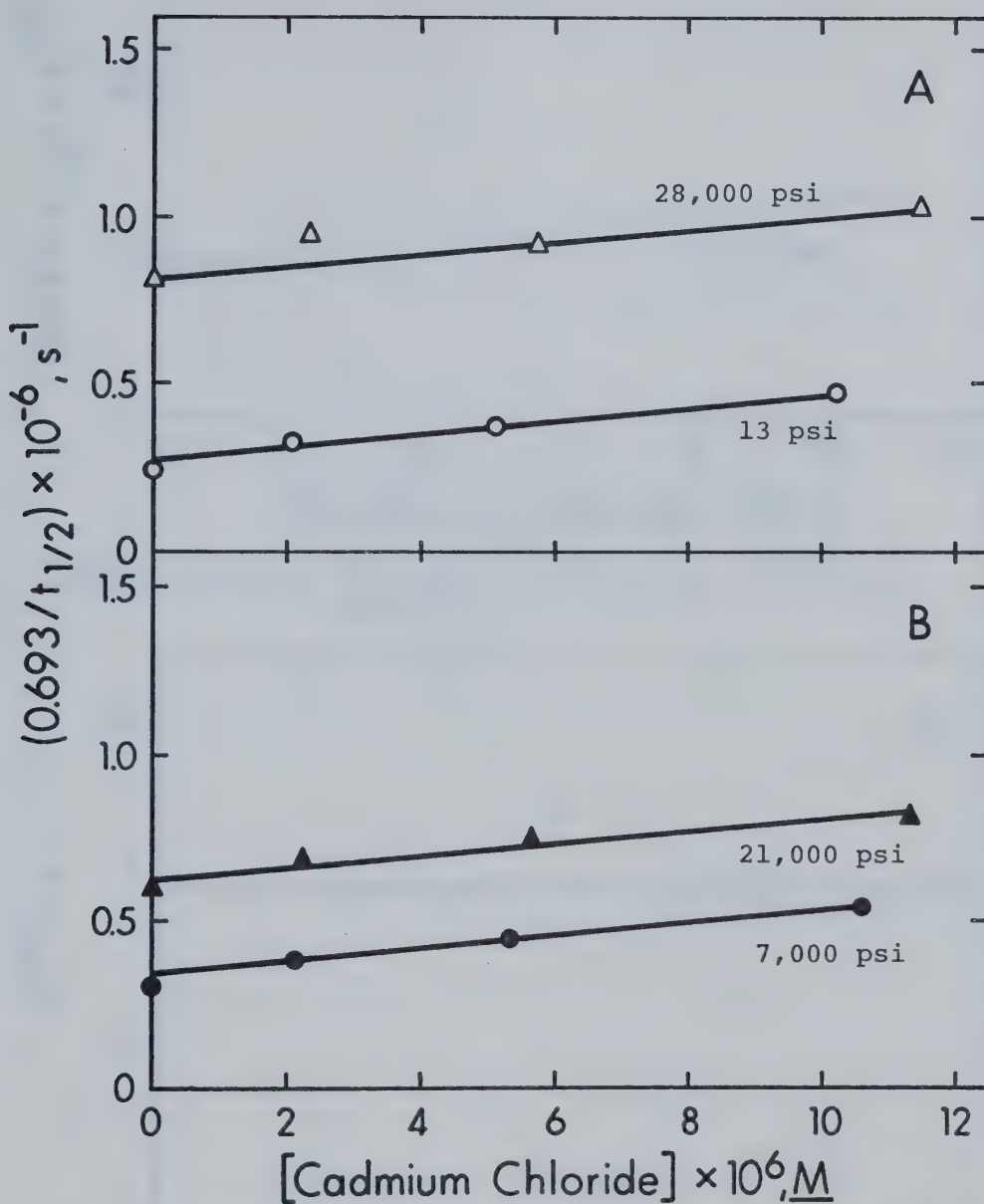


FIGURE III-38 A, B. The Effect of P on $e_s^- + \text{CdCl}_2$ in MeOH . 157

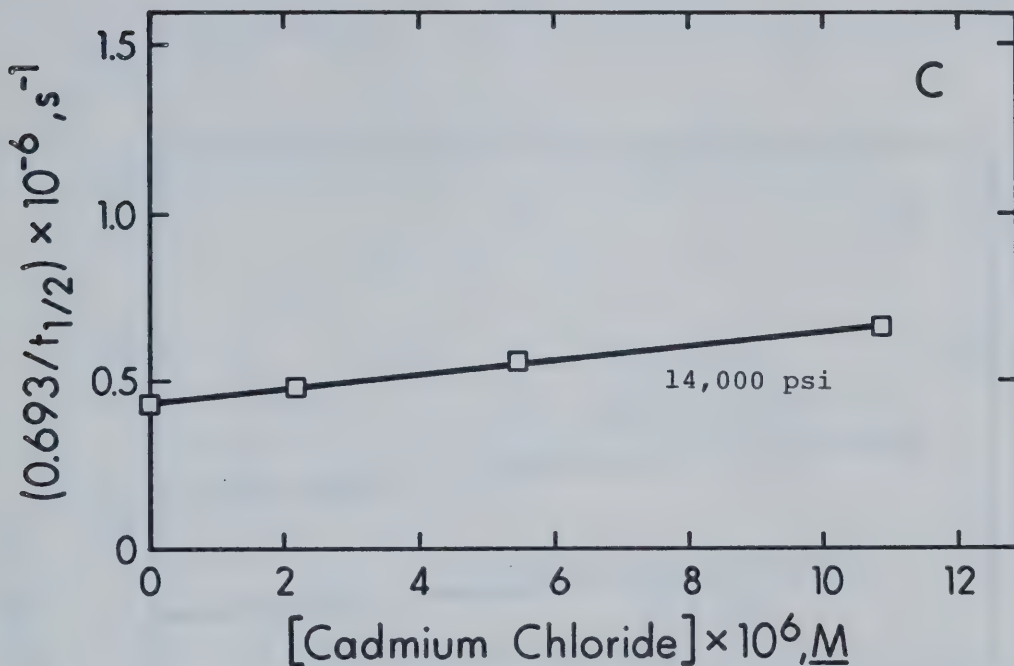


FIGURE III-38 C. The Effect of P on $e_s^- + \text{CdCl}_2$ in MeOH. 157

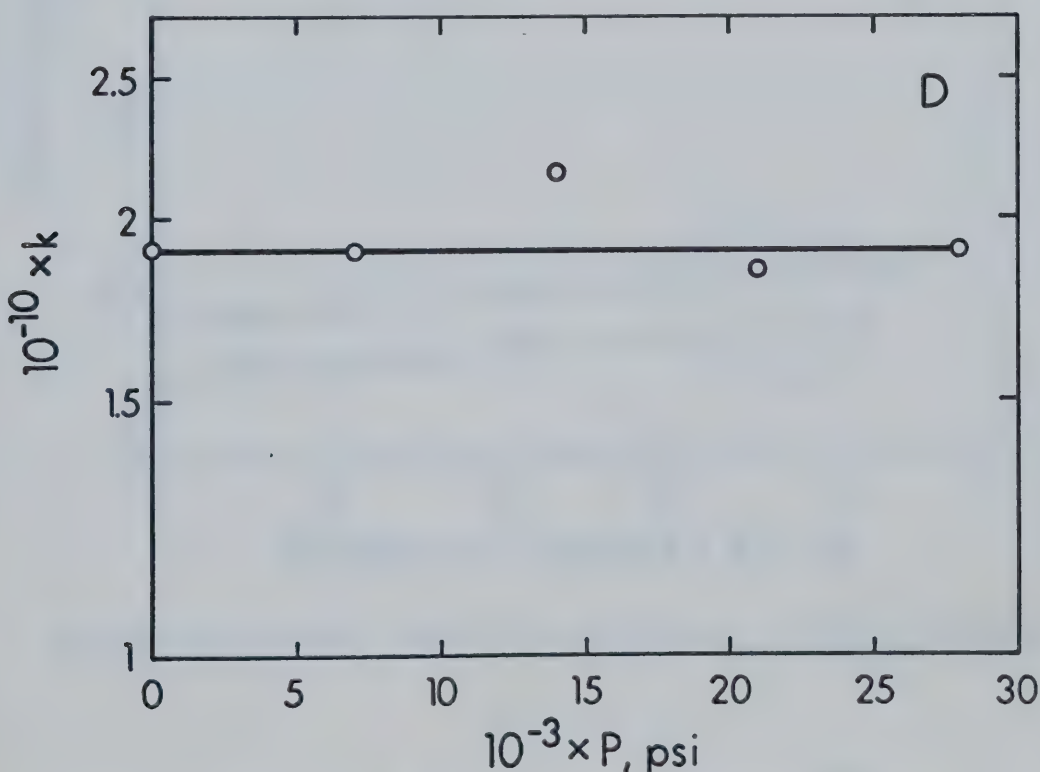


FIGURE III-38 D. ΔV^\ddagger for $e_s^- + \text{CdCl}_2$ in MeOH. 157

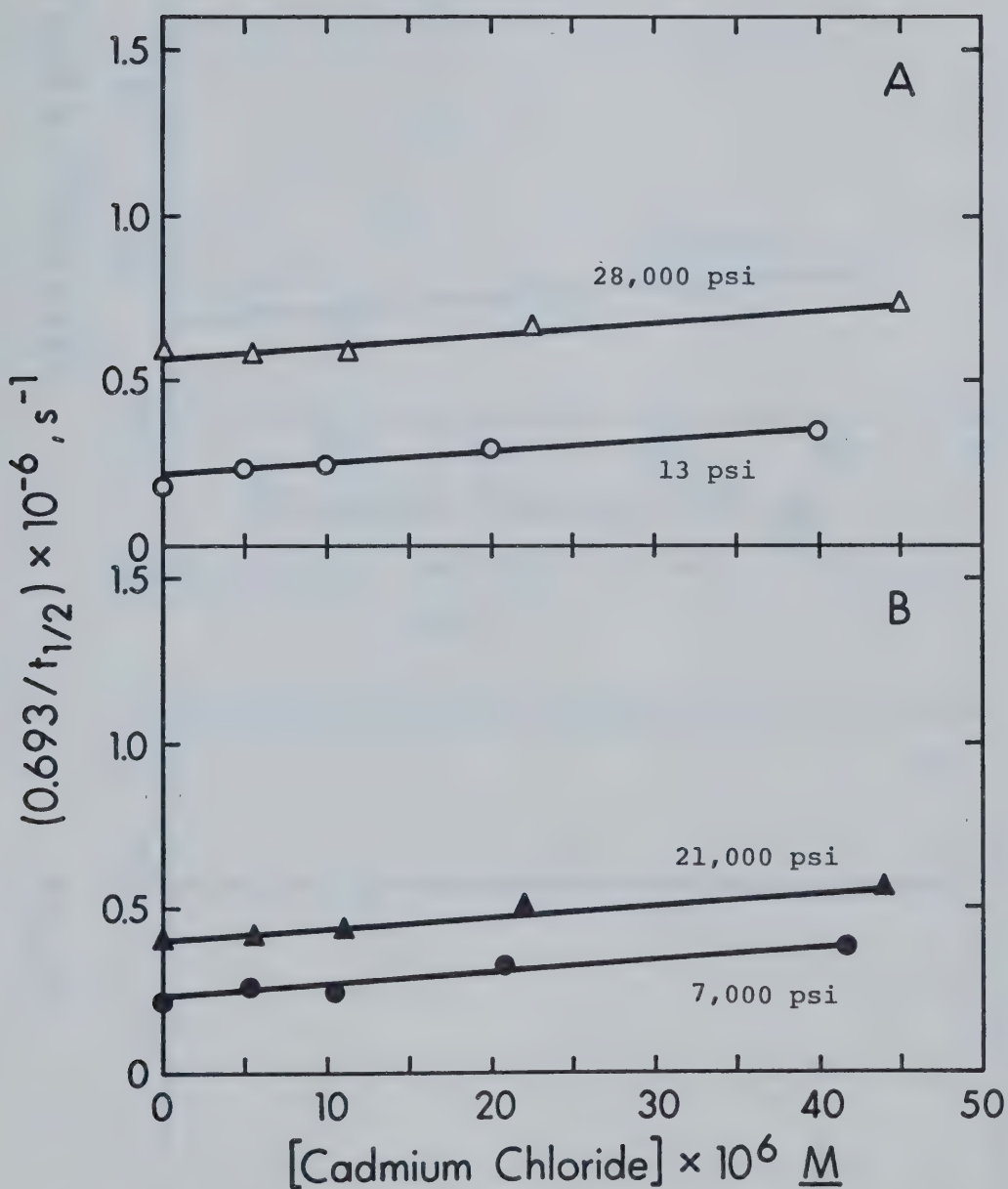


FIGURE III-39 A,B. The Effect of P on $e_s^- + \text{CdCl}_2$ in EtOH.

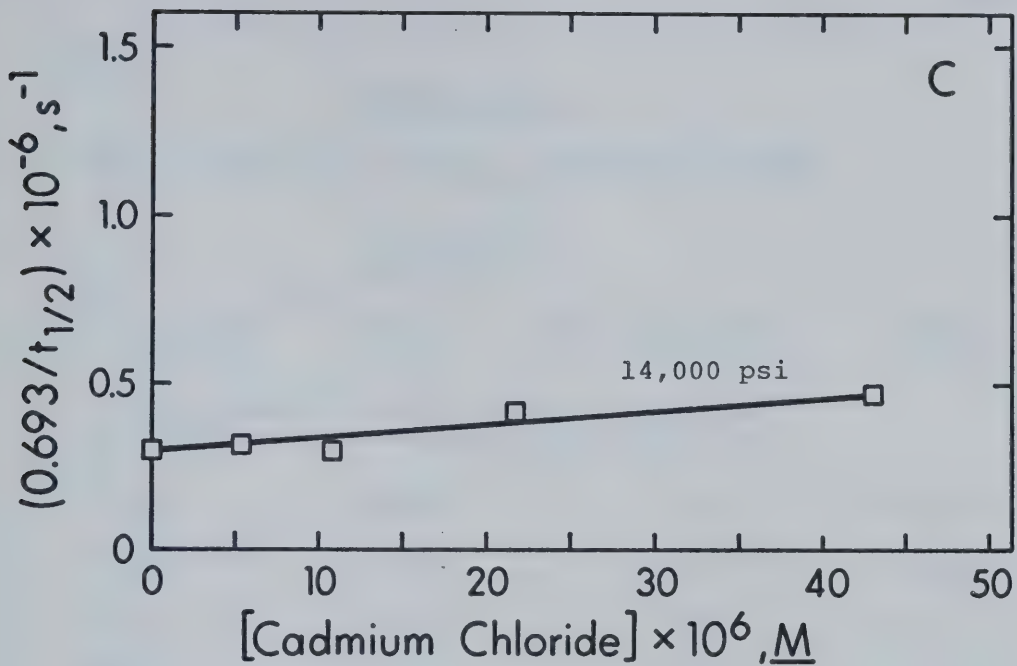


FIGURE III-39 C. The Effect of P on $e_s^- + \text{CdCl}_2$ in EtOH.

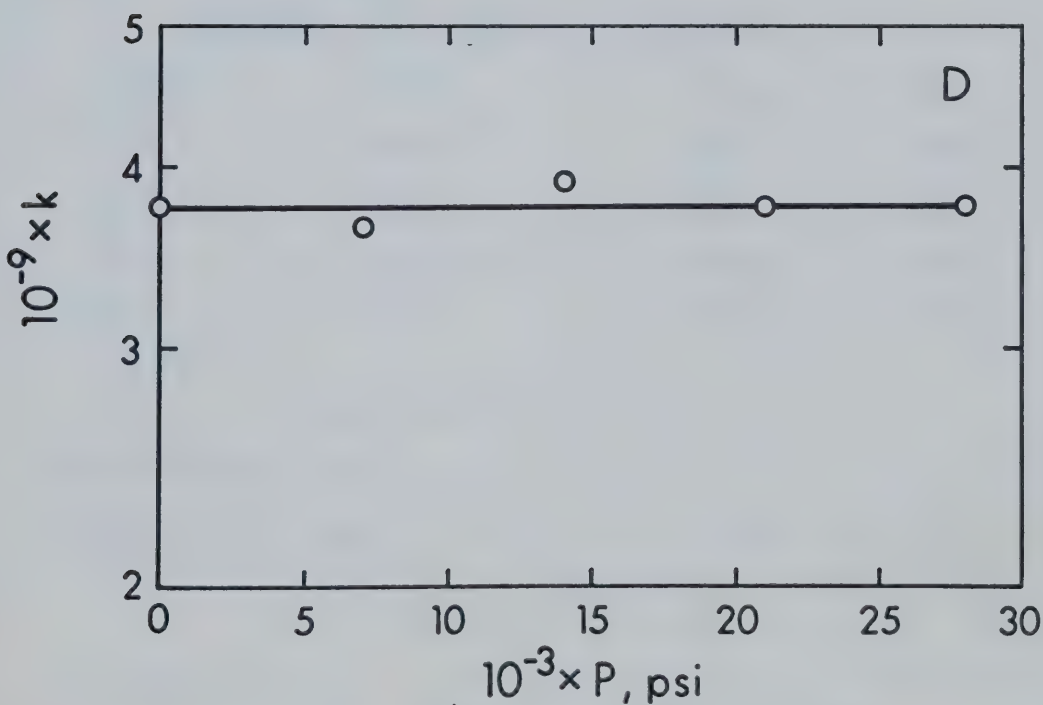


FIGURE III-39 D. ΔV^\ddagger for $e_s^- + \text{CdCl}_2$ in EtOH.

TABLE III-24

The k 's and ΔV^\ddagger 's for $e^- + \frac{Cd}{S} + \text{Cadmium Chloride}$

$T = 295 \pm 1\text{K}$

$10^{-3} \times P^a, \text{psi}$	P, kb	$10^{-9} \times k_5^b, \text{M}^{-1}\text{s}^{-1}$	$\log k_5$
Methanol ¹⁵⁷ , $\Delta V^\ddagger = 0.0 \pm 0.5 \text{ cm}^3 \text{ mol}^{-1}$			
0.013	0.001	19	10.28
7.0	0.48	19	10.28
14.0	0.96	21.5	10.33
21.0	1.45	18.5	10.27
28.0	1.93	19	10.28
Ethanol, $\Delta V^\ddagger = 0.0 \pm 1.0 \text{ cm}^3 \text{ mol}^{-1}$			
0.013	0.001	3.7_5	9.57
7.0	0.48	3.6	9.56
14.0	0.96	3.9	9.59
21.0	1.45	3.7_5	9.57
28.0	1.93	3.7_5	9.57

^a Error may be $\pm 3\%$.

^b Error may be $\pm 10\%$.

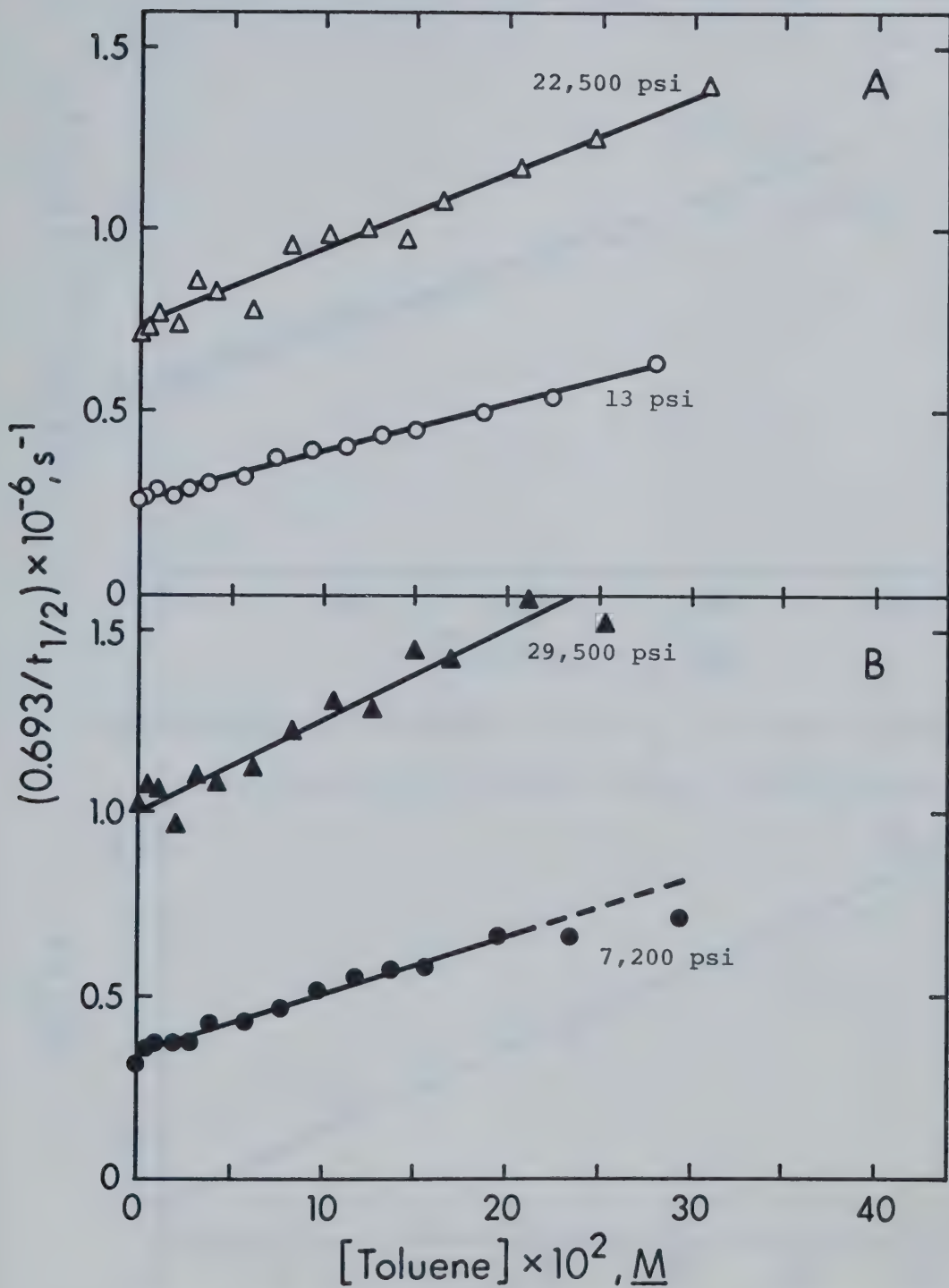


FIGURE III-40 A,B. The Effect of P on e_s^- + Toluene in MeOH.

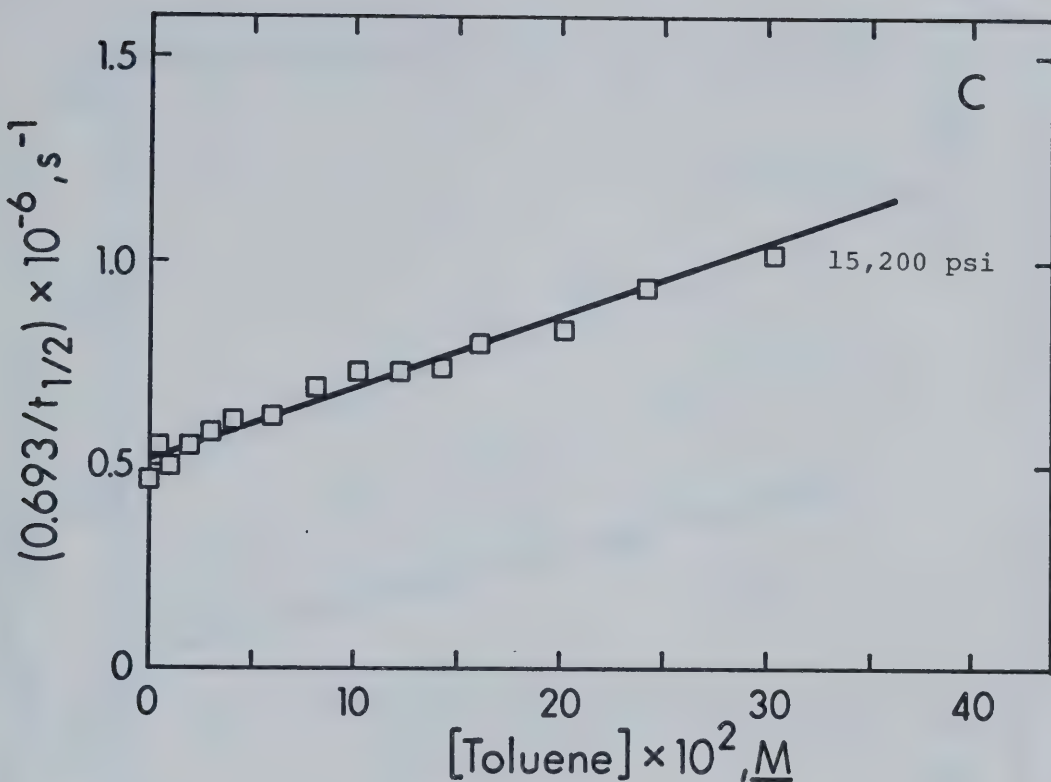


FIGURE III-40 C. The Effect of P on $e_s^- + \text{Toluene}$ in MeOH.

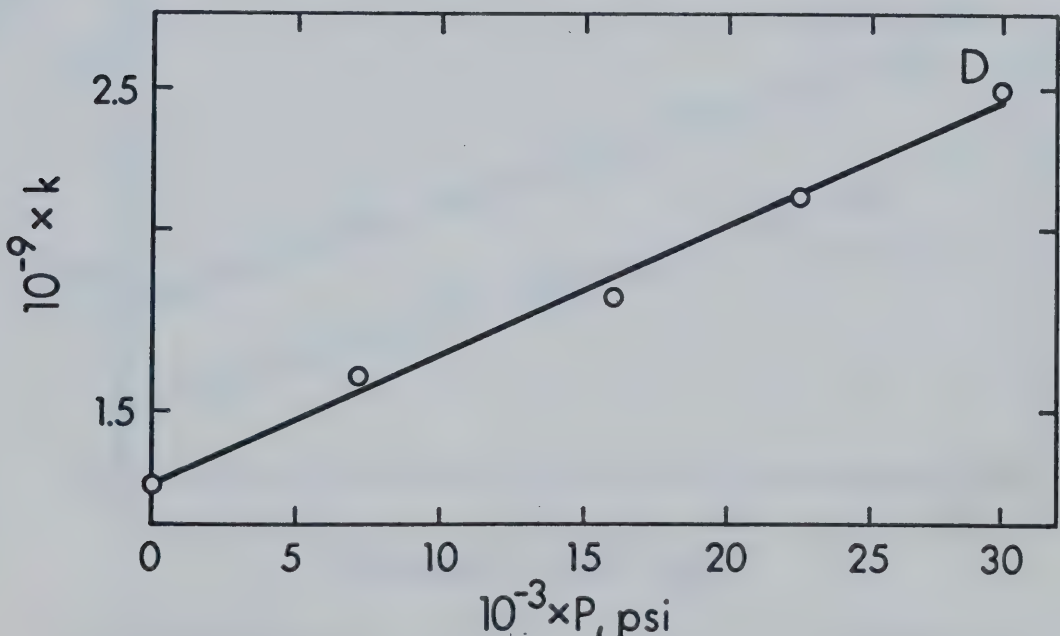


FIGURE III- 40 D. ΔV^\ddagger for $e_s^- + \text{Toluene}$ in MeOH.

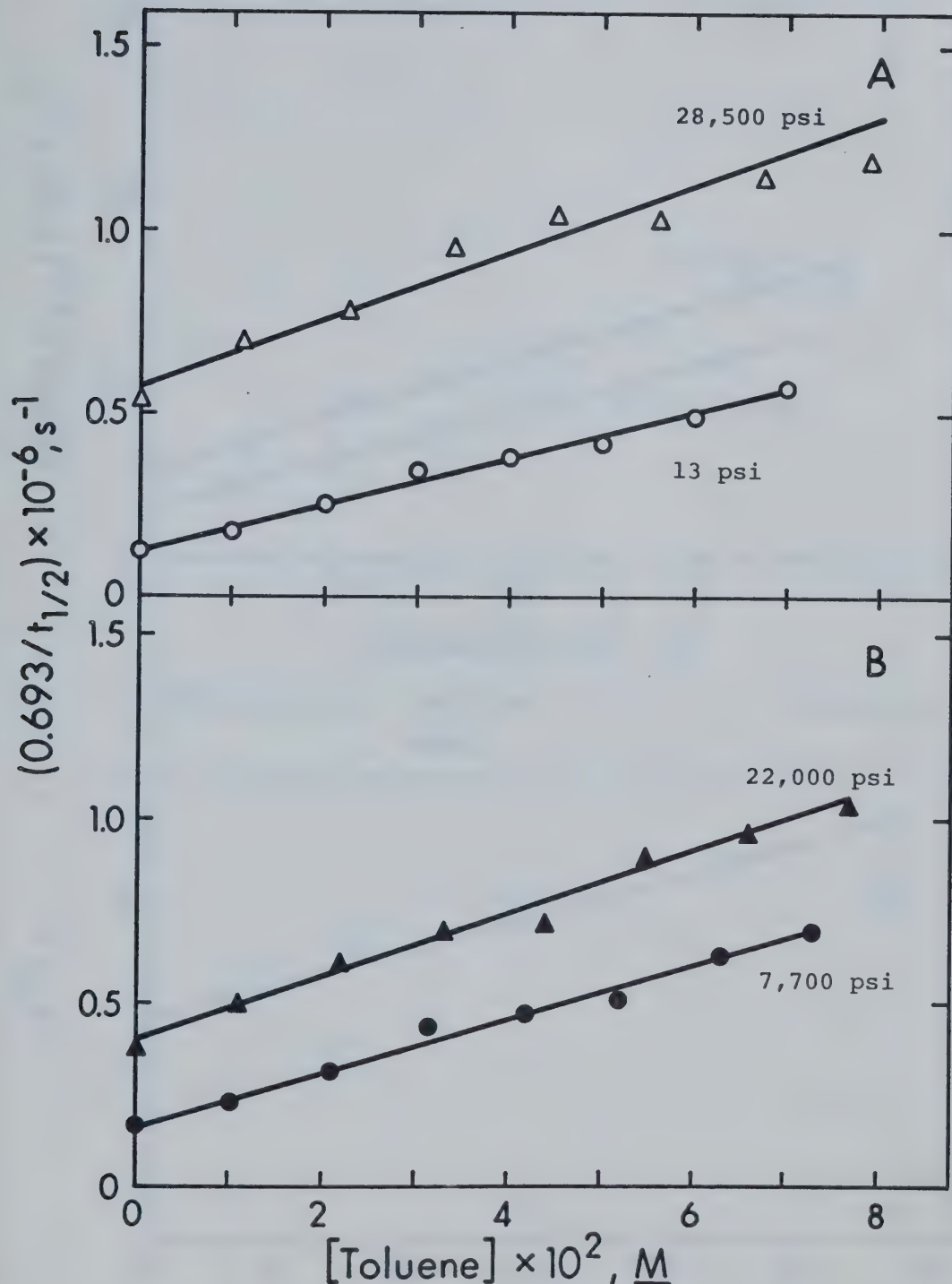


FIGURE III-41 A,B. The Effect of P on $e_s^- +$ Toluene in EtOH.

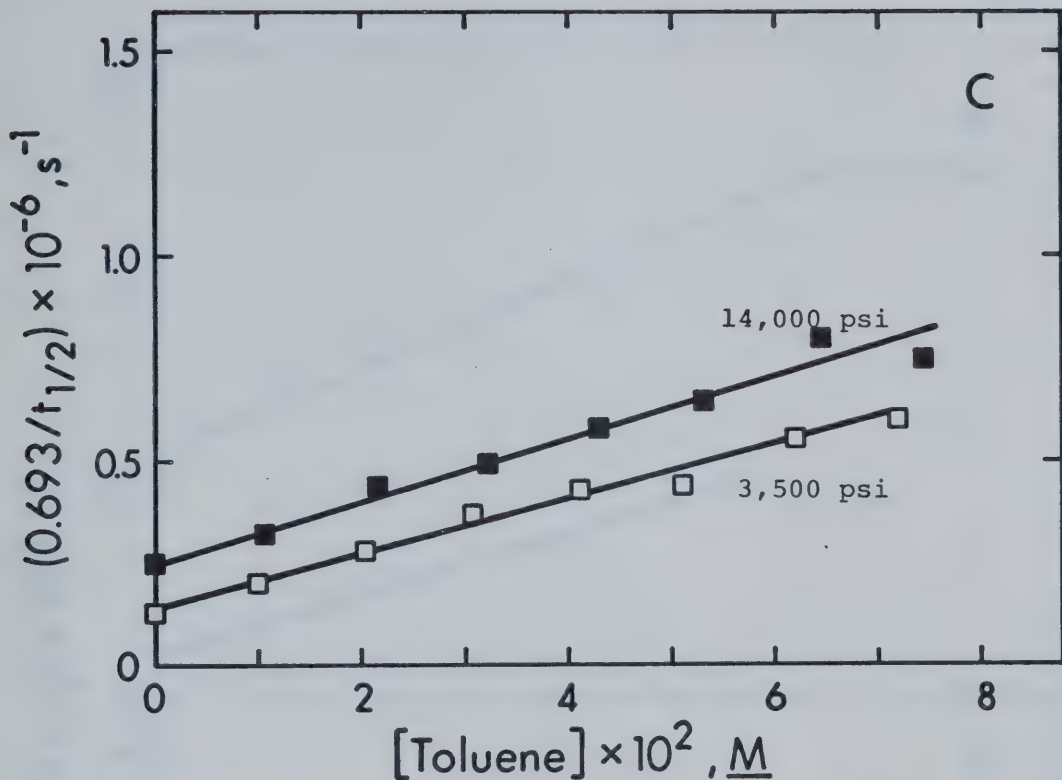


FIGURE III-41 C. The Effect of P on $e_s^- + \text{Toluene}$ in EtOH.

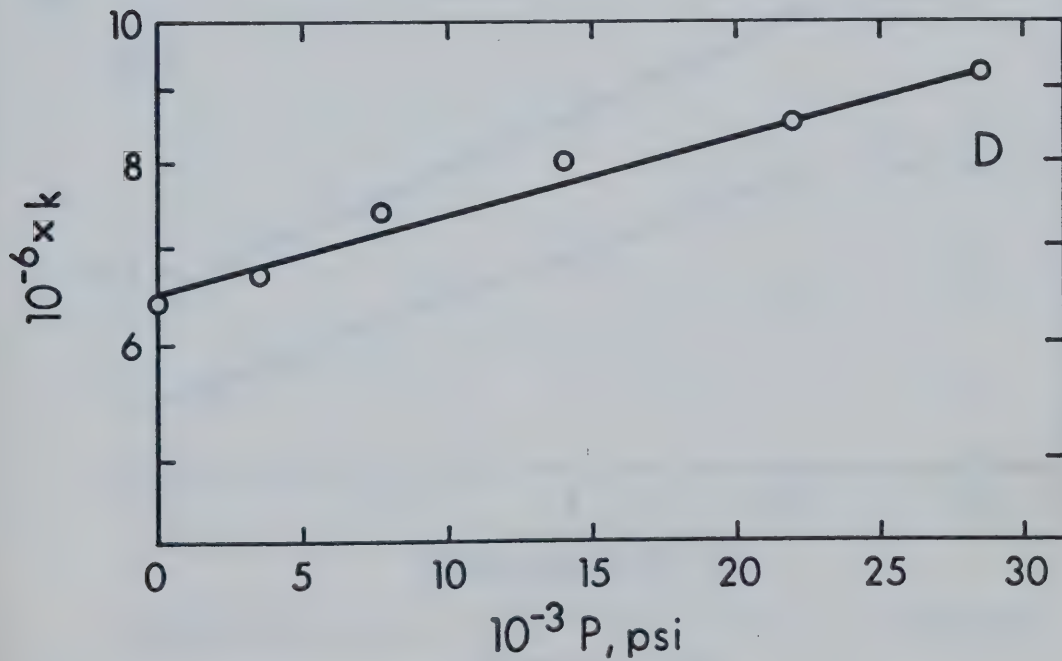


FIGURE III-41 D. ΔV^\ddagger for $e_s^- + \text{Toluene}$ in EtOH.

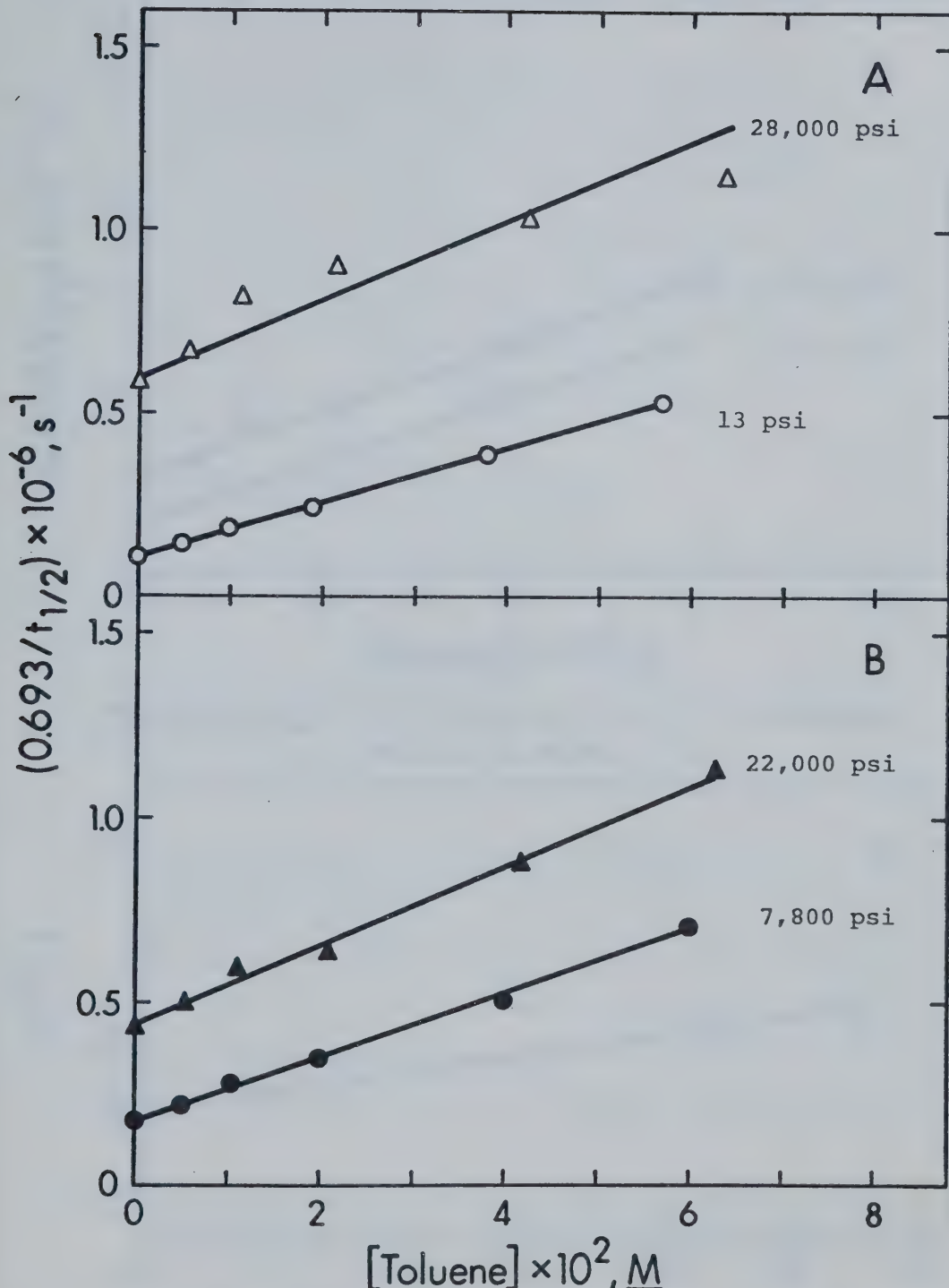


FIGURE III-42 A,B. The Effect of P on $e_s^- + \text{Untreated Toluene in EtOH}$.

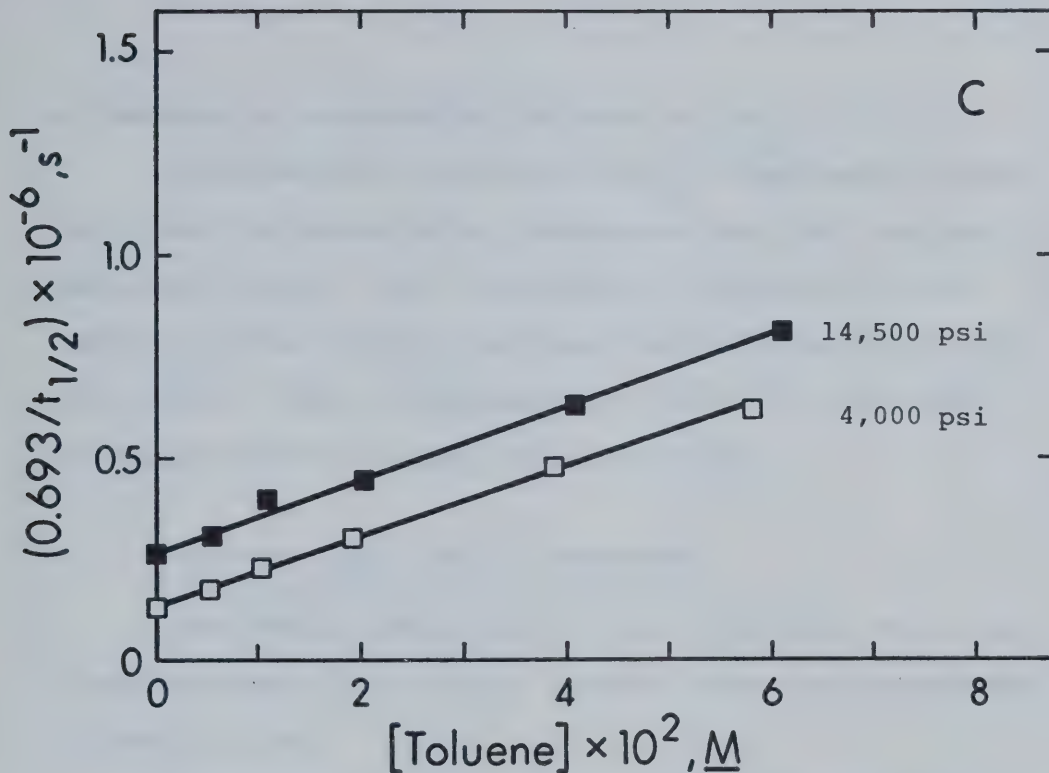


FIGURE III-42 C. The Effect of P on $e_s^- + \text{Untreated Toluene in EtOH.}$

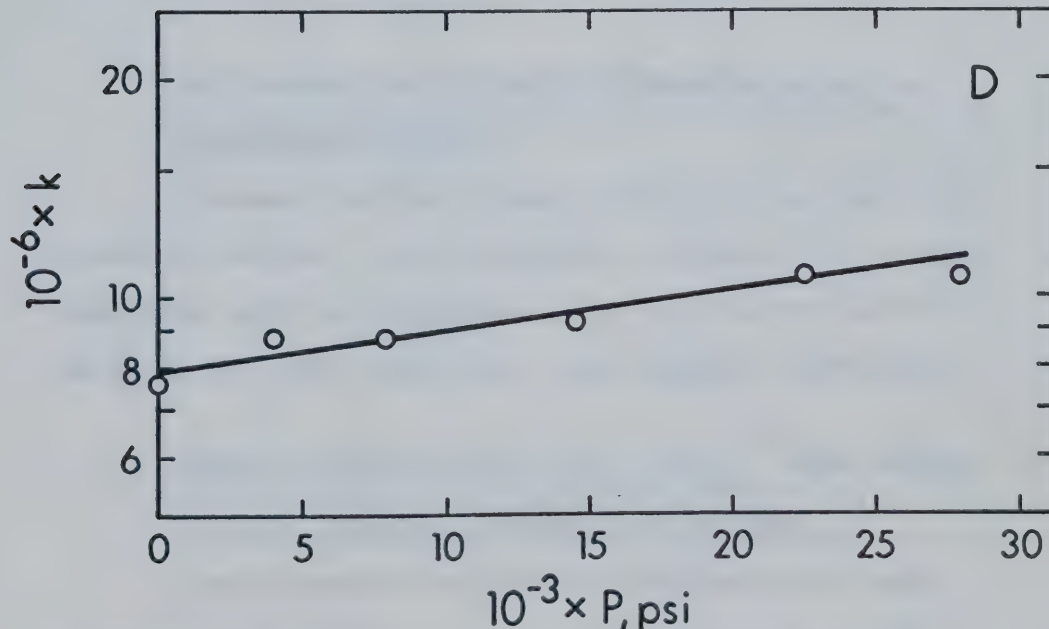


FIGURE III-42 D. ΔV^\ddagger for $e_s^- + \text{Toluene (untreated) in EtOH.}$

a function of pressure are included in Table III-25.

The reaction rate found for e_s^- + untreated toluene in ethanol is higher at all pressures than that for the purified toluene. This indicates the presence of some impurity in the solute which was removed by reaction with Na-K alloy. Within experimental error, ΔV^\ddagger is the same for the reaction in both ethanol solutions.

i. Benzene (C_6H_6) as e_s^- scavenger

The results are given in Figure III-43 A, B, C and D and in Figure III-44 A, B, C and D. They are summarized in Table III-26.

Values for k_5 at 1 bar and 295K agree well with those found in quartz cells for both solvents.

3. DATA SUMMARY FOR EFFECT OF PRESSURE ON e_s^- + SCAVENGER REACTION

A summary of the values of k_5 at 1 bar, and ΔV^\ddagger between 1 bar and 2 kb, is given in Table III-27. The compounds used as scavengers of e_s^- are listed in the table in the same order that they appeared previously.

D. REACTION RATE CONSTANTS (k_5) FOR e_s^- WITH GASEOUS SOLUTES IN WATER, METHANOL AND ETHANOL

A novel sample preparation technique was used, as explained in II-C-1,b. Stock solutions, saturated

TABLE III-25

The k 's and ΔV^\ddagger 's for $e_s^- + \text{Toluene}$

$10^{-3} \times P^a, \text{ psi}$	$P, \text{ kb}$	$10^{-6} \times k_5^b, \text{ M}^{-1} \text{ s}^{-1}$	$\log k_5$
Methanol, $\Delta V^\ddagger = -7.4 \pm 0.5 \text{ cm}^3 \text{ mol}^{-1}$			
0.013	0.001	1.3	6.11
7.2	0.50	1.6	6.20
15.2	1.05	1.8	6.26
22.5	1.55	2.1	6.32
29.5	2.03	2.5	6.40
Ethanol, $\Delta V^\ddagger = -4.3 \pm 0.2 \text{ cm}^3 \text{ mol}^{-1}$			
0.013	0.001	6.4	6.81
3.5	0.24	6.7	6.83
7.7	0.53	7.4	6.87
14.0	0.96	8.0	6.90
22.0	1.52	8.5	6.93
28.0	1.93	9.2	6.96
Ethanol, $\Delta V^\ddagger = -4.5 \pm 1.5 \text{ cm}^3 \text{ mol}^{-1}$ (toluene used was not treated with Na-K alloy)			
0.013	0.001	7.6	6.88
4.0	0.28	8.8	6.94
7.8	0.54	8.8	6.94
14.5	1.00	9.2	6.96
22.0	1.52	10.6	7.03
28.0	1.93	10.7	7.03

^a Error may be ± 300 psi for $P > 13$ psi

^b Error may be $\pm 5\%$ for $P \leq 1$ kb, and $\pm 20\%$ for $P > 1$ kb

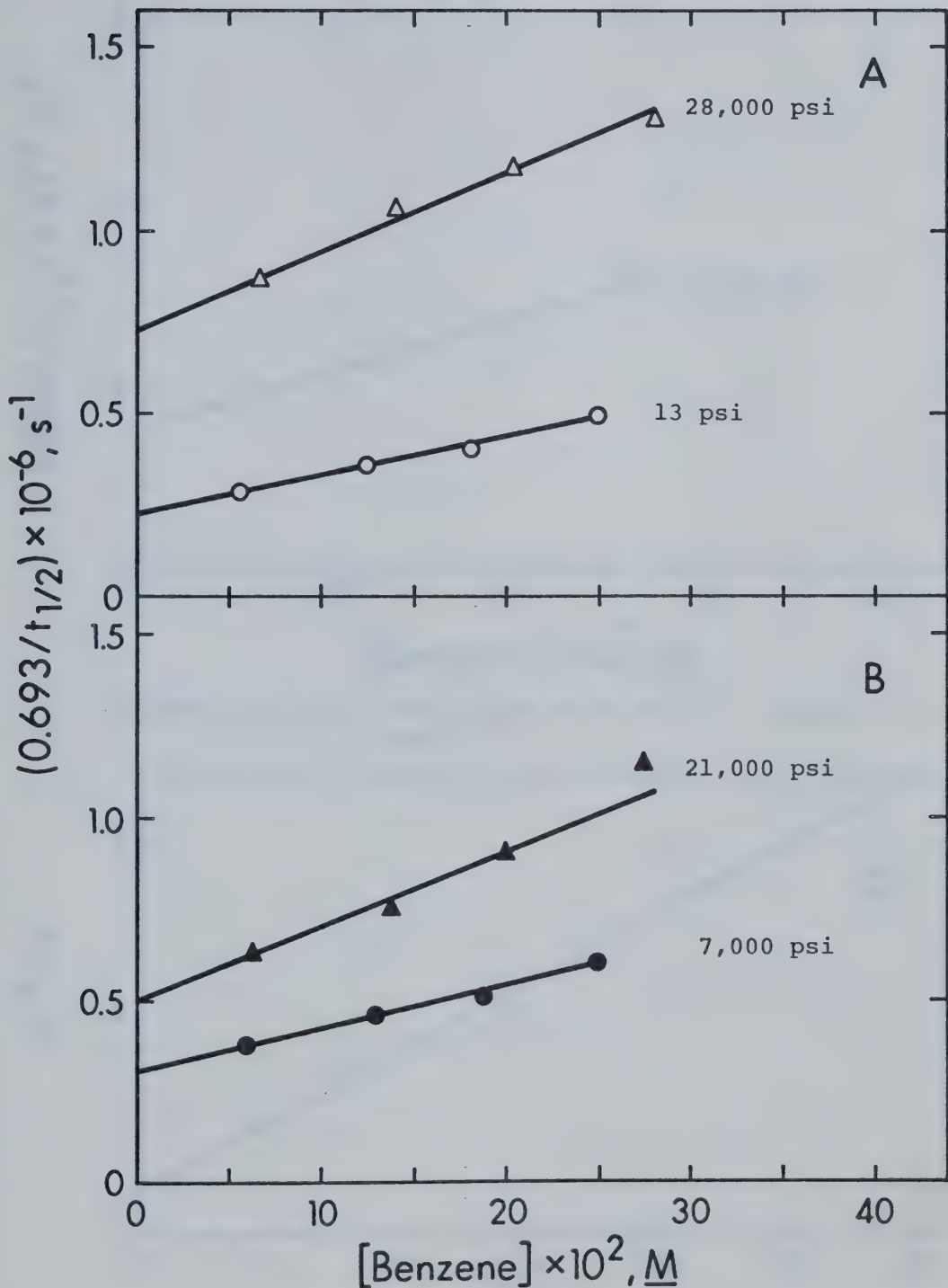


FIGURE III-43 A,B. The Effect of P on $e^- +$ Benzene in MeOH.¹⁵⁷

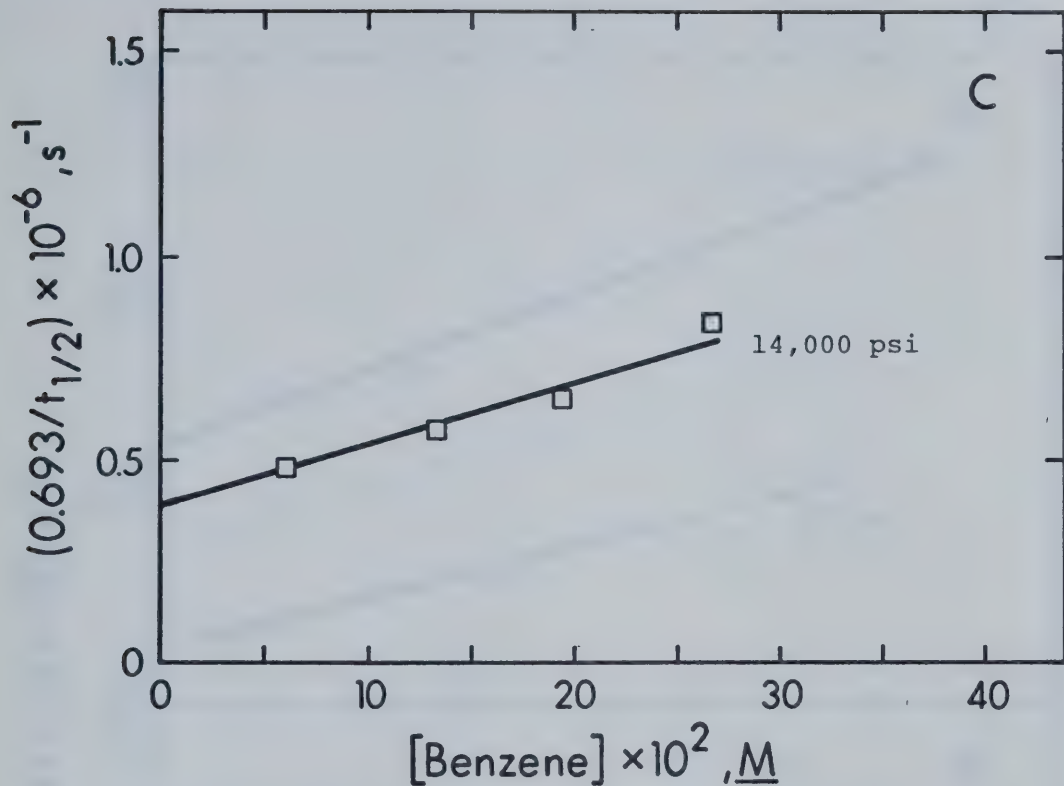


FIGURE III-43 C. The Effect of P on $e_s^{-} + \text{Benzene}$ in MeOH.¹⁵⁷

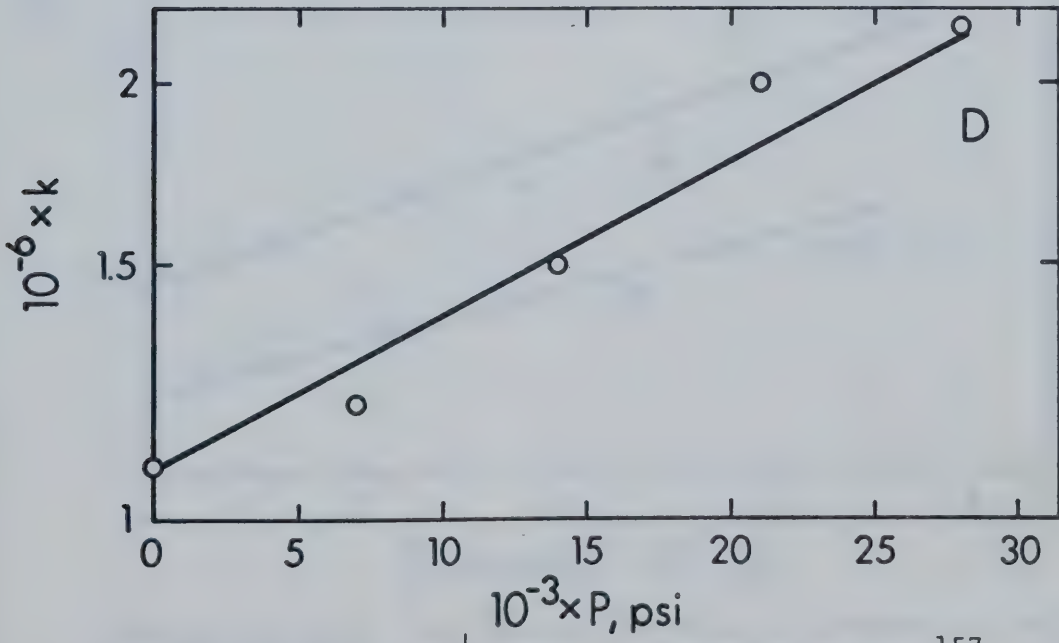


FIGURE III-43 D. ΔV^{\ddagger} for $e_s^{-} + \text{Benzene}$ in MeOH.¹⁵⁷

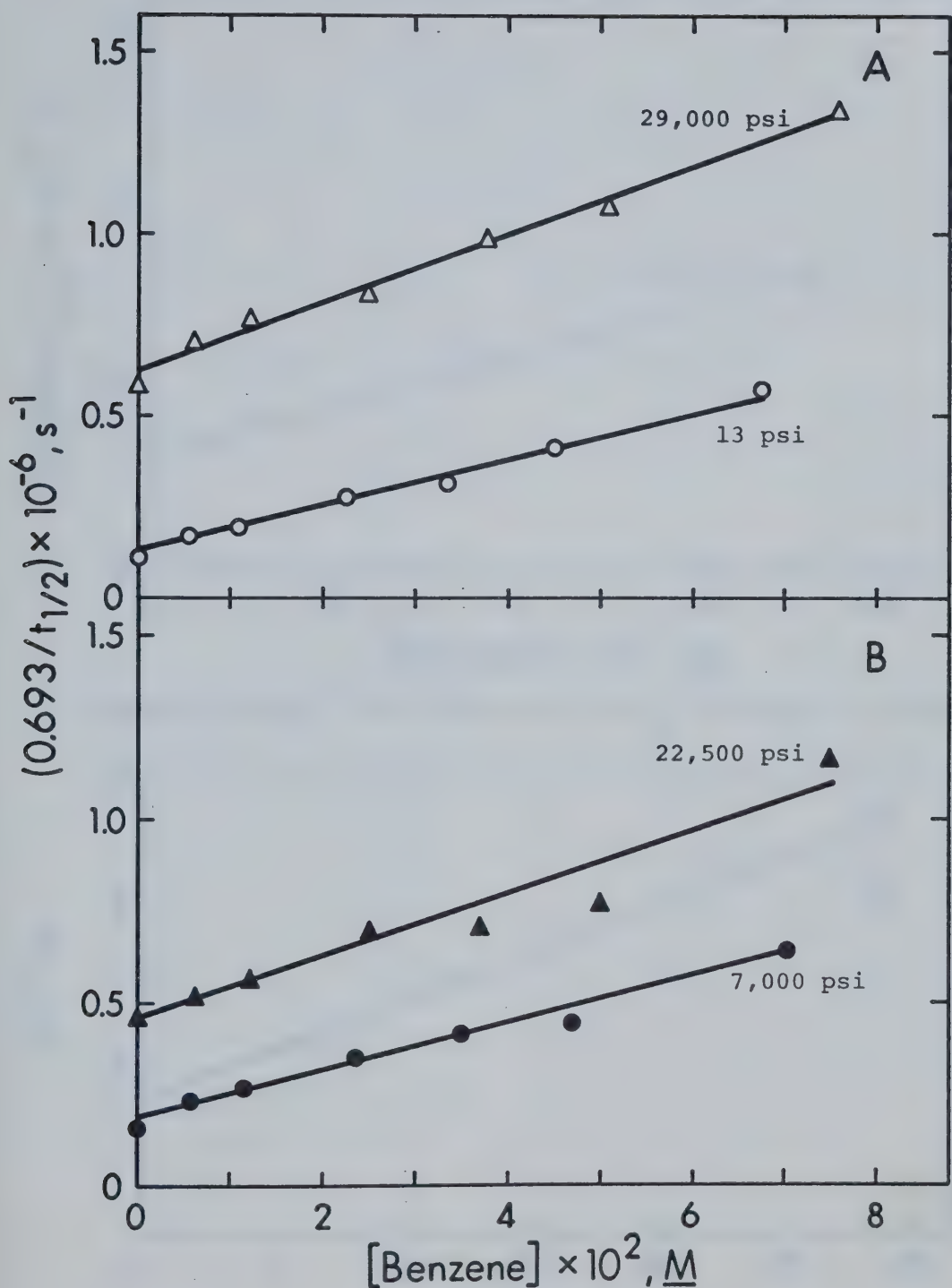


FIGURE III-44 A, B. The Effect of P on $e_s^- + \text{Benzene}$ in EtOH.

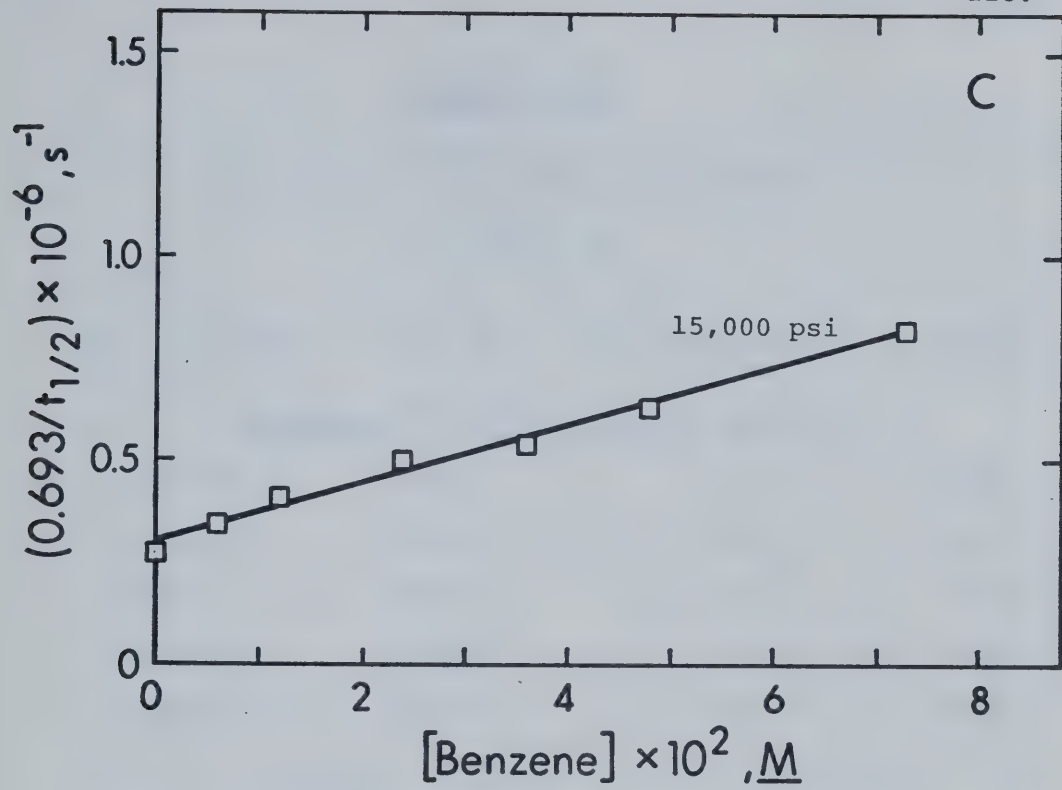


FIGURE III-44 C. The Effect of P on $e_s^- + \text{Benzene}$ in EtOH.

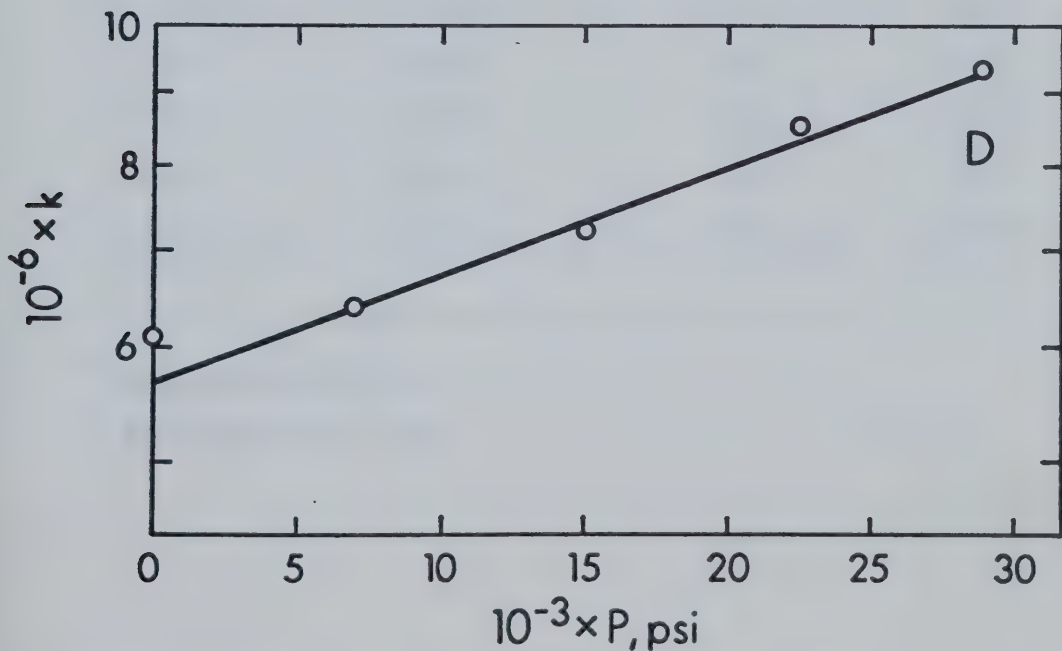


FIGURE III-44 D. ΔV^\ddagger for $e_s^- + \text{Benzene}$ in EtOH.

TABLE III-26

The k 's and ΔV^\ddagger 's for $e_s^- + \text{Benzene}$ $T = 295 \pm 1\text{K}$

$10^{-3} \times P^a, \text{psi}$	$P, \text{ kb}$	$10^{-6} \times k_5^b, \text{ M}^{-1}\text{s}^{-1}$	$\log k_5$
<u>Methanol, $157 \Delta V^\ddagger = -8.8 \pm 1 \text{ cm}^3 \text{ mol}^{-1}$</u>			
0.013	0.001	1.1	6.04
7.0	0.48	1.2	6.08
14.0	0.96	1.5	6.18
21.0	1.45	2.0	6.30
28.0	1.93	2.2	6.34
<u>Ethanol, $\Delta V^\ddagger = -6.0 \pm 0.5 \text{ cm}^3 \text{ mol}^{-1}$</u>			
0.013	0.001	6.1	6.79
7.0	0.48	6.4	6.81
15.0	1.03	7.2	6.86
22.5	1.55	8.5	6.93
29.0	2.00	9.3	6.97

^a Error may be $\pm 3\%$.^b Error may be $\pm 10\%$.

TABLE III-27

Data Summary for Effect of Pressure on e_s^- + Scavenger Reaction, 295 ± 1 K

Scavenger Species	Methanol		Ethanol	
	$k_5^a, \text{M}^{-1} \text{s}^{-1}$	$\Delta V^\ddagger b, \text{cm}^3 \text{mol}^{-1}$	$k_5^a, \text{M}^{-1} \text{s}^{-1}$	$\Delta V^\ddagger b, \text{cm}^3 \text{mol}^{-1}$
naphthalene	4.4×10^9	2 ± 1	6.2×10^9	7.3 ± 1
acetonitrile	8.6×10^7	4.7 ± 1.3	3.3×10^8	6.3 ± 0.2
perchloric acid			3.4×10^{10}	5.9 ± 1
nitrobenzene	2.6×10^{10}	4.7 ± 1.4	1.5×10^{10}	5.2 ± 1
acetone	4.0×10^9	3.1 ± 1.5	4.2×10^9	4.4 ± 1
ethyl acetate	2.2×10^7	-0.6 ± 1.5	5.3×10^7	0.0 ± 0.5
cadmium chloride	1.9×10^{10}	0.0 ± 0.5	3.7×10^9	0.0 ± 1.0
toluene	1.3×10^6	-7.4 ± 0.5	6.4×10^6	-4.3 ± 0.2
toluene (untreated)			7.6×10^6	-4.5 ± 1.5
benzene	1.1×10^6	-8.8 ± 1	6.1×10^6	-6.0 ± 0.5

^a Values at 1 bar. Error limits were normally $\pm 5\%$, but vary as indicated for individual tables.

^b Average value between 1 bar and 2 kb.

with the gaseous solute being used, were prepared in the apparatus shown in Figure II-10. The method used to obtain an aliquot of a stock solution is given in II-B-5,c.

Seven compounds, which are gases under normal conditions, were used as e_s^- scavengers in the solvents water, methanol, and ethanol. The gases chosen were nitrous oxide (N_2O), sulphur hexafluoride (SF_6), oxygen (O_2), carbon dioxide (CO_2), 1,3 butadiene (C_4H_6), acetylene (C_2H_2) and ethylene (C_2H_4). The results are presented in the above order.

The rate constants for reaction of N_2O and SF_6 with solvated electrons are important because these compounds are frequently used as electron scavengers in competition kinetics studies.^{41,161-163} In competition kinetics, rate constant ratios are obtained. To solve the ratio, one of the rate constants must be known absolutely.

For the same reason, it is important to know the rate constants for $e_s^- + O_2$ and CO_2 . However, there is an additional reason in that these two compounds are the most common reactive gaseous impurities in solutions.

The reactivity of e_s^- towards the carbon-carbon double bond, conjugated double bonds, and triple bond was investigated using C_2H_4 , C_4H_6 and C_2H_2 , respectively.

The samples of solvent were first deaerated by bubbling with UHP Ar, then irradiated to determine $t_{1/2}$ of e_s^- in the pure solvent. Some solute stock solution was

then added, and the irradiation was repeated to determine the effect of the scavenger on $t_{\frac{1}{2}}$ of e_s^- . The sample could be made more concentrated in scavenger by further addition of stock solution. Usually, only two solute concentrations were made before preparing fresh solvent. This was to limit the number of pulses to a sample.

The rate constants tabulated were calculated from (9).

$$k_5 = \frac{k_T - k_4}{[S]} \quad (9)$$

k_T is a pseudo-first order rate constant equal to the sum of k_4 and $k_5[S]$. It equals $0.693/t_{\frac{1}{2}}(T)$, where $t_{\frac{1}{2}}(T)$ is the observed e_s^- half-life after the addition of solute. k_4 and k_5 were previously defined. Where a rate constant is referred to as k_5 , it is the rate constant for (5) where S is the solute under discussion. If more than one solute is being discussed, k_5 is replaced by $k_{(e_s^- + S)}$ to avoid confusion.

The k 's are usually the average value determined from three experiments. The values for k_4 are included in the tables because of slight variations from sample to sample, which were large enough to affect the value calculated for k_5 when k_5 was small.

In order to calculate k_5 it was necessary to know the solubility of the gas in the solvent being used to

make a stock solution. In some cases these data were not available in the literature, or there was disagreement in the reported values. Solubilities were then determined by gas chromatography. In every case the Ostwald coefficient (L) used is reported in the appropriate table. Concentrations were calculated in the following way.

$$L = V_G/V_L \quad (10)$$

V_G is the volume of gaseous solute

V_L is the volume of liquid solvent.

Both are at the same temperature and pressure.

$$[S] = \frac{L}{22.41} \times \frac{P}{760} \times \frac{273}{T} \quad (11)$$

L is the Ostwald coefficient in litres of gas/litre of solution.

P is the pressure in torr

T is the temperature in °K.

For the tabulated data to follow, the temperature reported for L is the temperature at which the stock solution was made. The temperature given at the top of each table is the irradiation temperature.

Electron pulses of 1.87 MeV energy and 0.1 μ s duration were used.

1. NITROUS OXIDE (N₂O) AS e_s⁻ SCAVENGER

The results are presented in Table III-28, 29 and 30 for water, methanol and ethanol, respectively.

The value for k₅ of $(7.9 \pm 0.4)10^9 \text{ M}^{-1} \text{ s}^{-1}$ obtained in neutral water compares well with a previous report of $8.67 \times 10^9 \text{ M}^{-1} \text{ s}^{-1}$, for k₅ at pH 7.⁴⁸ At pH 11, a lower value of $5.6 \times 10^9 \text{ M}^{-1} \text{ s}^{-1}$ was obtained.¹⁶⁴ It has been found in this work that in basic alcohols, the k₅ is also generally lower than in the neutral solvent.

The value of L of 0.63 obtained at 295K was used. This agrees well with the literature value of 0.638.^{165, 166a, 167a}

In methanol, there is excellent agreement between the values for k₅ of $(6.1 \pm 0.4)10^9 \text{ M}^{-1} \text{ s}^{-1}$ at 296K, obtained in this work, and $(6.2 \pm 1.6)10^9 \text{ M}^{-1} \text{ s}^{-1}$ calculated from competition kinetics using $k = 5.6 \times 10^{10} \text{ M}^{-1} \text{ s}^{-1}$.⁴⁷ A considerably higher value of $1.3 \times 10^{10} \text{ M}^{-1} \text{ s}^{-1}$ for k₅ has been reported.¹⁶⁸ That work used the pulse radiolysis method. A similarly high value at 298K of $1.4 \times 10^{10} \text{ M}^{-1} \text{ s}^{-1}$ has been calculated from competition kinetics using $k = 5.0 \times 10^9 \text{ M}^{-1} \text{ s}^{-1}$.¹⁶⁹ However, as Baxendale points out⁴⁷, these high values are not consistent with results of competition kinetic studies using acid.^{154, 170, 171}

The literature value for the solubility of N₂O in methanol at 296K was about 13% lower (L = 3.25, ref.

TABLE III-28

k for $e_s^- + N_2O$ in Water

$10^5 \times [N_2O]^a, \underline{M}$	$10^{-5} \times k_T^b, s^{-1}$	$10^{-4} \times k_4^b, s^{-1}$	$10^{-9} \times k_5^b, \underline{M}^{-1} s^{-1}$
1.2	1.34	4.15	7.71
1.9 ₆	1.82	3.85	7.34
2.3	2.34	4.15	8.37
3.5	3.50	4.15	8.93
3.7	3.25	3.70	7.79
5.5 ₅	4.56	3.70	7.55
7.4	5.78	4.95	7.14
7.8	6.48	3.30	7.88
8.2	6.93	3.40	8.04
9.7 ₅	8.35	3.30	8.22
11.1	9.63	4.95	8.22

$$k_5 = (7.9 \pm 0.4) 10^9 \underline{M}^{-1} s^{-1}$$

^a $[N_2O]$ calculated using $L = 0.63$ at 295K.

^b Rate constants as defined for (9).

TABLE III-29

k for $e^- + N_2O$ in MethanolT = 296 \pm 1KP = 700 \pm 5 torr

$10^5 \times [N_2O]^a, M$	$10^{-5} \times k_T^b, s^{-1}$	$10^{-5} \times k_4^b, s^{-1}$	$10^{-9} \times k_5^b, M^{-1} s^{-1}$
---------------------------	--------------------------------	--------------------------------	---------------------------------------

Neutral, $k_5 = (6.1 \pm 0.4) 10^9 M s^{-1}$
--

1.27	2.97	2.27	5.51
4.6	4.81	2.18	5.72
7.2	6.42	1.94	6.22
9.1	7.88	1.86	6.62
12.1	9.76	2.08	6.35
14.2	11.18	2.07	6.42

$\sim 30 mM$	$NaOCH_3$, $k_5 = (6.3 \pm 0.4) 10^9 M^{-1} s^{-1}$
--------------	--

2.4	3.25	1.73	6.33
5.0	4.39	1.73	5.32
9.7	7.79	1.73	6.25
11.4	9.36	1.79	6.64
12.3	10.34	1.73	7.00

^a $[N_2O]$ calculated using L = 3.75 at 296K.

^b Rate constants as defined for (9).

TABLE III-30

k for $e_s^- + N_2O$ in EthanolT = 296 \pm 1KP = 695 \pm 5 torr

$10^5 \times [N_2O]^a, \underline{M}$	$10^{-5} \times k_T^b, s^{-1}$	$10^{-5} \times k_4^b, s^{-1}$	$10^{-9} \times k_5^b, \underline{M}^{-1} s^{-1}$
---------------------------------------	--------------------------------	--------------------------------	---

Neutral, $k_5^c = (7.2 \pm 0.4) 10^9 \underline{M}^{-1} s^{-1}$

2.1	2.76	1.17	7.57
3.5	3.77	1.12	7.57
4.5	4.39	1.14	7.22
6.3	5.78	1.39	6.97
7.9	6.42	1.22	6.58
12.5	10.66	1.13	7.62

$\sim 4.3 \text{ mM NaOC}_2H_5, k_5 = (5.7 \pm 0.7) 10^9 \underline{M}^{-1} s^{-1}$

4.9	3.14	0.87	4.63
7.3	4.95	0.99	5.42
9.6	6.54	0.87	5.91
12.3	9.43	0.99	6.86

^a $[N_2O]$ calculated using L = 3.30 at 296K.

^b Rate constants as defined for (9).

^c A separate series of 7 samples gave k $(e_s^- + N_2O) = (7.2 \pm 1.1) 10^9$.

165, 166a, 167a) than the L of 3.75 reported here. This was also noted by Dainton et. al.¹⁶⁹ who found the literature value to be 18% lower at 298K. Use of the lower, incorrect Ostwald coefficient, could account in part for the high value of k_5 obtained previously by pulse radiolysis.

There is good agreement between the pulse radiolysis value for k_5 of $(7.2 \pm 0.4)10^9 \text{ M}^{-1} \text{ s}^{-1}$ obtained here at 296K in neutral ethanol, and that calculated from competition kinetics at 298K. The calculated value is $8 \times 10^9 \text{ M}^{-1} \text{ s}^{-1}$ ¹⁷² assuming $k = \frac{1}{(e_s^- + \text{CH}_3\text{CHO})} = 4 \times 10^9 \text{ M}^{-1} \text{ s}^{-1}$ ⁴⁴

2. SULPHUR HEXAFLUORIDE (SF_6) AS e_s^- SCAVENGER

The results are presented in Tables III-31, III-32 and III-33.

It was difficult to determine the SF_6 concentration in water because of the very low solubility of the gas. Neither the gas chromatography system used, nor fluorine NMR, could detect SF_6 in saturated aqueous solutions of the gas.

When SF_6 saturated water was used as the stock solution, relatively large injection volumes were required. It was therefore necessary to leave a small gas volume in the sample cells to avoid cell breakage during injection. This volume was usually less than 0.5 ml.

There was some difference between solubility of

TABLE III-31

k for $e_s^- + SF_6$ in WaterT = 297 \pm 1KP = 700 \pm 5 torr

$10^6 \times [SF_6], \underline{M}$	$10^{-5} \times k_T^a, s^{-1}$	$10^{-4} \times k_4^a, s^{-1}$	$10^{-9} \times k_5^a, \underline{M}^{-1} s^{-1}$
4.2 ^b (4.7) ^c	.88	4.53	10.1 (9.0)
8.2 (9.3)	1.27	4.53	10.0 (8.9)
12.1 (13.7)	1.56	4.53	9.2 (8.1)
19.6 (22.1)	2.31	4.53	9.5 (8.4)
26.5 (30.0)	3.15	4.53	10.2 (9.1)
$k_5 = [9.8(8.7) \pm 0.4]10^9 \underline{M}^{-1} s^{-1}$			

1.3	.98	3.79	4.6
1.4	1.28	3.08	6.9
2.1	1.39	3.30	5.0
2.6	1.75	3.79	5.3
3.2	2.48	3.08	6.8
4.3	2.31	3.30	4.6
5.4	4.85	3.08	8.4
6.4	3.38	3.30	4.8
7.7	7.22	3.08	9.0
8.6	4.62	3.30	5.0

$$k_5^d = (6.0 \pm 1.4)10^9 \underline{M}^{-1} s^{-1}$$

(continued.....)

Footnotes to Table III-31

- ^a Rate constants as defined for (9).
- ^b $[\text{SF}_6]$ calculated using $L = 6.2 \times 10^{-3}$ at 296 K (ref. 173).
- ^c $[\text{SF}_6]$ calculated using $L = 7.0 \times 10^{-3}$ at 296K (ref. 148).
- ^d SF_6 saturated ethanol (0.0265 M) used as stock solution.

TABLE III-32

k for $e_s^- + SF_6$ in Methanol

$10^5 \times [SF_6]^a, M$	$10^{-5} \times k_T^b, s^{-1}$	$10^{-5} \times k_4^b, s^{-1}$	$10^{-10} \times k_5, M^{-1} s^{-1}$
Neutral, $k_5 = (1.3 \pm 0.07) 10^{10} M^{-1} s^{-1}$			
1.3	3.43	1.85	1.2
1.5	4.01	2.06	1.3
2.3	4.85	1.91	1.3
2.9	6.13	2.06	1.4
4.4	8.45	2.06	1.4 ₅
$\sim 30 \text{ mM NaOCH}_3^c, k_5 = (1.2 \pm 0.03) 10^{10} M^{-1} s^{-1}$			
1.4	3.61	2.12	1.1
2.1	4.01	1.50	1.2
2.7	5.41	2.12	1.2
3.7	5.78	1.48	1.3
4.1	7.53	2.12	1.3
4.3	6.66	1.50	1.2
5.4	9.00	2.12	1.3
6.4	9.24	1.50	1.2
7.0	10.04	1.48	1.2
8.5	11.75	1.50	1.2

^a Calculated using $L = 0.535$ at 294K. ^b Rate constants as defined in (9). ^c SF_6 in ethanol stock solution used to make samples.

TABLE III-33

k for $e_s^- + SF_6$ in Ethanol

$10^5 \times [SF_6]^a, \underline{M}$	$10^{-5} \times k_T^b, s^{-1}$	$10^{-5} \times k_4^b, s^{-1}$	$10^{-9} \times k_5, \underline{M}^{-1} s^{-1}$
Neutral, $k_5 = (1.0 \pm 0.1)10^{10} \underline{M}^{-1} s^{-1}$			
1.4	2.54	1.22	9.4
2.1	3.55	1.22	11.2
2.7	4.39	1.22	11.7
3.5	4.41	1.14	9.3
4.1	5.82	1.22	11.3
4.2	6.19	1.22	11.9
4.9	6.03	1.16	9.9
7.0	7.88	1.14	9.6
9.7	9.24	1.16	8.3
$\sim 4.3 \text{ mM } NaOC_2H_5, k_5 = (9.6 \pm 0.5)10^9 \underline{M}^{-1} s^{-1}$			
1.3	2.01	0.92	8.4
2.3	3.05	0.90	9.3
2.6	3.47	0.92	9.8
3.6	4.47	0.92	9.9
3.8	4.65	0.92	9.8
4.5	5.68	0.90	10.6
6.1	6.60	0.92	9.3
6.8	7.62	0.90	9.9

^a $[SF_6]$ calculated using $L = 0.70$ at 294K. ^b Rate constants as defined in (9).

SF_6 in water reported in the literature¹⁷³, and that found by measuring the F^- concentration in irradiated water which had been saturated with SF_6 .¹⁴⁸ Therefore, $[\text{SF}_6]$ and k_5 have been tabulated using two different Ostwald coefficients. The lower L , which results in a higher k_5 of $(9.8 \pm 0.4)10^9 \text{ M}^{-1} \text{ s}^{-1}$ is preferred because of better agreement with values for k_5 in the alcohols, found in this work (1.3 and $1.0 \times 10^{10} \text{ M}^{-1} \text{ s}^{-1}$ in methanol and ethanol, respectively), and because L was measured directly in the former case.

In order to overcome the problem of large injection volumes and low solubility, an attempt was made to use a stock solution of SF_6 in ethanol to prepare the aqueous samples. Sulphur hexafluoride is $\sim 10^2$ more soluble in ethanol than in water. There was a lot of scatter in the values obtained for k_5 , and they were generally lower than those obtained using an aqueous stock solution. This was interpreted as a solubility problem since after injection of the SF_6 saturated ethanol into the Ar saturated water, a gas bubble formed which did not completely disappear even with vigorous mixing.

A value for $k_{(\text{e}_s^- + \text{SF}_6)}$ in water of $1.65 \pm 0.1 \times 10^{10} \text{ M}^{-1} \text{ s}^{-1}$ has been reported.⁷ However, in this report, no correction was made for reaction with impurity in the neutral water. A reasonable $t_{1/2}$ for e_s^- in triply distilled neutral deaerated water is $20 \mu\text{s}$. Making the correction, assuming this $t_{1/2}$, gives $k_{(\text{e}_s^- + \text{SF}_6)} =$

$1.45 \times 10^{10} \text{ M}^{-1} \text{ s}^{-1}$. This is still higher than the preferred value of $9.8 \times 10^9 \text{ M}^{-1} \text{ s}^{-1}$ reported here.

In methanol ^{47,174}, calculation of k from competition kinetics gives $k = 2.3 \pm 0.8 \times 10^{10} \text{ M}^{-1} \text{ s}^{-1}$ assuming $k = 6.2 \times 10^9 \text{ M}^{-1} \text{ s}^{-1}$, and allowing for a probable 18% error in the N_2O concentration. ^{47,169} This is considerably higher than the value of $(1.3 \pm 0.07) \times 10^{10} \text{ M}^{-1} \text{ s}^{-1}$ reported here for 296K.

A similar calculation using $k = 1 \times 10^5 \text{ s}^{-1}$ gives $k = 5.4 \times 10^9 \text{ M}^{-1} \text{ s}^{-1}$ in ethanol. ^{48,174} This is much lower than the value of $(1.0 \pm 0.1) \times 10^{10} \text{ M}^{-1} \text{ s}^{-1}$ reported here. It should be noted that the values for k in methanol and ethanol calculated from competition kinetics differ by nearly a factor of five. This is not consistent for a reaction rate which is diffusion controlled.

3. OXYGEN (O_2) AS e_s^- SCAVENGER

The results are presented in Tables III-34 and III-35. Since the results tended to confirm previously published results for methanol ^{89,147,175} and ethanol ^{89,147} as solvents, the k for $e_s^- + \text{O}_2$ in water was not checked. It would have involved similar solubility problems to those experienced with SF_6 . Values reported for

TABLE III-34

k for $e_s^- +$ Oxygen in MethanolT = 296 \pm 1KP = 700 \pm 5 torr

$$10^5 \times [O_2]^a, \underline{M} \quad 10^{-5} \times k_T^b, \underline{s^{-1}} \quad 10^{-5} \times k_4^b, \underline{s^{-1}} \quad 10^{-10} \times k_5^b, \underline{M^{-1} s^{-1}}$$

$$\text{Neutral, } k_5 = (1.8 \pm 0.06) 10^{10} \underline{M^{-1} s^{-1}}$$

0.69	3.15	1.91	1.8
1.3	4.01	1.78	1.7
2.1	5.87	1.91	1.9
2.6	6.60	1.78	1.8 ₅

$$\sim 27 \text{ mM NaOCH}_3, k_5 = (2.0 \pm 0.05) 10^{10} \underline{M^{-1} s^{-1}}$$

0.73	3.04	1.58	2.0
1.3 ₅	4.41	1.58	2.1
1.5	4.68	1.58	2.1
2.7	7.07	1.58	2.0

^a $[O_2]$ calculated using L = 0.224 at 296K.

^b Rate constants as defined in (9).

TABLE III-35

k for e_s^- + Oxygen in Ethanol $T = 296 \pm 1K$ $P = 700 \pm 5 \text{ torr}$

$10^5 \times [O_2]^a, \underline{M}$	$10^{-5} \times k_T^b, \underline{s}^{-1}$	$10^{-5} \times k_4^b, \underline{s}^{-1}$	$10^{-10} \times k_5^b, \underline{M}^{-1} \underline{s}^{-1}$
--------------------------------------	--	--	--

$\text{Neutral, } k_5 = (2.0 \pm 0.1) 10^{10} \underline{M}^{-1} \underline{s}^{-1}$
--

1.4	4.36	1.44	2.1
2.9	6.93	1.44	1.9

$\sim 12 \text{ mM NaOC}_2\text{H}_5, k_5 = (1.5 \pm 0.05) 10^{10} \underline{M}^{-1} \underline{s}^{-1}$

0.71	2.04	0.98	1.5
1.35	3.71	1.61	1.55
2.1	3.96	0.98	1.4
2.7	5.13	1.07	1.5

^a Solutions made using O_2 saturated methanol as the stock ($8.5 \times 10^{-3} \underline{M}$).

^b Rate constants as defined in (9).

$k_{(e_s^- + O_2)}$ in water are from 1.5 to $2.16 \times 10^{10} \text{ M}^{-1} \text{ s}^{-1}$ at pH 7^{48,49,60,176}, and $1.9 \times 10^{10} \text{ M}^{-1} \text{ s}^{-1}$ at pH 11.¹⁶⁴

Solutions of oxygen saturated methanol were used in making samples in both methanol and ethanol. There was disagreement in literature values for the solubility of O_2 in methanol. The value of L varied from 0.251^{177,178} to 0.194^{179,180} at 298K. The value for L of 0.224 obtained at 296K in this work was therefore used.

4. CARBON DIOXIDE (CO_2) AS e_s^- SCAVENGER

The data are presented in Tables III-36, III-37 and III-38.

Solubilities of CO_2 in water at 297K reported in the literature varied from $L = 0.834$ ^{166a,167a} to 1.58 .^{167a} Therefore, the value of $L = 1.03$ at 296K determined in this work was used in calculating the CO_2 concentration. The value obtained for k_5 of $(7.3 \pm 0.4)10^9 \text{ M}^{-1} \text{ s}^{-1}$ agrees well with a previously reported value of $7.67 \times 10^9 \text{ M}^{-1} \text{ s}^{-1}$ ^{48,49}

The value for L of 4.85 in methanol at 295K obtained and used in this work is considerably higher than the literature value of 3.4.^{166a,177} Both the calibration of the gas chromatograph and the solubility determination were checked, and the higher value was reproduced.

The effect of base on the rate of the reaction of e_s^- with CO_2 could not be measured, due to removal of

TABLE III-36

k for e_s^- + Carbon Dioxide in Water

$T = 296 \pm 1K$	$P = 695 \pm 5 \text{ torr}$		
$10^5 \times [CO_2]^a, \text{ M}$	$10^{-5} \times k_T^b, \text{ s}^{-1}$	$10^{-4} \times k_4^b, \text{ s}^{-1}$	$10^{-9} \times k_5^b, \text{ M}^{-1} \text{ s}^{-1}$
$k_5 = (7.3 \pm 0.4) 10^9 \text{ M}^{-1} \text{ s}^{-1}$			
3.3 ₅	3.19	5.8	7.8
4.7	4.03	5.3	7.4
6.6	4.88	5.6	6.6
7.8	6.42	5.3	7.4 ₅
10.0	8.45	5.8	7.8
13.2	9.76	5.6	7.0

^a $[CO_2]$ calculated using $L = 1.03$ at 296K.

^b Rate constants as defined in (9).

TABLE III-37

k for $e_s^- + \text{Carbon Dioxide in Methanol}$ $T = 296 \pm 1\text{K}$ $P = 700 \pm 5 \text{ torr}$

$10^5 \times [\text{CO}_2]^a, \text{M}$	$10^{-5} \times k_T^b, \text{s}^{-1}$	$10^{-5} \times k_4^b, \text{s}^{-1}$	$10^{-9} \times k_5^b, \text{M}^{-1} \text{s}^{-1}$
Neutral, $k_5 = (6.7 \pm 0.6) 10^9 \text{ M}^{-1} \text{s}^{-1}$			
3.5	4.05	1.94	6.0
5.9	5.68	1.87	6.5
9.2	7.07	1.74	5.7
10.1	8.88	1.95	6.9
11.9	10.10	1.87	7.6
15.6	13.59	1.74	7.6

^a $[\text{CO}_2]$ calculated using $L = 4.85$ at 295K.

^b Rate constants as defined in (9).

TABLE III-38

k for e_s^- + Carbon Dioxide in Ethanol

	$T = 296 \pm 1K$	$P = 700 \pm 5 \text{ torr}$	
	$10^5 \times [CO_2]^a, \underline{M}$	$10^{-5} \times k_T^b, \underline{s}^{-1}$	$10^{-9} \times k_5^b, \underline{M}^{-1} \underline{s}^{-1}$
Neutral, $k_5 = (4.9 \pm 0.7) 10^9 \underline{M}^{-1} \underline{s}^{-1}$			
3.1	2.57	1.35	3.9
5.9	4.33	1.64	4.6
7.5	4.78	1.53	4.3
11.9	9.24	1.64	6.4
13.7	9.03	1.53	5.5
15.1	8.74	1.61	4.7

^a Solutions made using CO_2 saturated methanol as the stock ($0.18 \underline{M}$).

^b Rate constants as defined in (9).

CO_2 from solution by carbonate formation when base was added.

5. 1,3-BUTADIENE (C_4H_6) AS e_s^- SCAVENGER

The results are given in Tables III-39, 40 and 41.

Stock solution was 1,3-butadiene saturated water for use in the solvents water, methanol and ethanol. This was necessary because of the very high solubility of the gas in methanol and ethanol. Diminishingly small injection volumes would have been necessary if stock solution in the alcohols had been used.

Not more than 60 μl of aqueous stock solution was used in 6 ml alcohol samples. Injection of 60 μl of UHP Ar bubbled water had no effect on the $t_{1/2}$ of e_s^- in methanol.

1,3-Butadiene was a relatively good scavenger of e_s^- in all three solvents. The k_5 was lower in the basic than in the neutral alcohols, but in every case it was $> 10^9 \text{ M}^{-1} \text{ s}^{-1}$.

The value for k_5 of $(3.0 \pm 0.7) 10^9 \text{ M}^{-1} \text{ s}^{-1}$ in water was lower than the value of $8 \times 10^9 \text{ M}^{-1} \text{ s}^{-1}$ given in a previous report.¹⁸¹

6. ACETYLENE (C_2H_2) AS e_s^- SCAVENGER

The results are given in Tables III-42, 43 and 44.

TABLE III-39

k for $e_s^- + 1,3\text{-Butadiene in Water}$ $T = 296 \pm 1\text{K}$ $P = 700 \pm 5 \text{ torr}$

$10^5 \times [C_4H_6]^a, M$	$10^{-5} \times k_T^b, s^{-1}$	$10^{-4} \times k_4^b, s^{-1}$	$10^{-9} \times k_5^b, M^{-1} s^{-1}$
-----------------------------	--------------------------------	--------------------------------	---------------------------------------

Neutral, $k_5^c = (3.0 \pm 0.7) 10^9 M^{-1} s^{-1}$			
---	--	--	--

3.1	2.00	9.0	3.5
6.3	3.63	9.0	4.3
7.1	2.08	3.8	2.4
9.4	4.62	9.0	4.0
14.2	3.75	3.8	2.4
21.3	5.54	3.8	2.4
28.4	7.29	3.8	2.4

^a $[C_4H_6]$ calculated using $L = 0.47$ at 293K.

^b Rate constants as defined for (9).

^c High values for k_5 were obtained in impure water. The lower limit for k_5 is therefore preferred.

TABLE III-40

k for $e_s^- + 1,3\text{-Butadiene}$ in Methanol $T = 296 \pm 1\text{K}$ $P = 700 \pm 5 \text{ torr}$

$$10^5 \times [C_4H_6]^a, M \quad 10^{-5} \times k_T^b, s^{-1} \quad 10^{-5} \times k_4^b, s^{-1} \quad 10^{-9} \times k_5^b, M^{-1} s^{-1}$$

$$\text{Neutral, } k_5 = (1.65 \pm 0.2) 10^9 M^{-1} s^{-1}$$

3.1	2.50	1.94	1.8
5.8	3.01	2.06	1.6
6.1	3.18	1.94	2.0
12.3	3.83	1.94	1.5
14.6	4.08	2.06	1.4
18.4	4.85	1.94	1.6

$$\sim 30 \text{ mM NaOCH}_3, k_5 = (1.4 \pm 0.1) 10^9 M^{-1} s^{-1}$$

6.0	2.39	1.50	1.5
1.2	3.07	1.50	1.3
1.9	4.05	1.50	1.3

^a All samples made using 1,3-butadiene saturated water as stock solution, $L = 0.47$ at 293K.

^b Rate constants as defined for (9).

TABLE III-41

k for $e_s^- + 1,3\text{-Butadiene}$ in EthanolT = 296 \pm 1KP = 700 \pm 5 torr

$$10^5 \times [C_4H_6]^a, M \quad 10^{-5} \times k_T^b, s^{-1} \quad 10^{-5} \times k_4^b, s^{-1} \quad 10^{-9} \times k_5^b, M^{-1} s^{-1}$$

$$\text{Neutral, } k_5 = (2.9 \pm 0.2) 10^9 M^{-1} s^{-1}$$

3.2	2.37	1.39	3.1
5.9	2.83	1.24	2.7
6.4	3.40	1.39	3.1
9.6	4.53	1.39	3.3
11.8	4.47	1.24	2.7
18.3	6.24	1.24	2.7

$$\sim 4.3 \text{ mM NaOC}_2H_5, k_5 = (2.4 \pm 0.1) 10^9 M^{-1} s^{-1}$$

5.8	2.17	0.92	2.2
11.6	3.75	0.92	2.4
17.5	5.21	0.92	2.5

^a All samples made using 1,3-butadiene saturated water as stock solution. L = 0.47 at 293K.

^b Rate constants as defined for (9).

TABLE III-42

k for $e_s^- +$ Acetylene^a in Water

$[C_2H_2]^b, \underline{M}$	$10^{-5} \times k_T^c, s^{-1}$	$10^{-4} \times k_4^c, s^{-1}$	$10^{-6} \times k_5^c, \underline{M}^{-1} s^{-1}$
$k_5^a \leq 6.6 \times 10^6 \underline{M}^{-1} s^{-1}$			
0.037	2.95	6.2	6.3
0.037	3.00	4.5	6.9

^a Mass spectrometry indicated 0.04 to 0.07% O_2 in the acetylene. $O_2 + e_s^-$ could account for all the difference between k_T and k_4 ($k_{(e_s^- + O_2)} = 2 \times 10^{10} \underline{M}^{-1} s^{-1}$) if O_2 were 0.04% of the gas in solution.

^b $[C_2H_2]$ calculated using $L = 0.97$ at 295K.

^c Rate constants as defined for (9).

TABLE III-43
 k for $e_s^- +$ Acetylene^a in Methanol

$[C_2H_2]^b, \underline{M}$	$10^{-5} \times k_T^c, s^{-1}$	$10^{-5} \times k_4^c, s^{-1}$	$10^{-6} \times k_5^c, \underline{M}^{-1} s^{-1}$
Neutral, $k_5^a \leq 3.4 \times 10^6 \underline{M}^{-1} s^{-1}$			
0.0052	2.21	1.93	5.2
0.016	2.43	1.93	3.1
0.029	2.82	1.93	3.1
0.50	12.8	2.21	2.1
$\sim 27 \text{ mM NaOCH}_3, k_5^a \leq 2.3 \times 10^6 \underline{M}^{-1} s^{-1}$			
0.0052	1.70	1.55	2.9
0.011	1.76	1.59	1.5
0.015	1.90	1.55	2.3
0.021	2.04(1.93) ^d	1.59	2.1(1.6)
0.031	2.19(2.10)	1.59	1.9(1.65)
0.50	15.4	1.44	2.8

^a Mass spectrometry indicated 0.04 to 0.07% O_2 in the acetylene. $O_2 + e_s^-$ could account for all the difference between k_T and k_4 ($k = 1.8 \times 10^{10} \underline{M}^{-1} s^{-1} (e_s^- + O_2)$) if O_2 were 0.04% of the gas in solution.

^b $[C_2H_2]$ calculated using $L = 13.1$ at 295K.

^c Rate constants as defined for (9).

^d Results in brackets are after 3 pulses, indicating probable partial removal of oxygen.

TABLE III-44

k for e_s^- + Acetylene^a in Ethanol

$[C_2H_2]^b$, \underline{M}	$10^{-5} \times k_T^c, s^{-1}$	$10^{-5} \times k_4^c, s^{-1}$	$10^{-6} \times k_5^c, \underline{M}^{-1} s^{-1}$
Neutral, $k_5^a \leq 5 \times 10^6 \underline{M}^{-1} s^{-1}$			
0.005	1.50	1.15	7.0
0.010	1.47	1.15	3.2
0.27 ₅	13.9	1.27	4.6
0.29	17.2	1.34	5.5
$\sim 12 \text{ mM NaOC}_2H_5, k_5^a \leq 2.9 \times 10^6 \underline{M}^{-1} s^{-1}$			
0.0024	1.40	1.00	1.7
0.0072	1.76	1.00	1.1
0.011	1.31	0.92	3.5
0.0145	1.52	0.98	3.7
0.021	1.78(1.65) ^d	0.92	4.1(3.5)
0.031	1.95(1.77)	0.92	3.3(2.7)

^a Mass spectrometry indicated 0.04 to 0.07% O_2 in the acetylene. $O_2 + e_s^-$ could account for all the difference between k_T and k_4 ($k_{(e_s^- + O_2)} = 1.8 \times 10^{10} \underline{M}^{-1} s^{-1}$) if O_2 were 0.04% of the gas in solution.

^b $[C_2H_2]$ calculated using $L = 7.6$ at 295K.

^c Rate constants as defined for (9).

^d Results in brackets are after 3 pulses, indicating probable partial removal of oxygen.

More than eighty samples were used in this study. A major problem was removal of electron scavenging impurities, such as acetone and oxygen, from the acetylene. Acetone was removed by running the gas from the storage cylinder through first a cold trap (210K), then two flasks of triply distilled water. Oxygen could not be removed using Oxysorb "G" due to reaction of C_2H_2 with the column packing material.

Analysis of the acetylene by mass spectrometry indicated that it contained from 0.04 to 0.07% O_2 . Assuming the lower value of O_2 impurity was also contained in a stock solution, it was calculated that all of the observed decrease in $t_{\frac{1}{2}}$ of e_s^- could be due to the reaction of e_s^- with O_2 .

Tabulated values for k_5 are those determined from the observed decrease in $t_{\frac{1}{2}}$ for e_s^- in solutions containing the indicated amount of C_2H_2 . No correction for O_2 was applied because the actual O_2 concentration in a stock solution was not known.

7. ETHENE (C_2H_4) AS e_s^- SCAVENGER

The results are given for water, methanol and ethanol in Table III-45.

Saturated solutions were used in each case. As for C_2H_2 , the rate constants for $e_s^- + C_2H_4$ were all small, with the largest being $6.1 \times 10^6 \text{ M}^{-1} \text{ s}^{-1}$ in

TABLE III-45

k for $e_s^- + \text{Ethene}$

$T = 297 \pm 1\text{K}$

$P = 700 \pm 5 \text{ torr}$

$10^2 \times [C_2H_4]^a, \underline{M} \quad 10^{-5} \times k_T^b, s^{-1} \quad 10^{-5} \times k_4^b, s^{-1} \quad 10^{-6} \times k_5^b, \underline{M}^{-1} s^{-1}$

Neutral Ethanol

9.8	3.08	1.37	1.7
-----	------	------	-----

$\sim 12 \text{ mM NaOC}_2H_5$ in Ethanol

9.8	3.08	0.95	2.2
-----	------	------	-----

Neutral Methanol

9.2	2.88	2.41	0.5
-----	------	------	-----

$\sim 27 \text{ mM NaOCH}_3$ in Methanol

9.2	2.63	1.50	1.2
-----	------	------	-----

Neutral Water

0.38	0.92	0.69	6.1
------	------	------	-----

^a $[C_2H_4]$ calculated using $L = 2.59$ at 296 for EtOH,
 $L = 2.43$ at 296 for MeOH and $L = 0.1$ at 296 for H_2O .

^b Rate constant as defined for (9).

water, and the smallest being $5 \times 10^5 \text{ M}^{-1} \text{ s}^{-1}$ in neutral methanol.

The problem of possible impurity of the order of a few μM in the bubbled sample makes the reported k 's upper limit values.

Ethene was previously reported to be "unreactive" with e_s^- in water, ¹⁸¹ but no value for k_5 was quoted because of impurity problems.

E. THE EFFECT OF DOSE ON $t_{1/2}$

The effect of pulse dose on the $t_{1/2}$ for neutral and basic methanol and ethanol is given in Figures III-45 and III-46.

Larger pulse doses result in shorter $t_{1/2}$ for e_s^- due to the creation of a higher concentration of scavenging impurity. This impurity can largely be removed before reacting with e_s^- by adding base.

Extrapolation of the plots to zero dose gives minimum half lives of 5.3 μs and 8.7 μs for methanol and ethanol, respectively, at 295K.

The ethanol used was untreated U.S.I. alcohol. The methanol was from Monsanto, and had been treated by the Na-NaBH_4 purification method.

Baxendale and Wardman ³¹ report $t_{1/2}$ for e_s^- of 7 and 9 μs in ~1 mM NaOR solutions of methanol and ethanol, respectively, at 293K. In their work, 5 - 10 ns pulses

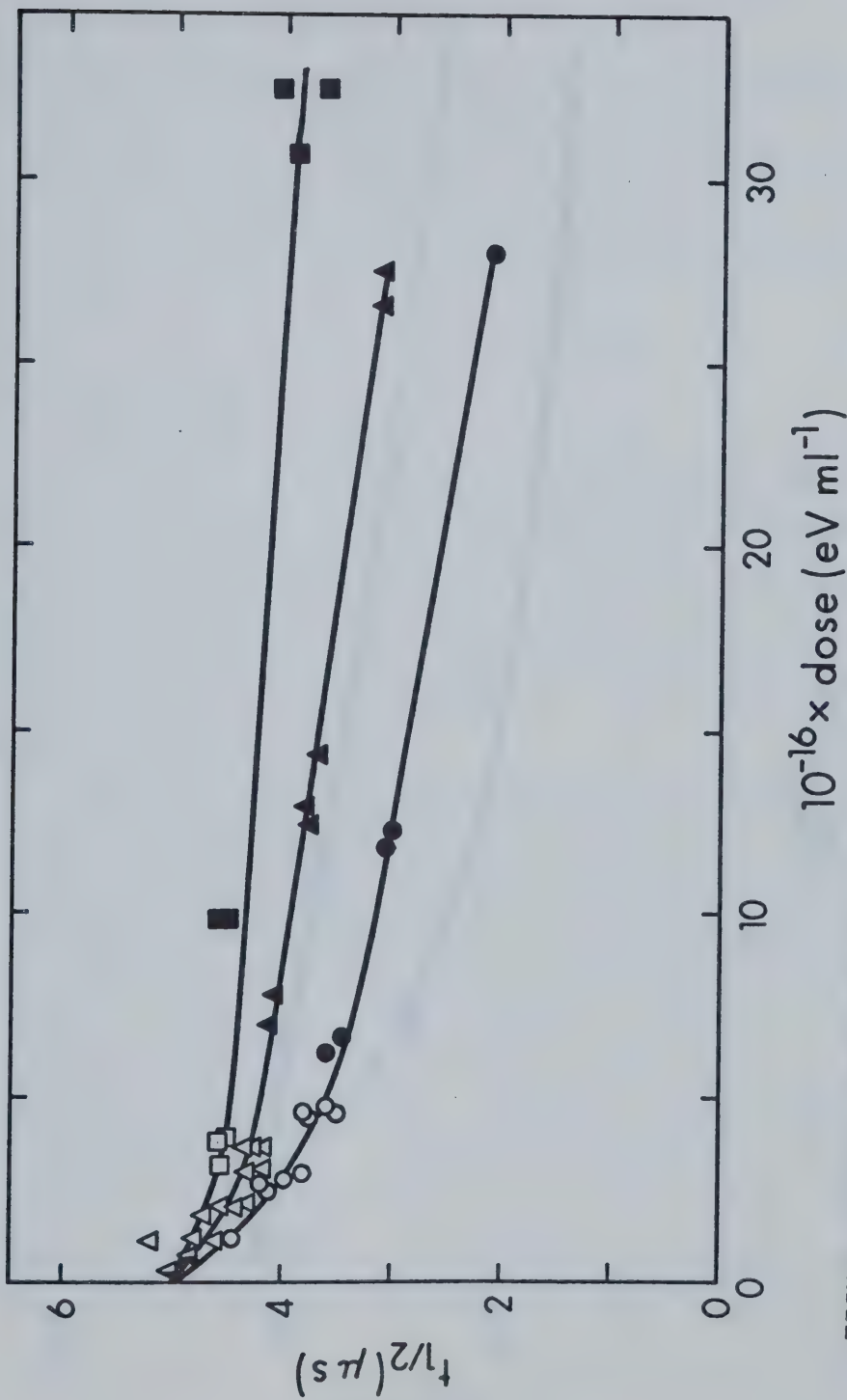


FIGURE III-45. The Effect of Dose on $t_{1/2}$ of e_s^- in MeOH. $295 \pm 1K$. Open Points, $0.1 \mu s$ Pulses; Closed Points, $1.0 \mu s$ Pulses; half closed, $0.03 \mu s$ Pulses. 0 , Neutral; Δ , $\sim 1 \text{ mM NaOCH}_3$; \square , $\sim 31 \text{ mM NaOCH}_3$.

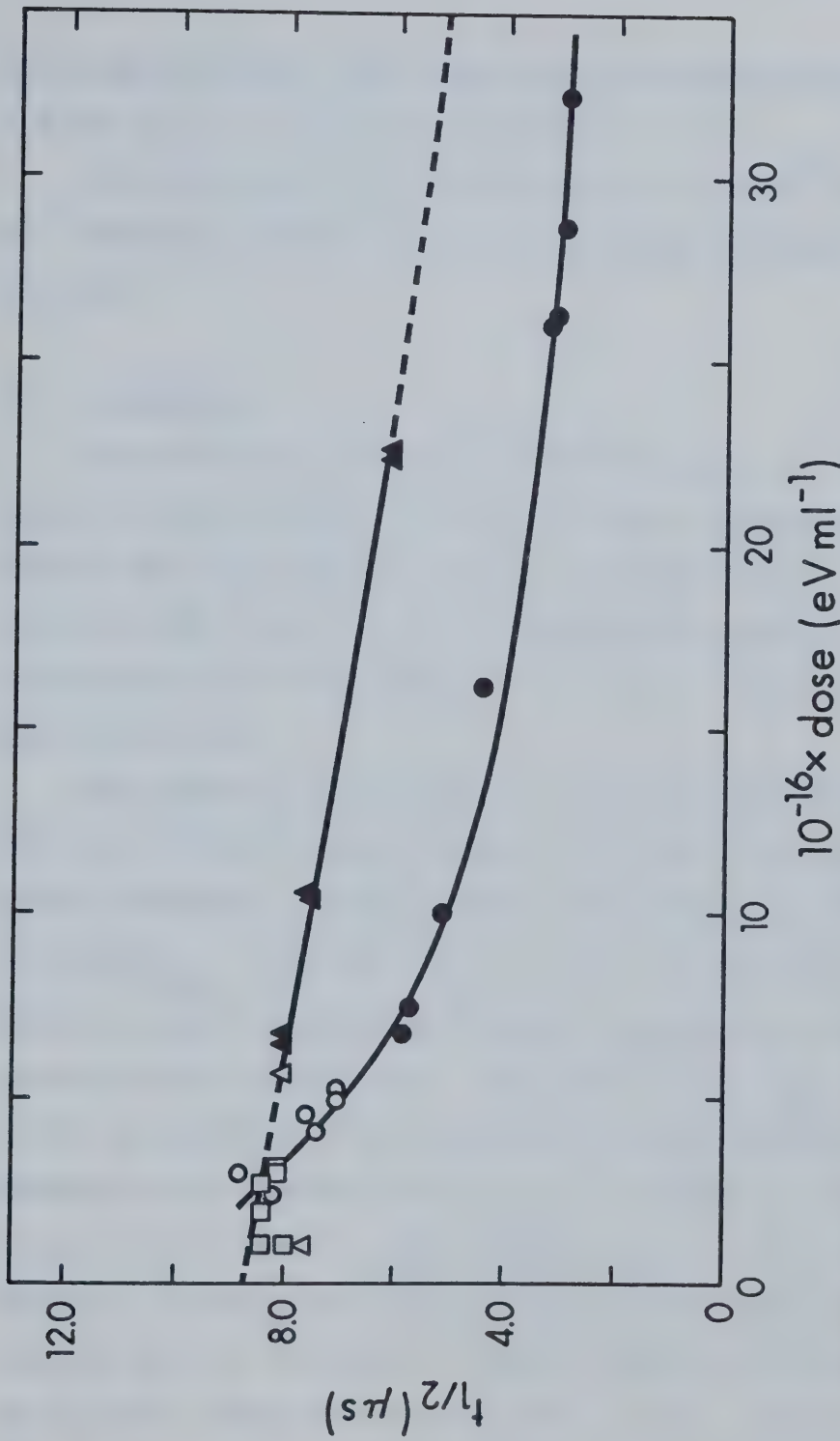


FIGURE III-46. The Effect of Dose on $t_{1/2}$ of e^- in EtOH. 295 \pm 1K. Open Points, 0.1 μs Pulses; Closed Points, 1.0 μs Pulses. O, Neutral; Δ , 10^{-2} M KOH; \square , 4.3 mM NaOC_2H_5 .

of 12 MeV electrons were used, giving a sample dose of 1 - 2 Krads ($6 - 12 \times 10^{16}$ ev) per pulse.

In this work, doses in water of $4 - 5 \times 10^{16}$ ev ml^{-1} were obtained for each ncoul of charge collected from the SEM.

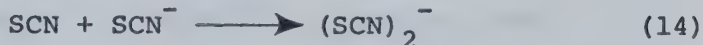
F. DOSIMETRY

The relative dose in each electron pulse was determined from the current caused by passage of the pulse through the thin metal foils of a secondary emission monitor (SEM) (Figure II-11). The SEM was regularly calibrated to the dose absorbed by a sample using in situ actinometry.

The standard actinometer in radiation chemistry has been the $\text{Fe}^{+2}/\text{Fe}^{+3}$ aqueous system, referred to as the Fricke dosimeter. In this system, the values of $G(\text{Fe}^{+3}) = 15.5$ and $\mathcal{E}_{\lambda_{\text{max}}} = 2110 \text{ M}^{-1} \text{ cm}^{-1}$ at 292K are well known.¹⁸² However, use of the Fricke dosimeter routinely was inconvenient for two reasons. First, Fe^{+3} has a λ_{max} of 304 nm. Monitoring this wavelength required several changes to the optical system, such as removal of the Perspex filter from the lamp housing, use of a U.V. monochromator grating, and installation of a photomultiplier detector and its amplifier. Second, and most important, the dosimeter response was very slow (~3 s). Fluctuation in the analyzing light, or diffusion of Fe^{+3} from

the analyzed volume (Figure III-12) during this time, would limit the accuracy of a dose measurement.

The actinometer chosen for routine use was aqueous, O_2 saturated KSCN solution, in which the absorbing species was $(SCN)_2^-$.



The KSCN dosimeter was ideal in that the response occurred within the pulse, the absorption was in the visible region, and there was no appreciable decay in A during a measurement.

The A obtained following irradiation of actinometer solution depends upon the product of the concentration of the absorbing species and its ϵ . The concentration of $(SCN)_2^-$ is relative to $G(OH)$ in aqueous solution, as shown by (13) and (14). Therefore, A is relative to $G(OH) \cdot \epsilon_{(SCN)_2^-}$ (units are (radicals/100 eV \underline{M} cm)).

Although this dosimeter was being used in several laboratories 43,65,69,73, some confusion existed in the literature over the value of $\epsilon_{\lambda_{max}}$. Early reports by Adams et. al. 137,183 indicated that λ_{max} was 480 nm and ϵ was $7100 \underline{M}^{-1} \text{ cm}^{-1}$ at 500 nm. The ϵ was determined relative to $\epsilon_{\lambda_{max}} = 1.0 \times 10^3 \underline{M}^{-1} \text{ cm}^{-1}$ for ferricyanide in aqueous solution.¹⁸⁴ However, it was pointed out that this was consistent with a value for $G(OH)$ of 2.9.^{137,185}

The value of $7100 \text{ M}^{-1} \text{ cm}^{-1}$ for ϵ_{500} was later quoted by Baxendale *et. al.*¹³⁸ as being for $\epsilon_{\lambda_{\max}}$. These authors found $\lambda_{\max} = 475 \text{ nm}$, and $\epsilon_{\lambda_{\max}} = 7600 \text{ M}^{-1} \text{ cm}^{-1}$, assuming $G(\text{OH}) = 2.8$.¹⁸⁶ Their measurement of $G(\text{OH}) \cdot \epsilon_{(\text{SCN})_2^-}$ was relative to the Fricke dosimeter.

Another report gave a $G(\text{OH}) \cdot \epsilon_{\lambda_{\max}} (\text{SCN})_2^-$ of $2.15 \times 10^{+4}$ in 10^{-2} M KSCN.¹⁸² Assuming $G(\text{OH})$ to be 2.9¹⁸⁵, this gives $\epsilon_{\lambda_{\max}} = 7400 \text{ M}^{-1} \text{ cm}^{-1}$.

To establish which $G(\text{OH}) \cdot \epsilon_{\lambda_{\max}} (\text{SCN})_2^-$ should be used, the KSCN dosimeter was compared with the Fricke dosimeter. The results are given in Table III-46. Absorbances relative to the same SEM dose were found in irradiated aqueous KSCN/O₂ solution and in aqueous 5, 10 and 50 mM Fe⁺² solution. Values of $G(\text{OH}) \cdot \epsilon_{\lambda_{\max}} (\text{SCN})_2^-$ were then calculated using (15), where $G(\text{Fe}^{+3}) = 15.5$ and $\epsilon_{304} = 2110 \text{ M}^{-1} \text{ cm}^{-1}$ at 292K for the Fricke dosimeter.

$$G(\text{OH}) \cdot \epsilon_{\lambda_{\max}} (\text{SCN})_2^- = \frac{G(\text{Fe}^{+3}) \epsilon_{\lambda_{\max}} (\text{Fe}^{+3})_{\text{A}_{\max}} (\text{SCN})_2^-}{\text{A}_{\max} (\text{Fe}^{+3})} \quad (15)$$

Using the average value for $G(\text{OH}) \cdot \epsilon_{\lambda_{\max}} (\text{SCN})_2^-$ of 2.20×10^4 and assuming $G(\text{OH})$ to be 2.9, a value of $7600 \text{ M}^{-1} \text{ cm}^{-1}$ is obtained for $\epsilon_{\lambda_{\max}} (\text{SCN})_2^-$. These values were used in all subsequent dosimetry.

TABLE III-46

$10^3 \times [\text{Fe}^{++}]$, M		Pulse length μs	$10^2 \times A_{\text{max}} (\text{Fe}^{+3})$ ^a	$10^2 \times A_{\text{max}} ((\text{SCN})_2^-)$ ^b	$10^4 \times G(\text{OH}) \cdot \mathcal{E}_{\lambda_{\text{max}}}$	$(\text{SCN})_2^-$ max	
5	0.1	2.70		1.50		1.82	
		2.20				2.23	
	1.0	2.34		1.41		2.10	
		2.00				2.31	
10	0.1	2.33		1.50		1.97	
		1.89				2.44	
	1.0	2.18		1.41		2.25	
		2.21				2.22	
50	0.1	2.25		2.00		2.18	
		1.81				2.55	
	1.0	2.09		2.09		2.31	
		2.53				2.20	
1.0	0.1	2.40		1.50		1.94	
		2.30				2.04	
	1.0	2.20		1.41		2.13	
		2.05				2.10	
		1.86				2.25	
						2.46 (continued...)	

TABLE III-46 continued

$$\text{Average } G(\text{OH}) \cdot \mathcal{E}_{\lambda_{\text{max}}} (\text{SCN})_2^- = 2.20 \pm 0.14 \times 10^4$$

^a A per unit SEM dose at $\lambda = 304$ nm.

^b A per unit SEM dose at $\lambda = 478$ nm in 5 mM KSCN solution.

^c Calculated using (15). Units are (radicals $\ell/100$ eV mol cm).

The value for λ_{\max} was checked and the effect of temperature change on λ_{\max} and A_{\max} was determined. Results are given in Figure III-47. A λ_{\max} of 478 ± 4 nm was found, in good agreement with previous values.^{137,138,183} Both A_{\max} and λ_{\max} were independent of temperature between 295 and 332K.

As is evident in Figure III-48, $G(OH) \cdot \epsilon_{\lambda_{\max}}^{(SCN)_2^-}$ is nearly independent of concentration between 10^{-3} and 10^{-4} M KSCN. This was also found by Adams et. al.¹³⁷. Solutions of either 2.0 or 5.0 mM KSCN were used for dosimetry purposes.

Above about 10^{-2} M KSCN, there is a gradual rise in the relative A up to about 1 M KSCN. This was interpreted as due to an increase in scavenging of OH in the spurs. The decrease in relative A at KSCN concentrations above 1.0 M is not understood. It was not due to contamination of the solutions, because the lower concentrations were made by dilution of the more concentrated ones.

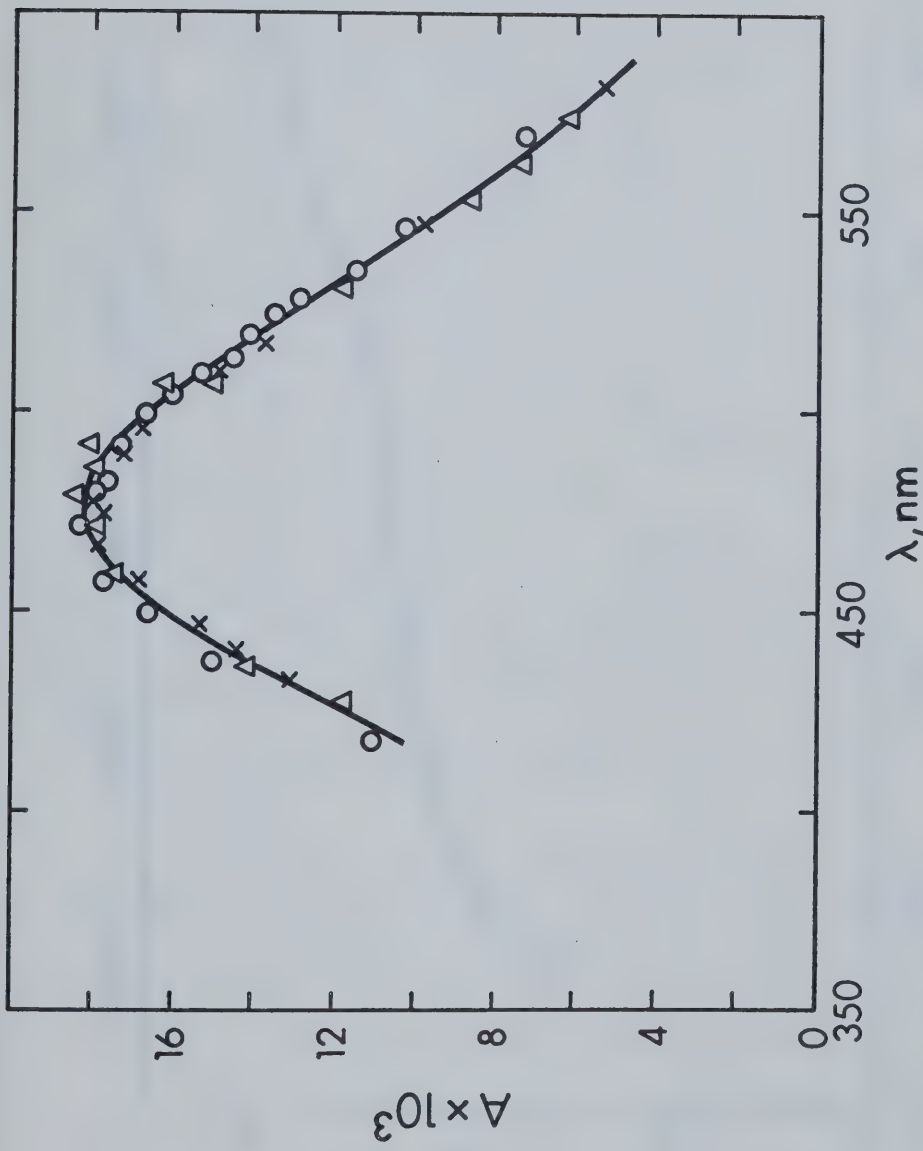


FIGURE III-47. The $(SCN)_2^-$ Absorption Spectrum in Water. Effect of Temperature. X, 295K; Δ , 307K; O, 332K.

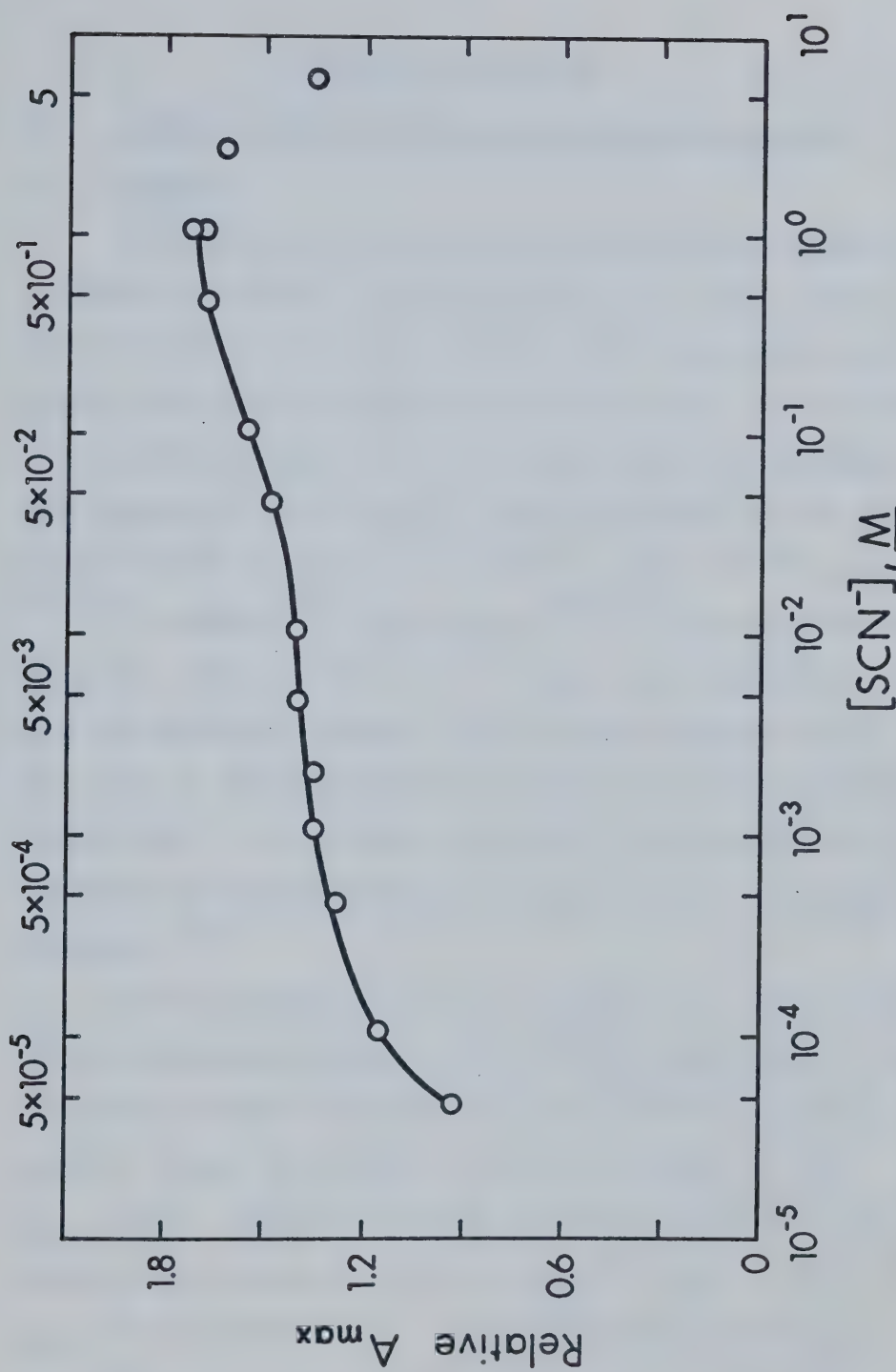


FIGURE III-48. The Effect of $[SCN^-]$ on Δ_{max} of $(SCN)_2^-$ in Aqueous Solution.

0.1 μ s Pulses, $295 \pm 1K$.

DISCUSSION

A. SOLVATED ELECTRON OPTICAL ABSORPTION SPECTRA

1. GENERAL

The solvated electron optical absorption spectrum in dilute solutions of alkali metals in liquid ammonia has been known for many years.¹⁸⁷ Over the past twelve years, the pulse radiolysis method has been used to generate solvated electrons in a wide variety of solvents. The absorption spectrum has been determined in the liquids water^{63,188}, alcohols^{30-32,64,65}, ethers^{72,73}, amines^{190,191}, ammonia¹⁹² and others.¹⁹³⁻¹⁹⁶ Representative data are shown in Table IV-1. There are similarities in all the observed spectra, the two most apparent being the lack of any resolvable structure, and the broadness of the band. It has been shown that the spectrum is independent of the method used to generate e_s^- in several solvents.¹⁸⁸

There are also dissimilar properties. The energy of the absorption maximum (E_{max}) varies from about 1.7 eV in water and many alcohols to about 0.5 eV in several ethers. There is, however, a marked grouping of the E_{max} values, depending on the type of compound.^{72b} The value of $W_{1/2}$ varies from 51% of E_{max} in water to 96% of E_{max} in ethylenediamine. It has been said that $W_{1/2}$ is approximately equal to 60% of the E_{max} .¹¹² The more

TABLE IV-1

Comparison of ϵ_s^- Spectral Data from Different Solvents

Solvent	T, K	λ_{max} , nm	E_{max} , eV	$W_{1/2}$, eV	$10^{-3} G \cdot \mathcal{E}_{\lambda_{\text{max}}}$ ^a	$10^{-3} \mathcal{E}_{\lambda_{\text{max}}}$ ^a	$G(\epsilon_s^-)_{\text{f1}}$	Ref.
Water	298	720	1.73	0.885	52.29	18.4(18.9)	2.8 ^b	63(65)
Heavy water	293	700	1.77	0.88	61.8	20.2	3.1	189
Methanol	294	635	1.95	1.3	20.4	10.2	2.0	65
	~298	630	1.96	1.29	18.7	17.0	1.1	64
Ethanol	296	688	1.80	1.4	16.0	9.4	1.7	65
	~298	700	1.77	1.55	15.0	15.0	1.0	64
n-Propanol	~298	740	1.67		13.0	13.0	1.0	64
n-Butanol	303	680	1.82	1.5	13.6			75
2-Methyl-2-butanol	303	1250	0.99	~0.8				75
Tetrahydrofuran	298	2100	0.59	0.43	15.6	40.0	0.39 ^c	72a
Diethyl ether	298	2050	0.54	0.43	11.6	40.0	0.29 ^c	72b
Dimethoxyethane	298	2050	0.60	0.50		34		72b
Diglyme	298	1915	0.65	0.58	7.5	30.0	0.25 ^c	72a
Diethyl amine	298	1900	0.65	0.58		20.0		190,191
Ethylene diamine	298	1360	0.91	0.876				192a (192b)
Ammonia	240	1550	0.80	0.39	49.0(40.0)			
Dimethyl sulfoxide	298	≥ 1500	0.83	~0.5 ^d			~1.8 ^e	193,194
HMPA ^f	298	2250	0.55	0.42	38	19	~2.0	195,196 (continued...)

FOOTNOTES TO TABLE IV-1

a Units of $G.\mathcal{E}$ are $(e_s^-/100 \text{ eV M cm})$

b Yield at pH = 9.5

c F. Y. Jou, Private communication

d Determined from a long extrapolation of the low energy side of the spectrum

e Assumed from anthracene scavenging results

f Data all from both alkali metal 196 and pulse irradiated 195 solutions.
HMPA = Hexamethylphosphine triamide.

extensive data now available indicate that this is not true in many solvents.

2. THE EFFECTS OF TEMPERATURE AND PRESSURE ON E_{\max}

Jortner¹¹² has said that the location of the maximum in the optical absorption of the electron is not very enlightening from the theoretical point of view. Nevertheless, most attempts to correlate data from different solvents with physical properties of the solvent have used E_{\max} .^{64-66,72,189,197} The determination of what solvent properties affect the spectrum, and how they do so, will be of benefit to future theoretical developments.

One of the first correlations was of E_{\max} to the dielectric constant (ϵ). It was shown that for the C_1 to C_3 alcohols and ethylene glycol, E_{\max} for the spectrum at room temperature varied linearly with ϵ .⁶⁴ This relation fails for higher normal and branched alcohols⁶⁶, as well as for water, liquid ammonia⁶⁴ and many other solvents. It also fails for methanol and ethanol when ϵ is changed in different ways.^{65,198}

Using the extreme temperature and pressure values from Tables III-1 and III-5, respectively, the ratio (16) has a value of 3.7 in ethanol and 4.0 in methanol.

$$\left(\frac{\Delta E_{\max}}{\Delta \epsilon} \right)_T \left/ \left(\frac{\Delta E_{\max}}{\Delta \epsilon} \right)_P \right. \quad (16)$$

This means that E_{\max} increases more rapidly when ϵ is increased by the application of pressure (constant T) than when ϵ is increased by lowering the temperature (constant P). The same is true in water, but the difference between the pressure and temperature effects is not as apparent.^{65,118} Since the relation between E_{\max} and ϵ is not linear for either pressure or temperature variation, the values obtained from (16) may vary depending on where the comparison is made. However, they are always greater than 1.0, which would be the result if E_{\max} depended only on ϵ .

Another physical property of the solvents which is affected by both pressure and temperature change is the density (ρ). There is not a direct correlation of E_{\max} to ρ either.

$$\left(\frac{\Delta E_{\max}}{\Delta \rho} \right)_T / \left(\frac{\Delta E_{\max}}{\Delta \rho} \right)_P \quad (17)$$

Again using the extreme values from Tables III-1 and III-5, the ratio (17) has values of 0.43 for ethanol and 0.65 for methanol. This shows that changing ρ by the application of pressure has less effect on E_{\max} than changing ρ by lowering the temperature. This is the opposite to the effect on E_{\max} of changing ϵ in the different ways, and suggests that the product of $\epsilon \cdot \rho$ might better correlate to E_{\max} . This is shown in Figure IV-1. There

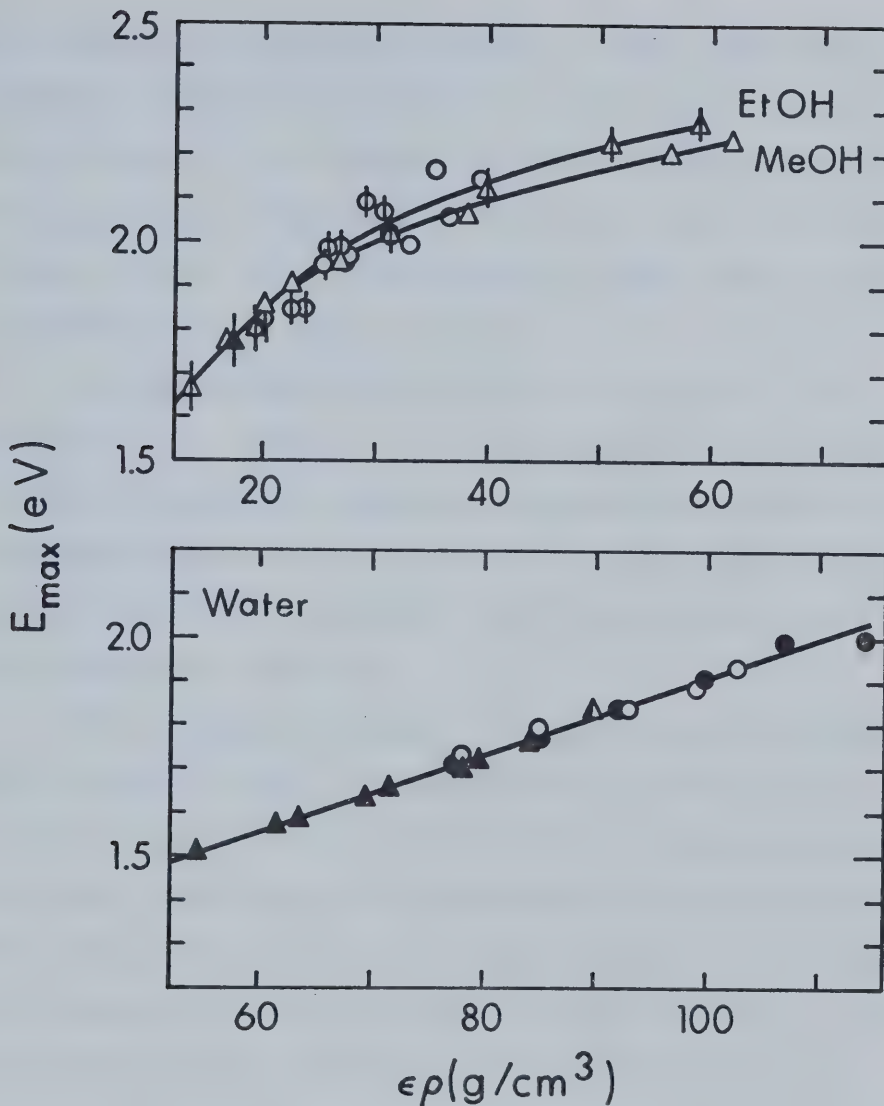


FIGURE IV-1. Plot of E_{\max} vs $\epsilon \cdot \rho$ for ethanol (\downarrow, ϕ), methanol (Δ, \circ) and water. Triangles are for temperature variation, circles are for pressure variation. \blacktriangle , ref. 67; \circ , ref. 115 for methanol and ethanol. \blacktriangle , ref. 134; \blacktriangle , ref. 63; \circ , ref. 115; \bullet , ref. 118 for water.

is still a fair amount of scatter in data from the alcohols, but the correlation is much improved over using either ϵ or ρ alone. For data from water $(\Delta E_{\max}/\epsilon \cdot \rho)_T / (\Delta E_{\max}/\epsilon \cdot \rho)_P = 1.0$ over the indicated range of $\epsilon \cdot \rho$. This is not meant to imply that no other properties affect E_{\max} in water.

No theoretical significance is given to the quantity $\epsilon \cdot \rho$. However, one may conclude that solvated electron excitation energies in hydroxylic solvents are determined as much by density, or by some other property of the media that correlates with the density, as by the dielectric constant.

The difference between the temperature and pressure effects on E_{\max} as indicated by (17) may be at least partly rationalized in terms of a simple physical picture. The electron is surrounded by dipoles, and the potential energy (E) is some function of the distance (r) between the electron and the dipoles, say r^{-x} . If r is decreased by increasing the pressure, then E increases. The value of r is proportional to $\rho^{-1/3}$, so E is proportional to $\rho^{x/3}$. Decreasing the temperature also decreases r , but at the same time the thermal agitation of the dipoles decreases. The dipoles are then able to line up more in the electric field of the electron, which further increases E . This amounts to

an increase in the "local" dielectric constant of the dipoles in the first solvation shell. Copeland, Kestner and Jortner ¹⁰² conclude that a major portion of dE_{max}/dT is due to this temperature effect. Since both temperature effects increase E , the effect of T should be greater than that of P for the same change in ρ . This was confirmed by observation.

Recent correlations of E_{max} to solvent properties have recognized the necessity of including the effect of the structure of the solvent ¹⁹⁷ and solvent molecules. ^{72,189} Freeman ¹⁹⁷ has illustrated the importance of solvent structure through the use of the Kirkwood correlation factor (g_k). ^{199,200} This factor indicates the extent to which molecules align themselves with their neighbors to create short-range order. The importance of molecular structure was expressed by α_p' , which is the polarizability of the polar group in the solvent molecule. It was found that if the total molecular polarizability (α) was used, correlation among the alcohols and amines was destroyed. This indicates that the electron is mainly associated with the polar ends of the molecules and that the most important interactions have relatively short ranges. When E_{max} was plotted versus $\epsilon \cdot \rho \cdot g_k^3 \cdot \alpha_p'$, a smooth curve could be drawn through the values for a wide variety of solvents at many different temperatures and

pressures. The curve approached a plateau near the highest plotted value of E_{\max} of 2.3 eV. It was therefore speculated that an upper limit for E_{\max} in liquids might be about 2.5 eV. It would be interesting to see if a theoretical treatment could lead to the same result.

The importance of molecular structure was again emphasized by the spectra obtained in 25 different alcohols.¹⁸⁹ Spectra in the C_1 to C_{11} normal alcohols were remarkably similar. However, for alcohols with branched alkyl groups, the spectrum was very dependent on the size and position of the branch with respect to the OH group. This may reflect a steric hindrance towards the formation of cavities suitable for electron localization. The fact that E_{\max} and $W_{\frac{1}{2}}$ are nearly independent of carbon number in normal alcohols shows that the electron interacts mainly with the OH group in these solvents. This was recognized by the use of α_p in the previous correlation.

The effects of pressure on the e_s^- spectra in methanol and ethanol have been treated by application of the semicontinuum model.²⁰¹ The only experimental data available were E_{\max} , and in methanol, these were at least 0.1 eV low. The best fit was achieved by assuming four solvent dipoles ($N=4$) surround the cavity containing most of the electron charge. The

calculated values for E_{\max} were quite a bit low for $N=6$. Values for $\Delta E_{\max}/\Delta P$ of 0.10 and 0.057 eV/kb were predicted for ethanol and methanol, respectively, between 0 and 2 kb. These may be compared to the experimental values of 0.075 eV/kb for ethanol and 0.15 eV/kb for methanol. The model calculation could only fit the data by emphasizing short range interactions, which is consistent with the empirical evidence.

Future models, or improvements to existing ones, must have still less reliance on long range interactions. Also, allowance must be made for solvent structure, the importance of which has been demonstrated by its effect on E_{\max} .

3. THE EFFECTS OF TEMPERATURE AND PRESSURE ON $W_{1/2}$

The $W_{1/2}$ of the e_s^- spectrum in methanol and ethanol is not greatly affected by temperature changes. The data in Table III-1 indicate a broadening of about 0.2 eV in the spectrum in ethanol as the temperature is raised from 155 to 343K. Results for methanol and $\sim m$ M basic ethanol (Table III-2) are incomplete, but the trend appears to be similar. Within experimental uncertainty, there is no effect of KOH concentration on the shape of the spectrum in ethanol up to 0.1 M KOH. However, as shown in Table III-4, the $W_{1/2}$ is smaller in

1 M KOH solution, probably due to the influence of water introduced with the KOH. The $W_{\frac{1}{2}}$ of the e_s^- spectrum in binary solutions of ethanol and water has been shown to be strongly influenced by water.⁶⁷

As indicated in Table III-5, the $W_{\frac{1}{2}}$ in methanol and ethanol is increased by the application of high hydrostatic pressures, the increase amounting to about 0.1 eV/kb in both solvents. The broadening is much greater in proportion to the effect on ρ and ϵ than was apparent in the temperature study. The same is true in water^{115,118}, where pressure broadens the band by about 28% between 1 bar and 6.3 kb.¹¹⁸ There is little or no effect on $W_{\frac{1}{2}}$ in water over a wide range of temperature.⁶³

4. THE EFFECT OF TEMPERATURE ON $G_{fi} \cdot \epsilon_{\lambda_{max}}$ IN NEUTRAL

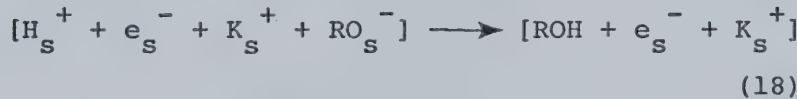
AND BASIC ALCOHOL

Values of $G_{fi} \cdot \epsilon_{\lambda_{max}}$ measured at different temperatures are given in Figure III-5 and Table III-3 for neutral and $\sim m$ M basic ethanol. Here, G_{fi} refers to solvated electron free ions. In neutral alcohol, $G_{fi} \cdot \epsilon_{\lambda_{max}}$ is independent of temperature, but it increases gradually in the basic solution. The same behavior has been observed in methanol.⁶⁵ The value for $G_{fi} \cdot \epsilon_{\lambda_{max}}$ is higher at all temperatures in the basic

alcohols due to a larger G_{fi} .

Free ion yields under different conditions have been estimated from earlier studies ^{43,44,92,202} with the aid of model calculations. ^{44,202} A value of 1.7 for G_{fi} in neutral ethanol was used at $295 \pm 2K$. ^{43,44,92,93,124,203} Values for $\epsilon_{\lambda_{max}}$ are given in Table IV-2. Extrapolation of $G_{fi} \cdot \epsilon_{\lambda_{max}}$ to higher temperatures was made when necessary. Results for methanol ⁶⁵ are included in the table for comparison purposes. A G_{fi} of 2.0 at $295 \pm 2K$ was used. ^{92,203-205}

In basic solution, the G_{fi} was enhanced by the scavenging of radiolytic cations in the spurs. The square brackets in (18) indicate that the species are within a spur.



where RO^- is either HO^- or an alkoxide ion. There is no reaction between e_s^- and K_s^+ , so (18) is followed by (19).



The average increase in the free ion yield in $\sim mM$ basic solution was 0.3 G units, as estimated by comparison with nitrous oxide scavenger studies in the manner described

TABLE IV-2

The Estimation of $\mathcal{E}_{\lambda_{\max}}$ in Ethanol and Methanol 65

T, K	$10^{-3} \cdot G_{fi} \mathcal{E}_{\lambda_{\max}}^a$	G_{fi}	$10^3 \cdot \mathcal{E}_{\lambda_{\max}} \text{, M}^{-1} \text{ cm}^{-1}$
Ethanol, neutral			
161	15	1.8	8.3
298	15	1.7	8.8
363	15	1.6	9.4
Ethanol, ~mM KOH			
161	20	2.0	10.0
298	20	2.0	10.0
363	21	2.2	9.5
418	22	2.3	9.6
Methanol, neutral			
176	19	1.9	10.0
298	19	2.0	9.5
423	19	1.9	10.0
Methanol, ~mM KOH			
176	23	2.2	10.5
298	23	2.2	10.5
423	25	2.3	10.9

^a Units are ($e_s^- / 100 \text{ eV M}^{-1} \text{ cm}^{-1}$).

in reference 65.

Within experimental uncertainty, the value of $\mathcal{E}_{\lambda_{\max}}$ is independent of both temperature and $\sim m\text{M}$ KOH in both alcohols. In ethanol $\mathcal{E}_{\lambda_{\max}} = (9.4 \pm 0.4) 10^3 \text{ M}^{-1} \text{ cm}^{-1}$, which is considerably lower than the previous estimate of $15 \times 10^3 \text{ M}^{-1} \text{ cm}^{-1}$.⁶⁴ There is no disagreement about the value of $G_{fi} \cdot \mathcal{E}_{\lambda_{\max}}$. The difference arises from the values of G_{fi} . To obtain the higher $\mathcal{E}_{\lambda_{\max}}$, a G_{fi} of 1.0 was used.^{45,64,95,174,206,207} This low value could easily arise from use of alcohol which contained an electron scavenging impurity. The value of $\mathcal{E}_{\lambda_{\max}} = (10.2 \pm 0.4) 10^3 \text{ M}^{-1} \text{ cm}^{-1}$ in methanol is lower than the previous estimate of $17 \times 10^3 \text{ M}^{-1} \text{ cm}^{-1}$ for the same reason as cited above. An indirect estimate of $\mathcal{E}_{\lambda_{\max}}$ in the alcohols can be made from knowledge of the oscillator strength (f), as will be discussed.

5. THE EFFECTS OF PRESSURE ON A_{\max}

There is a difference in magnitude between the effect of pressure on A_{\max} in the alcohols and water. In both methanol and ethanol, increasing the pressure causes A_{\max} to decrease substantially. In water, the decrease in A_{\max} is much less.^{115,116,118} If G_{fi} and $\mathcal{E}_{\lambda_{\max}}$ are not affected by pressure, the observed A_{\max} should in fact increase due to the increase in absorbed dose with increased solvent density. Since this did not

occur in water, either G_{fi} or $\epsilon_{\lambda_{max}}$, or some combination of these, must vary approximately as $1/\rho$. Steady state radiolysis results indicate G_{fi} is unaffected by pressure in water¹²³, so Hentz et.al. interpreted the constancy of A_{max} as being due to a decrease $\epsilon_{\lambda_{max}}$. An increase in $W_{\frac{1}{2}}$ compensates for the lower $\epsilon_{\lambda_{max}}$, resulting in little or no change in the oscillator strength.

In the alcohols, A_{max} decreases much more rapidly than it does in water for the same increase in pressure. As shown in Figure III-13, $dA_{max}/dP \approx -25\%$ per kb in methanol. Steady state results indicate that G_{fi} is unaffected, or even increases slightly, with increasing pressure in methanol¹²⁵ and ethanol.¹²⁴ By analogy to the conclusions of Hentz, since $A_{max} \propto G_{fi} \cdot \epsilon_{\lambda_{max}}$, a 25% per kb decrease in $\epsilon_{\lambda_{max}}$ would explain the observed behavior. However, there is a further possibility which cannot be ignored. There may also be a redistribution of the energy states of e_s^- . If pressure causes a relative increase in the population of states which give rise to absorption on the wings of the absorption curve, then the observed increase in $W_{\frac{1}{2}}$ can be explained. If this increase occurs at the expense of states represented by E_{max} , then both the pressure independence of G_{fi} and dA_{max}/dP can be rationalized.

6. THE OSCILLATOR STRENGTH f OF THE e_s^- OPTICAL
ABSORPTION

The oscillator strength f is defined as the ratio of the observed integrated absorption coefficient \mathcal{E} to the total value predicted by theory (\bar{A}).²⁰⁸

$$f = \frac{1}{\bar{A}} \int \frac{\mathcal{E}}{\bar{v}} d\bar{v} \quad (20)$$

The value of $\frac{1}{\bar{A}}$ is $4.32 \times 10^{-9} \text{ M cm}^2$, and the integral is the area under the absorption curve when it is plotted as \mathcal{E} versus wavenumber (\bar{v}). The area has units of $\text{M}^{-1} \text{ cm}^{-2}$, so that f is unitless. A correction for the refractive index (n_o) of the medium should also be applied, as shown in (21).^{1b}

$$f = 4.32 \times 10^{-9} \frac{\frac{9n_o}{(n_o^2 + 2)^2}}{\int \mathcal{E} \frac{d\bar{v}}{\bar{v}}} \quad (21)$$

Reported oscillator strengths for e_s^- vary depending on the value used for \mathcal{E} , and whether or not the refractive index correction was applied.⁶⁵ Usually a large extrapolation of the absorption band is necessary to determine the integral.

a. The Relative f for e_s^- in Various Solvents

The f is directly proportional to $\int \mathcal{E} \frac{d\bar{v}}{\bar{v}}$, and

the integral can be approximated as shown in (22).

$$\int \mathcal{E}_v^{-d\bar{v}} \approx W_{\frac{1}{2}} \cdot \mathcal{E}_{\lambda_{\max}} \quad (22)$$

This relation has been used to obtain the relative value for f in a variety of solvents. The results are compiled in Table IV-3. Excluding values for the alcohols and hexamethylphosphoric triamide (HMPA), the average product of $W_{\frac{1}{2}} \cdot \mathcal{E}_{\lambda_{\max}}$ is $(139 \pm 5) \cdot 10^6 \text{ M}^{-1} \text{ cm}^{-2}$. This indicates that f is remarkably constant considering the variety of workers, solvents and methods used to obtain the results.

Two values are given for each of the alcohols, the difference in them being entirely due to a difference in the value of G_{fi} used. Using the average $W_{\frac{1}{2}}$ reported for each alcohol, and $139 \times 10^6 \text{ M}^{-1} \text{ cm}^{-2}$ for $W_{\frac{1}{2}} \cdot \mathcal{E}_{\lambda_{\max}}$, give values of $\mathcal{E}_{\lambda_{\max}}$ of $13.3 \times 10^3 \text{ M}^{-1} \text{ cm}^{-1}$ for methanol and $11.7 \times 10^3 \text{ M}^{-1} \text{ cm}^{-1}$ for ethanol. Values for G_{fi} can then be calculated from known values of $G_{fi} \cdot \mathcal{E}_{\lambda_{\max}}$. The results predict a G_{fi} of 1.5 in methanol and 1.4 in ethanol. These values are intermediate to the ones most often reported in the literature, so do not provide a basis for a choice of either the higher or the lower values. It does indicate that additional work is necessary to resolve the discrepancy.

TABLE IV-3

Comparison of $W_{\frac{1}{2}} \cdot \mathcal{E}_{\lambda_{\max}}$ for the e_s^- Spectrum in a Variety of Solvents^a

Solvent	$W_{\frac{1}{2}}$, eV	$W_{\frac{1}{2}}$, cm^{-1}	$10^{-3} \cdot \mathcal{E}_{\lambda_{\max}}, \text{M}^{-1} \text{cm}^{-1}$		$10^{-6} \cdot W_{\frac{1}{2}} \cdot \mathcal{E}_{\lambda_{\max}}, \text{M}^{-1} \text{cm}^{-2}$
			$W_{\frac{1}{2}}$, cm^{-1}	$10^{-6} \cdot W_{\frac{1}{2}} \cdot \mathcal{E}_{\lambda_{\max}}, \text{M}^{-1} \text{cm}^{-2}$	
Water	0.885	7,140	18.4 (18.9)		131 (135)
Heavy Water	0.88	7,100	20.2		142
Methanol	1.3	10,500	10.2		107
	1.29	10,400	17.0		177
Ethanol	1.4	11,300	9.4		104
	1.55	12,500	15.0		188
Tetrahydrofuran	0.43	3,450	40.0		138
Diethyl ether	0.43	3,500	40.0		140
Dimethoxyethane	0.50	4,050	34.0		138
Diglyme	0.58	4,650	30.0		140
Diethylamine	0.58	4,680	30.0		140
Ethylenediamine	0.876	7,070	20.0		141
Ammonia	0.39	3,150	49.0 (40.0)		154 (126)
HMPA	0.42	3,390	19		64

a References are the same as in Table IV-1

In HMPA values for both $W_{1/2}$ and $\epsilon_{\lambda_{\max}}$ are uncertain, so a comparison with the relative f obtained in other solvents would not be meaningful.

b. The Effects of Temperature and Pressure on $W_{1/2} \cdot \epsilon_{\lambda_{\max}}$ in Methanol and Ethanol.

Theoretical calculations predict a small decrease in the free ion yield with increasing temperature.^{202,204} Experimental results show very little change in solvated electron yields over the range of temperature being considered in water^{63,209}, methanol²⁰⁴ and ethanol.²⁰² Therefore, in view of the fact that the value of $G_{fi} \cdot \epsilon_{\lambda_{\max}}$ is constant with temperature in the neutral liquids, (references 63, 65 and Figure III-5) $\epsilon_{\lambda_{\max}}$ either increases slightly or remains the same as the temperature increases. This is shown by the values listed in Table IV-4. In the alcohols, there is also an increase in the value of $W_{1/2}$ as the temperature is raised. The product $W_{1/2} \cdot \epsilon_{\lambda_{\max}}$ therefore increases with temperature.

The effect of pressure on the value of $W_{1/2} \cdot \epsilon_{\lambda_{\max}}$ is greater in the alcohols than is the effect of temperature, for similar changes in the physical properties of the bulk solvent. In water, the apparent decrease in $\epsilon_{\lambda_{\max}}$ is compensated for by an increased half-width as

TABLE IV-4

The Effect of T on $W_{1/2} \cdot \mathcal{E}_{\lambda_{\max}}$ in Alcohols and Water

T, K	$W_{1/2}^a$, eV	$10^{-3} \cdot W_{1/2}$, cm^{-1}	$10^{-3} \cdot \mathcal{E}_{\lambda_{\max}}$, $\text{M}^{-1} \text{cm}^{-1}$	$10^{-6} \cdot W_{1/2} \cdot \mathcal{E}_{\lambda_{\max}}$, $\text{M}^{-1} \text{cm}^{-2}$
<u>Methanol</u> ⁶⁵				
176	1.1	8.87	10.0	89
298	1.3	10.5	9.5	100
423	1.4	11.3	10.0	113
<u>Ethanol</u>				
161	1.3	10.5	8.3	87
298	1.4	11.3	8.8	99
363	1.5	12.1	9.4	113
<u>Water</u> ⁶³				
269	0.855	6.9	18.2	126
298	0.855	6.9	18.4	127
343	0.855	6.9	19.1	132

^a Extrapolated from reported values where necessary.

the hydrostatic pressure is increased. As a result, the oscillator strength seems to be independent of pressure in water, as shown by the data in Table IV-5.

In methanol and ethanol, the large decrease in the value of $W_{1/2} \cdot \epsilon_{\lambda_{\max}}$ with increasing pressure is due to a rapid drop in $\epsilon_{\lambda_{\max}}$. Although the $W_{1/2}$ increases at the same time, it is not enough to compensate. Application of the semicontinuum model to the solvated electron spectrum predicted a decrease in the oscillator strength with increasing pressure.²⁰¹ However, the predicted decrease of about 2% per kb is much less than the observed drop of about 20% per kb.

7. THE EFFECT OF ADDED WATER ON THE e_s^- OPTICAL ABSORPTION SPECTRUM IN ETHANOL

The values of E_{\max} for the e_s^- absorption spectrum is nearly the same in ethanol (1.8 eV) and water (1.73 eV) at 298K. Within experimental error, E_{\max} does not change in different mixtures of these two solvents.⁶⁷ However, the value of $W_{1/2}$ decreases rapidly towards the value in pure water as the water content of the mixture increases. This is accompanied by an increase in the maximum absorbance, as shown in Figure III-15. The increase is initially rapid, then more gradual, as the water content of the mixture is increased. Above about

TABLE IV-5

The Effect of P on $W_{\frac{1}{2}} \cdot \mathcal{E}_{\lambda_{\max}}$ in Alcohols and Water

P, kb	$W_{\frac{1}{2}}$, ev	$10^{-3} \cdot W_{\frac{1}{2}}$, cm^{-1}	$10^{-3} \mathcal{E}_{\lambda_{\max}}$, $\text{M}^{-1} \text{cm}^{-1}$ ^b	$10^{-6} W_{\frac{1}{2}} \cdot \mathcal{E}_{\lambda_{\max}}$, $\text{M}^{-1} \text{cm}^{-2}$
<u>Methanol</u>				
0	1.3 ₆	11.0	10.2	112
1	1.4 ₅	11.7	7.7 ^{b1}	90
2	1.5 ₄ ^a	12.4	5.5 ^{b1}	68
<u>Ethanol</u>				
0	1.4	11.3	9.4	106
1	1.5	12.1	7.1 ^{b2}	86
2	1.7	13.7	5.3 ^{b2}	73
<u>Water</u> ¹¹⁸				
0	0.81	6.5	18.4 ^{b3}	120
1.1	0.87	7.0	17.9	125
2.13	0.89	7.2	17.3	125
6.26	1.04	8.4	15.1	127

^a Extrapolated from values in Table III-5.

^b Calculated assuming G_{fi} at E_{\max} is pressure independent

¹ from data in Figure III-13. ² Relative to dA_{\max}/dp in methanol using data in Figures III-9, 10 and 13. ³ 1 bar

value from reference 63 was used to calculate $\mathcal{E}_{\lambda_{\max}}$ from separated values of A_{\max} .

1% by weight of water, the increase in absorbance is linear when absorbance is plotted versus the weight percent of water.

As a test of the possible solvent independence of the oscillator strength, it would be valuable to determine values of f in water-alcohol mixtures. This is only possible if the value of G_{fi} is known. Two studies, one using pulse radiolysis⁶⁷ and one using steady state radiolysis²⁰⁷, have been conducted to determine G_{fi} in water-ethanol solutions. In the former study, biphenyl was used to scavenge e_s^- ($k_5 = 4.3 \times 10^9 \text{ M}^{-1} \text{ s}^{-1}$ in ethanol at 298K).⁸⁹ The absorbance of the biphenyl negative ion was used to calculate G_{fi} . The assumptions made were that the absorptivity of the biphenyl ion is the same in the mixtures as in pure ethanol, that all of $e_{s,fi}^-$ and only $e_{s,fi}^-$ are scavenged, and that G_{fi} in pure ethanol is 1.0. The latter two assumptions at least could be incorrect. Biphenyl is only slightly soluble in water, a saturated solution at 298K being $4.9 \times 10^{-5} \text{ M}$.^{167a} In ethanol, a saturated solution is 0.59 M in biphenyl at 294K.^{167b} A scavenger concentration of the order of 10^{-3} M would be necessary to scavenge all the free ions. It is possible that the solubility of biphenyl is not that high in water rich mixtures of ethanol and water. Even if solubility is not a problem, it is likely that biphenyl is selectively

solvated by alcohol molecules. It is evident from values of $W_{1/2}$ and A_{max} that electrons are selectively solvated by water. Therefore, the efficient scavenging of e_s^- by biphenyl would be impeded in the mixed solvent.

The effects of electron scavengers on the stable product yields were used to estimate G_{fi} in a steady state radiolysis study. Hydrogen, nitrite, acetaldehyde, 2,3-butanediol and hydrocarbon yields were measured after radiolysis of ethanol-water mixtures containing lithium nitrate. Extrapolation of the plotted data gave values of G_{fi} of 2.75 in pure water and 0.9 - 1.2 in pure ethanol. The former agrees well with the accepted free-ion yield in water, while the latter would support a G_{fi} of 1.0 in ethanol. However, extrapolation to the low value in pure ethanol depended on only one result, at 0.3 mole fraction water. All other results were at higher concentrations of water, and fell on a smooth curve which, if extrapolated to pure ethanol, would indicate a value of about 1.5 for G_{fi} . No experiments were done on solutions containing less than 0.3 mole fraction water, yet the largest effect on the e_s^- absorbance and spectrum half-width occur in more dilute solutions of water in ethanol. Therefore, the data from this study are least reliable in the concentration range where they are most needed.

Better values of G_{fi} in alcohol water mixtures

are needed, particularly at low water concentrations, before the oscillator strength for e_s^- absorption can be determined. Qualitatively, it seems that the rapid increase in the absorbance is compensated for by the decrease in the value of $W_{1/2}$ as the water content of the mixture is increased. Therefore, the oscillator strength does not change suddenly in the mixed solvent.

The large effect of low concentrations of water on the e_s^- spectrum in ethanol can be explained as scavenging of electrons by aggregates of water molecules. The result is a spectrum dominated more by water than would be predicted from the mole fraction of each solvent.

B. TEMPERATURE EFFECTS ON e_s^- REACTION KINETICS

1. GENERAL

Kinetic data over a range of temperature can usually be represented by use of an empirical equation (I-24) proposed by Arrhenius. The values found for the Arrhenius activation energy (E_a) and the frequency factor (A) are useful in obtaining an understanding of those things which determine the reaction rate.

Most temperature dependent kinetic data for solvated electron reactions have been determined in water. Many of the reported activation energies have values of 3.5 ± 0.5 kcal mol⁻¹.^{110,130} The rate constants for these

reactions vary from that calculated for a diffusion controlled reaction ($\sim 10^{10} \text{ M}^{-1} \text{ s}^{-1}$) to that for the first order decomposition reaction (890 s^{-1}). Reactions with rates near the diffusion controlled limit will have an observed activation energy equal to the activation energy required for diffusion. This is from 3 to 4 kcal mol⁻¹ for most solutes in water. However, for slower reactions, the observed activation energy should represent the actual energy barrier of the reaction.

Anbar¹³⁰ believes that all solvated electron reactions in water have the same activation energy. Since it is unlikely that a constant E_a arises from identical energy requirements of a transition state when many different substrates are involved, he attributes the constance of E_a to an intrinsic energy requirement of the solvated electron.

Cercek^{131,210} takes exception with this view. He reports values of E_a which vary from 1.65 to 4.5 kcal mol⁻¹ for different substrates.¹³¹ His data indicate that e_s^- reactions having similar rate constants may have different activation energies. For example, $k(e_s^- + \text{NO}_2^-) = 3.4 \times 10^9 \text{ M}^{-1} \text{ s}^{-1}$, $E_a = 1.65 \text{ kcal mol}^{-1}$ and $k(e_s^- + \text{pyridine}) = 3.7 \times 10^9 \text{ M}^{-1} \text{ s}^{-1}$, $E_a = 4.5 \text{ kcal mol}^{-1}$. The rate constant for reaction with pyridine is higher than the previously reported value of

$1.0 \times 10^9 \text{ M}^{-1} \text{ s}^{-1}$.¹⁸¹ It was concluded on the basis of these data that solvated electron reactions in water do not have a constant energy of activation. Therefore, both the activation entropy and the activation enthalpy contribute to the determination of the reaction rate constant. To rationalize the very low values of E_a , it was postulated that hydrated electrons migrate between existing potential traps instead of through the creation of new holes, as in conventional diffusion.^{56,132}

Since there are inconsistencies in the data and their interpretation, more results are necessary. The use of solvents other than water might provide complementary data over a wider temperature range. The effect of solvent has recently been demonstrated for the reaction of electrons with biphenyl.²¹¹ In n-hexane, cyclopentane and iso-octane, the activation energies are respectively, 6.4, 4.2 and 0.51 kcal mol⁻¹. This indicates that the nature of the reaction of electrons with biphenyl is different in each solvent.

2. NEUTRAL AND ~mM KOH SOLUTIONS OF ETHANOL

Non-Arrhenius behavior for the solvated electron decomposition reaction was observed in both neutral and basic ethanol, as shown in Figure III-16. Similar results were found in methanol.¹⁴⁸ The data obtained in the basic solution can nearly be fitted by two straight

lines. The high temperature results indicate an activation energy of 4.8 kcal mol⁻¹, in good agreement with the value of 4.86 kcal mol⁻¹ found by Baxendale and Wardman³¹ over much of the normal liquid range of the solvent. However, below about 240K, an E_a of 2.5 kcal mol⁻¹ is indicated. This is lower than any of the activation energies found for e_s^- scavenging reactions, so cannot be attributed solely to an increasing importance of reaction (5) as the temperature decreases.

Another possible explanation is that the observed solvated electron absorption could have contained an increasing component due to faster decaying geminate ions as the temperature was lowered. Some geminate electron absorption was observed as an initial "spike", amounting to about 25% of the observed absorption immediately following a 0.1 μ s pulse at 180K in ethanol. It decayed rapidly, having a half-life of about 1 μ s at the temperature. First order plots were linear between 20 and at least 400 μ s following the pulse. This portion of the decay was attributed entirely to free ions. Vermeer and Freeman⁴¹ found that a nonhomogeneous kinetics treatment could explain a portion of the solvated electron absorption decay at times up to 80 μ s after the pulse in di-n-propyl ether at 149K. A long time contribution of the geminate neutralization reaction could not be confirmed using available data in ethanol.

Very long half lives ($>100 \mu\text{s}$) could not be measured with confidence with the spectrophotometer used, due to fluctuations in the analyzing light intensity with time. Because of this, and the reasons discussed above, a value of $4.8 \pm 0.2 \text{ kcal mol}^{-1}$ for E_a of reaction (4) in ethanol is recommended over the whole temperature range. This agrees well with a value of $4.6 \pm 1 \text{ kcal mol}^{-1}$ determined from steady state radiolysis.³⁷

3. THE REACTION OF e_s^- WITH SCAVENGERS

The activation energy data from Figures III-17 to 22 are summarized in Tables IV-6 and IV-7. Calculated values of the frequency factor are between 10^{10} and $10^{13} \text{ M}^{-1} \text{ s}^{-1}$. The lowest values are for the reaction of e_s^- with benzene or phenol. All reactions having a measured rate constant greater than $10^9 \text{ M}^{-1} \text{ s}^{-1}$ gave an activation energy of $3.0 \pm 0.3 \text{ kcal mol}^{-1}$, with the exception of acid in ethanol. This exception is not considered to be significant, since the difficulty encountered due to adsorption of H_s^+ onto the walls of the cells and reaction with the solvent at high temperature, could result in a 1 kcal mol^{-1} error.

The apparent constant value of E_a for efficient scavenging reactions in the alcohols implies that there is a common rate determining step, such as diffusion of the solvated electron.

TABLE IV-6
Summary of Arrhenius Activation Energy Data
for the Reaction of e_s^- with Scavenger

Scavenger	<u>Methanol as Solvent</u>	<u>$k_5^a, M^{-1} s^{-1}$</u>	<u>$\log_{10} A_5, M^{-1} s^{-1}$</u>	<u>$E_a, \text{ kcal mol}^{-1}$</u>
Acetone	4.3×10^9	11.7		2.7 ₄
Nitrobenzene	2.1×10^{10}	12.5		3.0
Naphthalene	3.0×10^9	11.9		3.2 ₄
Perchloric Acid	5.5×10^{10}	13.1		3.2
Benzene	1.2×10^6	10.8		6.4
Phenol	6.7×10^6	10.1		4.5

^a k_5 's at 295 \pm 3K

TABLE IV-7
Summary of Arrhenius Activation Energy Data
for the Reaction of e^- with Scavenger

Scavenger	$k_5^a, M^{-1} s^{-1}$	$\log_{10} A_5, M^{-1} s^{-1}$	$E_a, kcal mol^{-1}$
Acetone	4.9×10^9	11.9	3.0
Nitrobenzene	1.5×10^{10}	12.4	3.0
Naphthalene	4.2×10^9	12.0	3.2 ₄
Perchloric Acid	3.3×10^{10}	13.5	4.0
Benzene	6.4×10^6	11.2	6.0
Phenol	$5.0_5 \times 10^7$	10.9	4.4

^a k_5 's at 295 \pm 3K

For the less efficient solvated electron scavengers benzene and phenol, higher activation energies were found. The lower rate constant is largely due to the higher enthalpy of activation. A reaction of a nature different from that for efficient scavengers is indicated. One especially different result is the much larger effect of solvent. For efficient scavengers, the ratio of $k_{5,\text{EtOH}}/k_{5,\text{MeOH}}$ is less than one. For benzene and phenol the ratio is 5.3 and 7.5, respectively. In methanol the electron is more strongly localized than it is in ethanol. This is indicated by the E_{\max} values of 1.97 eV in methanol and 1.80 in ethanol at 295K. The difference in the binding energy may account for the slower reaction rate in methanol. Furthermore, the increase in E_{\max} with decrease in temperature in both alcohols could account for the higher temperature dependence of the rate constant.

4. OTHER EFFECTS OF BENZENE-SOLVATED ELECTRON REACTIONS

The yield of $e_{s,\text{fi}}^-$ is decreased in the alcohols when high concentrations of benzene are added. This effect is demonstrated by the data in Figure IV-2 and Table IV-8.

In the figure, the plotted points are for the relative absorbance immediately following a 0.1 μs electron pulse in benzene solutions of ethanol. They

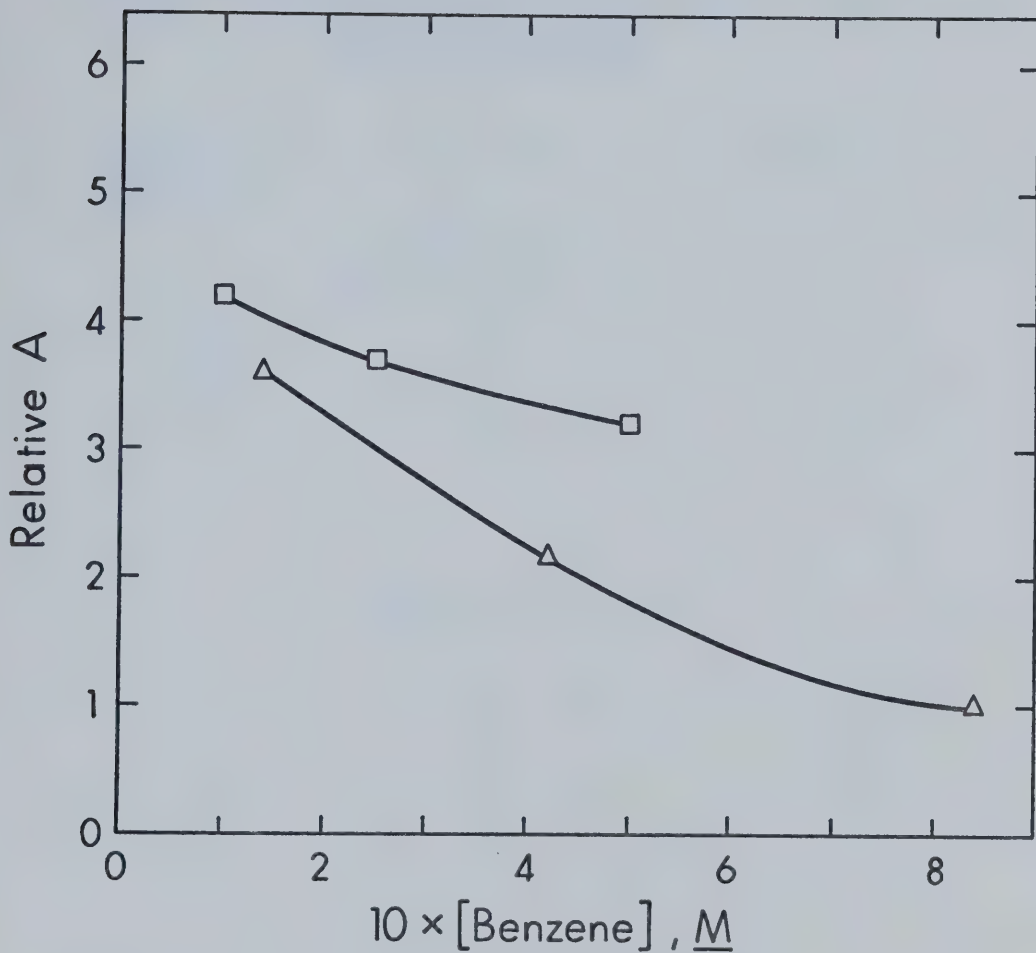


FIGURE IV-2. The Effect of Benzene Concentration on the e_s^- Absorbance. \square , 295K; Δ , 195K; 0.1 μ s pulses; 690 nm. Relative A in arbitrary units.

TABLE IV-8

The Effect of Benzene Concentration on the Absorbance in
Methanol and Ethanol

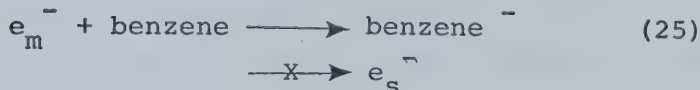
 M ^a	$t_{1/2}$, μ s	Relative A ^b
Methanol, 204 \pm 3K		
0.28	25	0.38
0.83	20	0.20
1.65	16	0.11
Ethanol, 195 \pm 1K		
0.14	29	0.36
0.42	17	0.21
0.84	17	0.10

^a Adjusted for change in solvent density.

^b Relative A at 602 nm in both solvents, in arbitrary units.

have been corrected for decay during the pulse. There is a monotonic decrease in the A as the concentration of benzene is increased which could not be due to the slow ($k_5 = 6.4 \times 10^6 \text{ M}^{-1} \text{ s}^{-1}$) reaction of benzene with solvated electrons. Ogura and Hamill²¹² have observed this effect in n-propanol and ethanol. It has been attributed to scavenging of mobile (e_m^-) or "dry" (e_s^-) electrons which are the precursors of e_s^- (23).²¹²⁻²¹⁴

The data in Table IV-8 are especially interesting, and clearly demonstrate that two benzene-electron



reactions occur. At low temperatures, (24) becomes much less efficient, due to the increased binding energy of e_s^- . This is shown by the values of $t_{1/2}$ of e_s^- given in the table. However, (25) is still efficient, as indicated by the pronounced effect of benzene concentration on the absorbance. Reaction (25) competes with (23) for the mobile electrons.

Similar effects were noted for both phenol and toluene in methanol and ethanol in this work. No quantitative treatment was attempted, as the effect was incidental to the $e_{s,fi}^-$ kinetic data desired.

Previous attempts to distinguish between solvated electrons and their precursors have generally made use of scavengers which are not as selective as benzene appears to be.^{13,215,216} An exception is the hydrogen ion which reacts with e_s^- , but not with its precursor.^{13,213,214} Benzene, and some of its derivatives, offer a way of obtaining less ambiguous results regarding electrons which are not fully solvated, particularly in systems where solvated free ions are not scavenged.

The effect of the solvated electron binding energy on the efficiency of the benzene scavenging reaction might be demonstrated by the e_s^- absorption spectrum. There should be preferential scavenging of the solvated electrons giving rise to absorptions on the low energy side of the spectrum, resulting in a slight decrease in the half-width of the band. This effect might be more evident at low temperature in the alcohols. It was not noted between 500 and 800 nm in n-propanol at room temperature.²¹²

It is unlikely that a sharp distinction can be made between species given symbols like e^- , e_m^- and e_s^- . The transitions between them are probably continuous. It is especially difficult to identify a distinction between e^- and e_m^- , if in fact any exists. These two terms are therefore used interchangeably here, although e_m^- is preferred.

C. PRESSURE EFFECTS ON e_s^- REACTION KINETICS

1. GENERAL

Laidler¹²⁷ has said, "Pressure studies provide at least as much insight into mechanisms as do temperature studies, and there is need for much more work in this field." This statement applies particularly well to the reactions of solvated electrons in polar solvents.

Experiments to study the effects of high hydrostatic pressure on the reaction kinetics of electrons solvated in water, methanol and ethanol have been conducted at two laboratories.^{115,118-126} The majority of the work done has utilized the steady state method, since there are experimental difficulties associated with the formation and fast detection of solvated electrons in solutions under high pressure. It is only recently that the desire for new kinetic information has spurred efforts in the area of pulse radiolysis at high pressure.^{115,119}

The effect of pressure on reaction rates is usually expressed in terms of the volume of activation (ΔV^\ddagger). This quantity can be calculated from observed rate constants at two different pressures using (7). In steady state radiolysis, values for a rate constant cannot be determined absolutely. Rather, a ratio of rate constants is inferred from measurements of final product yields. It is therefore also impossible to obtain a

value of ΔV^\ddagger for a single reaction via the steady state radiolysis method. A difference in the volumes of activation for two competing reactions can be calculated from their rate constant ratio. The value of ΔV^\ddagger for one of the competing reactions must be either assumed or calculated from absolute reaction rates, before the other can be determined. Hentz et. al.¹²⁰ assumed that for a diffusion controlled reaction (5) in water, the activation volume could be approximated from the pressure dependence of viscosity in water. They calculated a value for ΔV^\ddagger of $1.6 \text{ cm}^3 \text{ mol}^{-1}$, which was applied to all diffusion controlled reactions of solvated electrons in water. Later, direct measurements of the effect of pressure on the rates of eleven presumably diffusion controlled reactions led to activation volumes of from -1.1 to $1.2 \text{ cm}^3 \text{ mol}^{-1}$ between 1 bar and 6.4 kb.^{119a} This indicates the original assumption was not strictly correct. However, the data do confirm that fast reactions of solvated electrons are rather insensitive to changes in pressure. Combining the pulse radiolysis results, and previous data from steady state radiolysis, yields a value of $-15.8 \text{ cm}^3 \text{ mol}^{-1}$ for the activation volume of the solvated electron decomposition reaction in water.

The volume of activation can be taken to be comprised of two components, one due to a volume change of the reactants themselves as they enter the transition

state, and the other due to a rearrangement of surrounding solvent molecules. The latter effect is large and negative where charged species are created, because of electrostriction. A large negative value for ΔV^\ddagger therefore implies a considerable contribution due to electrostriction.

The volume of activation is pressure dependent.^{1c,217} The amount of the dependency is difficult to predict. However, where electrostriction plays a role, the volume of activation becomes more positive with increasing pressure. This is connected with the fact that at high pressures, the compressibility of a solvent, and therefore the amount of its contraction around an electrical charge, is greatly reduced. When comparing data obtained over different pressure ranges, the pressure dependence of the activation volume must be considered.

2. THE EFFECT OF PRESSURE ON THE e_s^- DECOMPOSITION REACTION

a. Pure Neutral Methanol and Ethanol

The values of ΔV^\ddagger for the decomposition reaction of electrons solvated in methanol and ethanol were found to be -16.7 ± 0.5 and $-23.4 \pm 0.5 \text{ cm}^3 \text{ mol}^{-1}$, respectively. Within experimental error, there was no dependence on pressure between 1 bar and 2 kb, although the values at 2 kb fell below the line (Figure III-23). This could be interpreted as indicating the onset of a noticeable

pressure dependence.

A previously reported value for ΔV^\ddagger of $-16 \text{ cm}^3 \text{ mol}^{-1}$ between 1 bar and 3 kb for the e_s^- decomposition reaction in ethanol is not negative enough.¹¹⁵ The probable reason is that some electrons were scavenged by impurity. Fast reactions generally have an activation volume greater than $0 \text{ cm}^3 \text{ mol}^{-1}$, and the measured value would be the weighted sum of the activation volumes of all the $e_{s,fi}^-$ reactions occurring in the solution. Steady state results have been used to estimate a value of $-11 \text{ cm}^3 \text{ mol}^{-1}$ for the activation volume of the decomposition in methanol, averaged between 1 bar and 5.3 kb.¹²⁵ Results from this work indicate this value may not be negative enough.

The very large negative value for ΔV^\ddagger of reaction (4) in ethanol may be used as evidence of the solvent's purity, as explained below. The molar volume for solvated electrons in water has been found to be approximately $0 \text{ cm}^3 \text{ mol}^{-1}$.^{119a} Assuming an electrostriction contribution of $-3 \text{ cm}^3 \text{ mol}^{-1}$, one estimates $3 \text{ cm}^3 \text{ mol}^{-1}$ for the cavity volume of an electron in water. Due largely to the lack of knowledge of the molar volume of alkoxide ions, similar values cannot be calculated for the alcohols. However, by analogy to the water results, the cavity volume and the electrostriction effect will be assumed to approximately cancel each

other for the purpose of this discussion. The molar volume of the reacting alcohol molecule should increase slightly as the O-H bond stretches. Therefore, in the formation of the transition state, the largest negative volume contribution should be that due to electrostriction as the electronic charge becomes concentrated on the oxygen in the forming alkoxide ion. Theoretical treatments predict that the decrease in volume accompanying the development of a full electronic charge on a small spherical molecule is between 10 and $30 \text{ cm}^3 \text{ mol}^{-1}$, for most solvents (ref. 1c, p.165). It is not possible to determine how highly concentrated the charge has become in the transition state. However, a maximum contribution of $-30 \text{ cm}^3 \text{ mol}^{-1}$ would be expected even if the charge were fully developed on the oxygen atom in the transition state. This is unlikely, so one would expect less than the maximum electrostriction. The value of $-23.4 \text{ cm}^3 \text{ mol}^{-1}$ for ΔV^\ddagger in ethanol, although not necessarily due totally to electrostriction, is about as negative a value as can be easily rationalized. This implies that reactions having near zero or positive values of ΔV^\ddagger are not competing successfully for solvated electrons in the pure solvent.

b. The Effect of Base on ΔV^\ddagger of e_s^- Decomposition

The addition of base to alcohols normally increases the e_s^- yield and half life by reacting with the positive

ions formed during radiolysis, and possibly also removing some impurities originally present. In the case of methanol, the activation volume for e_s^- decomposition was made more negative by the addition of base, as shown in Figure III-24 and Table III-15. This is considered to be an indication that the methanol used contained some impurity, and that the true activation volume may be more negative than $-16.7 \text{ cm}^3 \text{ mol}^{-1}$.

Both the value of $t_{\frac{1}{2}}$ and the absolute value of the ΔV^\ddagger were initially decreased by the addition of base to the ethanol. The lowering of the e_s^- half-life is unusual, and is attributed to sample contamination, perhaps by the use of dirty KOH for these samples. The more concentrated base solutions gave a longer half-life for e_s^- than was observed in the neutral solvent, which is as expected. The pertinent fact is that even when the half-life increased, the value of ΔV^\ddagger remained less negative than that found in the neutral solvent. This is further evidence for the purity of the ethanol used in this work.

c. The Effect of Water on ΔV^\ddagger of e_s^- Decomposition in Ethanol

The addition of water to ethanol caused ΔV^\ddagger for the solvated electron decomposition reaction to become less negative. There was also a large effect of pressure

on ΔV^\ddagger at low pressures, as shown in Figure III-26 and Table III-17. This was due, at least in part, to the occurrence of an efficient scavenging reaction. As the pressure increased, the rate of the scavenging reaction would decrease, corresponding to a positive activation volume. At the same time, the rate of the decomposition reaction would be increasing, so that it would compete more favourable for electrons at the higher pressure.

The small positive value for ΔV^\ddagger in "pure" water was due to reaction of e_s^- with impurities in the water.

3. THE EFFECT OF PRESSURE ON THE SCAVENGING OF e_s^-

The data illustrating the pressure dependence of the rate of reaction (5) for nine different solutes in methanol and ethanol are summarized in Table III-27. Within experimental error, all the reactions studied which have a $k_5 > 10^7 \text{ M}^{-1} \text{ s}^{-1}$ are characterized by a value of ΔV^\ddagger which is $\geq 0.0 \text{ cm}^3 \text{ mol}^{-1}$. Only toluene and benzene react with solvated electrons via a scheme which results in a substantial decrease in volume as the reactants enter the transition state. This is difficult to understand unless the transition state is assumed to be very near to a benzene negative ion, and occupies much less volume than did the benzene molecule. This can be rationalized by considering two effects. First, electrostriction around the forming benzene ion would result

in some volume decrease. Second, the benzene molecule may occupy a larger volume in alcohol solutions than would be expected from its molar volume in the pure liquid. If benzene occupies a small cavity in alcohol solutions, the collapse of the cavity on entering the transition state would also contribute a volume decrease. The slightly endothermic heat of solution of benzene in methanol and ethanol ($0.36 \text{ kcal mol}^{-1}$ at infinite dilution²²⁴) might indicate an energy requirement of cavity formation.

A limited amount of data are available from steady state radiolysis^{124,125} for comparison of the effects of pressure on efficient e_s^- scavenging reactions with the results of this work. A summary is presented in Table IV-9. The activation volumes from the γ radiolysis studies were determined by assuming values for ΔV^\ddagger of the e_s^- decomposition reaction to be -14.4 and $-11 \text{ cm}^3 \text{ mol}^{-1}$ in ethanol and methanol respectively. While these values may seem too positive when compared to the results reported in this thesis, allowance must be made for the fact that the former data were averaged between 1 bar and 5.3 kb. The latter data were determined between 1 bar and 2.0 kb. A pressure dependence of the activation volume is expected. The agreement among the tabulated data is satisfactory.

The results listed in Table III-27 indicate that,

TABLE IV-9

Comparison of ΔV^\ddagger Data from Pulse Radiolysis and
Steady State Radiolysis Studies

Scavenger	$T = 295 \pm 2\text{K}$	ΔV_p^\ddagger , $\text{cm}^3 \text{mol}^{-1}$	ΔV_γ^\ddagger , $\text{cm}^3 \text{mol}^{-1}$
<u>Ethanol</u>			
Nitrobenzene		+ 5.2 \pm 1	+ 7.5
Acetone		+ 4.4 \pm 1	+ 5.1
Naphthalene		+ 7.3 \pm 1	+ 5.6
H_s^+		+ 5.9 \pm 1	+ 4.3 - 4.6
<u>Methanol</u>			
Nitrobenzene		4.7 \pm 1.4	$\sim + 4$
Acetone		3.1 \pm 1.5	$\sim + 4$

^a Pulse radiolysis, reported in this work (Table III-27).

^b γ radiolysis results from ref. 124 (EtOH) and 125 (MeOH).

ΔV^\ddagger 's are averaged values between 1 bar and 5.3 kb, calculated by assuming ΔV^\ddagger for the e_s^- decomposition reaction is $-14.4 \text{ cm}^3 \text{mol}^{-1}$ in EtOH and $-11 \text{ cm}^3 \text{mol}^{-1}$ in MeOH.

in general, the activation volume for a particular solvated electron-scavenger reaction is more positive in ethanol than in methanol. The magnitude of the difference for fast reactions is, very roughly, $2 \text{ cm}^3 \text{ mol}^{-1}$. A correlation of this difference to the difference in magnitude of some physical property of the solvents could be enlightening.

The activation volume for viscous flow ($\Delta V_{\eta}^{\ddagger}$) has been determined from existing data.¹⁴³ It is $8 \text{ cm}^3 \text{ mol}^{-1}$ in ethanol¹²⁴ and $6 \text{ cm}^3 \text{ mol}^{-1}$ in methanol¹²⁵, averaged between 1 bar and 5.3 kb. The difference is in the right direction and of the right magnitude. It implies that the diffusion coefficient of solvated electrons in alcohols correlates with the viscosity. However, all the observed values of ΔV^{\ddagger} for reaction (5) are lower than $\Delta V_{\eta}^{\ddagger}$, so other factors might be involved. Jha and Freeman¹²⁵ expect $\Delta V_{\eta}^{\ddagger}$ to be about $2 \text{ cm}^3 \text{ mol}^{-1}$ greater than that for diffusion, based on the effects of pressure on diffusion of sodium picrate, sodium bromide and hydrogen bromide in methanol. This would lead to a better numerical correlation with the observed activation volumes for reaction (5).

D. REACTION RATE CONSTANTS (k_5) FOR e_s^- WITH GASEOUS SOLUTES IN WATER, METHANOL AND ETHANOL

The values of the absolute reaction rate constants for reaction of e_s^- with seven gaseous solutes are given

in Tables III-28 to III-45. These data, along with those from other pulse radiolysis and steady state radiolysis studies, are summarized in Tables IV-10 to IV-12. In most instances there is very good agreement between the values determined in this work, and those obtained by others. However, in some cases, they differ by a factor of up to two.

Where the rate constant is calculated from a ratio of rate constants, there are two major reasons for incorrect results. First, the rate constant used to solve the ratio might be incorrect. Second, an impurity reaction might also be competing for electrons. The latter reason would explain the different results from different studies for e_s^- scavenging by N_2O in methanol, when benzyl chloride (BzCl) is the competing scavenger (Table IV-11).

The compounds N_2O , SF_6 , O_2 , CO_2 and 1,3-butadiene are efficient scavengers of solvated electrons in water, methanol and ethanol. Acetylene and ethene are very poor scavengers, indicating a low reactivity of carbon-carbon double and triple bonds toward electrons. However, when double bonds are conjugated, as in 1,3-butadiene, the compound's electron affinity is increased. The difference between olefins and conjugated diolefins also shows up in electron mobility measurements. Electron mobilities in various olefins are $10^{-1} \pm 1$ square centi-

TABLE IV-10

Gaseous Solute Rate Constant Data Summary

Water, 295 \pm 3K					
Solute	$k_5, M^{-1} s^{-1}$ (This work)	$k_5, M^{-1} s^{-1} a$ (Other's work)	Ref.	Competing Scavenger and its $k_5, M^{-1} s^{-1}$	Ref. b
N_2O	$(7.9 \pm 0.4) 10^9$	8.67×10^9	48		
		5.6×10^9	218		
		12.9×10^9	219	H^+ , 2.2×10^{10}	88
		8.8×10^9	219	$(CH_3)_2CO$, 5.9×10^9	48
		15.9×10^9	219	CO_2 , 7.3×10^9	T.W
SF_6	$(9.8 \pm 0.4) 10^9$	1.65×10^{10}	7		
CO_2	$(7.3 \pm 0.4) 10^9$	7.67×10^9	48, 49		
		7.3×10^9	221	H^+ , 2.2×10^{10}	88
		3.6×10^9	219	N_2O , 7.9×10^9	T.W
1, 3-Butadiene	$(3.0 \pm 0.7) 10^9$	8×10^9	181		
Acetylene	$< 6.6 \times 10^6$				
Ethene	$< 6.1 \times 10^6$	$< 2.5 \times 10^6$	222		

a Where no competing scavenger is indicated, the result is from pulse radiolysis

b T.W. = This work

TABLE IV-11

Gaseous Solute Rate Constant Data Summary

Solute	$k_5, \text{M}^{-1} \text{s}^{-1}$		Ref.	Competing scavenger and its $k_5, \text{M}^{-1} \text{s}^{-1}$	Ref. ^c
	(this work)	(other's work)			
N_2O	$(6.1 \pm 0.4)10^9$	13×10^9	168	$\text{H}^+, 6.5 \times 10^{10}$	88
	$[(6.3 \pm 0.4)10^9]$	8.2×10^9	220	$\text{H}^+, 5.6 \times 10^{10}$	47
		6.2×10^9	47	$\text{BzCl}, 5.0 \times 10^9$	85
		14×10^9	169	$\text{BzCl}, 5.0 \times 10^9$	85
		6.7×10^9	154	$\text{BzCl}, 5.0 \times 10^9$	85
		4.1×10^9	174	$\text{SF}_6, 1.3 \times 10^9$	T.W.
SF_6	$(1.3 \pm 0.07)10^{10}$	2.0×10^{10}	174	$\text{N}_2\text{O}, 6.1 \times 10^9$	T.W.
	$[(1.2 \pm 0.03)10^{10}]$				
O_2	$(1.8 \pm 0.06)10^{10}$	1.9×10^{10}	89,147		
	$[(2.0 \pm 0.05)10^{10}]$		175		
CO_2	$(6.7 \pm 0.6)10^9$				
1,3-Butadiene	$(1.65 \pm 0.2)10^9$				
	$[(1.4 \pm 0.1)10^9]$				

(continued.....)

Table IV-11 (continued)

Solute	$k_5, \text{M}^{-1} \text{s}^{-1}$ ^a
	(this work)
Acetylene	$\underline{<3.4 \times 10^6}$
	$[<2.3 \times 10^6]$
Ethene	$\underline{<5 \times 10^5}$
	$[<1.2 \times 10^6]$

a Values in square brackets determined in basic solution.

b Where no competing scavenger is indicated, the result is from pulse radiolysis.

c T.W. = This work.

TABLE IV-12
Gaseous Solute Rate Constant Data Summary

Solute		$k_5, \frac{M}{s}^{-1} s^{-1}$ (this work)		$k_5, \frac{M}{s}^{-1} s^{-1}$ (other's work)		Ref.		Competing Scavenger and its $k_5, \frac{M}{s}^{-1} s^{-1}$		Ref. ^c	
N_2O		$(7.2 \pm 0.4)10^9$	8×10^9		172			$CH_3CHO, 4 \times 10^9$			44
		$[(5.7 \pm 0.7)10^9]$	6×10^9		44			$k_4 = 1 \times 10^5 s^{-1}$			T.W.
				4.2×10^9	202			$k_4 = 1 \times 10^5 s^{-1}$			T.W.
				6.8×10^9	174			$SF_6, 1.0 \times 10^{10}$			T.W.
SF_6		$(1.0 \pm 0.1)10^{10}$	1.1×10^{10}		174			$N_2O, 7.2 \times 10^9$			T.W.
		$[(9.6 \pm 0.5)10^9]$									
O_2		$(2.0 \pm 0.1)10^{10}$		1.9×10^{10}				$89, 147$			
				$[(1.5 \pm 0.05)10^{10}]$							
CO_2		$(4.9 \pm 0.7)10^9$									
1,3-Butadiene		$(2.9 \pm 0.2)10^9$									
		$[(2.4 \pm 0.1)10^9]$									
Acetylene		$\frac{<5}{[<2.9 \times 10^6]}$									

(continued,)

Table IV-12 (continued)

<u>Solute</u>	$k_5 \text{M}^{-1} \text{s}^{-1}$ a (this work)
Ethene	$\leq 1.7 \times 10^6$ $[\leq 2.2 \times 10^6]$

a Values in square brackets determined in basic solution.

b Where no competing scavenger is indicated, the result is from pulse radiolysis.

c T.W. = This work.

meters per volt second. However, in conjugated diolefins, electron mobilities could not be measured, presumably due to capture of the thermalized electrons by the dienes to form molecular negative ions.²⁶

E. THE EFFECT OF PULSE DOSE ON THE e_s^- HALF-LIFE ($t_{1/2}$)

The determination of the true solvated electron lifetime in a polar solvent is very difficult, and is never completely unambiguous. Progress is made by an upward revision of the lower limit of the value of $t_{1/2}$. This limit is governed by the reaction of e_s^- with electron scavenging impurities. Some impurities are present prior to irradiation. More are created by the radiation induced reactions which follow a pulse. Impurities which are initially present in the solvent can sometimes be reduced in concentration by rigorous purification. In the case of the ethanol used in this work, attempts at purification did not increase the value of $t_{1/2}$, indicating an initial high purity. The value of $t_{1/2}$ of e_s^- was increased in methanol treated with sodium metal and sodium borohydride, then distilled in an inert atmosphere.

There are two methods which can be used to overcome the problem of creation of electron scavenging impurities by the radiation. First, a dose study can be made, and the observed values of $t_{1/2}$ of e_s^- can then be

extrapolated to zero dose. Second, an additive which reacts with an electron scavenging impurity can be used to remove the scavengers before they can react with electrons. An example is base, which reacts with radio-lytically formed positive ions. Both the above methods were used to obtain the data given in Figures III-45 and III-46.

The data for both neutral and basic methanol extrapolate to a zero dose half-life of about 5.3 μ s at 295K. This is considerably longer than most previous values and therefore supports the value of 7 μ s reported by Baxendale and Wardman.³¹ For basic ethanol, a minimum value of 8.7 μ s is found for $t_{1/2}$ at 295K, in good agreement with the 9 μ s value recently reported³¹, and higher than the value of 6.0 μ s determined in a previous dose study.⁴³ However, extrapolation of the data from neutral ethanol to zero dose indicated a value of $t_{1/2}$ of about 11 μ s. A higher value for $t_{1/2}$ of e_s^- in neutral solution at zero dose would indicate some electron scavenging impurity was introduced with the sodium metal added to generate the ethoxide ion.

Further upward revisions for the $t_{1/2}$ of e_s^- are possible as purification techniques become more refined. Photolytically produced electrons may have a $t_{1/2}$ as long as 30 μ s in ethanol.²²⁴ While this value may be approached by pure radiolysis, a much longer $t_{1/2}$

for e_s^- in alcohols at room temperature is not expected.

If solvated electrons decayed by simple proton abstraction from the solvent in the absence of scavengers⁵⁶, the decay rate would increase with increasing acid strength of the solvent. Relative acid strengths are $H_2O \approx CH_3OH > CH_3CH_2OH > NH_3^{225}$, so on the above mentioned basis, the solvated electron half life in ethanol should be between that in water (0.28 ms) and in ammonia (~stable). This is not observed, indicating proton abstraction is not the decomposition scheme.

Reaction (4) is driven by the difference in solvation energy of the alkoxide ion and the electron:



**F. COMPARISON OF REACTION RATES OF e_s^- IN METHANOL
AND ETHANOL**

For reaction rates shown by solution of the Debye equation to be near the diffusion controlled limit, the ratio of the observed rate constants in ethanol and methanol is ~ 0.6 . This is consistent with the difference in the diffusion coefficient for solvated electrons ($D_{e_s^-}$) in the two solvents. Values for $D_{e_s^-}$ in ethanol and methanol are 0.8×10^{-5} and $1.55 \times 10^{-5} \text{ cm}^2 \text{ s}^{-1}$, respectively.⁹² In alcohol containing one percent by weight water, values for $D_{e_s^-}$ of $1.14 \times 10^{-5} \text{ cm}^2 \text{ s}^{-1}$ in ethanol and $1.64 \times 10^{-5} \text{ cm}^2 \text{ s}^{-1}$ in methanol have been reported.²²⁶

Vermeer and Freeman ⁴¹ have indicated that these values of $D_{e_s^-}$ may be about a factor of five low. As only the ratio of the diffusion coefficients is used, and this remains unchanged, the correlation made here would be unaffected by the higher values of $D_{e_s^-}$. Therefore, due to the difference in the diffusion coefficient for the solvated electron alone, the rate in ethanol should be about half that in methanol when diffusion is rate determining.

For slower reactions, the ratio $k_{5,\text{EtOH}}/k_{5,\text{MeOH}}$ is much greater than unity. That is, the reaction with solvated electrons proceeds faster in ethanol than in methanol. This is interpreted as being due to the electron being more tightly bound in methanol than in ethanol. Values for the rate constant ratio for the reaction of electrons solvated in ethanol or methanol with the same solute are given in Table IV-13. The trend in the ratio is illustrated in Figure IV-3. The dashed line on the figure is significant only in that it draws attention to the trend. The ratio of the rate constant for scavenging by phenol in methanol and ethanol fall well above the line. As wide a range as possible in reaction rates has been used. There are, unfortunately, no additional data from the literature which can be used in the table. Very few rate constants have been determined in both solvents by other workers.

TABLE IV-13

Comparison of k_5 in Methanol and Ethanol for a Variety of

Scavenger	Electron Scavengers			Ref. ^a
	$295 \pm 3K$	$k_5, M^{-1} s^{-1}$ (Ethanol)	$k_5, M^{-1} s^{-1}$ (Methanol)	
Cd _s ⁺⁺		$3.7_5 \times 10^9$	1.9×10^{10}	0.20
H _s ⁺		3.6×10^{10}	6.5×10^{10}	0.55
Nitrobenzene		1.5×10^{10}	$2.6_5 \times 10^{10}$	0.57
Carbon dioxide		4.9×10^9	6.7×10^9	0.73
Sulphur hexafluoride		1.0×10^{10}	1.3×10^{10}	0.77
Oxygen		2.0×10^{10}	1.9×10^{10}	1.05
Acetone		4.9×10^9	4.3×10^9	1.14
Nitrous oxide		7.2×10^9	6.1×10^9	1.18
Naphthalene		4.2×10^9	3.0×10^9	1.40
1,3-Butadiene		2.9×10^9	1.65×10^9	1.76
Ethyl acetate		5.3×10^7	2.2×10^7	2.41
Acetonitrile		3.3×10^8	8.6×10^7	3.84
o-Xylene		2.5×10^6	4.8×10^5	5.20
Benzene		6.4×10^6	1.2×10^6	5.33
Toluene		6.1×10^6	1.1×10^6	5.55
Phenol		$5.0_5 \times 10^7$	6.7×10^6	7.53

^a T.W. means this work. (P) and (T) means rate constants were determined in pressure and temperature cells, respectively.

^b G. L. Bolton, unpublished results.

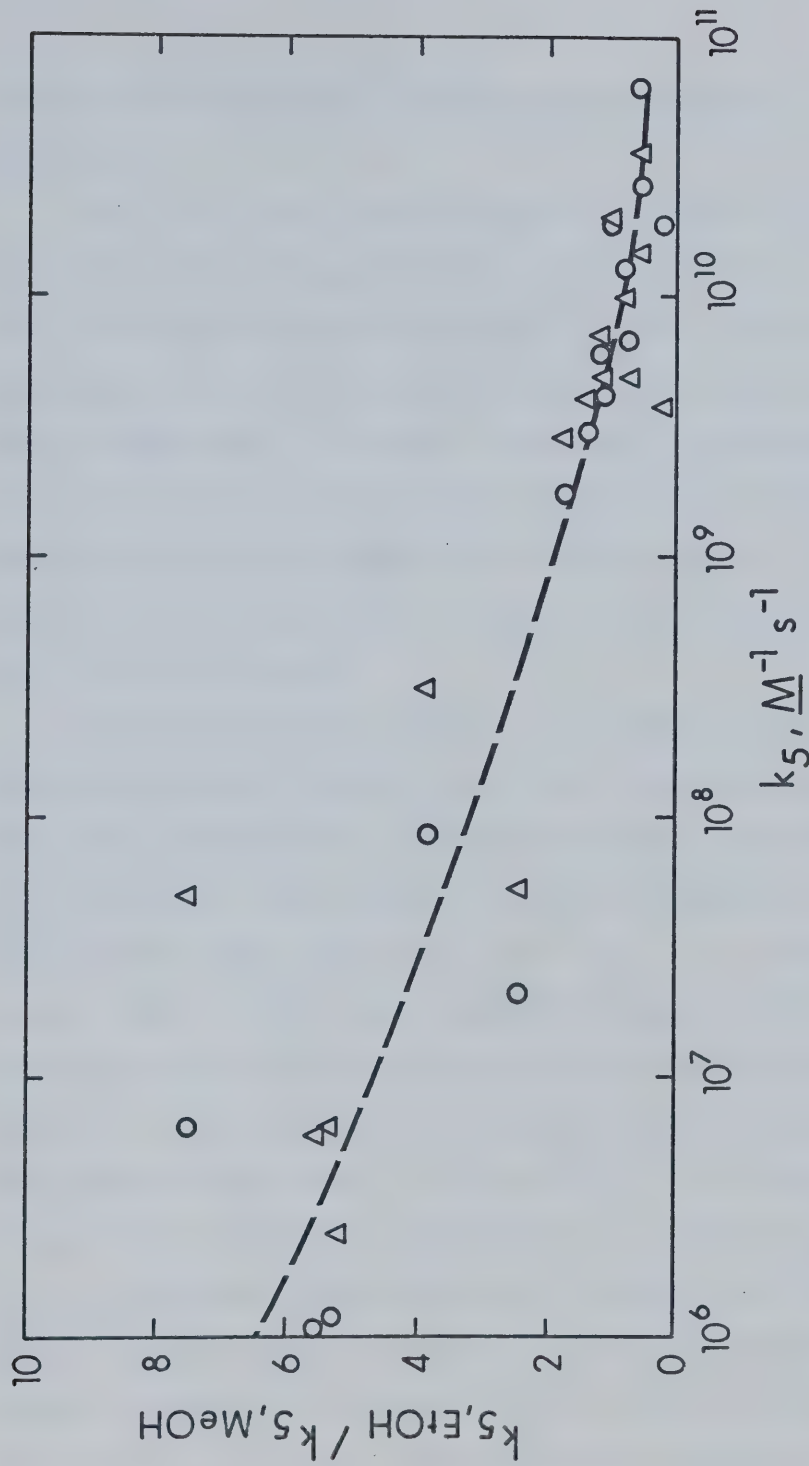


FIGURE IV-3. Comparison of ϵ_s^- Scavenging Reaction Rates (k_5) in Methanol (Δ) and Ethanol (\circ).

However, the data from this work are sufficiently illustrative.

An attempt was made to extend to water the correlation between rates and the effect of solvent. However, the reported rate constants in water for the slow reactions of solvated electrons are often high, probably due to impurities. To make a meaningful comparison, many of these rates should be redetermined in water. It would be a valuable comparison to make, since it could indicate the correct value of $D_{e_s^-}$ in the alcohols relative to that in water.

The lowest value in Table IV-13 is for a rate constant ratio where cadmium ion is the electron scavenger. The value of the rate constant in ethanol ($3.8 \times 10^9 \text{ M}^{-1} \text{ s}^{-1}$) seems low when compared to that in methanol ($1.9 \times 10^{10} \text{ M}^{-1} \text{ s}^{-1}$) and water ($5.0 \times 10^{10} \text{ M}^{-1} \text{ s}^{-1}$), and the actual value of the ratio should be larger. The rate constants were therefore redetermined in methanol and ethanol. The value for k_5 in ethanol was reproduced, but a lower value of $k_5 = 1.1 \times 10^{10} \text{ M}^{-1} \text{ s}^{-1}$ was found in methanol, resulting in a value of 0.3 for $k_{5,\text{EtOH}}/k_{5,\text{MeOH}}$. For both determinations in ethanol, and the second determination in methanol, a similar cadmium chloride concentration range ($10^{-5} - 10^{-4} \text{ M}$) was used. In methanol, the first study had used a cadmium chloride concentration range about a factor of ten lower than

did the second study. The rate constant in the more dilute solution of cadmium chloride in methanol was a factor of 1.7 higher than that in the more concentrated solution. Both the concentration dependence, and the greater than expected effect of solvent on the rate constant, are due to the incomplete dissociation of CdCl_2 . The dependence of the rate constant on the cadmium chloride concentration has previously been noted in water ¹⁴, but at much higher concentrations of cadmium chloride. In the case of water, concentrations of 0.1 to 0.5 M cadmium chloride were used, and the rate constant for electron scavenging varied with the cadmium salt concentration. Species coexisting in solution were Cd^{++} , CdCl^+ , CdCl_2 and CdCl_3^- .²²⁷ The three species containing chloride would not scavenge electrons as efficiently as the doubly charged cadmium ion.

A value of about 0.6 would be expected for $k_{5,\text{EtOH}}/k_{5,\text{MeOH}}$ if the reaction of electrons with Cd^{++} was assumed to be diffusion controlled. The values found for the ratio indicate that Cd^{++} is in two to three times higher concentration in methanol than in ethanol for about the same concentration of dissolved cadmium chloride. The difference is due to the higher dielectric constant of methanol (33 at 293K) than of ethanol (25 at 293K). The dissociation constant varies exponentially with the difference in the dielectric constants of the

different solvents.²²⁸

Dissociation of salts is favoured by increasing pressure because of the associated volume decrease due to electrostriction as the ions are solvated. This means that for cadmium chloride, complex formation would be less at high pressure, and the Cd^{++} concentration would be higher. Therefore the observed independence of the reaction rate with pressure (Table III-24) in both alcohols is the result of a decrease in the real rate with a compensating increase in the Cd^{++} concentration. A decrease in the real rate constant with pressure would result in a positive value for the volume of activation. The value of $0.0 \text{ cm}^3 \text{ mol}^{-1}$ given in Table III-27, is therefore too negative, as it appears when compared with the volumes of activation found for other efficient e_s^- scavenging reactions.

The scavengers acid and nitrobenzene give a ratio the same as the ratio of diffusion coefficients for solvated electrons in ethanol and methanol. This is convincing evidence that the diffusion of the electrons is rate determining in the reaction with these scavengers.

Throughout the table there is a general trend that the ratio increases as the reaction rate constant decreases. This trend can be used to determine if an observed small rate constant is due to slow scavenging by the known solute, or fast scavenging by an unknown

impurity present in low concentration. With this in mind, it is useful to look again at the apparently slow scavenging rates determined for acetylene in this work. The value of $k_{5,\text{EtOH}}/k_{5,\text{MeOH}}$ is 1.5 in the neutral solvent, and 1.3 in basic solution. This suggests the observed decrease in the solvated electron half-life was due to a reaction which has a rate constant greater than $10^9 \text{ M}^{-1} \text{ s}^{-1}$, which supports the contention that oxygen was present as an impurity.

The most interesting result of the comparison is for benzene, and some of its derivatives. Rate constants as low as $10^6 \text{ M}^{-1} \text{ s}^{-1}$ are difficult to justify for solvated electron reactions, because μM impurity could account for the observed effects. However, for benzene, several facts dispute any suggestion that impurity is the sole electron scavenger in its alcohol solutions. These are:

- (i) The higher activation energy than observed for fast electron reactions (Tables IV-6 and IV-7).
- (ii) The negative activation volume (Table III-27).
- (iii) The fact that $k_{5,\text{EtOH}}/k_{5,\text{MeOH}}$ is much greater than 0.6 (Table IV-13).

The same arguments can be used for toluene, phenol, and probably o-xylene.

B I B L I O G R A P H Y

1. (a) Advisory Board, *Anal. Chem.*, 34, 1852 (1962).
(b) W. Kauzmann, "Quantum Chemistry", Academic Press, New York (1957) p.581.
(c) S. D. Hamann, "Physico-Chemical Effects of Pressure", Butterworths, London (1957) p.163.
2. J. W. T. Spinks and R. G. Woods, "An Introduction to Radiation Chemistry" Wiley, New York (1964).
3. G. Fiedlander and J. W. Kennedy, "Nuclear and Radiochemistry", Wiley, New York (1955).
4. F. S. Dainton and D. B. Peterson, *Proc. Roy. Soc. A*, 267, 443 (1962).
5. J. M. Warman, K.-D. Asmus and R. H. Schuler, *Advances in Chemistry Series No. 82*, American Chemical Society, Washington, D.C. (1968), p.25.
6. F. S. Dainton and D. C. Walker, *Proc. Roy. Soc. A*, 285, 339 (1965).
7. K.-D. Asmus and J. H. Fendler, *J. Phys. Chem.*, 72, 4285 (1968).
8. A. O. Allen, "The Radiation Chemistry of Water and Aqueous Solutions", Van Nostrand, Princeton, N. J., (1961) pp.75-98.
9. M. S. Matheson and L. M. Dorfman, *J. Chem. Phys.*, 32, 1870 (1960).

10. R. L. McCarthy and A. MacLachlan, *Trans. Farad. Soc.*, 56, 1187 (1960).
11. J. P. Keene, *Nature*, 188, 843 (1960).
12. (a) M. J. Bronskill, R. K. Wolff and J. W. Hunt, *J. Chem. Phys.*, 53, 4201 (1970).
(b) R. K. Wolff, M. J. Bronskill, J. E. Aldrich and J. W. Hunt, *J. Phys. Chem.*, 77, 1350 (1973).
(c) L. Gilles, J. E. Aldrich and J. W. Hunt, *Nature Phys. Sc.*, 243, 70 (1973).
13. R. K. Wolff, M. J. Bronskill and J. W. Hunt, *J. Chem. Phys.*, 53, 4211 (1970).
14. J. E. Aldrich, M. J. Bronskill, R. K. Wolff and J. W. Hunt, *J. Chem. Phys.*, 55, 530 (1971).
15. M. J. Bronskill and J. W. Hunt, *J. Phys. Chem.*, 72, 3762 (1968).
16. M. J. Bronskill, W. B. Taylor, R. K. Wolff and J. W. Hunt, *Rev. Sci. Instr.*, 41, 333 (1970).
17. A. J. Swallow, "Radiation Chemistry", Longman, London (1973).
18. A. K. Pikaev, "Pulse Radiolysis of Water and Aqueous Solutions", Indiana University Press, Bloomington, Ind., (1967).
19. J. P. Keene, in "Pulse Radiolysis", M. Evert, J. P. Keene, A. J. Swallow and J. H. Baxendale, Eds., Academic Press, London (1965).

20. J. W. Boag, in "Actions Chimiques et Biologiques des Radiations", M. Haissinsky, Ed., Sixième Série, Masson et C^{ie}, Paris (1963).
21. P. K. Ludwig, in "Advances in Radiation Chemistry", M. Barton and J. L. Magee, Eds., Vol. 3, Wiley-Interscience, New York (1972), p.1.
22. F. T. Howard, O. R. N. L. Rep. 2644, Oakridge National Laboratory, U.S.A. (1958).
23. R. J. van de Graaff, J. G. Trump and W. W. Buechner, Rep. Prog. Phys., 11, 1 (1948).
24. L. M. Dorfman, Science, 141, 493 (1963).
25. R. A. Holroyd, in "Fundamental Processes in Radiation Chemistry", P. Ausloos, Ed., Interscience, New York (1968), p.413.
26. J.-P. Dodelet, K. Shinsaka and G. R. Freeman, J. Chem. Phys., 59, 1293 (1973).
27. M. G. Robinson and G. R. Freeman, Can. J. Chem., 52, 440 (1974).
28. W. F. Schmidt and G. Bakale, Chem. Phys. Let., 17, 617 (1972).
29. W. F. Schmidt and A. O. Allen, J. Chem. Phys., 52, 2345 (1970).
30. J. H. Baxendale and P. Wardman, Nature, 230, 449 (1971).
31. J. H. Baxendale and P. Wardman, Chem. Comm., 429 (1971).

32. J. H. Baxendale and P. Wardman, *J. Chem. Soc., Farad. Trans.*, 69, 584 (1973).
33. G. R. Freeman, "Radiation Chemistry" notes of Chem. 591 course.
34. J. H. O'Donnell and D. F. Sangster, "Principles of Radiation Chemistry", Edward Arnold Ltd., London (1970).
35. H. A. Bethe and J. Ashkin, in "Experimental Nuclear Physics", E. Segré, Ed., Vol. 1, Wiley, New York (1953).
36. A. Mozumder, in "Advances in Radiation Chemistry", M. Burton and J. L. Magee, Ed., Vol. 1, Wiley-Interscience, New York (1969) p.1.
37. G. R. Freeman, in "Actions Chimiques et Biologiques des Radiations", M. Haissinsky, Ed., 14^e Série, Masson et C^{ie}, Paris (1969).
38. G. R. Freeman, *J. Chem. Phys.*, 46, 2822 (1967).
39. A. H. Samuel and J. L. Magee, *J. Chem. Phys.*, 21, 1080 (1953).
40. G. R. Freeman, in "Advances in Radiation Research" J. I. Duplan and A. Chapiro, Eds., Vol. 2, Gordon and Breach, London (1973).
41. R. A. Vermeer and G. R. Freeman, *Can. J. Chem.*, 52, 1181 (1974).
42. (a) G. R. Freeman and J. M. Fayadh, *J. Chem. Phys.*, 43, 86 (1965).

42. (b) R. Schiller, J. Chem. Phys., 47, 2278 (1967).
(c) A. Mozumder, J. Chem. Phys., 50, 3153 (1969).
(d) P. M. Rentzepis, R. P. Jones and J. Jortner, J. Chem. Phys., 59, 766 (1973).
43. J. W. Fletcher, P. J. Richards and W. A. Seddon, Can. J. Chem., 48, 1645 (1970).
44. S. M. S. Akhtar and G. R. Freeman, J. Phys. Chem., 75, 2756 (1971).
45. G. E. Adams and R. D. Sedgwick, Trans. Farad. Soc., 60, 865 (1964).
46. G. R. Freeman, Radiation Chemistry of Ethanol: A Review of Data----, NSRDS-NBS48, Nat. Stand. Ref. Data Syst., Nat. Bur. Stand. (U.S.) (1974).
47. J. H. Baxendale, The Radiolysis of Methanol:----, NSRDS-NBS (U.S.) in press.
48. S. Gordon, E. J. Hart, M. S. Matheson, J. Rabani and J. K. Thomas, Disc. Farad. Soc., 36, 193 (1963).
49. E. J. Hart, J. K. Thomas and S. Gordon, Rad. Res. Suppl., 4, 74 (1964).
50. G. Stein, Discuss. Farad. Soc., 12, 227 (1952).
51. D. E. Lea, "Actions of Radiation on Living Cells", 2nd Ed., Cambridge University Press, Cambridge (1955).
52. L. H. Gray, J. Chem. Phys., 48, 172 (1951).
53. R. L. Platzman, U. S. Nat. Acad. Sci. - N.R.C. Reports, No. 305, 22 (1953).

54. H. Fröhlich and R. L. Platzman, *Phys. Rev.*, 92, 1152 (1953).
55. E. J. Hart and J. W. Boag, *J. Amer. Chem. Soc.*, 84, 4090 (1962).
56. D. C. Walker, *Quart. Revs.*, 21, 79 (1967).
57. S. Gordon, E. J. Hart, M. S. Matheson, J. Rabani and J. K. Thomas, *J. Amer. Chem. Soc.*, 85, 1375 (1963).
58. M. S. Matheson, *Rad. Res.*, 4, 1 (1964).
59. D. F. Burow and J. J. Lagowski, in "Solvated Electron", R. F. Gould, Ed., *Advances in Chemistry Series* 50, American Chemical Society, Washington (1965) p.125
60. (a) A. Habersbergerová, I. Janovský and J. Teply, *Rad. Res. Revs.*, 1, 109 (1968).
(b) A. Habersbergerová, I. Janovský and P. Kourim, *Rad. Res. Revs.*, 4, 123 (1972).
61. (a) J. P. Keene, *Nature*, 197, 47 (1963).
(b) J. W. Boag and E. J. Hart, *Nature*, 197, 45 (1963).
62. J. Rabani, W. A. Mulac and M. S. Matheson, *J. Phys. Chem.*, 69, 53 (1965).
63. B. D. Michael, E. J. Hart and K. H. Schmidt, *J. Phys. Chem.*, 75, 2798 (1971).
64. M. C. Sauer, Jr., S. Arai and L. M. Dorfman, *J. Chem. Phys.*, 42, 708 (1965).

65. K. N. Jha, G. L. Bolton and G. R. Freeman, *J. Phys. Chem.*, 76, 3876 (1972).
66. R. R. Hentz and G. Kenney-Wallace, *J. Phys. Chem.*, 76, 2931 (1972).
67. S. Arai and M. C. Sauer, Jr., *J. Chem. Phys.*, 44, 2297 (1966).
68. F. A. Taub, D. A. Harter, M. C. Sauer, Jr., and L. M. Dorfman, *J. Chem. Phys.*, 41, 979 (1964).
69. A. K. Pikaev, G. K. Sibirskaya, E. M. Shirshov, P. Ya. Glazunov, and V. I. Spitsyn, *Dokl. Phys. Chem.*, *Proc. Acad. Sci. U.S.S.R. (Eng.)*, 200, 786 (1971).
70. F. A. Taub and L. M. Dorfman, *J. Am. Chem. Soc.*, 85, 4053 (1962).
71. J. F. Gavlas and L. M. Dorfman, *Int. J. Radiat. Phys. Chem.*, in press.
72. (a) L. M. Dorfman, F. Y. Jou and R. Wagemen, *Ber. Buns. Phys. Chem.*, 75, 681 (1971).
(b) L. M. Dorfman and F. Y. Jou, in "Electrons in Fluids", J. Jortner and N. R. Kestner, Eds., Springer-Verlag, New York (1973) p.447.
73. F. Y. Jou and L. M. Dorfman, *J. Chem. Phys.*, 58, 4715 (1973).
74. W. A. Seddon, J. W. Fletcher, F. C. Sopchyshyn and J. Jevcak, *Can. J. Chem.*, submitted for publication.
75. R. R. Hentz and G. A. Kenney-Wallace, *J. Phys. Chem.*,

- 78, 514 (1974).
76. R. Olinger and U. Schindewolf, *Ber. Buns. Phys. Chem.*, 75, 693 (1971).
77. B. J. Brown, N. T. Baker and D. F. Sangster, *Aust. J. Chem.*, 26, 2089 (1973).
78. E. M. Fielden and E. J. Hart, *Trans. Farad. Soc.*, 63, 2975 (1967).
79. H. Greenshields and W. A. Seddon, "Pulse Radiolysis, A Comprehensive Bibliography", A.E.C.L.-3524 (1970).
80. J. Shankar, *J. Indian Chem. Soc.*, 48, 97 (1971).
81. M. Anbar, *Quart. Revs.*, 22, 578 (1968).
82. J. K. Thomas, *Rad. Res. Revs.*, 1, 103 (1968).
83. E. J. Hart, *Accts. of Chem. Res.*, 2, 161 (1969).
84. E. J. Hart, *Survey of Prog. Chem.*, 5, 140 (1969).
85. I. A. Taub, M. C. Sauer, Jr., L. M. Dorfman, *Disc. Farad. Soc.*, 36, 206 (1963).
86. S. Arai and L. M. Dorfman, *J. Chem. Phys.*, 41, 2190 (1964).
87. J. H. Baxendale, *Int. J. Radiat. Phys. Chem.*, 4, 113 (1972).
88. K. N. Jha, G. L. Bolton and G. R. Freeman, *Can. J. Chem.*, 50, 3073 (1972).
89. L. M. Dorfman, *Advan. Chem. Ser.*, 50, 36 (1965).
90. J. K. Thomas and R. V. Bensasson, *J. Chem. Phys.*, 46, 4147 (1967).
91. S. Arai, A. Kira and M. Imamura, *J. Phys. Chem.*, 74,

- 2102 (1970).
92. P. Fowles, Trans. Farad. Soc., 67, 428 (1971).
93. J. Rabani, M. Graetzel and S. A. Chaudri, J. Phys. Chem., 75, 3893 (1971).
94. J. K. Thomas, K. Johnson, T. Klippert and R. Lowers, J. Phys. Chem., 48, 1608 (1968).
95. E. Hayon, J. Chem. Phys., 53, 2353 (1970).
96. A. V. Rudnev, V. A. Vannikov and N. A. Bakh, High Energy Chem. (Eng.), 6, 416 (1972).
97. S. Pekar, J. Phys. (U.S.S.R.), 10, 341 (1946).
98. L. Landau, Sov. Phys., 3, 664 (1933).
99. R. A. Ogg, Jr., Phys. Rev., 69, 243 (1946).
100. J. Jortner, J. Chem. Phys., 30, 839 (1959).
101. J. Jortner, in "Radiation Chemistry of Aqueous Systems", G. Stein, Ed., Weizmann Science Press, Jerusalem (1968) p.91.
102. D. A. Copeland, N. R. Kestner and J. Jortner, J. Chem. Phys., 53, 1189 (1970).
103. (a) K. Fueki, D.-F. Feng and L. Kevan, J. Phys. Chem., 74, 1976 (1970).
- (b) K. Fueki, D.-F. Feng, L. Kevan and R. E. Christoffersen, J. Phys. Chem., 75, 2297 (1971).
104. K. Fueki, D.-F. Feng and L. Kevan, Chem. Phys. Lett., 10, 504 (1971).
105. D.-F. Feng, K. Fueki and L. Kevan, J. Chem. Phys., 57, 1253 (1972).

106. L. Raff and H. A. Phol, *Advan. Chem. Ser.*, 50, 173 (1965).
107. M. Natori and T. Watanabe, *J. Phys. Soc. Japan*, 21, 1573 (1966).
108. G. Howat and B. C. Webster, *J. Phys. Chem.*, 76, 3714 (1972).
109. B. C. Webster and G. Howat, *Rad. Res. Revs.*, 4, 259 (1972).
110. E. J. Hart and M. Anbar, "The Hydrated Electron", Wiley-Interscience, New York (1970).
111. F. S. Dainton, *Ber. Buns. Phys. Chem.*, 75, 608 (1971).
112. (a) J. Jortner, *Ber. Buns. Phys. Chem.*, 75, 696 (1971).
(b) N. R. Kestner in "Electrons in Fluids", J. Jortner and N. R. Kestner, Eds., Springer-Verlag, New York (1973) p.1.
113. B. J. Nicholson, *Advan. Chem. Phys.*, 18, 249 (1970).
114. G. Howat and B. C. Webster, *Ber. Buns. Phys. Chem.*, 75, 626 (1971).
115. M. G. Robinson, K. N. Jha and G. R. Freeman, *J. Chem. Phys.*, 55, 4933 (1971).
116. U. Schindewolf, H. Kohrmann and G. Long, *Angew. Chem. Internat. Edit.*, 8, 512 (1969).
117. U. Schindewolf, G. Lang and H. Kohrmann, *Chemie. Ing. Thechn.*, 41, 830 (1969).
118. R. R. Hentz, Farhataziz and E. M. Hansen, *J. Chem.*

- Phys., 55, 4974 (1971).
119. (a) R. R. Hentz, Farhataziz and E. M. Hansen, J. Chem. Phys., 56, 4485 (1972).
- (b) R. R. Hentz, Farhataziz and E. M. Hansen, J. Chem. Phys., 57, 2959 (1972).
120. R. R. Hentz, Farhataziz, D. J. Milner and M. Burton, J. Chem. Phys., 46, 2995 (1967).
121. R. R. Hentz, Farhataziz, D. J. Milner and M. Burton, J. Chem. Phys., 47, 374 (1967).
122. R. R. Hentz, Farhataziz and D. J. Milner, J. Chem. Phys., 47, 5381 (1967).
123. R. R. Hentz and R. J. Knight, J. Chem. Phys., 52, 2456 (1970).
124. K. N. Jha and G. R. Freeman, J. Chem. Phys., 57, 1408 (1972).
125. K. N. Jha and G.R. Freeman, J. Amer. Chem. Soc., 95, 5891 (1973).
126. K. N. Jha and G. R. Freeman, Can. J. Chem., 51, 2033 (1973).
127. K. J. Laidler, "Chemical Kinetics", 2nd Ed., McGraw Hill, Toronto (1965).
128. U. Schindewolf, Angew. Chem. Internat. Ed., 6, 575 (1967).
129. I. S. Jacobs, Phys. Rev., 93, 993 (1954).
130. M. Anbar, Quart. Rev., 22, 578 (1968).

131. B. Cercek, *Nature*, 223, 491 (1969).
132. B. Cercek, *Nature Phys. Sc.*, 229, 12 (1971).
133. G. V. Buxton, F. C. R. Cattell and F. S. Dainton, *Trans. Farad. Soc.*, 67, 687 (1971).
134. W. C. Gottschall and E. J. Hart, *J. Phys. Chem.*, 71, 2102 (1967).
135. National Research Council, "International Critical Tables", McGraw-Hill, New York (1926). Vol. 1, p.58.
136. "C.R.C. Handbook of Chemistry and Physics", 48th Ed., p. D101.
137. G. E. Adams, J. W. Boag, J. Cunant and B. D. Michael, "Pulse Radiolysis", Academic Press Inc., New York, (1965) p.117.
138. J. H. Baxendale, P. L. T. Bevan and D. A. Stott, *Trans. Farad. Soc.*, 64, 2389 (1968).
139. D. Behar, P. L. T. Bevan and G. Scholes, *J. Phys. Chem.*, 76, 1537 (1972).
140. R. W. Gallant, "Physical Properties of Hydrocarbons", Vol. 1, Gulf Publishing Co, Houston, Tex., (1968). Chap. 8.
141. W. Dannhauser and L. W. Bahe, *J. Chem. Phys.*, 40, 3058 (1964).
142. F. Buckley and A. A. Maryott, *Nat. Bur. Stand. U. S. Circ.*, No. 589 (1958).

143. P. W. Bridgeman, "The Physics of High Pressure", G. Bell and Sons, London (1958).
144. W. E. Danforth, Jr., Phys. Rev., 38, 1224 (1931).
145. S. Kyropoulos, Zeit. Für Physik, 40, 507 (1926).
146. A. V. Vannikov and V. S. Marevtsev, Int. J. Radiat. Phys. Chem., 5, 453 (1973).
147. I. A. Taub, M. C. Sauer, Jr., and L. M. Dorfman, Disc. Farad. Soc., 36, 206 (1963).
148. K. N. Jha, private communication.
149. A. K. Pikaev, G. K. Sibirskaya and S. A. Kabakchi, Dokl. Phys. Chem. Proc. Acad. Sci. U.S.S.R., 198, 554 (1971).
150. F. S. Dainton, J. P. Keene, T. J. Kemp, G. A. Salmon and J. Teply, Proc. Chem. Soc., 265 (1964).
151. B. E. Conway, "Electrochemical Data", Elsevier Publishing Co., Amsterdam (1952).
152. H. Strehlow, Z. Phys. Chem. (N.F.), 24, 240 (1960).
153. J. Holcman, S. Karolczak, J. Kroh, J. Mayer and M. Mienska, Int. J. Radiat. Phys. Chem., 1, 457 (1969).
154. W. V. Sherman, J. Phys. Chem., 71, 4245 (1967).
155. L. M. Dorfman and M. S. Matheson, in "Progress in Reaction Kinetics", Vol. III, Pergamon Press, London (1965).
156. R.S. Bradley, Ed., "High Pressure Physics and Chemistry", Vol. 1 and 2, Academic Press, London

- (1963).
157. M. G. Robinson, to be published.
 158. M. Walter and L. Ramaley, *Anal. Chem.*, 45, 165 (1973).
 159. J. F. Coetzee, *Pure and Appl. Chem.*, 13, 429 (1966).
 160. J. H. Baxendale, E. M. Fielden and J. P. Keene, *Proc. Royal Soc. A*, 286, 320 (1965).
 161. T.E.M. Sambrook, Ph.D. Thesis, The University of Alberta (1973) pg. 15, and references therein.
 162. J. Niedzielski and J. Gawlowski, *Int. J. Radiat. Phys. Chem.*, 5, 239 (1973).
 163. J. Gawlowski and J. Niedzielski, *Int. J. Radiat. Phys. Chem.*, 5, 419 (1973).
 164. E. J. Hart and E. M. Fielden, *Advances in Chemistry Series* 50, 253 (1965).
 165. W. Kunerth, *Phys. Rev.*, 19, 519 (1922).
 166. W. F. Linke, "Solubilities of Inorganic and Metal Organic Compounds", 4th Ed., Amer. Chem. Soc., Washington (1965). a, Vol. I; b, Vol. II.
 167. H. Stephen and T. Stephen, Eds., "Solubilities of Inorganic and Organic Compounds", Macmillan, New York (1963). a, Part I, b, Part II.
 168. H. Seki and M. Imamura, *Bull. Chem. Soc. Japan*, 44, 1538 (1971).
 169. F. S. Dainton, G. A. Salmon and P. Wardman, *Proc. Roy. Soc. A*, 313, 1 (1969).

170. G. V. Buxton, F. S. Dainton and M. Hammerli, *Trans. Farad. Soc.*, 63, 1191 (1967).
171. D. M. Pinkerton, *Atomic Energy Res. Estab.*, Harwell, AERE-R 6541 (1970).
172. J. W. Fletcher, unpublished results (1969).
173. H. L. Friedman, *J. Amer. Chem. Soc.*, 76, 3294 (1954).
174. S. G. Rzad and J. H. Fendler, *J. Chem. Phys.*, 52, 5395 (1970).
175. K. Suryanarayanan and N. N. Lichtin, *J. Phys. Chem.*, 73, 1384 (1969).
176. M. Anbar and P. Neta, *Internat. J. Appl. Rad.*, 16, 227 (1965).
177. E. Wilhelm and R. Battino, *Chem. Revs.*, 73, 1 (1973).
178. C. B. Kretschmer, J. Nowakowska and R. Wieve, *Ind. Eng. Chem.*, 38, 506 (1946).
179. J. H. Hildebrand and R. L. Scott, "The Solubility of Nonelectrolytes", Dover Publications, Inc., New York, (1964), p.243.
180. G. Levi, *Gazz. Chim. Ital.*, 31, 513 (1901).
181. E. J. Hart, S. Gordon and J. K. Thomas, *J. Phys. Chem.*, 68, 1271 (1964).
182. N. W. Holm and R. J. Berry, Eds., "Manual of Radiation Dosimetry", Marcel Dekken Inc., New York (1970).
183. G. E. Adams, J. W. Boag and B. D. Michael, *Trans. Farad. Soc.*, 61, 1679 (1965).

184. G. E. Adams, personal communication.
185. G. Czapski and B. H. J. Bielski, *J. Phys. Chem.*, 67, 2180 (1963).
186. J. H. Baxendale, personal communication.
187. J. Jortner, S. A. Rice and E. G. Wilson, in "Metal-Ammonia Solutions", G. Lepoutre and M. J. Sienko, Eds., W. A. Benjamin, New York, (1964) p.222 and references contained therein.
188. E. M. Fielden and E. J. Hart, *Radiat. Res.*, 33, 426 (1968).
189. R. R. Hentz and G. Kenney-Wallace, *J. Phys. Chem.*, 78, 514 (1974).
190. J. L. Dye, M. G. DeBacker and L. M. Dorfman, *J. Chem. Phys.*, 52, 6251 (1970).
191. M. G. DeBacker and J. L. Dye, *J. Phys. Chem.*, 75, 3092 (1971).
192. (a) R. K. Quinn and J. J. Lagowski, *J. Phys. Chem.*, 73, 2326 (1969).
(b) D. M. J. Compton, J. F. Bryant, R. A. Cesena and B. C. Gehman, p.43 of reference 19.
193. D. C. Walker, N. V. Klassen and H. A. Gillis, *Chem. Phys. Lett.*, 10, 636 (1971).
194. R. Bensasson and E. J. Land, *Chem. Phys. Lett.*, 15, 195 (1972).
195. N. Nauta and C. van Huis, *J. Chem. Soc., Farad. Trans.*, 68, 647 (1972).

196. J. M. Brooks and R. R. Dewald, *J. Phys. Chem.*, 72, 2655 (1968).
197. G. R. Freeman, *J. Phys. Chem.*, 77, 7 (1973).
198. M. G. Robinson, K. N. Jha, G. L. Bolton and G. R. Freeman, in a paper presented at the C.I.C. Pulse Radiolysis Symposium, Pinawa, Manitoba, Oct. 26, 1971.
199. J. G. Kirkwood, *J. Chem. Phys.*, 7, 911 (1939).
200. G. Oster and G. J. Kirkwood, *J. Chem. Phys.*, 11, 175 (1943).
201. D. Feng, K. Fueki and L. Kevan, *J. Chem. Phys.*, 57, 1253 (1972).
202. K. N. Jha and G. R. Freeman, *J. Chem. Phys.*, 51, 2846 (1969).
203. F. Busi and M. D. Ward, *Int. J. Radiat. Phys. Chem.*, 5, 521 (1973).
204. K. N. Jha and G. R. Freeman, *J. Chem. Phys.*, 48, 5480 (1968).
205. H. Seki and M. Imamura, *J. Phys. Chem.*, 71, 870 (1967).
206. J. J. J. Myron and G. R. Freeman, *Can. J. Chem.*, 43, 381 (1965).
207. J. C. Roux, Ch. Baquey and J. Sutton, *Int. J. Radiat. Phys. Chem.*, 5, 309 (1973).
208. G. M. Barrow, "Molecular Spectroscopy", McGraw-Hill, New York (1962) p.81.

209. I. Kules and R. Schiller, *J. Phys. Chem.*, 75, 2997 (1971).
210. B. Cercek and M. Ebert, *J. Phys. Chem.*, 72, 766 (1968).
211. G. Beck and J. K. Thomas, *J. Chem. Phys.*, 60, 1705 (1974).
212. H. Oguara and W.H. Hamill, *J. Phys. Chem.*, 78, 504 (1974).
213. W. H. Hamill, *J. Chem. Phys.*, 49, 2446 (1968).
214. W. H. Hamill, *J. Phys. Chem.*, 73, 1341 (1969).
215. H. B. Steen, O. Kaalhus and M. Kongshaug, *J. Phys. Chem.*, 75, 1941 (1971).
216. H. B. Steen, *J. Phys. Chem.*, 74, 4059 (1970).
217. D. L. Gay, *Can. J. Chem.*, 49, 3231 (1971).
218. J. H. Baxendale, E. M. Fielden, C. Capellos, J. M. Francis, J. V. Davis, M. Ebert, C. M. Gilbert, J. P. Keene, E. J. Land, A. J. Swallow and J. M. Nosworthy, *Nature*, 201, 468 (1964).
219. J. Appleby, G. Scholes and M. Simic, *J. Amer. Chem. Soc.*, 85, 3891 (1963).
220. G. V. Buxton, F. S. Dainton and M. Hammerli, *Trans. Farad. Soc.*, 63, 1191 (1967).
221. J. I. Allen, N. Getoff, H. P. Lehmann, K. E. Nixon, G. Scholes and M. Simic, *J. Inorg. and Nucl. Chem.*, 19, 204 (1961).

222. C. F. Cullis, J. M. Francis and A. J. Swallow, Proc. Roy. Soc., A287, 15 (1965).
223. G. Dobson and L. I. Grossweiner, Rad. Res., 23, 290 (1964).
224. National Research Council, "International Critical Tables", McGraw-Hill, New York (1926). Vol. 5, pp.151-152.
225. E. J. King, "Acid-base Equilibria", The MacMillan Co. New York (1965) p.293.
226. J. Barat, L. Gilles, B. Hickel and B. Lesigne, J. Phys. Chem., 77, 1711 (1973).
227. E. L. King, J. Amer. Chem. Soc., 71, 319 (1949).
228. I. M. Kolthoff and S. Bruckenstein, in "Treatise on Analytical Chemistry", I. M. Költhoff, P. J. Elving, and E. B. Sandell, Eds., Interscience, New York (1959). Part 1, Vol. 1, Chap. 13, p.488.

B30102